An anatomical exploration of the extracranial (V1-V3) and intracranial (V4) components of the vertebral arteries in a select KwaZulu-Natal population

UNIVERSITY OF KWAZULU-NATAL
INYUVESI YAKWAZULU-NATALI

By

BUKOLA RUKAYAT OMOTOSO

(Student no. 217080986)

May 2021

An anatomical exploration of the extracranial (V1-V3) and intracranial (V4) components of the vertebral arteries in a select KwaZulu-Natal population

By

BUKOLA RUKAYAT OMOTOSO

(Student no. 217080986)

A Thesis submitted to

Discipline of Clinical Anatomy

School of Laboratory Medicine and Medical Sciences College of Health Sciences

University of KwaZulu-Natal Durban, South Africa

In fulfilment of the Requirement for the Degree of Doctor of Philosophy in the Discipline of Clinical Anatomy

Supervisor: **Prof Lelika Lazarus**

Co-supervisors: **Prof Kapil Satyapal**

Dr Rohen Harrichandparsad

Preface

The information presented in this thesis is an original work by the candidate. It was carried out in the Discipline of Clinical Anatomy, School of Laboratory Medicine and Medical Sciences, College of Health Sciences, University of KwaZulu-Natal and Lenmed Ethekwini Hospital and Heart Center, Durban, South Africa from June 2018 to February 2021, under the supervision of Prof L Lazarus, Prof KS Satyapal, and Dr R Harrichandparsad for the award of Doctor of Philosophy Degree in Clinical Anatomy and has not otherwise been submitted in any form for any degree or diploma to any other University. Where use has been made of the work of others, it has been duly acknowledged in the text in the form of reference.

Declaration

I, Bukola Rukayat Omotoso, declare as follows:

1. That the research reported in this thesis, to my knowledge has not been submitted to UKZN or any other tertiary institution for the purpose of obtaining an academic qualification either by me or any other person.
2. That my contributions to the project were as follows:
    a. I was involved in the design and submission of the proposal for ethics approval by the Biomedical Research Ethics Committee.
    b. I was wholly responsible for the data collection, collation, and analyses.
    c. I was responsible under supervision, for writing all the manuscripts and this thesis.
3. This thesis does not contain any other person's writing, data, pictures, or other information unless specifically acknowledged as being sourced from other persons or researchers.
   Where other written sources have been quoted then:
    a. Their words have been rewritten, but the general information attributed to them has been referenced.
    b. Where their exact words have been used, then it has been properly referenced in the reference section.
4. This thesis does not contain text, graphics or tables copied and pasted from the Internet, unless specifically acknowledged, and the source being detailed in the thesis and in the References sections.

[redacted]

03/05/2021

---------------------- ------------------------

Signed Date

Presentations

Part of the findings observed in this study was presented at the following conferences or symposia:

1. **BR Omotoso**, R Harrichandparsad, IG Moodley, KS Satyapal, L Lazarus; Fenestration of the Intracranial Vertebral Artery and Vertebrobasilar Junction Detected with Multi Detector Computed Tomography Angiography, **ASSA World Anatomy Day Virtual Conference October 2020.**
2. **BR Omotoso**, R Harrichandparsad, IG Moodley, KS Satyapal, L Lazarus; An Anatomical Investigation of the Vertebral Arteries in a Select South African Cohort of Patients, **School of Laboratory Medicine and Medical Sciences, September 2020 Research Symposium, University of Kwazulu-Natal, Durban, South Africa.**
3. **BR Omotoso**, R Harrichandparsad, J. NAIDOO, KS Satyapal, L Lazarus; Fenestration of the Intracranial Vertebral Artery and Vertebrobasilar Junction Detected with Multi Detector Computed Tomography Angiography, **16th Annual Conference of the Australian and New Zealand Association of Clinical Anatomists, December 2019, Perth, Western Australia.**
4. **BR Omotoso**, R Harrichandparsad, IG Moodley, KS Satyapal, L Lazarus; Fenestration of the Vertebrobasilar Junction Detected with Multi Detector Computed Tomography Angiography, **College of health Sciences Research Symposium November 2019, University of KwaZulu-Natal, Durban, South Africa.**
5. **BR Omotoso**, R Harrichandparsad, IG Moodley, KS Satyapal, L Lazarus; Tortuosity of the Vertebral Arteries in a Select South African Population, **19th Congress of International Federation of Anatomists, August 2019, London, United Kingdom.**
6. **BR Omotoso**, R Harrichandparsad, IG Moodley, KS Satyapal, L Lazarus; Anatomical Variation in Origin of the Left Vertebral Artery, **47th Congress of Anatomical Society of Southern Africa, April 2019.**

Statement

The following publications has been included as chapters in this thesis (i.e., Chapter 2 to 6)

Published/accepted

1. **Omotoso, B.R**., Harrichandparsad, R., Moodley, I.G, Satyapal K.S, Lazarus L. An anatomical investigation of the proximal vertebral arteries (V1, V2) in a select South African population. *Surg Radiol Anat* (2021). https://doi.org/10.1007/s00276-021-02712-x
2. **BR Omotoso**, IG Moodley, R Harrichandparsad, KS Satyapal, L Lazarus. Fenestration of the Vertebrobasilar Junction Detected with Multidetector Computed Tomography Angiography. Folia Morphologica. (2021) **DOI:** 10.5603/FM.a2021.0028
3. **Omotoso, B.R**., Harrichandparsad, R., Satyapal K.S, Moodley, I.G, Lazarus L. Radiological Anatomy of the Intracranial Vertebral Artery in a Select South African Cohort of Patients. Scientific Reports. 2021 Jun 9;11(1):1-9. https://doi.org/10.1038/s41598-021-91744-9
4. **Bukola R. Omotoso**, Rohen Harrichandparsad, Lelika Lazarus (2021) Radiological Anatomy of the Suboccipital Segment of the Vertebral Artery in a Select South African Population. Eur J Anat, 25(5): 553-562 (2021)

In press (publication was halted by the publisher due to COVID-19 please see appendix)

1. **BR Omotoso**, IG Moodley, R Harrichandparsad, KS Satyapal, L Lazarus (2019). Anatomical Variations of the Vertebral Arteries in a Select South African Population; Evaluation with Multidetector Computed Tomography Angiography. Italian Journal of Anatomy and Embryology. Manuscript number: **IJAE 47-2019-DRFP** Accepted for publication

The PhD candidate performed experimental work described in this publication, where others have made contributions, it is duly acknowledged in the text. The candidate drafted this publication in full and it has been reviewed by co-authors.

B.R Omotoso……[redacted]…… Date…03/05/2021

Professor Lelika Lazarus…[redacted] Date…14/05/2021

Professor KS Satyapal… [redacted] Date…14/05/2021

Dr Rohen Harrichandparsad… [redacted] Date…03/05/2021

Dedication

To my parents – Mr. Rasheed Adeleke and Mrs. Idiat Abiola Omotoso, for their support in every aspect. To my adorable siblings Oluwasegun and Opeyemi who inspire me daily.

Acknowledgement

The author wishes to convey her gratitude to the following:

- The Almighty God for the opportunity, grace, hope, and knowledge given to me to complete this program.
- My sincere gratitude to my supervisors Prof L Lazarus, Dr. R Harrichandparsad, and Prof KS Satyapal, for their never-ending support, displayed all through my Doctor of Philosophy journey. Your guidance did not only help me all through but also make me a better researcher.
- Thank you, Prof. Nancy Eik-Nes, for your constructive comments, support, guidance, and valuable contributions to my writing. May God reward you immensely.
- I appreciate everyone's support in the Discipline of Clinical Anatomy and the Radiology Unit of Lenmed Ethekwini Hospital and Heart Center in Durban whom I worked with during this project: Mrs. Kumarie, Mrs. Urvash, Ms. Raksha, Mrs. Bukola, Dr. P Pillay, Dr. Brenda De-Gama, Ms. Ntombifuthi, Mr. Celumusa Mbokazi, Mr. Joastin Naidoo. You all have been wonderful.
- I cannot but acknowledge my friends and colleagues for their fun times, comfort, and support in achieving this, Dr. Oladapo, Olakunle Sanni, Segun Oladipupo, Veronica Salau, Olayemi Ijomone, Dr. Abiola, Sodiq Lawal, Samuel Olojede, and Okiki Aladeyelu.
- Special gratitude goes to the College of Health Sciences for providing the funding necessary for this doctorate.

Table of content

List of tables

List of figures

Abbreviations

VA -	Vertebral artery
CTA -	Computed Tomography Angiography
MDCTA -	Multidetector Computed Tomography Angiography
PICA -	Posterior inferior cerebellar artery
VAH -	Vertebral artery hypoplasia
VAD -	Vertebral artery dominance
C1 -	Atlas vertebra
C2 -	Axis vertebra

Abstract

The risk of injury to the vertebral artery is a significant complication of surgery. The presence of anatomical variation in the course of the vertebral artery increases the likelihood of injury. Due to inadequate understanding of the presence and location of anatomical variations in the morphology and morphometry, the vertebral artery can be injured during surgical intervention. Apart from the vascular injury that can occur during surgical intervention, anatomical variations have implications for some pathologies in the posterior circulation territory. These include aneurysm formation, cerebrovascular disorders, posterior circulatory stroke, and some neurovascular problems. In this retrospective observational study, we investigated the anatomical features of the extracranial (V1-V3) and intracranial (V4) components of the vertebral arteries in a South African population. The study is an observational, retrospective chart review of 554 consecutive South African patients (Black, Indian, and White) who had undergone computed tomography angiography (CTA) at Lenmed Ethekwini Hospital and Heart Centre, Durban, South Africa, from January 2009 to September 2019. The vertebral artery exhibited various morphological variations in its course. We report the incidence of variant origin of the left vertebral artery (6.9%). The level of entry into the transverse foramen ranged between C7-C3. We report the incidence of vertebral artery tortuosity at V1, V2: 76.6%, and 32.1%, respectively. We observed fenestration at V3 (0.18%) and V4 (0.4%) segments. We registered the incidence of the persistent first intersegmental artery (1.1%), extradural PICA origin (2.8%), atresia (6.7%), and hypoplastic terminal vertebral artery (13.2%). Average length and diameter at each vertebral artery segment were registered; we also report on hypoplasia of the vertebral artery. Anatomical variations of the vertebral artery are common in the South African population studied in the present study. Imaging of the complete segments of the vertebral artery from the origin to the point of convergence to form the basilar artery may be necessary to decide a treatment strategy for interventions in the vicinity of the vertebral artery. Understanding the patterns of anatomical variations of the vertebral arteries will contribute significantly to the diagnosis of various diseases in the posterior circulatory territory. The average diameter was significantly larger on the left in all the racial groups, but there were no significant gender differences. We registered a left dominance pattern in all the segments (V1-V4).

Iqoqa

Ingozi yokulimala emithanjeni yomgogodla iyinkinga enzima kakhulu yokuhlinzwa. Ukuba khona kokwehlukahlukana kokwakheka komzimba ekuhambeni komthambo womgogodla kwandisa amathuba okulimala. Ngenxa yokuqonda okunganele kokukhona kanye nendawo yokwehlukahlukana kwesakhikwo somzimba ekwakhekeni nokulinganisa umumo, umthambo womgogodla ungalimala ngesikhathi sokuhlinzwa. Ngaphandle kokulimala kwemithambo yegazi okungenzeka ngesikhathi sokuhlinzwa, ukuhlukahlukana kwemithamdo yomgogodla kunomthelela ngezinye izimbangela ngokuthola umsuka wesifo ngokuhamba kwegazi emigudwini. Lokhu kubandakanya ukwakheka kokuvuvukala komthambo, ukuphazamiseka kokuhamba kwegazi engqondweni, ukushaywa yisifo sohlangothi, nezinye izinkinga ngezinzwa nemithambo. Kulolu cwaningo lokubheka ngokuqhathanisa abanesifo nabangenaso, sibheke ukwakheka komzimba kwamathambo ekhanda ngaphandle (V1-V3) kanye nokwakheka kwawo ngaphakathi (V4) nezingxenye zemithambo yomgogodla emphakathini waseNingizimu Afrikha. Ucwaningo lungukuzibonela ngqo, ukuqhathanisa ngokubuyekeza amashadi eziguli zaseNingizimu Afrikha angama-554 ngokulandelana (abaNsundu, amaNdiya, nabaMhlophe) abafakwe emshinini bahlolwa wonke umzimba ngekhompuyutha ukubona okusemithanjeni (isibonathambomzimba) (CTA) esibhedlela i-Lenmed Ethekwini neSikhungo seNhliziyo, eThekwini, eNingizimu Afrikha, kusukela kuMasingana wowezi-2009 kuya kuMandulo wowezi-2019. Umthambo womgogodla ukhombisa ukwehlukahluka kwesakhiwo ekuthubelezeni kwawo. Sibika isehlakalo semvelaphi esehlukile somthambo womgogodla kwesokunxele (6.9%). Izinga lokungena esikhaleni esiphakathi komthambo womgogodla laliphakathi kwe-C7 ne-C3. Sibika isehlakalo esihambisana nokuguga komthambo womgogodla nomfutho wegazi okulinganiselwa phakathi kuka-V1, V2: 76.6% no-32.1%, ngokulandelana. Sibone ukuhlinzwa kwesakhiwo sendlebe ngaphakathi kwezingxenye ezingu-V3 (0.18%) nezingu-V4 (0.4%). Sabhalisa izehlakalo zomthambo wokuqala ngezingxenye ezilokhu zikhona ngo-1.1%, imvelaphi ye-PICA yamathambo ekhanda (2.8%), isicubu esingenayo embotsheni ngokwemvelo (6.7%), nokungakhuli kwesitho ngokuphelele (13.2%). Isilinganiso sobude nobubanzi engxenyeni ngayinye yomthambo womgogodla yabhaliswa; siphinde sibike ngokungasebenzi ngokwejwayelekile komthambo womgogoda. Ukwehlukahlukana kokwakheka komthambo womgogodla kuvamile kubantu baseNingizimu Afrikha ocwaningweni lwamanje. Ukufanekisa kwezingxenye eziphelele zomthambo womgogodla lapho zihlangana khona ukwenza umthambo ophakathi nendawo ekhanda kungadingakala ukunquma ngamasu okwelapha ngokungenelela endaweni eseduze nomthambo womgogodla. Ukuqonda ukuphiceka kwesakhiwo esahlukahlukene semithambo yomgogodla kuzodlala indima ebalulekile ekuhlonzeni izifo ezahlukahlukene ekuhlinzekweni kokuhamba kwegazi. Isilinganiso sobubanzi besisikhulu kakhulu kwesokunxele kuwo wonke amaqembu ezinhlanga, kodwa kwakungekho mehluko obalulekile phakathi kobulili. Sibhalise indlelakwenza ebihamba phambili kuzo zonke izingxenye ebe ngu-V1-V4.

1.0 CHAPTER ONE

1.1 Introduction

The risk of injury to the vertebral artery (VA) is one of the major complications of surgery (Yamazaki et al., 2012). The likelihood of injury is increased by the presence of anatomical variation in the course of the VA (Decarvalho et al., 2019). Due to inadequate understanding of the presence and location of anatomical variations in the morphology and morphometry, the artery can be injured during surgical intervention. Studies conducted in England and the USA to quantify the risk of injury to the VA during surgery reported an injury rate of 8.2% (Madawi et al., 1997) and 4.1% (Wright and Lauryssen, 1998), respectively. Each of the studies acknowledged the importance of knowledge of anatomical variations, which can increase the risk of injury. A review of the literature and case series studies have reported incidences ranging from 1.7% - 9.0% (Liang et al., 2004, Vergara et al., 2012, Elliott et al., 2014), while a survey on the incidence of injury from neurosurgeons reported an incidence rate of 4.1% (Wright and Lauryssen, 1998). Sometimes lesions of the VA are unrecognized and misinterpreted as preoperative venous bleedings, especially when patients are asymptomatic (Golfinos et al., 1994). Therefore, variations in the course of the artery at any of its segments should be considered by surgeons during cervical spine surgery and manipulation around the craniospinal region (Vicenzini et al., 2010).

Previous reports of anatomical variations of the VA include variant origin (duplicate or triplicate origin) (Uchino et al., 2013, Gailloud, 2019), variation in the level of entering the transverse foramen (between C7-C3) (Uchino et al., 2013), asymmetry and hypoplasia (Gaigalaite et al., 2016), VA terminating as posterior inferior cerebellar artery (PICA) (Liu et al., 2017) and PICA originating from the third segment (V3) of the artery (Arslan et al., 2019). Others include fenestration, persistent first intersegmental artery (Fortuniak et al., 2016), tortuosity (medial and lateral loop) (Yenigun et al., 2016), while the incidence of aplasia or unilateral absence of the VA is uncommon (Abd El Gawad et al., 2019).

Apart from the vascular injury that can occur during surgical intervention, anatomical variations have implications for some pathologies in the posterior circulation territory. For instance, the VA plays a significant role in the perfusion of the upper spinal cord, cerebellum, brainstem, thalamus, and occipital lobes (Sonje et al., 2015). Therefore, morphologic variations in the course of the VA may influence the hemodynamics of blood flow to these central nervous system structures. This situation can predispose to some pathological processes in the posterior circulation territory due to inadequate perfusion of these structures. For instance, authors have hypothesized that posterior circulation infarctions of the PICA and basilar artery territory are higher in vertebral artery dominant patients (Zhu et al., 2016). Similarly, posterior circulatory stroke and VA occlusion frequency have been found to be related to VA hypoplasia (Mitsumura et al., 2016).

As a result of suspected hemodynamic alterations, variation in origin has been linked with intracranial aneurysm formation and can predispose to cerebrovascular disorders (Lazaridis et al., 2018). Other morphological variations like tortuosity have been diagnosed in association with neurovascular problems such as cervical radiculopathy (Doweidar et al., 2014) and may encourage build-up of atherosclerosis (Kornieieva, 2014). The incidence of PICA originating from the third segment of the artery can complicate surgical intervention at the atlantoaxial region. Consequently, in-depth knowledge of variation is essential for diagnoses of some pathologies in the area supplied by the VAs.

The presence of variation is often overlooked due to a lack of obvious clinical symptoms and is mostly detected accidentally during the evaluation of head and neck pathologies (Shi, 2017). Because of the diverse nature of anatomical variation, the morphology of the VA needs to be wholly understood and evaluated along its entire course for operative indication in the cervical, suboccipital and intracranial region to prevent damage to the artery. Anatomically, the VA is segmented into four sections: prevertebral (V1), vertebral (V2), atlantoaxial (V3), and intracranial (V4) segments (Jecko et al., 2015). The first three segments (V1-V3) are the extracranial segments. The V1 segment, unlike the other segments, is not guarded by bony structures and is at risk of injury when the muscles around it are separated (Bruneau et al., 2006c). Thus, recognizing the variation in its level of entrance into the transverse foramen on preoperative investigations is essential to avoid iatrogenic injury (George and Laurian, 2012).

Previous studies regarding the morphology and morphometry of the VAs have hypothesized the existence of variation with demographic and ethnic/racial differences (Sikka and Jain, 2012, Kornieieva, 2014, Gaigalaite et al., 2016). Prevalence of variation in the morphology and morphometry has been previously reported at each segment of the VA in the US, Egyptian, Turkish, Asian, and Kenyan populations (Uchino et al., 2012, O'donnell et al., 2014, Yenigun et al., 2016, Abd El Gawad et al., 2019). Previous reports from the South African population did not give information about the morphology and morphometry of the entire segments but focused on the diameter of the suboccipital and intracranial VAs (Mitchell and Mckay, 1995, Mitchell, 2004). There have been controversies in the literature regarding the cut-off value for hypoplastic VA and VA dominance (Ergun et al., 2016). There is no consensus as regards which side is dominant in several populations. Some authors have reported left dominance (Abd El Gawad et al., 2019), others reported right (Akar et al., 1994, Ergun et al., 2016), while a similar study reported no difference (co-dominance) (Mitchell, 2004). For these reasons, it is essential to describe the morphology and morphometry of the VA based on ethnicity, as data from one population group may not apply to another. Knowledge of anatomical variation is essential for the interpretation of imaging studies (Pekcevik and Pekcevik, 2014). Proper identification of variant anatomy during preoperative planning may reduce the risk of iatrogenic injury and contribute to the interpretation of ischemic areas in the posterior circulatory territory. Inadequate information about this variation can expose the VA to the risk of injury that can result in grave consequences if the dominant artery is involved in a case of asymmetry (Guan et al., 2017).

Furthermore, knowledge of variation in the anatomical features of the VA in different human populations can provide indicators for understanding and prognosis of the pathological processes in the posterior circulation territory (Kornieieva, 2014). In this retrospective observational study, we sought to investigate the anatomical features of the extracranial (V1-V3) and intracranial (V4) components of the VAs in a South African population using multidetector computed tomography angiography (MDCTA). This information is important to describe the prevalence of variations in the origin and course of the VA and the pattern of dominance in a South Africa population.

1.1.1 Justification for the study

VA injuries remain the most common type of injury during cervical spine surgery (Decarvalho et al., 2018) and the risk of injury as a complication of surgery is a major problem (Yamazaki et al., 2012). The artery is at risk of damage during anterior, posterior, and lateral approaches to cervical spine surgery and during surgical procedures that involve the occipito-atlanto-axial region (Wright and Lauryssen, 1998, Neo et al., 2008), with the presence of variation in its course increasing the likelihood of injury (Lunardini et al., 2014). The intensity and degree of variation depend on age, gender, and the population being sampled. There is a need for a thorough understanding of the complex anatomy of the VA, which will enable the surgeons to know when the artery is at risk of damage during surgery and, if damage occurs, how to deal with it (Schroeder and Hsu, 2013). There are studies on the prevalence of variations in the origin, course, and diameter of the VAs from various countries: Egypt (Abd El Gawad et al., 2019), Bosnia and Herzogovina (Vujmilović et al., 2018), Turkey (Yenigun et al., 2016), USA (O'donnell et al., 2014), Asia (Kornieieva, 2014), Japan (Uchino et al., 2012). However, it appears there is dearth of study on the morphology of the VA among the South African population. Although two South African studies (Mitchell and Mckay, 1995, Mitchell, 2004) have reported on the diameter of the third and fourth segment, both studies are limited in terms of sample size, lack of consideration of major population groups, and non-availability of data on the morphology (origin and course) of the four segments of the VA. Previous studies have shown that there are population differences with regards to the course of the vertebral arteries, and the application of data from one population to another is not encouraged (Jeng et al., 2004). Furthermore, the incidence of some cerebrovascular diseases such as posterior circulation stroke and arterial dissection in different populations may be established by understanding the variations that may occur in the artery (Eftekhar et al., 2006).

1.1.2 Research questions

1. What are the anatomical parameters (viz. origin, course, diameter, and length) of the extracranial part of the vertebral artery among the KwaZulu-Natal population?

2. What are the anatomical parameters (viz. diameter, length, and branches) of the intracranial part of the vertebral artery among the KwaZulu-Natal population?

3. What is the dominant pattern of the artery?

4. What is the clinical implication of the anatomical features present in the above-mentioned part of the vertebral artery?

1.1.3 Aim

This study aims to investigate anatomical features of the extracranial and intracranial components of the vertebral arteries in a South African population. This information is important to describe the prevalence of variations in the origin and course of the vertebral artery and the pattern of dominance in different population groups in KwaZulu-Natal, South Africa.

1.1.4 Objectives

The objectives of this study were:

1. To describe the typical and prevalence of variation in the origin of the VA.
2. To determine the incidence of the VA entering the foramen transversarium of the cervical vertebra (viz. C7, C6, C5, C4, or C3).
3. To evaluate the morphology of the VA (V1-V4) and their dimensions (external diameter and length) at each segment.
4. To describe the morphometry and angles between the proximal and distal loops at the third segment.
5. To determine the pattern of dominance of the VA in a South African population.
6. To compare the parameters of the VA between males and females in a South African population.
7. To determine the angle at the vertebrobasilar junction by measuring the confluence angle where the two arteries join to form the basilar on the 3D reconstructed CT images.

1.2 Literature review

1.2.1 Background

The VA is one of the medium-sized arteries in the body that originates from the subclavian artery and ascends superiorly and posteriorly up the neck to enter the sixth cervical vertebrae (Standring, 2015). It has numerous characteristics such as its smaller diameter in relation to its great length, asymmetry, and the convergence of the two arteries from each side of the neck to form a single basilar artery in the direction of upward flow (Rawal and Jadav, 2012). The VAs and the paired internal carotid arteries are the primary sources of blood supply to the brain (Iqbal, 2013, Standring, 2015).

The VA is well protected by the transverse foramina of the cervical vertebrae along its extracranial course, specifically the second segment and part of the third segment (Shin et al., 2014). However, from its origin to its entry at the sixth cervical vertebra, the artery is unprotected. Therefore, the artery is susceptible to injury during surgical procedures at the root of the neck (Peng et al., 2009).

The origin of the VAs are variable. In addition to typical origin from the subclavian artery, there are reports of the VA arising from the aortic arch, carotid arteries, brachiocephalic trunk, and thyrocervical trunk; thus, the recognition of such variations during head and neck surgery, non-invasive vascular procedures, and supra-aortic arch surgery are important (Matula et al., 1997). The level of entry into the transverse foramen is usually at the sixth cervical vertebrae (C6), although this may vary from the seventh to third cervical vertebrae (C7-C3) (Wakao et al., 2014). Therefore, this parameter should be carefully assessed as it may differ from one side to the other (left and right) in the same individual (Al-Habib et al., 2018). Details and prevalence of anatomical variation at the entry-level are necessary to avoid vertebral artery injury during anterior or posterior cervical spine instrumentation (Cheung and Luk, 2016).

Bilateral VAs are asymmetrical in most individuals, with a reported left dominance in approximately 50% of the population, while similarly sized right and left VAs are present in about 25% (Katsanos et al., 2013b). However, studies from different population groups have shown that this percentage may vary from one population to another (Ergun et al., 2016, Abd El Gawad et al., 2019, Li et al., 2019). Additionally, there is no consensus with regard to the standard definition of hypoplastic VAs.

Researchers have used diameter criteria ranging from less than 2.0 mm to less than 3.0 mm to define vertebral artery hypoplasia (VAH). Preoperative knowledge of hypoplasia of the VA is vital in selecting and moulding catheters during interventional neuroradiological procedures and in mitigating complications of endovascular treatment and improving prognosis of cerebrovascular disease (Chaturvedi et al., 1999).

1.2.2 Embryology of the vertebral artery

Vertebral arteries are formed between the 32nd and 40th gestational days by the development of longitudinal anastomoses between the first six (or seven) cervical intersegmental arteries, that later regress except for the sixth, which becomes the proximal subclavian artery and the point of origin of the adult VA (Luh et al., 1999) (Figure 1.1) [Six cervical intersegmental arteries that form the VAs are primitive branches from the Dorsal Aortae (right and left) and not direct branches of the six pairs of aortic arches. Several of the aortic arches regress. All six pairs are not present simultaneously; they develop and regress at different stages. Six pairs of aortic arches end in the dorsal aorta, which gives off the cervical intersegmental arteries (Bloch and Danziger, 1974)]. Usually, the V1 segment of the VA develops from the proximal part of the dorsal branch of the seventh cervical intersegmental artery proximal to post-costal anastomosis. The V2 segment is derived from longitudinal communications of the post-costal anastomosis with the consequent regression of the stems of the upper six intersegmental arteries. The V3 segment develops from the spinal branch of the first cervical intersegmental artery, while the V4 segment develops from the pre neural division of the spinal branch (Panicker et al., 2002). According to Padget's classification, the first cervical intersegmental artery has been designated the "proatlantal intersegmental artery" because of its course between the occiput and the atlas (Padget, 1948) (Figure 1.1). Luh and colleagues later hypothesized that the horizontal part of the V3 segment of the VA develops from the proatlantal intersegmental artery (Luh et al., 1999). These complex anastomoses of multiple primitive vessels during embryogenesis may result in a variety of anatomical variations. Also, any complication during this developmental phase can result in either morphologic or morphometric variation in the course of the artery. For instance, anatomical variation such as VA duplication is due to the persistence of two segmental arteries (Meila et al., 2012). These variations may influence the development of arterial disease, and the first stage at which variations can occur is during angiogenesis (Menshawi et al., 2015).

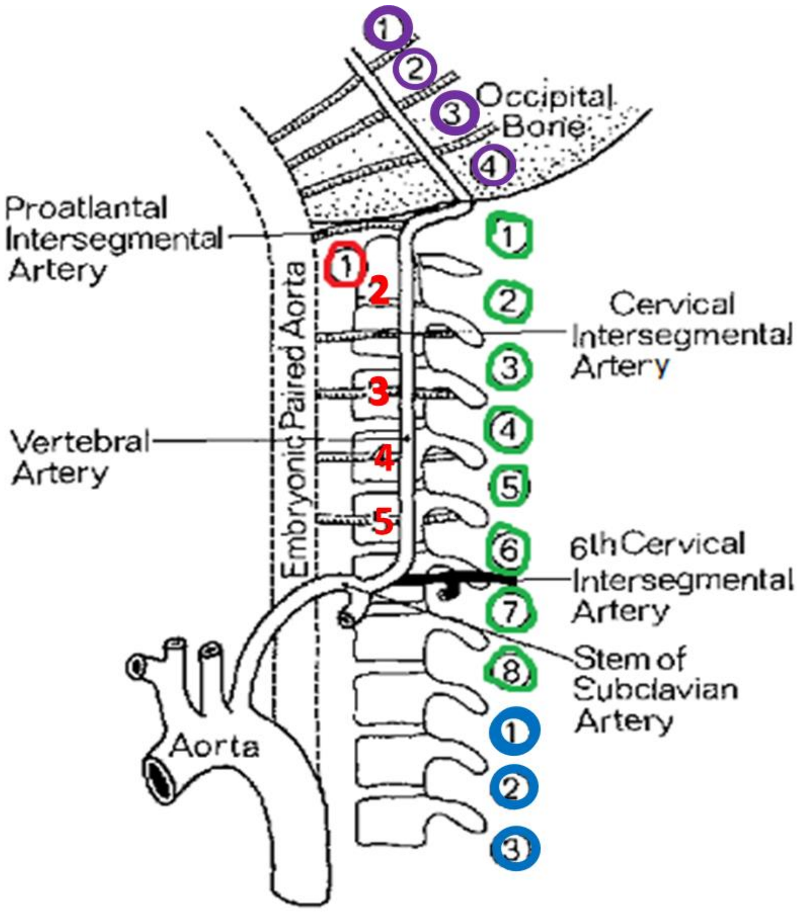

Figure 1.1: Illustration of the development of the vertebral artery. Purple (1-posterior communicating artery, 2-hypoglossal artery, 3-otic artery, 4-trigeminal artery). Red (1-

proatlantal intersegmental artery, 2-5; cervical intersegmental arteries). Green (body of vertebrae). Blue (thoracic vertebrae)

(Adapted from Bloch and Danziger, 1974)

1.2.3 Origin of the vertebral artery

Standard anatomical textbooks describe the VA arising from the superior posterior aspect of the first part of the subclavian artery (George and Laurian, 2012, Standring, 2015, Netter, 2017). It runs superiorly and posterior in the scalenovertebral triangle formed by scalenus anterior and longus colli muscles. The common carotid arteries and the vertebral vein are located anterior to the VAs (Dodevski and Tosovska-Lazarova, 2012). It is crossed on the right by the right lymphatic duct and on the left by the thoracic duct (Bruneau et al., 2006b). Posterior to the first segment of the VA is the stellate ganglion (Figure 1.2), inferior cervical ganglia, and the ventral rami of the sixth and seventh cervical spinal nerves. The VA enters the foramen in the transverse process of the sixth cervical vertebra and then ascends superiorly in the subsequent transverse processes of other cervical vertebrae to the level of the atlas (Figure 1.3) (Clark and Benzel, 2005). The entire length of the VA from the origin to the point where it penetrates the dura mater (to enter the skull) is described as its extracranial component (V1-V3) (Figure 1.3)

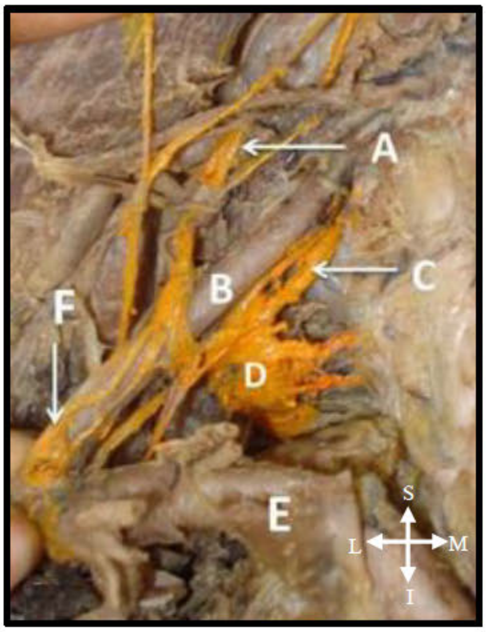

Figure 1.2: The vertebral artery and the stellate ganglion. A- sympathetic chain; B- vertebral artery; C- cervical spinal nerve; D- stellate ganglion; E- subclavian artery; F- ansa subclavia

(Adapted from Raveendran and Kamalamma, 2018)

Key: S- superior; I- inferior; L- lateral; M- medial

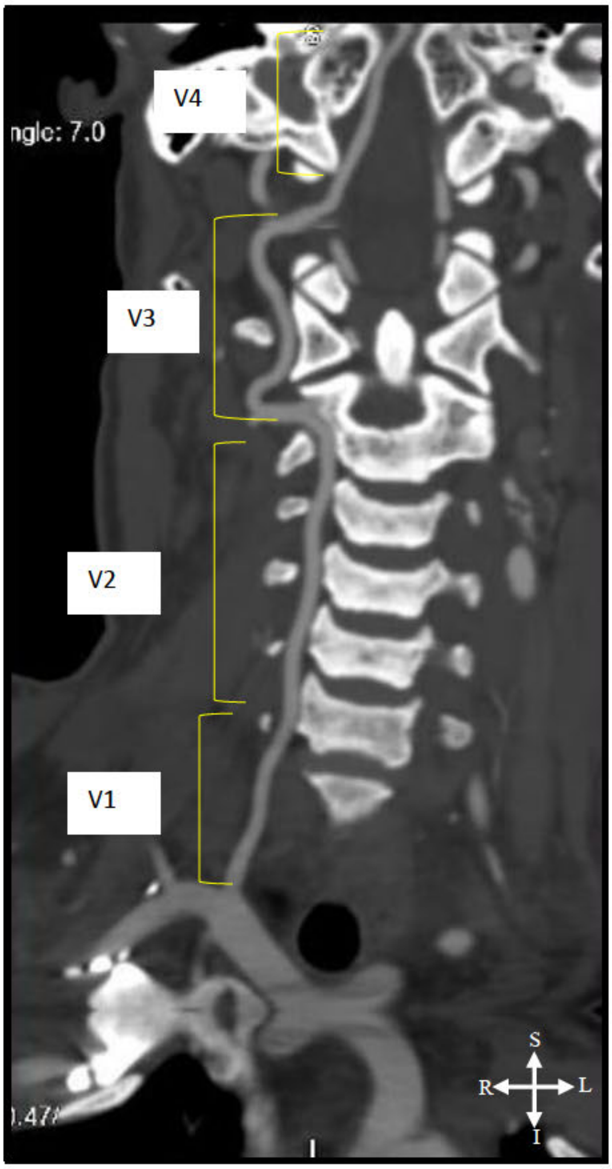

Figure 1.3: Coronal View 3D CTA illustrating the typical course of the entire segments (V1 – V4) of the right vertebral artery

(Image is obtained from Lenmed Ethekwini Hospital and Heart Centre Durban, South Africa)

Key: S- superior; I- inferior; R- right; L- left

From the literature, the VA has been described to vary from its classical origin. It has been reported to originate from the arch of the aorta directly (Komiyama et al., 2001, Panicker et al., 2002, Nayak et al., 2006, Satti et al., 2007, Poonam and Sharma, 2010), from the thyrocervical trunk (Matula et al., 1997, Strub et al., 2006), from the brachiocephalic trunk (Bhatia et al., 2005), from the common carotid artery (Matula et al., 1997, Buckenham and Wright, 2014), and the external carotid artery (Matula et al., 1997, Poonam and Sharma, 2010). This wide range of possible origins results from the complex embryogenesis of the artery (Dodevski and Tosovska-Lazarova, 2012). The prevalence of variant origin is higher on the left than the right and occurs mostly from the aortic arch, with the rate generally reported between 3 and 16% (Table 1). Reports of anomalous origin of the VA are essential because of its clinical significance and surgical implications during endovascular treatment of aortic arch injuries, angioplasty, and stent procedures (Ka-Tak et al., 2007). Preoperative knowledge of anatomical variation will reduce the risk of iatrogenic injury and contribute to the advancement of non-invasive imaging studies. The aortic arch origin of the VA is associated with predilection for arterial dissection (Lazaridis et al., 2018). The incidence of bilateral variation in origin has also been reported (Kim et al., 2009, Hadimani et al., 2013). The VA may have duplicate origins (Cagnie et al., 2006, Ionete and Omojola, 2006, Satti et al., 2007, Uchino et al., 2013), mostly one from the aortic arch and the other from the subclavian artery that have fused (Komiyama et al., 2001) and cases of bilateral aortic arch origin being an unusual anatomic variant (Albayram et al., 2002). Recently, an extremely rare case of triplicate origin of the right VA from the right subclavian artery was reported in a 3-year-old boy (Gailloud, 2019). In duplicate and triplicate origin, the VAs arose from 2 or 3 different sites on the parent artery and later merged in the course of the artery to become a single arterial channel. Some authors agreed that the atypical origin of the VA did not result in clinical symptoms (Lemke et al., 1999, Ka-Tak et al., 2007). However, in some cases, patients with atypical left VA origin may complain of syncope and dizziness (Satti et al., 2007). Anomalous origin of the vertebral arteries may also lead to intracerebral disorders by altering vascular hemodynamics, thereby putting patients at greater risk of arterial dissection, potential atherosclerosis, intracranial aneurysm, and occlusion (Satti et al., 2007, Nasir et al., 2010, Lazaridis et al., 2018).

Table 1.1: Prevalence of variation in origin of the vertebral artery from different population groups

Author	Year	Country	Type of study	Sample size (N)	Sex Male/ Female	Laterality of reported variation	Incidence of reported variation (%)	Variant origin
Tsai et al.,	2007	China	Multidetector CTA	102	-	Left /Right	15.7	AOA, RCCA.
Meila et al.,	2012	Caucasia	CTA	539	13/21	Left/Right	6.3/0.19	AOA
Uchino et al.,	2013	Japan	CTA	2287	132/92	Left/Right	6.0/3.8	AOA and others, RCCA and others
Karacan et al.,	2014	Turkey	CTA	1000	32/21	Left	5.3	AOA
Lale et al.,	2014	Turkey	CTA	881	14/12	Left/Right	2.8/0.1	AOA
Alicioglu et al.,	2015	Turkey	Multidetector CTA	110	-	-	3.6	AOA
Vujmilovic et al.,	2018	Bosnia and Herzogovina	CTA	112(224)	6/5	Left	4.47/0.45	AOA, others
Abd El Gawad et al.,	2019	Egypt	Multidetector CTA	100	-	Left	7.0	AOA

Key: AOA - Arch of aorta, RCCA - Right common carotid artery.

1.2.4 Levels of entry of the vertebral arteries into the transverse foramen

The presence of variation in the origin of the VA can also influence variation in the level of entry into the transverse foramen (Meila et al., 2012, Uchino et al., 2013, Kośla et al., 2014). The typical level of entry of the VAs into the foramen transversarium is at the transverse foramen of the sixth cervical vertebra. However, the atypical entry points into the foramen transversarium may be C7, C5, C4, or C3 (Figure 1.4). In imaging studies, it is mostly reported at the level of the fifth transverse foramen (Vujmilović et al., 2018, Zibis et al., 2018) (Table 2). This relation of the point of entry of the VA is essential during spinal surgeries and transpedicular screw fixation. It is essential to note that variations in the point of entry into the transverse foramen could be missed on non-contrast computed tomography (CT) scans but can be easily detected on contrast-enhanced CT scans or magnetic resonance imaging (MRI) (Dodevski and Tosovska-Lazarova, 2012). When these anatomical variations are suspected on non-contrast CT scans, for instance, in the presence of unusually small or an unfilled foramen, a CT scan or MRI may be mandatory for surgery in the vicinity of the VA (Bruneau et al., 2006c).

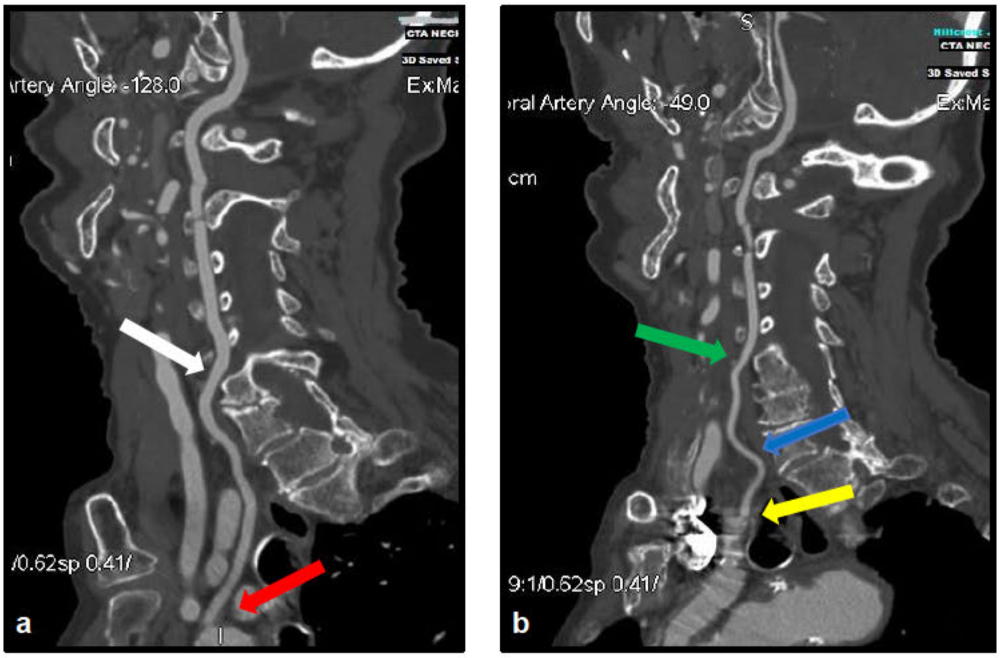

Figure 1.4: Sagittal view 3D CTA illustrating variation in origin and level of entering the transverse foramen. a) The left VA (red arrow) originates directly from the AOA and enters through the transverse foramen of C5 (white arrow). b) The right VA took origin from the right subclavian artery (yellow arrow) and ascends through the transverse foramen of the C4 vertebra (green arrow). The blue arrow shows a single loop at the V1 segment

(Adapted from Omotoso et al., 2021a)

Table 1.2: Prevalence of variation in the level of entering the transverse foramen.

Author	Year	Country	Type of study	Sample Size	Entrance into the transverse foramen [Left/Right (%)]				
					C3	C4	C5	C6	C7
Uchino et al.,	2013	Japan	CTA	2287	0.04	1.1	4.4	93.8	0.6
Alicioglu et al.,	2015	Turkey	Multidetector CTA	110	-	1.8	5.4	92	-
Vujmilovic et al.,	2018	Bosnia and Herzogovina	CTA	112	-	3.12	8.93	87.5	0.45
Zibis et al.,	2018	Greece	CTA	50	-	2	8	-	4
Abd El Gawad et al.,	2019	Egypt	Multidetector CTA	100	-	1/1	4/5	91/93	2/1

1.2.5 Course of vertebral artery

This section describes the typical course and anatomical variation associated with each segment of the VA. The VA has both extracranial and intracranial components (George and Laurian, 2012). The artery is segmented into four parts. The first part is the pre-vertebral (V1) segment, which is that part of the artery from its origin at the subclavian artery to the point of entering the transverse foramen of the sixth cervical vertebra (Bruneau et al., 2006a) (Figure 1.5). This part courses posteriorly between the longus colli muscle medially and scalenus anterior muscle laterally. The second part of the artery is the vertebral segment (V2) and extends from the transverse foramina of the sixth to the second cervical vertebrae (Bruneau et al., 2006c). The third part, the suboccipital or atlanto-axial (V3) segment, extends from the transverse process of the axis (C2), curves laterally to pass through the transverse foramen of the atlas (C1), and courses in the vertebral artery groove (An and Simpson, 1994). This part ends at the dura mater before passing through the foramen magnum (Bruneau et al., 2006a). At this point, the VA pierces the dura and arachnoid as it passes supero-medially to continue as the fourth part known as the intracranial segment (V4). The fourth segment passes anterior to the root of the hypoglossal nerve and converges with the contralateral VA to form the basilar artery at the lower border of the pons (Standring, 2015) (Figure 1.3). This segmentation and mobility of the bone structures at the V3 segment supports preservation of the vascular supply during neck movement or rotation (Bruneau et al., 2006a).

The V1 segment is the most proximal part of the artery and is prone to atherosclerotic changes, especially at its origin (Nouh et al., 2014). Details of the course of the V1 segment, including the point of entry into the transverse foramen, are required for anterior approach to the cervical spine (Eskander et al., 2010). This is to prevent catastrophic laceration of the VA during surgical procedures in the lower region of the neck (Sastry and Manjunath, 2006). Previously reported anatomical variation associated with the V1 segment includes variation in origin and tortuosity (including medial, lateral, and mild loops). According to a study by Matula and co-authors using cadaveric and angiographic samples, the course of the V1 segment is tortuous in 39 % of cases (Matula et al., 1997).

The rate of injury to the VA at the V2 segment during cervical spine surgery was estimated to be between 0.22–2.77 %. This is partially due to its variable course while running in the transverse foramina of the cervical vertebrae (Güvençer et al., 2006). The midline migration associated with an atypical course of the VA within the transverse foramen can predispose the VA to direct risk of injury during corpectomy (Eskander et al., 2010). Some authors have also described a rare course of the VA located at the back of the nerve root in the inter-transverse space (Nourbakhsh et al., 2015). This morphologic variation can interfere with Cervical Transforaminal Epidural Steroid Injections (CTESI), which is part of the treatment employed for painful cervical radiculopathy as the typical path of the VA through this segment is anterior to the target zone. Similar to the V1 segment, reports on fenestration are also rare (Wang et al., 2020). Knowledge of anatomical variation of the V2 segment involving the transverse process of the axis (C2) and the dural part of the V3 segment is important for procedures targeting the 3rd occipital nerve and lateral atlantoaxial joint (C1/C2 joint) (Zibis et al., 2018).

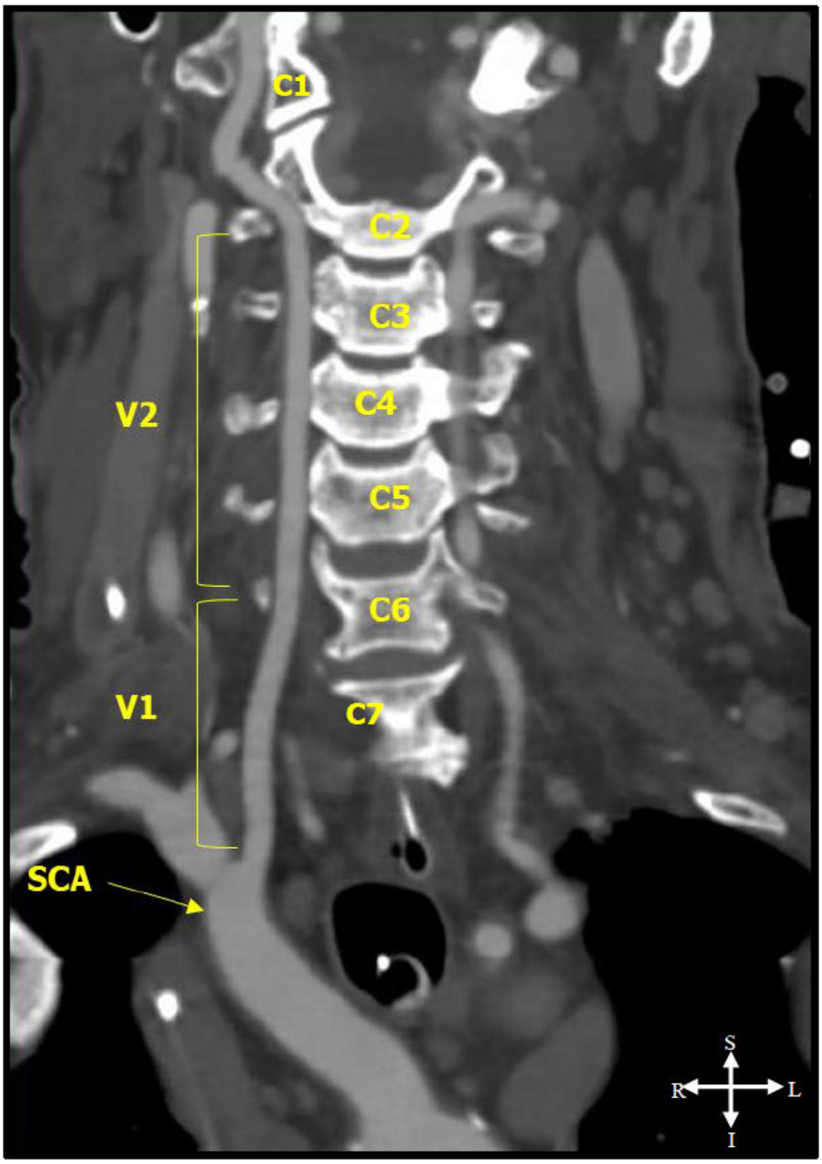

Figure 1.5: Coronal View 3D CTA illustrating the typical course of the V1 and V2 segments of the right vertebral artery. SCA- subclavian artery; C1-C7- cervical vertebrae

(Image is obtained from Lenmed Ethekwini Hospital and Heart Centre Durban, South Africa)

Key: S- superior; I- inferior; L- left; R- right

The V3 segment is also known as the suboccipital part, and it is located at the craniovertebral junction (Figure 1.6, 1.7). According to some authors, it is the anatomically complicated part of the VA as this part of the artery undergoes a series of bends to form a proximal and a distal loop while passing through the transverse foramen of the C2 and C1 vertebrae (Wakao et al., 2014). The proximal loop may descend toward the C2/C3 joint, thereby exposing the VA to possible injury during blocks or radiofrequency ablation performed at these levels (Zibis et al., 2018). The suboccipital segment lies near C2/C3 and C1/C2 zygapophyseal joints, which are often targeted during the treatment of cervicogenic headaches. Regarding pathology, the loops may also increase resistance to blood flow, which can later predispose the segment to atherosclerosis, thrombosis, and wall calcification (Alfaouri-Kornieieva and Al-Hadidi, 2014). These pathologies could consequently predispose the V3 segment to sudden dissection (Alfaouri-Kornieieva and Al-Hadidi, 2014). Natural tortuosity at this segment should prevent distortion. However, some authors agree that the portion of the VA most vulnerable to distortion is the part between the C2 and C1, where most cervical spine rotation takes place (Mitchell and Mckay, 1995, Park et al., 2007, Alfaouri-Kornieieva and Al-Hadidi, 2014). Anatomical variations associated with this segment include persistent FIA (first intersegmental artery), extradural origin of the PICA, and most cases of fenestration are also reported at this segment.

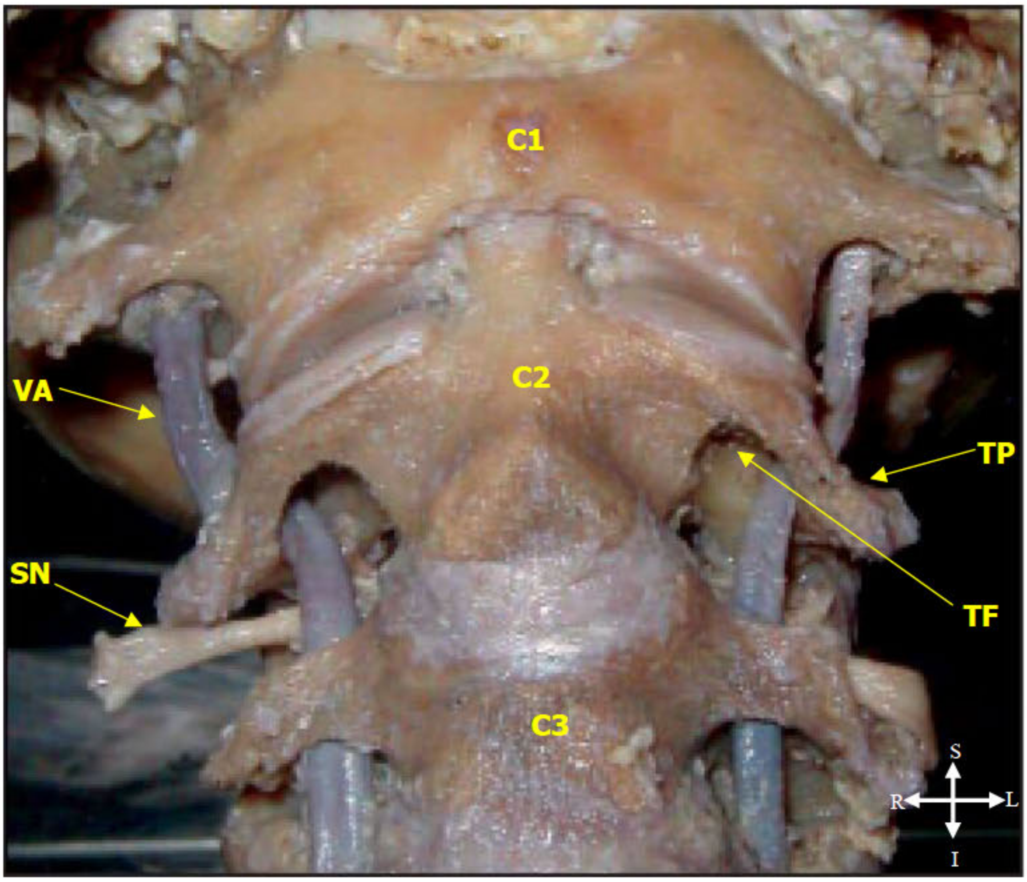

Figure 1.6: Anterior view of upper cervical region depicting the V3 segment of the vertebral arteries. VA- vertebral artery; C1- atlas; C2- axis; C3- 3rd cervical vertebra; TP- transverse process of C2; SN- spinal nerve; TF- transverse foramen

(Adapted from Cacciola et al., 2004)

Key: S- superior; I- inferior; L- left; R- right

The intracranial segment (V4) of the VA is the unique part of the artery at which the two VAs join to form a single vascular channel, viz. the basilar trunk (Figure 1.7). Consequently, the geometry of the basilar trunk depends on the pattern of the bilateral VAs. When the bilateral VAs are asymmetrical, the basilar trunk bends away from the midline (Li et al., 2019). This deviation of the basilar trunk may cause compression of the cranial nerves (Pekcevik and Pekcevik, 2014). The causal link between the vertebrobasilar junction's geometry and the occurrence of an aneurysm is yet to be established (Dzierzanowski et al., 2017). However, it is also essential to consider the geometry of the vertebrobasilar junction while planning for surgical interventions in this region. This region is of particular interest to neurosurgeons and radiologists due to various interventional neuroradiological procedures conducted in the area to treat vascular diseases such as arterial dissections, aneurysms, arteriovenous malformations, dural fistula, or repair of an occlusive disease (Mercier et al., 2008). For instance, the shape can influence the choice of surgical approach for aneurysm clipping in this region (Dzierzanowski et al., 2017). A few international studies have reported the average angle at the vertebrobasilar junction (Songur et al., 2008, Dzierzanowski et al., 2017). Other anatomical variations at this segment include fenestration, atresia, and hypoplasia.

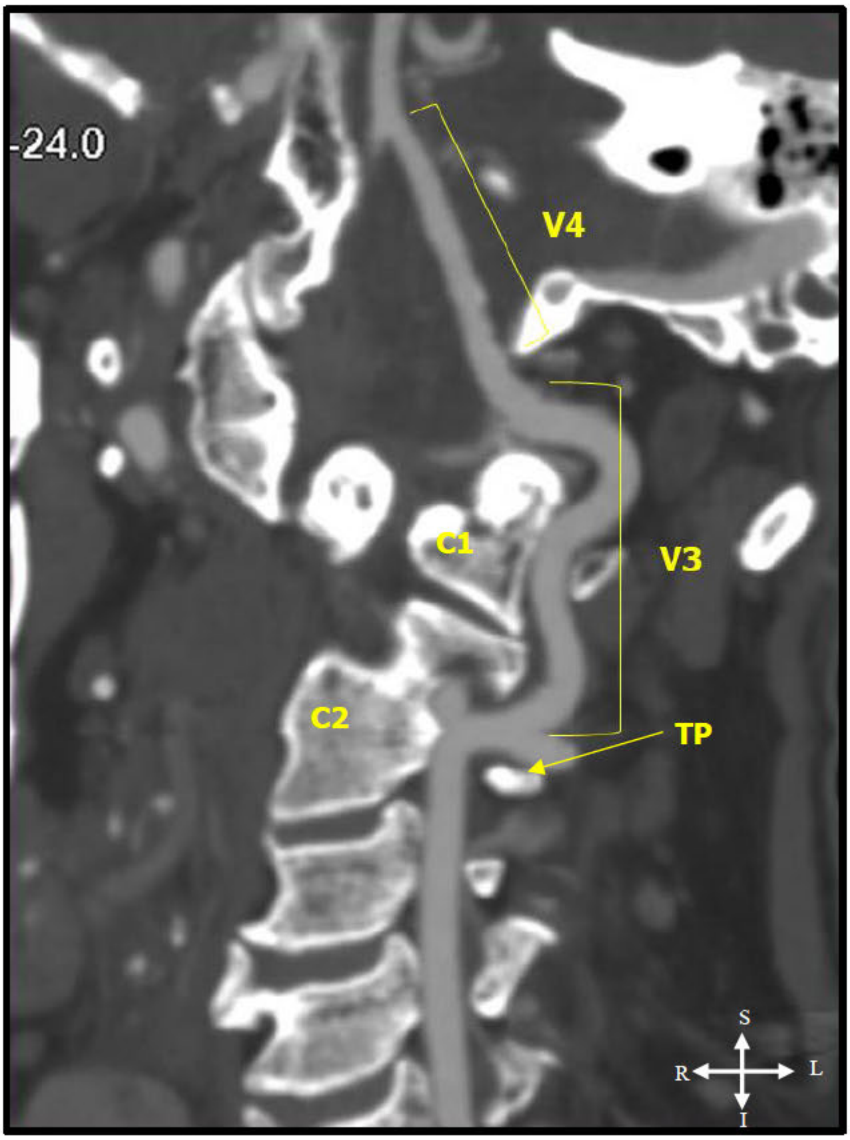

Figure 1.7: Oblique view 3D CTA illustrating the typical course of the V3 and V4 segments of the left vertebral artery. C1, atlas; C2, axis; TP, transverse process of C2

(Image is obtained from Lenmed Ethekwini Hospital and Heart Centre Durban, South Africa)

Key: S- superior; I- inferior; L- left; R- right

Prevalence of anatomical variations of the intracranial VA has been previously reported in a Western population (Caucasians) (Dzierzanowski et al., 2017), Asian population (Liu et al., 2017), and Turkish population (Songur et al., 2008). In the African continent, Ogeng'o et al. (2014) reported VA hypoplasia in a Black Kenyan population using post-mortem histological samples (Ogeng'o et al., 2014). Similar to the latter, a previous study of a South African population reported on average diameter using histological samples (Mitchell and Mckay, 1995, Mitchell, 2004). Adequate knowledge of variation in morphology and morphometry is clinically relevant in diagnosis and surgical intervention, including neurosurgery, facial surgery, and otolaryngology (Dzierzanowski et al., 2017).

Incomplete knowledge of anatomy during surgical procedures can lead to severe complications (Sikkal and Jain, 2012). Complications such as accidental breach of the VA after lower cervical procedures like stellate ganglion block and C5 to C7 transforaminal injections (Rathmell et al., 2004) as well as the ones targeting upper cervical segments (for example, C1/C2 intra-articular facet injections) can result in significant morbidity (Rathmell et al., 2004, Edlow et al., 2010). For this reason, it is necessary to describe the prevalence of anatomical variations at each of the segments of the VA and their clinical significance.

Vertebral Artery Tortuosity

The VA course is typically straight except for the V3 segment. However, the VA course can be tortuous, leading to a significant and potentially dangerous medial or lateral artery displacement (Figure 1.8). VA tortuosity (or loop formation) has been described as a congenital or acquired anomaly. However, it is challenging to assess the suggested genetic origin since vascular tortuosity increases with age (Matula et al., 1997, Curylo et al., 2000, Elgueta et al., 2018). According to other researchers, the mechanism of formation of tortuous vessels is not clear (Kim et al., 2010, Han, 2012). Sakaida et al. (2001) hypothesized that loop formation developed due to VA elongation caused by narrowing of the disc space (Sakaida et al., 2001). Some authors suggested reduced elasticity, degeneration of blood vessels, and vascular wall shear stress as a possible cause (Han, 2012, Lee et al., 2012). Another study suggested vascular risk factors such as hypertension, diabetes, and lipid metabolism disorders. These factors can promote atherosclerosis, aging, and degeneration of blood vessels, thereby aggravating vertebrobasilar artery tortuosity (Ikeda et al., 2010).

The prevalence of tortuosity ranges between 1% –78.3% (Table 3). It is commonly reported at the V1, followed by the V2 segment, and rarely reported at the intracranial part of the artery (Table 3). Naturally, the VA demonstrates a serpentine course while passing through the transverse process of the C2 and C1 at the V3 segment. This segment has been reported to be straight only in patients with atlantoaxial dislocation (Sardhara et al., 2015). From the origin to the point of entry into the foramen transversarium, the VA may show different levels of tortuosity (Matula et al., 1997, Curylo et al., 2000, Dodevski and Tosovska-Lazarova, 2012). The VA can also exhibit a tortuous path during its course through the transverse foramina at the V2 segment, as previously reported in cadaveric and angiographic studies (Cagnie et al., 2006, Alicioglu et al., 2015).

VA tortuosity has been diagnosed in association with various neurovascular problems. Recent findings suggested that vertebrobasilar tortuosity, combined with cerebrovascular risk factors like hypertension and diabetes, may lead to vascular vertigo (Hong-Tao et al., 2014). Paksoy et al., (2003) examined 173 patients with cervicobrachial pain and diagnosed 13 of them with VA loop formation. The authors concluded that the incidence of VA loop formation should be suspected in patients with cervicobrachialgic symptoms (Paksoy et al., 2003). Doweida et al., (2014), in their report, described VA loop formation as an uncommon cause of nerve root compression (Doweidar et al., 2014). According to a report on stroke patients, the coexistence of tortuosity with hypoplasia has been identified as a risk factor for posterior circulatory stroke (Bentsen et al., 2014). In addition to the suspected clinical sequelae, the formation of loops at the V2 segment may erode bony structures such as the uncinate process, transverse process, and the vertebral body (Hong et al., 2008, Kiresi et al., 2009, Alicioglu et al., 2015), or widening of the intervertebral foramen (Kim et al., 2010). Erosion of these bony structures may complicate cervical instrumentation surgery, especially in older patients (Curylo et al., 2000).

In contrast, some investigators have suggested that VA tortuosity is asymptomatic and does not have any hemodynamic consequences. These researchers further stated that the presence of tortuosity might go undetected because of the lack of symptoms and sometimes incidentally diagnosed during evaluation of neck problems and trauma (Matula et al., 1997, Chibbaro et al., 2012). Therefore, it is essential to report the prevalence of this morphological variation, which could significantly contribute to diagnosis of pathologies and safety of surgical procedures in the vicinity of the VA.

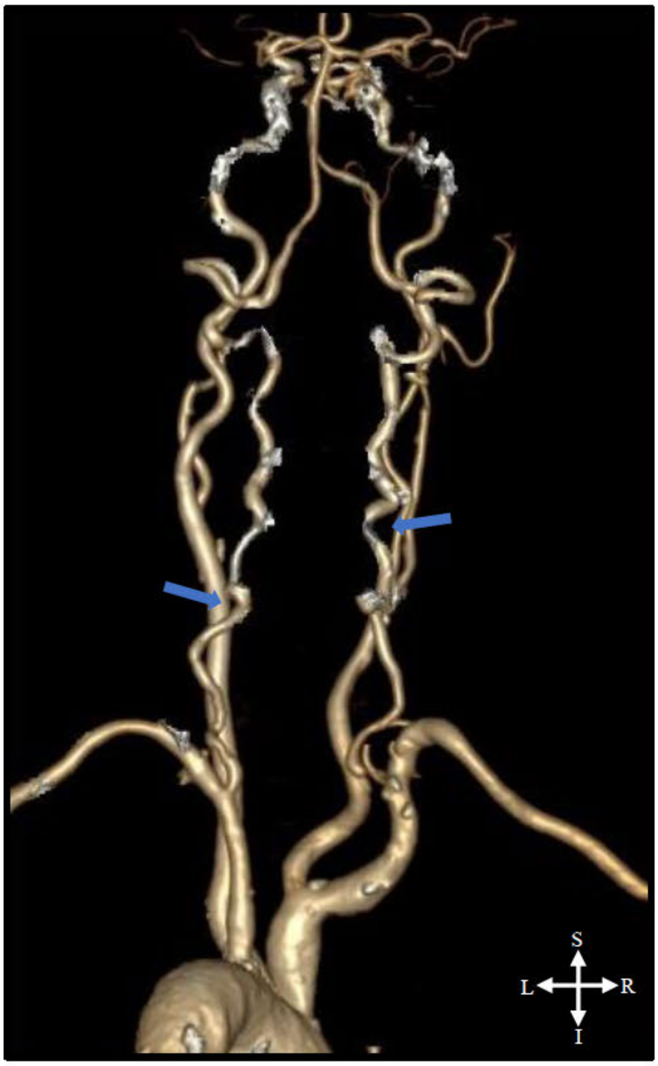

Figure 1.8: Posterior view 3D reconstructed image illustrating multilevel tortuosity in the V1-V2 segment of the bilateral vertebral artery (blue arrows)

(Image is obtained from Lenmed Ethekwini Hospital and Heart Centre Durban, South Africa)

Key: S- superior; I- inferior; L- left; R- right

Table 1.3: Incidence of vertebral artery tortuosity in different population groups

Author	Year	Country	Type of study	Sample Size	Sex Male/ Female	Segment of VA Cervical level	Incidence (%)
Paksoy et al.,	2003	Turkey	MRI	173	4/9	V1	7.51
Bruneau et al.,	2006	France/ Belgium	MRI	250	-	V2	2
Ono et al.,	2009	Brazil	MRI (Case report)	-	F	V2	-
Hong-tao et al.,	2014	China	MRA (Case report)	2	1/1	V2, V4	-
Alicioglu et al.,	2015	Turkey	CTA	110	10/5	V2	13.6
Wakao et al.,	2016	Japan	CTA	1054	4/6	V2	1
Yenigun et al.,	2016	Turkey	MRA	37	-	V1, V2	78.3, 21.6

Key: F-female

Vertebral Artery Hypoplasia and Dominance

A condition when the width of the VA is reduced below specific values, or a significant reduction in the width of a unilateral VA compared to the contralateral artery, is defined as vertebral artery hypoplasia (VAH) (Figure 1.9). VAH is a frequent anatomical variation with underemphasized clinical significance and an ambiguous cut-off value (Gaigalaite et al., 2016). Vertebral artery hypoplasia has been reported in about 10% of normal individuals (Hu et al., 2013). Authors have used criteria ranging from less than 2.0 mm to less than 3.0 mm to define VAH. Some authors classified VAH as a vessel with a diameter less than or equal to 2.0 mm (Thierfelder et al., 2014), others used criteria less than or equal to 2.5 mm (Chen et al., 2010, Szárazová et al., 2012) while a recent report used the criterion of less than 3.0 mm (Gaigalaite et al., 2016). Other specifications for diagnosing VAH is a significant decrease in flow volume (Chen et al., 2010) or a caliber disparity greater than or equal to 1:1.7 between the right and left VAs (Zhou et al., 2015). The discrepancies in cut-off value may be due to differences in the modality of studies, demographic and racial differences in the population group and the segment of the artery studied. Gaigalaite and co-authors (2016) reported a strong correlation between the diameter of the VA and anthropometric parameters such as height; these can also contribute to the differences reported in the literature. The range of diameter in different study groups will inform the choice of appropriate cut-off values for the definition of hypoplasia, the reason why the value cannot be generalized. Emerging evidence from prospective studies has shown that VAH predisposes to ischemic events in the posterior circulatory territory (Katsanos et al., 2013a) and spontaneous VA dissection (Zhou et al., 2015).

VA dominance (VAD) is a congenital structural variation of the VA characterized by a significant difference in diameter between bilateral VAs of the same individual. The prominent VA is now described as dominant. Until recently, VAD was previously described as a mere structural variation without clinical relevance. Researchers now identify VAD as a risk factor for posterior circulation infarction, brainstem infarction, and transient ischemic attack (Zhu et al., 2016, Meng et al., 2018). Similar to VAH, the cut-off value of vertebral artery dominance (VAD) is debatable. Scholars have adopted numerous criteria for the definition of VAD in the literature, and currently, there is no agreement on the standard criteria. The selected criterion for the definition of dominancy may depend on the average diameter in the studied group. Authors have used a size difference of ≥ 0.3 mm (Ngo et al., 2020), a size difference of ≥ 1.2 mm (Zhu et al., 2016), and criteria of any size difference between the bilateral VAs (Ozdemir et al., 2002). In addition to the associated pathologies, it may be essential to protect the dominant VA during surgical interventions and endovascular procedures. Iatrogenic injury to the dominant VA may increase the risk of vertebrobasilar insufficiency, brainstem ischemia and can even result in death (Sardhara et al., 2015, Guan et al., 2017).

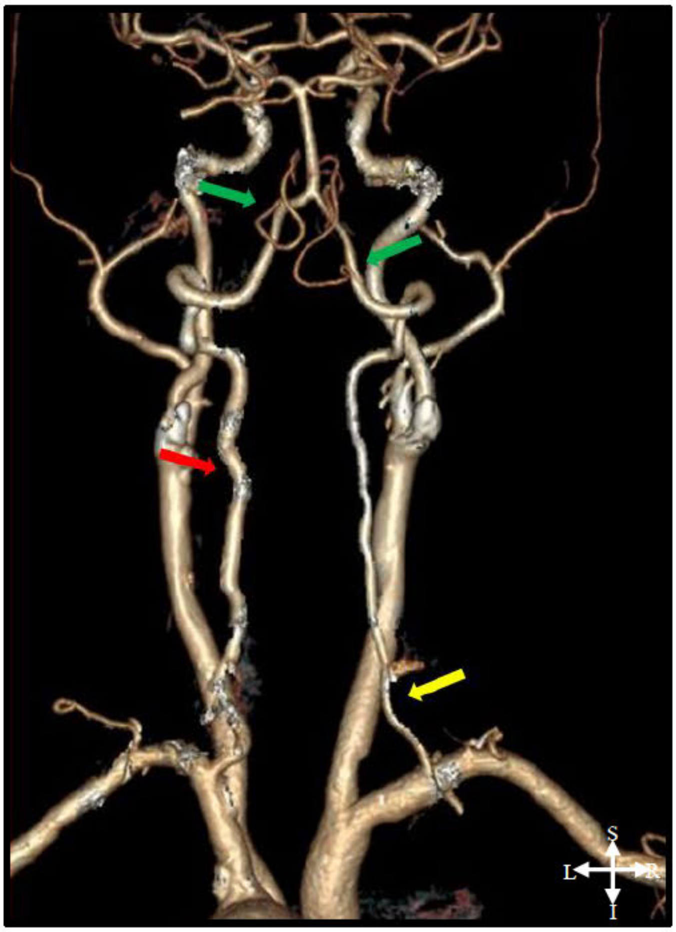

Figure 1.9: Posterior view 3D reconstructed image illustrating the bilateral vertebral artery and the posterior inferior cerebellar artery. The red arrow shows dominant left VA; the yellow arrow shows hypoplastic right VA while the green arrows show bilateral PICA

(Image is obtained from Lenmed Ethekwini Hospital and Heart Centre Durban, South Africa)

Key: S- superior; I- inferior; L- left; R- right

Vertebral Artery Atresia

An atretic VA is defined as a VA of small calibre that does not anastomose with the contralateral VA to form the basilar trunk but rather terminates as the PICA (George et al., 2013) (Figure 1.10). However, a recent report has shown that an atretic VA may not necessarily be hypoplastic, although the diameter may be smaller than the contralateral VA (Liu et al., 2017). The reported prevalence of VA atresia ranged between 1.0 to 9% (Lister et al., 1982, Kovač et al., 2014, Ohkura et al., 2014, Liu et al., 2017). In this morphological variation, the contralateral VA solely proceeds to form the basilar artery. Because there is no connection between the right and left VAs, compression, or occlusion of one of these arteries can lead to ischemia of the cerebellum or lateral medulla due to reduced blood flow in the vertebrobasilar system (Kovač et al., 2014). Furthermore, VA atresia has been previously linked to rotational vertebral artery syndrome (RVAS) (Noh et al., 2011) and Bow Hunter's Syndrome (Yeh et al., 2005, Miao et al., 2020), which may result from compression of this variant vessel.

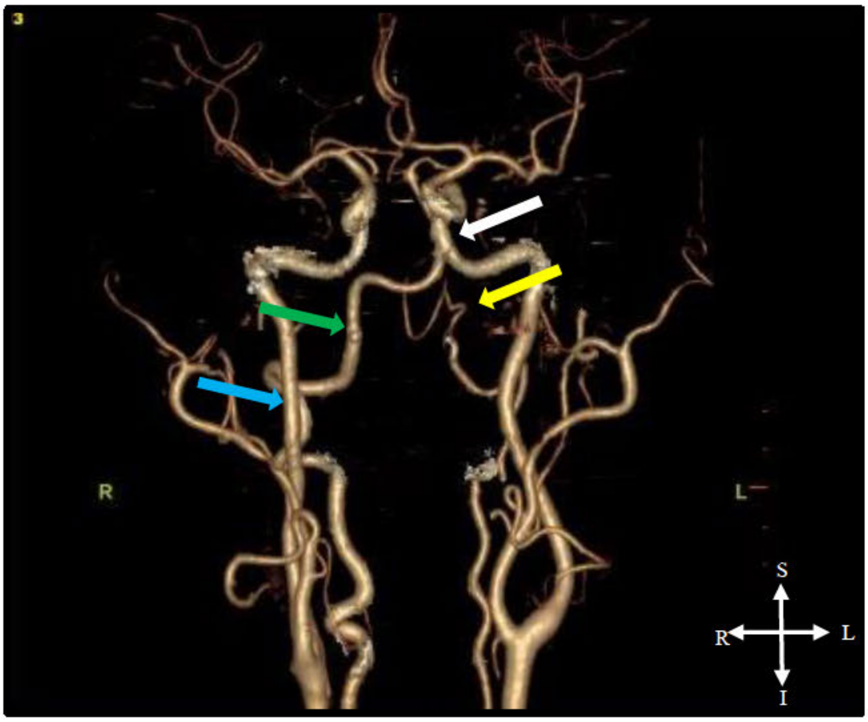

Figure 1.10: Anterior view 3D reconstructed image illustrating the bilateral vertebral artery. The yellow arrow illustrated left vertebral artery atresia. The white arrow illustrated the left internal carotid artery. The green arrow illustrated the right vertebral artery. The blue arrow illustrated the right internal carotid artery

(Image is obtained from Lenmed Ethekwini Hospital and Heart Centre Durban, South Africa)

Key: S- superior; I- inferior; L- left; R- right

Fenestration

Fenestration is an uncommon congenital morphological variation that involves a luminal division of an artery that has a common origin into two separate and parallel channels anywhere along its course to reunite distally (Omotoso et al., 2021b) (Figure 1.11). The prevalence of fenestration ranges between 0.01 to 1.0% (Table 4). According to some authors, fenestration of the VA is an incidental finding on imaging and has no pathological and clinical importance (Tetiker et al., 2014). However, a recent case report hypothesized that fenestration could sometimes be associated with an aneurysm or arteriovenous malformations (Wang et al., 2020). Another case report also suggested the possibility of compromised blood flow at the proximal and distal end of the fenestrated segment of the VA, which may result in transient ischemic attacks (Omotoso et al., 2021b). It is commonly reported at the extracranial segments of the VA, most commonly at the V3 segment, with few reports on prevalence at the intracranial segment (Table 4); and rarely occurring at the V1 segment (Wang et al., 2020). The incidence of multiple concomitant fenestrations involving more than one segment of the VA has also been reported (Wang et al., 2020). Fenestration has been used interchangeably with duplication in the literature. However, it is worth noting that the two anatomical terms describe different morphological variations and should be clarified. Duplication typically involves double vascular origin, which later fuses in the course of the artery (Ionete and Omojola, 2006), while fenestration involves a luminal division of an artery with a single origin.

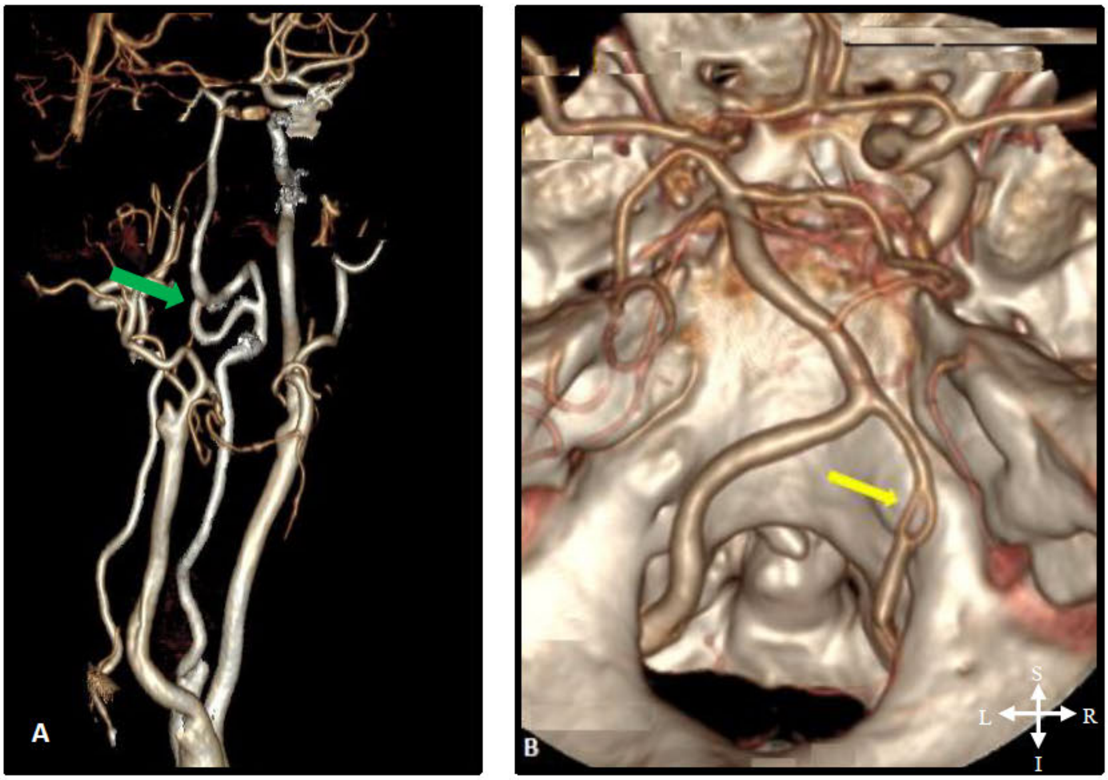

Figure 1.11: Anteroposterior (A) and posterior (B) view 3D reconstructed image illustrating the bilateral vertebral artery. A) The green arrow shows fenestration at the V3 segment of the left vertebral artery. B) The yellow arrow shows fenestration of the right intracranial vertebral artery

(Images are obtained from Lenmed Ethekwini Hospital and Heart Centre Durban, South Africa)

Key: S- superior; I- inferior; L- left; R- right

Table 1.4: Prevalence of fenestration in different population groups

Author	Year	Country	Type of study	Sample size	Number of cases	Laterality of reported variation (Left/Right)	Segment of VA
Tokuda et al.,	1985	Japan	DSA	300	3(1.0)	0/3	V3
Uchino et al.,	2012	Japan	MRA	2739	25(0.9%)	10/15	V3
O'Donnel et al.,	2014	US	CTA	975	1(0.01%)	-	V3
Wakao et al.,	2014	Japan	CTA	387	5(1.3%)	2/3	V3
Kim et al.,	2016	South Korea	CTA	3067 546 314	7(0.2) 2(0.4) 2(0.6)	2/5 - -	V4 V3 V3
Vaněk et al.,	2016	Czech Republic	CTA	511	1(0.2)	1/0	V3
Dzierzanowski et al.,	2017	Poland	CTA, DSA	100	2 (2%)	1/1	V4
Fortuniak et al.,	2019	Caucasian	CTA	1800	3(0.16%)	-	V3

Persistent First Intersegmental Artery

An atypical intradural course of the V3 segment of the VA through the spinal canal between the vertebral body of C2 and C1 (Figure 1.12) has been previously defined with different terminologies such as; an "aberrant VA coursing intradurally at the C2 level" (Kim, 2016), and "persistent first intersegmental artery (FIA)" (Uchino et al., 2012, Fortuniak et al., 2016), with the latter term being the most frequently used. The prevalence of this variation ranges between 0.01% and 3.2% (Uchino et al., 2012, O'donnell et al., 2014, Arslan et al., 2019). This variation can be present without any clinical symptoms and can sometimes be symptomatic when it coexists with a disease condition or vascular variations such as arteriosclerotic dilatation and tortuosity (Kim, 2018). Bilateral persistent FIAs have been previously reported to cause cervical cord myelopathy due to vascular compression when it coexists with other osseous anomalies at the CVJ (Takahashi et al., 2003). Persistent FIA has also been associated with clinical presentations such as cervical pain, occipital neuralgia, and accessory nerve palsy (Takahashi et al., 2003). Several embryological bases have been proposed for this type of variation. According to Uchino and co-authors (2012), when the first intersegmental artery persists without sufficient development of the typical VA branch during embryogenesis, the VA takes a variant course that enters the spinal canal between the C1 and C2 vertebral bodies (Uchino et al., 2012). Some researchers suggested that the intradural course of the distal VA at the C2 level is related to variations in size and connection of the lateral spinal artery (LSA) (Lasjaunias et al., 1985) or posterior spinal artery (PSA) (Siclari et al., 2007). The simultaneous persistence of the FIA and the typical branch of the VA results in fenestration at the V3 segment of the artery (Uchino et al., 2012). Both unilateral and bilateral persistent FIA can be easily overlooked (Uchino et al., 2012). An awareness of this variant anatomy and careful review of images will assist in proper identification to prevent VA injury.

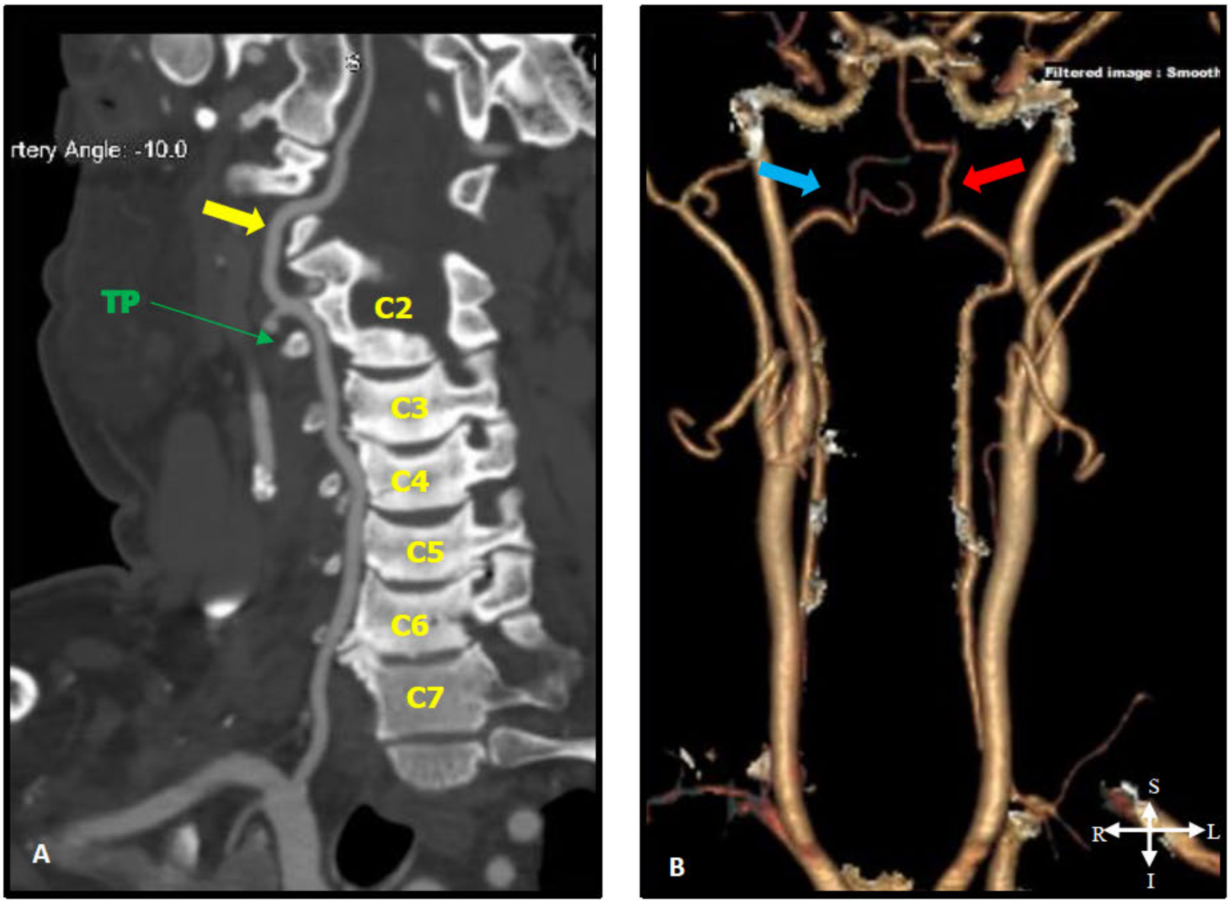

Figure 1.12: Coronal (A) and anterior (B) view 3D reconstructed image showing the bilateral vertebral artery. A) Yellow arrow shows persistent first intersegmental artery of the right vertebral artery. C2- axis; C3-C6 cervical vertebrae, TP-Transverse process of C2. B) Blue and the red arrow shows bilateral persistent first intersegmental artery

(Images are obtained from Lenmed Ethekwini Hospital and Heart Centre Durban, South Africa)

Key: S- superior; I- inferior; L- left; R- right

1.2.6 Branches of the vertebral artery

The VA branching pattern seems to be complex, which might increase the risk of surgical complications, especially if radicular or medullary branches are compromised, which might result in spinal cord ischemia (George and Laurian, 2012). In the neck region, the VA gives off small branches, which are rarely seen on angiograms. These are the spinal branches, the muscular branches (not always present, also known as the suboccipital artery of Salmon), and the cranial branches within the skull. The spinal branches and the muscular branches provide blood supply the spinal cord, posterior neck muscles, and bones of the cervical region (Tubbs et al., 2009). The cranial branches include the meningeal branch, posterior spinal artery, anterior spinal artery, small branches to the medulla oblongata, and the PICA.

The PICA is the largest branch of the VA (De Oliveira et al., 1985). It is the most variable of the cerebellar arteries and is occasionally absent (Ryan et al., 2011). It has a tortuous course, passing posteriorly and ascending at the lower border of the pons. It then courses inferolaterally around the fourth ventricle to reach the inferior surface of the cerebellum in the midline. The PICA terminates as the medial branch (inferior vermian artery) to the inferior vermis. Classically, the PICA arises from the intracranial part of the VA (4^{th} segment). However, the incidence of PICA arising from the third segment of the VA has also been reported (Miao et al., 2020). It is important to note that no perforating arteries emerge from the PICA of extradural origin (PICA arising from V3 segment). Instead, the medullary perforators originate from the intracranial VAs (Mercier et al., 2008).

1.3 Materials and methods

1.3.1 Computed Tomography Angiography

Computed tomography angiography (CTA) is a unique non-invasive imaging technique that can demonstrate the vascular anatomy, together with bones. It is commonly used in evaluating cerebral arteries for diagnoses of vascular pathology. Recent advances in multidetector CTA have shown that vascular structures can easily be depicted, which has caused some level of reduction in the use of invasive examinations such as digital subtraction angiography (DSA) (Akgun et al., 2013). Although DSA remains the gold standard procedure in assessing the vascular system, it is an invasive technique with potential complications (Akgun et al., 2013). CTA is also occasionally used as a complementary imaging technique to conventional angiography for follow-up (Chen et al., 2004). In addition, studies have shown that CTA allows reliable evaluation of intracranial arterial pathology, including aneurysm, stenosis, and occlusion (Kovač et al., 2014). Post-processed images in the 3D workstation of CTA and the raw images provide better details and opportunities for detailed description of the presence of anatomical variation (Wakao et al., 2014). However, CTA is not without its own risk. The disadvantage of the technique is ionizing radiation and iodinated contrast media, which has potential nephrotoxic effects, especially in patients with chronic kidney disease (Akgun et al., 2013, O'donnell et al., 2014).

1.3.2 Imaging Techniques

The imaging examination was performed on a 64-detector row 160-slice helical multidetector computed tomography scanner (Lightspeed CT, GE Healthcare Medical Systems, Milwaukee, WI, USA). In our standard MDCTA protocol for brain examinations, a scan coverage area from the aortic arch to the top of the brain in a supine position (headfirst) was adopted as a field of view (FOV). The scanning protocol was as follows: 120 kVp, 500 mAs, beam collimation 64 × 0.625 mm, speed 20.62mm/rotation, gantry rotation time 0.35s/rotation, the helical thickness of 0.625 mm, pitch 0.516:1, and reconstruction interval of 0.625 mm. Following the acquisition of the nonenhanced CT data, contrast-enhanced MDCTA was performed. During the procedure, a 20 Gauge needle (Pink Nexiva) was used to cannulate patients for IV access in the antecubital region to administer 60 mL of Ioversol (Optiray 350; Guerbet South Africa). This was followed by a 40 mL saline flush via a double power injector (Medex flowSens, Guerbet USA) into the patient's antecubital vein (4 mL/s), and the scan delay was individually adapted using a bolus-tracking technique. First, a single nonenhanced low-dose scan at the upper neck level was obtained for the bolus tracking. Then, repeated low-dose monitoring scans were obtained every second with the start of contrast material administration. Following the appearance of the first contrast in the aortic arch, the MDCTA was triggered automatically without delay. The region of interest was positioned at the aortic arch, and the threshold for the MDCTA was set as 150 Hounsfield Units. When the threshold was surpassed, helical scanning was automatically initiated.

1.3.3 Imaging Reconstruction

Postprocessing of three-dimensional images was performed using multiplanar reformation (MPR), maximum-intensity projection (MIP), multiplanar reconstruction (MPR), and 3D volume-rendering (VR) algorithms. The volumetric MDCTA data sets were processed on Advanced Workstation 4.2 (GE Healthcare, Milwaukee, WI, USA). A series of 17 projection images at every 20º around the cephalocaudal axis were generated and transfer to the PACS. The MDCTAs were performed for diagnostic purposes in the context of various cerebrovascular diseases or accidents. In some cases, the suspected diseases were not found on the MDCTA; thus, some materials in this study were derived from individuals without cerebrovascular diseases.

1.3.4 Patient Population

This study was an observational retrospective chart review of 554 radiographic images of the VA using MDCTA. We evaluated the extracranial (V1, V2, V3) and the intracranial (V4) segments of the VAs to describe the typical anatomy and establish the frequency of variations present in the morphology and morphometry of the VA. We retrospectively identified 554 MDCTAs obtained from Lenmed Ethekwini Hospital and Heart Centre, Durban, South Africa, from January 2009 to September 2019. The patient population represents the KwaZulu-Natal region.

The angiographies were from 247 females (44.6%) and 307 males (55.4%). The average age of the patients is reported as median (interquartile range (IQR)): 62 (23) (range: 10-99) years; 62 (25) for female patients and 61 (23) for male patients. The race was described according to the guidelines outlined in the modern systems of racial classification in the Republic of South Africa [60]. The criteria used in the scheme of racial classification include ancestry details and skin colour. The South African population is divided into four main racial groups: Black, White, Indian, and Coloured. Three population groups were included in this study: Black 91 (16.4%), White 287 (51.8%), and Indian 176 (31.8%). According to the modern system of classification, a Black individual was defined as having origins in indigenous Africa or Native groups. A White individual was defined as a person of European descent. An Indian individual was described as a person of Asian descent (Khalfani and Zuberi, 2001). Images were analyzed using a Picture Archiving Communication system (PACS) tool. The MDCTA images were examined for vascular variations by a neuroradiologist, neurosurgeon, and an anatomist using the anterior, posterior, coronal, anteroposterior, sagittal, and oblique view. Exclusion criteria included MDCTA scans that showed no clarity of the course of the VAs, scans that showed any sign of damage to the cervical vertebral bones, and scans with suboptimal image quality.

1.3.5 Ethical Considerations

The design of this study was approved by the Institutional Review Board/Ethics Committee (Biomedical Research Ethics Committee of the University of KwaZulu-Natal with ethical No: BE 148/19) and waived the need for informed consent as this study utilized retrospective chart reviews.

There was no patient contact, and no patient details were released from images. All methods were carried out in accordance with relevant guidelines and regulations.

1.3.6 Statistical Analysis

All data were analyzed using IBM SPSS version 27 program (SPSS for Windows; Chicago, IL, USA), and *p*-values less than 0.05 were considered statistically significant. The normal distribution of continuous variables was tested with the Kolmogorov-Smirnov test. Because the continuous variables are not normally distributed, the Wilcoxon Signed-Rank test was used to compare paired samples. The Kruskal-Wallis test was used to determine statistically significant differences in the dependent variables between the three racial groups. The Chi-square test was used for categorical variables. All measurements were taken three times (by a neurosurgeon, a neuroradiologist, and an anatomist) at each of the segments. The average value was subjected to intra-observer reliability testing using the intra-class correlation coefficient formula (ICC). Regarding the inter-observer reliability testing, another observer randomly selected 10% of the total sample size (55 images) and took measurements at each segment three times. The average value was compared with the initial value using ICC. The ICC values were reported for each segment, and details were recorded at the result session of each of the manuscripts (Chapter 2, 3, and 4). The Interclass coefficient correlation was used to examine the reliability of all continuous data (95% confidence intervals).

1.4 Publication outcomes

The following articles emanated from this thesis.

Table 1.5: Summary of the Manuscripts/Publications

Sn	Title	Journal	Remark
1.	An anatomical investigation of the proximal vertebral arteries (V1, V2) in a select South African population	Surgical and Radiological Anatomy (2021). https://doi.org/10.1007/s00276-021-02712-x	Published
2.	Fenestration of the Vertebrobasilar Junction Detected with Multidetector Computed Tomography Angiography	Folia Morphologica. (2021) **DOI:** 10.5603/FM.a2021.0028	Published
3.	Anatomical Variations of the Vertebral Arteries in a Select South African Population; Evaluation with Multidetector Computed Tomography Angiography	Italian Journal of Anatomy and Embryology.	Accepted for publication
4.	Radiological Anatomy of the Intracranial Vertebral Artery in a Select South African Cohort of Patients	Scientific Reports. Sci Rep. 2021 Jun 9;11(1):12138. doi: 10.1038/s41598-021-91744-9.	Published

5.	Radiological Anatomy of the Suboccipital Segment of the Vertebral Artery in a Select South African Population	European Journal of Anatomy. Eur J Anat, 25 (5): 553-562 (2021)	Published

References

Abd El Gawad, F. A., Shaaban, M. H., Shuaib, D. M. & Shallan, H. M. (2019). Anatomical variations of the vertebral artery and its relation to the atlas vertebra-Radiological and dry bone study. *Eur. j. anat,* 23**,** 49-58.

Akar, Z. C., Dujovny, M., Slavin, K. V., Gomez-Tortosa, E. & Ausman, J. I. (1994). Microsurgical anatomy of the intracranial part of the vertebral artery. *J Neurological research,* 16**,** 171-180.

Akgun, V., Battal, B., Bozkurt, Y., Oz, O., Hamcan, S., Sari, S. & Akgun, H. (2013). Normal anatomical features and variations of the vertebrobasilar circulation and its branches: an analysis with 64-detector row CT and 3T MR angiographies. *The scientific world journal,* 2013.

Al-Habib, A., Albadr, F., Ahmed, J., Aleissa, A. & Al, A. T. (2018). Quantitative assessment of vertebral artery anatomy in relation to cervical pedicles: surgical considerations based on regional differences. *J Neurosciences* 23**,** 104-110.

Albayram, S., Gailloud, P. & Wasserman, B. A. (2002). Bilateral arch origin of the vertebral arteries. *American journal of neuroradiology,* 23**,** 455-458.

Alfaouri-Kornieieva, M. & Al-Hadidi, A. M. (2014). Morphology of the vertebral artery in Asian population. *Asian Journal of Medical Sciences,* 5**,** 84-88.

Alicioglu, B., Gulekon, N. & Akpinar, S. (2015). Age-related morphologic changes of the vertebral artery in the transverse process. Analysis by multidetector computed tomography angiography. *The Spine Journal,* 15**,** 1981-1987.

An, H. S. & Simpson, J. M. 1994. *Surgery of the cervical spine*, CRC Press.

Arslan, D., Ozer, M. A., Govsa, F. & Kitis, O. (2019). Surgicoanatomical aspect in vascular variations of the V3 segment of vertebral artery as a risk factor for C1 instrumentation. *J. Clin. Neurosci.,* 68**,** 243-249.

Bentsen, L., Nygård, A., Ovesen, C., Christensen, A., Rosenbaum, S., Havsteen, I. & Christensen, H. (2014). Vascular pathology in the extracranial vertebral arteries in patients with acute ischemic stroke. *Cerebrovascular diseases extra* 4**,** 19-27.

Bhatia, K., Ghabriel, M. N. & Henneberg, M. (2005). Anatomical variations in the branches of the human aortic arch: a recent study of a South Australian population. *FOLIA MORPHOLOGICA-WARSZAWA-ENGLISH EDITION-,* 64**,** 217.

Bloch, S. & Danziger, J. (1974). Proatlantal intersegmental artery. *Neuroradiology,* 7**,** 5-8.

Bruneau, M., Cornelius, J. F. & George, B. (2006a). Antero-lateral approach to the V3 segment of the vertebral artery. *J Operative Neurosurgery,* 58**,** ONS-29-ONS-35.

Bruneau, M., Cornelius, J. F. & George, B. (2006b). Anterolateral approach to the V1 segment of the vertebral artery. *J Operative Neurosurgery,*58**,** ONS-215-ONS-219.

Bruneau, M., Cornelius, J. F., Marneffe, V., Triffaux, M. & George, B. (2006c). Anatomical variations of the V2 segment of the vertebral artery. *J Operative Neurosurgery,* 59**,** ONS-20-ONS-24.

Buckenham, T. & Wright, I. (2014). Ultrasound of the extracranial vertebral artery. *The British journal of radiology*.

Cacciola, F., Phalke, U. & Goel, A. (2004). Vertebral artery in relationship to C1-C2 vertebrae: an anatomical study. *J Neurology India* 52**,** 178.

Cagnie, B., Barbaix, E., Vinck, E., D'herde, K. & Cambier, D. (2006). Atherosclerosis in the vertebral artery: an intrinsic risk factor in the use of spinal manipulation? *Surg. Radiol. Anat.,* 28**,** 129-134.

Chaturvedi, S., Lukovits, T. G., Chen, W. & Gorelick, P. B. (1999). Ischemia in the territory of a hypoplastic vertebrobasilar system. *Neurology,* 52**,** 980-980.

Chen, C.-J., Tseng, Y.-C., Lee, T.-H., Hsu, H.-L. & See, L.-C. (2004). Multisection CT angiography compared with catheter angiography in diagnosing vertebral artery dissection. *American Journal of Neuroradiology,* 25**,** 769-774.

Chen, Y.-Y., Chao, A.-C., Hsu, H.-Y., Chung, C.-P. & Hu, H.-H. (2010). Vertebral artery hypoplasia is associated with a decrease in net vertebral flow volume. *Ultrasound Med Biol* 36**,** 38-43.

Cheung, J. P. Y. & Luk, K. D.-K. (2016). Complications of anterior and posterior cervical spine surgery. *Asian spine journal,* 10**,** 385-400.

Chibbaro, S., Mirone, G., Yasuda, M., Marsella, M., Di Emidio, P. & George, B. (2012). Vertebral artery loop—a cause of cervical radiculopathy. *World Neurosurg.,* 78**,** 375. e11-375. e13.

Clark, C. R. & Benzel, E. C. 2005. *The cervical spine*, Lippincott Williams & Wilkins.

Curylo, L. J., Mason, H. C., Bohlman, H. H. & Yoo, J. U. (2000). Tortuous course of the vertebral artery and anterior cervical decompression: a cadaveric and clinical case study. *Spine (Phila Pa 1976),* 25**,** 2860-2864.

De Oliveira, E., Rhoton Jr, A. L. & Peace, D. (1985). Microsurgical anatomy of the region of the foramen magnum. *Surgical neurology* 24**,** 293-352.

Decarvalho, S. A., Abd-El-Barr, M. M. & Groff, M. W. (2018). Vascular Complications in Cervical Spine Surgery (Anterior and Posterior Approach). *Complications in Neurosurgery E-Book***,** 314.

Decarvalho, S. A., Abd-El-Barr, M. M. & Groff, M. W. (2019). Vascular Complications in Cervical Spine Surgery (Anterior and Posterior Approach). *Complications in Neurosurgery.* Elsevier.

Dodevski, A. & Tosovska-Lazarova, D. (2012). Anatomical features and clinical importance of the vertebral artery. *Open Access Maced J Med Sci.,* 5**,** 328-335.

Doweidar, A., Al-Sayed, S. & Al-Kandery, S. (2014). Symptomatic Vertebral Artery Loop: A case report and review of literature. *J. Radiol. Case Rep.,* 8**,** 35.

Dzierzanowski, J., Szarmach, A., Bascik, B., Czapiewski, P., Muc, A., Piskunowicz, M., Krakowiak, M., Szmuda, T., Sloniewski, P., Szurowska, E. & Winklewski, P. J. (2017). Intracranial region of the vertebral artery: morphometric study in the context of clinical usefulness. *Folia Morphol. (Warsz.),* 76**,** 379-387.

Edlow, B. L., Wainger, B. J., Frosch, M. P., Copen, W. A., Rathmell, J. P. & Rost, N. S. (2010). Posterior circulation stroke after C1–C2 intraarticular facet steroid injection: evidence for diffuse microvascular injury. *The Journal of the American Society of Anesthesiologists* 112**,** 1532-1535.

Eftekhar, B., Dadmehr, M., Ansari, S., Ghodsi, M., Nazparvar, B. & Ketabchi, E. (2006). Are the distributions of variations of circle of Willis different in different populations?–Results of an anatomical study and review of literature. *BMC Neurol.,* 6**,** 22.

Elgueta, M. F., Jimenez, J. O., Wang, N. N., Lara, A. P., Chankowsky, J., Charghi, R., Tran, D. Q. & Finlayson, R. J. (2018). Anatomical Variations of the Vertebral Artery in the Upper Cervical Spine: Clinical Relevance for Procedures Targeting the C1/C2 and C2/C3 Joints. *Reg. Anesth. Pain Med.,* 43**,** 367-371.

Elliott, R. E., Tanweer, O., Boah, A., Morsi, A., Ma, T., Frempong-Boadu, A. & Smith, M. L. (2014). Comparison of screw malposition and vertebral artery injury of C2 pedicle and transarticular screws: meta-analysis and review of the literature. *Clinical Spine Surgery,* 27**,** 305-315.

Ergun, O., Tatar, I. G., Birgi, E. & Hekimoglu, B. (2016). Evaluation of vertebral artery dominance, hypoplasia and variations in the origin: angiographic study in 254 patients. *Folia Morphologica,* 75**,** 33-37.

Eskander, M. S., Drew, J. M., Aubin, M. E., Marvin, J., Franklin, P. D., Eck, J. C., Patel, N., Boyle, K. & Connolly, P. J. (2010). Vertebral artery anatomy: a review of two hundred fifty magnetic resonance imaging scans. *J Spine,* 35**,** 2035-2040.

Fortuniak, J., Bobeff, E., Polguj, M., Kośla, K., Stefańczyk, L. & Jaskólski, D. J. (2016). Anatomical anomalies of the V3 segment of the vertebral artery in the Polish population. *Eur. Spine J.,* 25**,** 4164-4170.

Gaigalaite, V., Vilimas, A., Ozeraitiene, V., Dementaviciene, J., Janilionis, R., Kalibatiene, D. & Rocka, S. (2016). Association between vertebral artery hypoplasia and posterior circulation stroke. *J BMC neurology,* 16**,** 118.

Gailloud, P. (2019). Vertebral artery triplication. *Surg. Radiol. Anat.,* 41**,** 841-843.

George, B., Bruneau, M. & Spetzler, R. F. (2013). *Pathology and surgery around the vertebral artery,* Springer Science & Business Media.

George, B. & Laurian, C. (2012). *The vertebral artery: pathology and surgery,* Springer Science & Business Media.

Golfinos, J. G., Dickman, C. A., Zabramski, J. M., Sonntag, V. & Spetzler, R. F. (1994). Repair of vertebral artery injury during anterior cervical decompression. *Spine (Phila Pa 1976),* 19**,** 2552-2556.

Guan, Q., Chen, L., Long, Y. & Xiang, Z. (2017). Iatrogenic vertebral artery injury during anterior cervical spine surgery: a systematic review. *J World neurosurgery* 106**,** 715-722.

Güvençer, M., Men, S., Naderi, S., Kiray, A., Tetik, S. (2006). The V2 segment of the vertebral artery in anterior and anterolateral cervical spinal surgery: a cadaver angiographic study. *J Clinical neurology &* neurosurgery 108**,** 440-445.

Hadimani, G., Desai, S., Bagoji, I. B., Sahana, B. N. (2013). Bilateral variation in the origin of vertebral artery. *Journal of Pharmaceutical Sciences Research and Clinical Studies in Headache* 5**,** 196.

Han, H.-C. (2012). Twisted blood vessels: symptoms, etiology and biomechanical mechanisms. *J. Vasc. Res.,* 49**,** 185-197.

Hong-Tao, Z., Shu-Ling, Z. & Dao-Pei, Z. (2014). Two case reports of bilateral vertebral artery tortuosity and spiral twisting in vascular vertigo. *J BMC neurology* 14**,** 14.

Hong, J. T., Park, D. K., Lee, M. J., Kim, S. W. & An, H. S. (2008). Anatomical variations of the vertebral artery segment in the lower cervical spine: analysis by three-dimensional computed tomography angiography. *Spine,* 33**,** 2422-6.

Hu, X.-Y., Li, Z.-X., Liu, H.-Q., Zhang, M., Wei, M.-L., Fang, S., Chen, W., Pan, H., Huang, J.-X. & Zhu, Y.-M. (2013). Relationship between vertebral artery hypoplasia and posterior circulation stroke in Chinese patients. *Neuroradiology,* 55**,** 291-295.

Ikeda, K., Nakamura, Y., Hirayama, T., Sekine, T., Nagata, R., Kano, O., Kawabe, K., Kiyozuka, T., Tamura, M. & Iwasaki, Y. (2010). Cardiovascular risk and neuroradiological profiles in asymptomatic vertebrobasilar dolichoectasia. *J Stroke Cerebrovasc Dis,* 30**,** 23-28.

Ionete, C. & Omojola, M. F. (2006). MR angiographic demonstration of bilateral duplication of the extracranial vertebral artery: unusual course and review of the literature. *American journal of neuroradiology* 27**,** 1304-1306.

Iqbal, S. (2013). A comprehensive study of the anatomical variations of the circle of Willis in adult human brains. *Journal of clinical and diagnostic research: JCDR,* 7**,** 2423.

Jecko, V., Rué, M., Castetbon, V., Berge, J. & Vignes, J.-R. (2015). Vertebral artery (V2) pseudo-aneurysm after surgery for cervical schwannoma. How to prevent it and a review of the literature. *Neurochirurgie,* 61**,** 38-42.

Jeng, J.-S., Yip, P.-K. (2004). Evaluation of vertebral artery hypoplasia and asymmetry by color-coded duplex ultrasonography. *J Ultrasound in medicine biology,* 30**,** 605-609.

Ka-Tak, W., Lam, W. W. & Yu, S. C. (2007). MDCT of an aberrant right subclavian artery and of bilateral vertebral arteries with anomalous origins. *American Journal of Roentgenology,* 188**,** W274-W275.

Karacan, A., Türkvatan, A. & Karacan, K. (2014). Anatomical variations of aortic arch branching: evaluation with computed tomographic angiography. *J Cardiology in the Young,* 24**,** 485-493.

Katsanos, A. H., Kosmidou, M. & Giannopoulos, S. (2013a). Vertebral artery hypoplasia in posterior circulation cerebral ischemia. *Clin. Neurol. Neurosurg.,* 115**,** 1194-1195.

Katsanos, A. H., Kosmidou, M., Kyritsis, A. P. & Giannopoulos, S. (2013b). Is vertebral artery hypoplasia a predisposing factor for posterior circulation cerebral ischemic events? A comprehensive review. *Eur. Neurol.,* 70**,** 78-83.

Khalfani, A. K. & Zuberi, T. (2001). Racial classification and the modern census in South Africa, 1911–1996. *Race and society,* 4**,** 161-176.

Kim, Y.-D., Yeo, H.-T. & Cho, Y.-D. (2009). Anomalous variations of the origin and course of vertebral arteries in patients with retroesophageal right subclavian artery. *Journal of Korean Neurosurgical Society,* 45**,** 297-299.

Kim, H. S., Lee, J. H., Cheh, G. & Lee, S.-H. (2010). Cervical radiculopathy caused by vertebral artery loop formation: a case report and review of the literature. *Journal of Korean Neurosurgical Society,* 48**,** 465.

Kim, M. S. (2016). Developmental anomalies of the distal vertebral artery and posterior inferior cerebellar artery: diagnosis by CT angiography and literature review. *Surg. Radiol. Anat.,* 38**,** 997-1006.

Kim, M. S. (2018). C2 segmental-type vertebral artery diagnosed using computed tomographic angiography. *Journal of Korean Neurosurgical Society,* 61**,** 194.

Kim, Y.-D., Yeo, H.-T. & Cho, Y.-D. (2009). Anomalous variations of the origin and course of vertebral arteries in patients with retroesophageal right subclavian artery. *Journal of Korean Neurosurgical Society,* 45**,** 297-299.

Kiresi, D., Gumus, S., Cengiz, S. L. & Cicekcibasi, A. (2009). The morphometric analysis of the V2 and V3 segments of the vertebral artery: normal values on MDCT. *Computerized Medical Imaging and Graphics,* 33**,** 399-407.

Komiyama, M., Morikawa, T., Nakajima, H., Nishikawa, M. & Yasui, T. (2001). High incidence of arterial dissection associated with left vertebral artery of aortic origin. *Neurol. Med. Chir. (Tokyo),* 41**,** 8-12.

Kornieieva, A. (2014). Morphology of the vertebral artery in Asian population. *Asian Journal of Medical Sciences (E-ISSN 2091-0576; P-ISSN 2467-9100),* 5**,** 84-88.

Kośla, K. N., Majos, M., Podgórski, M., Polguj, M., Topol, M., Stefańczyk, L. & Majos, A. (2014). Anomalous course and diameter of left-sided vertebral arteries–significance and predisposing factors in clinical practice. *Annals of Anatomy-Anatomischer Anzeiger,* 196**,** 360-364.

Kovač, J. D., Stanković, A., Stanković, D., Kovač, B. & Šaranović, D. (2014). Intracranial arterial variations: a comprehensive evaluation using CT angiography. *Medical science monitor: international medical journal of experimental and clinical research,* 20**,** 420.

Lale, P., Toprak, U., Yagız, G., Kaya, T. & Uyanık, S. A. (2014). Variations in the branching pattern of the aortic arch detected with computerized tomography angiography. *Advances in Radiology*

Lasjaunias, P., Vallee, B., Person, H., Ter Brugge, K. & Chiu, M. (1985). The lateral spinal artery of the upper cervical spinal cord: anatomy, normal variations, and angiographic aspects. *J. Neurosurg.,* 63**,** 235-241.

Lazaridis, N., Piagkou, M., Loukas, M., Piperaki, E.-T., Totlis, T., Noussios, G. & Natsis, K. (2018). A systematic classification of the vertebral artery variable origin: clinical and surgical implications. *Surg. Radiol. Anat.***,** 1-1.

Lee, S. H., Hur, N., Jeong, S.-K. J. J. O. A. & Thrombosis (2012). Geometric analysis and blood flow simulation of basilar artery. *Atheroscler Suppl,* 19**,** 397-401.

Lemke, A.-J., Benndorf, G., Liebig, T. & Felix, R. (1999). Anomalous origin of the right vertebral artery: review of the literature and case report of right vertebral artery origin distal to the left subclavian artery. *American journal of neuroradiology,* 20**,** 1318-1321.

Li, X., Guan, L., Zilundu, P. L. M., Chen, J., Chen, Z., Ma, M., Zhuang, H., Zhuang, Z., Qiu, Y. & Ye, F. (2019). The applied anatomy and clinical significance of the proximal, V1 segment of vertebral artery. *Folia Morphologica*

Liang, M.-L., Huang, M.-C., Cheng, H., Huang, W.-C., Yen, Y.-S., Shao, K.-N., Huang, C.-I., Shih, Y.-H. & Lee, L.-S. (2004). Posterior transarticular screw fixation for chronic atlanto-axial instability. *J. Clin. Neurosci.,* 11**,** 368-372.

Lister, R. J., Rhoton Jr, A. L., Matsushima, T. & Peace, D. A. (1982). Microsurgical anatomy of the posterior inferior cerebellar artery. *Neurosurgery,* 10**,** 170-199.

Liu, I.-W., Ho, B.-L., Chen, C.-F., Han, K., Lin, C.-J., Sheng, W.-Y., Hu, H.-H. & Chao, A.-C. (2017). Vertebral artery terminating in posterior inferior cerebellar artery: A normal variation with clinical significance. *PLoS One,* 12**,** e0175264.

Luh, G., Dean, B., Tomsick, T. & Wallace, R. (1999). The persistent fetal carotid-vertebrobasilar anastomoses. *AJR Am. J. Roentgenol,* 172**,** 1427-1432.

Lunardini, D. J., Eskander, M. S., Even, J. L., Dunlap, J. T., Chen, A. F., Lee, J. Y., Ward, T. W., Kang, J. D. & Donaldson, W. F. (2014). Vertebral artery injuries in cervical spine surgery. *The Spine Journal,* 14**,** 1520-1525.

Madawi, A. A., Casey, A. T., Solanki, G. A., Tuite, G., Veres, R. & Crockard, H. A. (1997). Radiological and anatomical evaluation of the atlantoaxial transarticular screw fixation technique. *Journal of neurosurgery* 86**,** 961-968.

Matula, C., Trattnig, S., Tschabitscher, M., Day, J. & Koos, W. T. (1997). The course of the prevertebral segment of the vertebral artery: anatomy and clinical significance. *Surg. Neurol.,* 48**,** 131.

Meila, D., Tysiac, M., Petersen, M., Theisen, O., Wetter, A., Mangold, A., Schlunz-Hendann, M., Papke, K., Brassel, F. & Berenstein, A. (2012). Origin and course of the extracranial vertebral artery: CTA findings and embryologic considerations. *Clin. Neuroradiol.,* 22**,** 327-333.

Meng, X., Ding, W., Wu, X. & Di, P. (2018). Clinical investigation and characterization of vertebrobasilar dolichoectasia and vertebral artery dominance. *Discov. Med.,* 25**,** 151-158.

Menshawi, K., Mohr, J. P. & Gutierrez, J. (2015). A functional perspective on the embryology and anatomy of the cerebral blood supply. *Journal of stroke,* 17**,** 144.

Mercier, P., Brassier, G., Fournier, H., Picquet, J., Papon, X. & Lasjaunias, P. (2008). Vascular microanatomy of the pontomedullary junction, posterior inferior cerebellar arteries, and the lateral spinal arteries. *Interv. Neuroradiol.,* 14**,** 49-58.

Miao, H.-L., Zhang, D.-Y., Wang, T., Jiao, X.-T. & Jiao, L.-Q. (2020). Clinical Importance of the Posterior Inferior Cerebellar Artery: A Review of the Literature. *Int. J. Med. Sci.,* 17**,** 3005-3019.

Mitchell, J. (2004). Differences between left and right suboccipital and intracranial vertebral artery dimensions: an influence on blood flow to the hindbrain? *Physiother. Res. Int.,* 9**,** 85-95.

Mitchell, J. & Mckay, A. (1995). Comparison of left and right vertebral artery intracranial diameters. *The Anatomical Record,* 242**,** 350-354.

Mitsumura, H., Miyagawa, S., Komatsu, T., Hirai, T., Kono, Y. & Iguchi, Y. (2016). Relationship between vertebral artery hypoplasia and posterior circulation ischemia. *Journal of Stroke Cerebrovascular Diseases,* 25**,** 266-269.

Nasir, S., Hussain, M., Khan, S. A., Mansoor, M. A. & Sharif, S. (2010). Anomalous origin of right vertebral artery from right external carotid artery. *J Coll Physicians Surg Pak* 20**,** 208-10.

Nayak, S. R., Pai, M. M., Prabhu, L. V., D'costa, S. & Shetty, P. (2006). Anatomical organization of aortic arch variations in the India: embryological basis and review. *Jornal Vascular Brasileiro,* 5**,** 95-100.

Neo, M., Fujibayashi, S., Miyata, M., Takemoto, M. & Nakamura, T. (2008). Vertebral artery injury during cervical spine surgery: a survey of more than 5600 operations. *Spine (Phila Pa 1976),* 33**,** 779-785.

Netter, F. H. 2017. *Atlas of Human Anatomy E-Book*, Elsevier Health Sciences.

Ngo, M. T., Kwak, H. S. & Chung, G. H. (2020). change in basilar artery length and bending according to aging and vertebral artery dominance: A longitudinal study. *Sci. Rep.,* 10**,** 1-8.

Noh, Y., Kwon, O.-K., Kim, H.-J. & Kim, J. S. (2011). Rotational vertebral artery syndrome due to compression of nondominant vertebral artery terminating in posterior inferior cerebellar artery. *J. Neurol.,* 258**,** 1775-1780.

Nouh, A., Remke, J. & Ruland, S. (2014). Ischemic posterior circulation stroke: a review of anatomy, clinical presentations, diagnosis, and current management. *Front. Neurol.,* 5**,** 30.

Nourbakhsh, A., Yang, J., Ziran, B. & Garges, K. J. (2015). An unusual course of the vertebral artery posterior to the nerve root in the inter-transverse space: a cadaveric study. *Patient Saf. Surg.,* 9**,** 19.

O'donnell, C. M., Child, Z. A., Nguyen, Q., Anderson, P. A. & Lee, M. J. (2014). Vertebral Artery Anomalies at the Craniovertebral Junction in the US Population. *Spine (Phila Pa 1976),* 39**,** E1053-E1057.

Ogeng'o, J., Olabu, B., Sinkeet, R., Ogeng'o, N. M. & Elbusaid, H. (2014). Vertebral artery hypoplasia in a Black Kenyan population. *J International scholarly research notices,* 2014.

Ohkura, K., Shiiya, N., Washiyama, N., Yamashita, K., Takahashi, D., Tsuda, K. & Kando, Y. (2014). Vertebral artery variations in thoracic aortic patients. *Eur. J. Cardiothorac. Surg.,* 46**,** 27-31.

Omotoso, B., Harrichandparsad, R., Moodley, I., Satyapal, K. & Lazarus, L. (2021a). An anatomical investigation of the proximal vertebral arteries (V1, V2) in a select South African population. *Surg. Radiol. Anat.***,** 1-13.

Omotoso, B., Harrichandparsad, R., Moodley, I., Satyapal, K. & Lazarus, L. (2021b). Fenestration of the vertebrobasilar junction detected with multidetector computed tomography angiography. *Folia Morphol. (Praha)*.

Ono, S. E., Kawasaki, C. S., Coelho, L. O. D. M., Lucaski, F. F. & Carvalho Neto, A. D. (2009). Widening of intervertebral foramen by tortuous vertebral artery. J Arquivos de neuro-psiquiatria 67**,** 115-116.

Ozdemir, S., Yildiz, C. & Cankur, N. (2002). Evaluation of vertebral artery system in a healthy population by using colour duplex Doppler ultrasonography. *Med School J Uludag,* 28**,** 95-99.

Padget, D. H. (1948). The development of the cranial arteries in the human embryo. *J Contrib Embryol* 32**,** 205-261.

Paksoy, Y., Levendoglu, F. D., Ögün, C. Ö., Üstün, M. E. & Ögün, T. C. J. S. (2003). Vertebral artery loop formation: a frequent cause of cervicobrachial pain. *Spine J,* 28**,** 1183-1188.

Panicker, H., Tarnekar, A., Dhawane, V. & Ghosh, S. (2002). Anomalous origin of left vertebral artery-embryological basis and applied aspects-a case report. *J. Anat. Soc. India,* 51**,** 234-5.

Park, J.-H., Kim, J.-M. & Roh, J.-K. (2007). Hypoplastic vertebral artery: frequency and associations with ischaemic stroke territory. *J. Neurol. Neurosurg. Psychiatry,* 78**,** 954-958.

Pekcevik, Y. & Pekcevik, R. (2014). Variations of the cerebellar arteries at CT angiography. *Surg. Radiol. Anat.,* 36**,** 455-461.

Peng, C. W., Chou, B. T., Bendo, J. A. & Spivak, J. M. (2009). Vertebral artery injury in cervical spine surgery: anatomical considerations, management, and preventive measures. *The Spine Journal,* 9**,** 70-76.

Poonam, S. R. & Sharma, T. (2010). Incidence of anomalous origins of vertebral artery–anatomical study and clinical significance. *Journal of Clinical and Diagnostic Research,* 4**,** 2626-2631.

Rathmell, J. P., Aprill, C. & Bogduk, N. (2004). Cervical transforaminal injection of steroids. *The Journal of the American Society of Anesthesiologists* 100**,** 1595-1600.

Raveendran, V. L. & Kamalamma, G. K. (2018). Inferior cervical ganglion and stellate ganglion-concepts revisited. *Journal of Evolution of Medical and Dental Sciences,* 7**,** 1653-1659.

Rawal, J. D. & Jadav, H. R. (2012). Histomorphometric comparison of diameter of right and left vertebral arteries. *National Journal of Medical Research,* 2**,** 260-263.

Ryan, S., Mcnicholas, M. & Eustace, S. J. (2011). *Anatomy for Diagnostic Imaging E-Book*, Elsevier Health Sciences.

Sakaida, H., Okada, M. & Yamamoto, A. (2001). Vascular reconstruction of a vertebral artery loop causing cervical radiculopathy and vertebrobasilar insufficiency: case report. *J. Neurosurg. Spine,* 94**,** 145-149.

Sardhara, J., Behari, S., Mohan, B. M., Jaiswal, A. K., Sahu, R. N., Srivastava, A., Mehrotra, A. & Lal, H. (2015). Risk stratification of vertebral artery vulnerability during surgery for congenital atlanto-axial dislocation with or without an occipitalized atlas. *Neurology India*

Sastry, V. R. & Manjunath, K. (2006). The course of the V1 segment of the vertebral artery. *Annals of Indian Academy of Neurology,* 9**,** 223.

Satti, S., Cerniglia, C. & Koenigsberg, R. (2007). Cervical vertebral artery variations: an anatomic study. *American journal of Neuroradiology,* 28**,** 976-980.

Schroeder, G. D. & Hsu, W. K. (2013). Vertebral artery injuries in cervical spine surgery. *Surg. Neurol. Int.,* 4**,** S362.

Shi, S. (2017). Arterial vascular variation of the head and neck and its clinical significance. *J Neurol Neurophysiol,* 8**,** 2.

Shin, H. Y., Park, J. K., Park, S. K., Jung, G. S. & Choi, Y. S. (2014). Variations in entrance of vertebral artery in Korean cervical spine: MDCT-based analysis. *The Korean journal of pain* 27**,** 266-270.

Siclari, F., Burger, I., Fasel, J. & Gailloud, P. (2007). Developmental anatomy of the distal vertebral artery in relationship to variants of the posterior and lateral spinal arterial systems. *American journal of neuroradiology,* 28**,** 1185-1190.

Sikka, A. & Jain, A. (2012). Bilateral variation in the origin and course of the vertebral artery. *Anatomy research international,* 2012.

Songur, A., Gonul, Y., Ozen, O. A., Kucuker, H., Uzun, I., Bas, O. & Toktas, M. (2008). Variations in the intracranial vertebrobasilar system. *Surg. Radiol. Anat.,* 30**,** 257-264.

Sonje, P., Arole, V. & Anand, R. (2015). Study of variations in the origin and course of vertebral artery. *International Journal of Current Research and Review,* 7**,** 85.

Standring, S. 2015. *Gray's anatomy e-book: the anatomical basis of clinical practice,* Elsevier Health Sciences.

Strub, W., Leach, J. & Tomsick, T. (2006). Left vertebral artery origin from the thyrocervical trunk: a unique vascular variant. *American journal of neuroradiology,* 27**,** 1155-1156.

Szárazová, A. S., Bartels, E. & Turčáni, P. (2012). Vertebral artery hypoplasia and the posterior circulation stroke. *J Perspectives in medicine,* 1**,** 198-202.

Takahashi, T., Tominaga, T., Hassan, T. & Yoshimoto, T. (2003). Cervical cord compression with myelopathy caused by bilateral persistence of the first intersegmental arteries: case report. *Neurosurgery,* 53**,** 234-237.

Tetiker, H., Çimen, M. & Koşar, M. (2014). Fenestration of the vertebral artery: case presentation. *FOLIA MORPHOLOGICA-WARSZAWA-ENGLISH EDITION-,* 73**,** 84-86.

Thierfelder, K. M., Baumann, A. B., Sommer, W. H., Armbruster, M., Opherk, C., Janssen, H., Reiser, M. F., Straube, A. & Von Baumgarten, L. (2014). Vertebral artery hypoplasia: frequency and effect on cerebellar blood flow characteristics. *Int J Stroke,* 45**,** 1363-1368.

Tsai, I.-C., Tzeng, W.-S., Lee, T., Jan, S.-L., FU, Y.-C., Chen, M.-C., Lin, P.-C., Liao, W.-C. & Chen, C. C.-C. (2007). Vertebral and carotid artery anomalies in patients with aberrant right subclavian arteries. *Pediatric radiology,* 37**,** 1007-1012.

Tubbs RS, Shah NA, Sullivan BP, Marchase, ND, & Cohen-Gadol, AA. (2009). Surgical anatomy and quantitation of the branches of the V2 and V3 segments of the vertebral artery. Journal of Neurosurgery: Spine ;11, 84-87.

Uchino, A., Saito, N., Takahashi, M., Okada, Y., Kozawa, E., Nishi, N., Mizukoshi, W., Nakajima, R. & Watanabe, Y. (2013). Variations in the origin of the vertebral artery and its level of entry into the transverse foramen diagnosed by CT angiography. *Neuroradiology,* 55**,** 585-594.

Uchino, A., Saito, N., Watadani, T., Okada, Y., Kozawa, E., Nishi, N., Mizukoshi, W., Inoue, K., Nakajima, R. & Takahashi, M. (2012). Vertebral artery variations at the C1–2 level diagnosed by magnetic resonance angiography. *Neuroradiology,* 54**,** 19-23.

Vaněk, P., Bradáč, O., De Lacy, P., Konopková, R., Lacman, J. & Beneš, V. (2017). Vertebral artery and osseous anomalies characteristic at the craniocervical junction diagnosed by CT and 3D CT angiography in normal Czech population: analysis of 511 consecutive patients. *Neurosurgical review,* 40**,** 369-376.

Vergara, P., Bal, J. S., Hickman Casey, A. T., Crockard, H. A. & Choi, D. (2012). C1-C2 posterior fixation: are 4 screws better than 2? *Operative Neurosurgery,* 71**,** ons86-ons95.

Vicenzini, E., Ricciardi, M. C., Sirimarco, G., Di Piero, V. & Lenzi, G. L. (2010). Extracranial and intracranial sonographic findings in vertebral artery diseases. *Journal of Ultrasound in Medicine* 29**,** 1811-1824.

Vujmilović, S., Spasojević, G., Vujnović, S., Malobabić, S. & Vujković, Z. (2018). Variability of the vertebral artery origin and transverse foramen entrance level—CT angiographic study. *Folia Morphol. (Praha),* 77**,** 687-692.

Wakao, N., Takeuchi, M., Nishimura, M., Riew, K. D., Kamiya, M., Hirasawa, A., Kawanami, K., Imagama, S., Sato, K. & Takayasu, M. (2014). Vertebral artery variations and osseous anomaly at the C1-2 level diagnosed by 3D CT angiography in normal subjects. *Neuroradiology,* 56**,** 843-849.

Wang, F., Wang, X., Li, X., Zheng, H. & Zhang, Z. (2020). A case of multiple Vertebrobasilar artery fenestration misdiagnosed as vertebral artery dissection. *BMC Neurol.,* 20**,** 1-5.

Wright, N. M. & Lauryssen, C. (1998). Vertebral artery injury in C1–2 transarticular screw fixation: results of a survey of the AANS/CNS section on disorders of the spine and peripheral nerves. *J. Neurosurg.,* 88**,** 634-640.

Yamazaki, M., Okawa, A., Furuya, T., Sakuma, T., Takahashi, H., Kato, K., Fujiyoshi, T., Mannoji, C., Takahashi, K. & Koda, M. (2012). Anomalous vertebral arteries in the extra-and intraosseous regions of the craniovertebral junction visualized by 3-dimensional computed tomographic angiography: analysis of 100 consecutive surgical cases and review of the literature. *Spine,* 37**,** E1389-E1397.

Yeh, J.-F., Lin, Y.-J., Po, H. L., Wang, S.-F., Pan, P.-Y., Cheng, S.-J. & Hseuh, I.-H. (2005). A case of bow hunter's stroke caused by non-dominant vertebral artery. *Acta Neurol. Taiwan.,* 14**,** 69-73.

Yenigun, A., Ustun, M., Tugrul, S., Dogan, R., Ozturan, O. J. T. J. O. L. & Otology (2016). Classification of vertebral artery loop formation and association with cervicogenic dizziness. *J. Laryngol. Otol.,* 130**,** 1115-1119.

Zhou, M., Zheng, H., Gong, S., Guo, J., Chen, N., Zhou, D., Yang, R., Zhu, C. & He, L. (2015). Vertebral artery hypoplasia and vertebral artery dissection a hospital-based cohort study. *Neurology*.

Zhu, W., Wang, Y.-F., Dong, X.-F., Feng, H.-X., Zhao, H.-Q. & Liu, C.-F. (2016). Study on the correlation of vertebral artery dominance, basilar artery curvature and posterior circulation infarction. *Acta Neurol Belg* 116**,** 287-293.

Zibis, A., Mitrousias, V., Galanakis, N., Chalampalaki, N., Arvanitis, D. & Karantanas, A. (2018). Variations of transverse foramina in cervical vertebrae: what happens to the vertebral artery? *European Spine Journal,* 27**,** 1278-1285.

BRIDGING TEXT

FROM CHAPTER ONE TO TWO

The introduction and the literature review from the previous chapter examined the typical anatomy of the VA and the incidence of various anatomical variations. We discussed extensively the prevalence of these variations in different population groups, including notes on the development of the artery and how some of the variant anatomies may have developed. Also, we highlighted the risk of iatrogenic injury and pathology associated with the morphological variations at each segment of the arteries. We realized that the best approach is to systematically review each segment to describe the typical anatomy and prevalence of associated variations. The next chapter comprehensively investigates the anatomy of the proximal VAs (V1 and V2 segments) in a South Africa population (KwaZulu-Natal region). The prevalence of variation and the morphometry of the two segments are compared to the previous report from other parts of the world.

CHAPTER TWO

MANUSCRIPT ONE

An Anatomical Investigation of the Proximal Vertebral Arteries (V1, V2) In a Select South African Population

Omotoso, B.R[1], Dr Harrichandparsad, R[2], Dr Moodley, I.G[3], Prof. Satyapal, K.S.[1], Prof. Lazarus, L[1]

[1]Discipline of Clinical Anatomy, School of Laboratory Medicine and Medical Sciences, College of Health Sciences, University of KwaZulu-Natal, Westville Campus, Private Bag X54001, Durban, South Africa.

[2]Department of Neurosurgery, School of Clinical Medicine, College of Health Sciences, Nelson R Mandela School of Medicine, University of KwaZulu-Natal, Durban, South Africa.

[3]Department of Radiology, Jackpersad and Partners Inc., Specialist Diagnostic Radiologists, Lenmed Ethekwini Hospital and Heart Centre, Durban, South Africa.

Corresponding Author: Professor L Lazarus

Address: Discipline of Clinical Anatomy, School of Laboratory Medicine and Medical Sciences, College of Health Sciences, University of KwaZulu-Natal, Westville Campus, Private Bag X54001, Durban, South Africa.

Email address: ramsaroopl@ukzn.ac.za

+27 31 260 7899

Published in Surgical and Radiologic Anatomy (2021)

https://doi.org/10.1007/s00276-021-02712-x

Published online on 10th March 2021

Surgical and Radiologic Anatomy
https://doi.org/10.1007/s00276-021-02712-x

ORIGINAL ARTICLE

An anatomical investigation of the proximal vertebral arteries (V1, V2) in a select South African population

B. R. Omotoso[1] · R. Harrichandparsad[2] · I. G. Moodley[3] · K. S. Satyapal[1] · L. Lazarus[1]

Received: 16 November 2020 / Accepted: 9 February 2021

Abstract

Introduction The most common type of vascular complication during cervical spine surgery is the vertebral artery (VA) injury. The presence of anatomical variation in the artery's morphology has been a significant factor for arterial injury during surgery. Therefore, physicians planning interventions in the craniospinal region need to be aware of the extents of variations. In addition to vascular injury, anatomical variations can predispose to some pathologies in the posterior circulation territory. To provide useful data to interventional radiologists, anatomists, and surgeons, we evaluated the anatomical features of the V1 and V2 segments of the VA in a South African population.

Materials and methods The study is an observational, retrospective chart review of 554 consecutive South African patients (Black, Indian and White) who had undergone computed tomography angiography (CTA) from January 2009 to September 2019.

Results The VA exhibited morphological variation in its course. We report the incidence of variant origin of the left VA, all from the aortic arch. Variation in the level of entry into the transverse foramen ranged between C7 and C3. A left dominant pattern was observed; we also report on hypoplasia of the VA. In addition, we report incidence of VA tortuosity at V1, V2 to be 76.6% and 32.1%, respectively.

Conclusions The baseline data established in this study regarding the diameter, variant origin, and level of entry into the transverse foramen will assist neurosurgeons and interventional radiologists in interpreting, diagnosing, and planning and executing various vascular procedures and treatment of pathology in the vicinity of the VA.

Keywords Vertebral artery dominance · Tortuosity · Vertebral artery hypoplasia · Arch of aorta · Iatrogenic injury · Anatomical variation

Introduction

Vertebral artery (VA) injury is the most common type of complication in cervical spine surgery [8]. A recent meta-analysis has revealed that patients with variant anatomy are more prone to iatrogenic injury of the VA [17]. Other authors also confirmed that the presence of anatomical variations in the morphology of the VA increases the likelihood of injury [8]. Therefore, variations in the origin and course of the artery should be considered by vascular surgeons and radiologists working in the craniospinal region. A possible explanation for this may be that variant arteries are often situated in an unanticipated position. In addition to the risk of injury, anatomical variations have been associated with some pathologies in the posterior circulatory territory. Important central nervous system structures such as the cervical spinal cord, brainstem, thalamus,

✉ L. Lazarus
ramsaroopl@ukzn.ac.za

1 Department of Clinical Anatomy, School of Laboratory Medicine and Medical Sciences, College of Health Sciences, University of KwaZulu-Natal, Westville Campus, Private Bag X54001, Durban 4000, South Africa

2 Department of Neurosurgery, School of Clinical Medicine, College of Health Sciences, Nelson R Mandela School of Medicine, University of KwaZulu-Natal, Durban, South Africa

3 Department of Radiology, Jackpersad and Partners Inc, Specialist Diagnostic Radiologists, Lenmed Ethekwini Hospital and Heart Centre, Durban, South Africa

Published online: 10 March 2021

cerebellum, and occipital lobes are primarily supplied by the VA [36]. Sometimes, morphologic variations may influence the hemodynamics of blood flow to these central nervous system structures. Inadequate perfusion of these structures can predispose to some pathological process in the posterior circulation territory of the brain.

Authors have hypothesized that the incidence of posterior circulation infarctions of the posterior inferior cerebellar and basilar artery territories is higher in VA dominant patients [44]. Similarly, posterior circulatory stroke and VA occlusion are found to be related with VA hypoplasia [31]. Other previously reported variations include variant origin and duplicate or triplicate origin, variation in the level of entering the transverse foramen (TF) (between C7 and C3), fenestration, and presence of tortuosity. According to some researchers, prevalence of variation sometimes can be linked with anthropometric parameters, demographic and ethnic/racial differences [9, 12]. There have been controversies regarding the cut-off value for hypoplastic VAs and VA dominance in the literature [11]. There was no consensus with regard to which side is dominant in several populations. Some authors have reported left dominance [1, 28] whilst others reported right [11]. However, Mitchell (2004) reported no difference (codominance) [30]. For these reasons and considering the multiracial background of the South African population, there is a need for data on the morphology of the proximal VAs to describe the trend of variation in the local population group. Population-specific data will be more appropriate as data from one population group may not be applicable to another.

VAs are large major arteries of the neck which have their origin from the supero-posterior aspect of the first part of the subclavian artery [15]. It is divided into four segments: the first segment (V1) extends from the origin at the subclavian artery to the C6 transverse process. The second segment (V2) extends from C6 to C2 transverse processes. The third segment (V3) extends from C2 to the site of passage through the foramen magnum. The intracranial segment (V4) extends from the foramen magnum dura to the vertebrobasilar junction [6]. Proper identification of variant anatomy during preoperative planning can reduce the risk of iatrogenic injury. Inadequate information about variation can expose the VA to the risk of injury resulting in grave consequences, especially if the dominant artery is involved in asymmetry [17].

In this retrospective observational study, using images produced by multidetector computed tomography angiography (MDCTA), we sought to investigate the anatomical variations of the V1 and V2 segments of the VA and their clinical relevance for procedures in the vicinity of this part of the artery in a select South African population. Due to the multiracial composition of South African population, in addition to overall incidence of variation, we also report variations based on the three racial groups present: Black, Indian, and White South African.

Materials and methods

Study population

This study was a retrospective observational chart review of 554 radiographic images, MDCTA of the extracranial segments (V1, V2) of the VAs to establish the variations that may be present in the morphology and the morphometry of the artery. The design was approved by the Institutional Review Board/Ethics Committee (Biomedical Research Ethics Committee of the University of KwaZulu-Natal with ethical No: BE 148/19). We retrospectively identified 554 CTAs obtained from Lenmed Ethekwini Hospital and Heart Centre, Durban, South Africa, from January 2009 to September 2019.

The angiographies were of 307 males (55.4%) and 247 females (44.6%). The average age of the patients is reported as median (IQR): 62 (23) (range 10–99) years; 62 (25) for female patients and 61 (23) for male patients. Race was defined according to the guidelines outlined in the modern systems of racial classification in the Republic of South Africa [23]. The criteria used in the scheme of racial classification include skin color and ancestry. The South African population is divided into four main racial groups: White, Black, Indian, and Colored. Three population groups were included in the present study: Black 91 (16.4%), Indian 176 (31.8%), and White 287 (51.8%). According to the modern system of classification, a White individual was defined as a person of European descent. A Black individual was defined as a person having origins in any of indigenous Africa or Native group. An Indian individual was defined as a person of Asian descent [23].

Images were analyzed using a Picture Archiving Communication system (PACS). The 3D-MDCTA images were examined for vascular variations by a neurosurgeon, a neuroradiologist, and an anatomist using the coronal and sagittal view. Exclusion criteria included CTA scans that showed no clarity of the VA's course, scans that showed any sign of damage to the vertebral bones and scans with motion artifacts or poor-quality imaging. Cases of variant origin were analyzed differently and together with the typical group.

CTA imaging protocol

The imaging examination was performed on a 64-detector row computed tomography (CT) scanner (Lightspeed CT, GE Healthcare Medical Systems, Milwaukee, WI, USA) with the scanning protocol as follows: 120 kVp, 697 mAs, beam collimation 64×0.625 mm, gantry rotation time 0.4 s, section thickness of 0.625 mm, pitch 0.969:1 and reconstruction interval of 0.625 mm. During the procedure, infused 80 mL of non-ionic iodinated contrast was followed by 40 mL saline and injected via a double power injector (Medex flowSens, Geubert USA) into the patient's antecubital vein (4 mL/s).

Imaging reconstruction

Postprocessing of three-dimensional images was performed by using a multiplanar reformation (MPR), maximum intensity projection (MIP), multiplanar reconstruction (MPR), and volume rendering (VR) algorithms. The volumetric MDCTA data sets were processed on Advanced Workstation 4.2, (GE Healthcare, Milwaukee, USA). The CTAs were performed for diagnostic purposes in the context of various cerebrovascular accidents or diseases. In some cases, the suspected diseases were not found on CT angiography; thus, some materials in this study were derived from a healthy population.

Each radiological image was evaluated for the following parameters, and variables were recorded:

1. Origin of the bilateral VA.
2. Level at which each of the VA entered the TF.
3. Tortuosity at V1 and V2 segment if present. When the artery was tortuous, the software was used to straighten it, after which the length was measured.
4. Total length of the V1 segment from the origin to the point of entry into the TF and the V2 segment, as measured from the point of entry into the TF to the TF of the C2 cervical vertebra (Fig. 1).
5. Diameter of the V1 segment, measured at a midpoint between origin and point of entry into the TF. The diameter of V2 segment was measured at a fixed point between C4 and C3 pedicles. The VA was categorized as dominant if the diameter was significantly larger than the contralateral side by any size [34]. Each VA with a diameter of less than 2.7 mm was noted and classified as hypoplastic [12].

The accuracy and repeatability of the measurements were determined by random sampling of 55 scans, and a second observer took measurements for inter-observer reliability testing.

Statistical analysis

Statistical analysis was conducted using SPSS version 27 (SPSS Inc., Chicago, IL, USA), and p-values less than 0.05 were considered statistically significant. The normal distribution of continuous variables was tested with the Kolmogorov–Smirnov test. Because the continuous variables

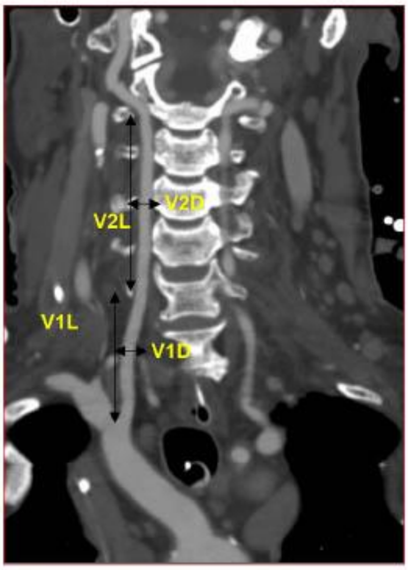

Fig. 1 Coronal view of CTA image, V1 and V2 segments of the vertebral artery. Measured variables; V1L—the length of the VA from the origin to the point of entry into the transverse foramen; V2L—the length of the VA from the point of entry into the transverse foramen to the transverse foramen of the C2 cervical vertebra; V1D—the diameter of the V1 segment at a midpoint between origin and point of entry into the transverse foramen; V2D—the diameter of the VA V2 segment at a fixed point between C4 and C3 pedicles

are not normally distributed, Wilcoxon Signed Rank test was used to compare paired samples. Kruskal–Wallis test was used to determine statistically significant differences in the dependent variables between the three racial groups and the Chi-square test was used for categorical variables. The continuous variables are presented as median (interquartile range), and the categorical variables were represented by a number (N) and percentage. The Interclass coefficient correlation was used to examine the reliability of measurements.

Results

The interclass coefficient correlation for intra-observer reliability testing was 99% for the V1 length, and 96% for diameter, 96% for the V2 length, and 95% for the V2 diameter. For inter-observer reliability testing, the intraclass correlation was 85% for the V1 length and diameter, 87% for the V2 length and 85% for the V2 diameter, with a 95% confidence interval.

Vertebral artery origin

Much of the VA showed typical origin from the subclavian artery bilaterally in this study. The left VA arose directly from the arch of aorta (AOA) in 6.9% of the patients (38/554: 4.0% males and 2.9% females) (Fig. 2). Of these total variations in origin registered, 3.6% were White, 2.5% Indian, and 0.7% Black South Africans. All the right VAs took their origin from the subclavian artery, although two of the right VAs arose close to the bifurcation of the brachiocephalic artery (Fig. 3b). No significant racial or gender differences were noted in the site of origin of the VA ($p=0.54, p=1.0$).

Level of entry into the TF

In most cases, the first segment of the VA entered the TF of C6 vertebra (Table 1). On both sides including the variation group (AOA origin), atypical entrance level was most common at the TF of C5.

Tortuosity

We classified tortuosity as a mild, single loop, and multiple loop formation (Table 2). Mild tortuosity was noted more commonly in the observed cases. At the V1 segment on the left, cases of tortuosity was 22.9% in White, 12.8% in Indian and 6.5% in Black ($p=0.058$). There was no significant difference across the racial groups. At the V1 segment on the

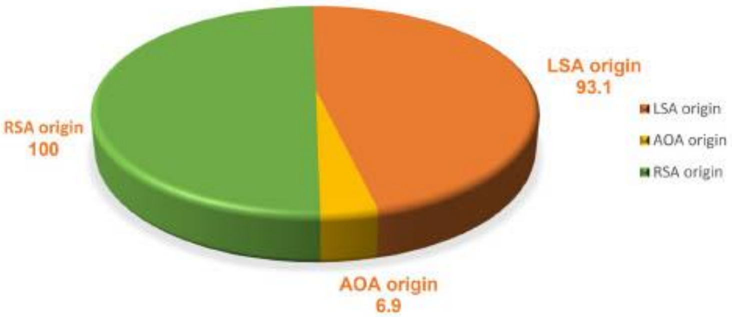

Fig. 2 Pie chart of the frequency (percent for each laterality) of variation in origin. LSA: left subclavian artery, *RSA* right subclavian artery, *AOA* arch of aorta.

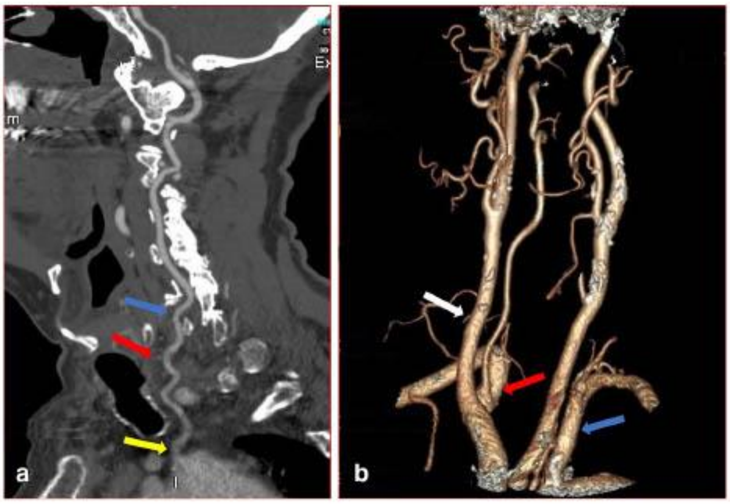

Fig. 3 CTA images of a male (sagittal view a) and female (3D reconstructed image b) patients showing variation in origin, level of entering the transverse foramen and tortuosity at V1 segment. **a** The left VA (yellow arrow) originates directly from the AOA with multiple loops (red arrow) and enters through the transverse foramen of C5 vertebra. (blue arrow). **b** 3D reconstructed image shows origin of the right VA from the right subclavian artery close to the bifurcation of the brachiocephalic trunk (red arrow). The right common carotid artery (white arrow) and left subclavian artery (blue arrow) are illustrated (color figure online)

Table 1 Relationship between VA origin and level of entry the TF

Entry level	LVA		RVA
	LSA origin *n* (%)	AOA origin *n* (%)	RSA origin *n* (%)
C3	–	–	1 (0.2%)
C4	3 (0.6%)	5 (13.2%)	9 (1.6%)
C5	16 (3.1%)	31 (81.6%)	40 (7.2%)
C6	489 (94.8%)	1 (2.6%)	502 (90.6%)
C7	8 (1.6%)	1 (2.6%)	2 (0.4%)

LSA left subclavian artery, *RSA* right subclavian artery, *AOA* arch of aorta, *LVA* left VA, *RVA* right VA

Table 2 Classification of incidence of tortuosity at the V1 and V2 segments

Tortuosity	Mild (%)	Single loop (%)	Multiple loop (%)	Total (%)
V1 Left side	27.4	13.9	0.9	42.2
V1 Right side	25.5	7.6	1.3	34.4
V2 Left side	9.2	4.5	2.5	16.3
V2 Right side	10.6	2.9	2.3	15.8

right, a significant difference was noted across the racial groups (21.1% White, 9.2% Indian and 4% Black: $p=0.012$) (Fig. 4).

At the V2 segment on the left, differences observed were not significant across the racial groups (7.6% White, 4.2% Indian and 4.5% Black: $p=0.093$), but the differences were significant on the right (8.6% White, 4.2% Black and 3% Indian: $p=0.008$). A total of 30% of the cases of tortuosity at the V1 segment on the left is among the elderly patients above 60 years ($p<0.001$); on the right, 26.1% also for the elderly group ($p<0.001$). At the V2 segment on the left, 10.4% is among the elderly patients $p=0.514$ left 10.4% for the elderly ($p=0.514$), and on the right, 10.7% ($p=0.243$) (Fig. 5).

Diameter

The average diameter of the VA in the typical + variation group, the typical group only, and the variation group only at V1 is summarized in Table 3. The average diameter on the left side was significantly larger than the right in all (typical + variation group, typical group $p=0.000$) except in variation group where we registered significantly larger right than the average diameter on the left side ($p=0.011$). Considering sex difference, males [right 3.61 (0.78), left 3.69 (0.88)] and females [right 3.61 (0.79), left 3.69 (0.97)] had the same diameter on both sides. The average diameter within the racial groups at the V1 segment is summarized in Table 4.

At the V2 segment, the average diameter was significantly larger on the left compared to the right $p=0.000$ (Table 5). The average diameter within the racial groups at the V2 segment is summarized in Table 4. Considering sex difference, the average diameter in males [right 3.43 (0.71), left 3.60 (0.79)] was not significantly different from that of females [right 3.52 (0.71), left 3.62 (0.88)] (right $p=0.250$, left $p=0.750$).

Hypoplasia and pattern of dominance

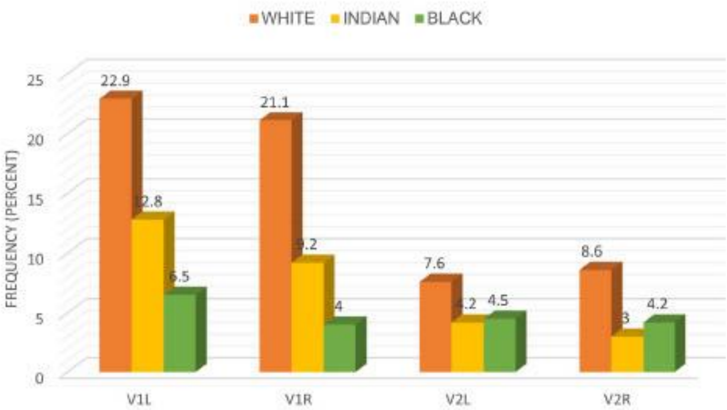

Fig. 4 Bar chart of the incidence of tortuosity across the racial groups (color figure online)

Incidence of VA hypoplasia and pattern of dominance at the V1 and V2 segments are summarized in Table 6. Males had

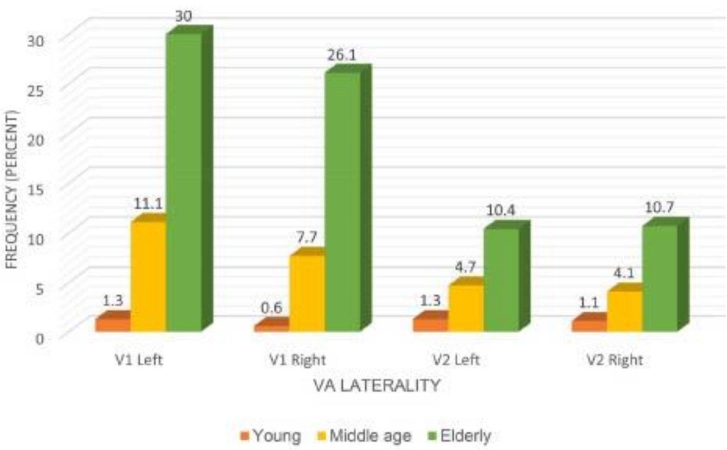

Fig. 5 Bar chart of the incidence of tortuosity in relationship with age. We categorized the age as young (10–39), middle age (40–59) and elderly (60–99) (color figure online)

a slightly higher proportion of hypoplastic arteries (4.2%) compared to females (2.9%) on the right side, though this was not significant ($p=0.643$). On the left side, 3.6% were females, 2.3% were males ($p=0.056$).

Considering sex differences, there was no significant difference in the average length of males [right 38.49 (11.89), left 43.37 (12.01)] and females [right 37.92 (10.59), left 42.24 (11.77)]: right ($p=0.685$), left ($p=0.376$). The average length within the racial groups at V1 segment is summarized in Table 4.

Table 3 Average diameter, length, and laterality of the VA V1 segment in all the cases, variation group only and typical group only

	Typical + variation group morphometrics		Variation group morphometrics		Typical group morphometrics	
	Laterality		Laterality		Laterality	
	Left median (IQR)	Right median (IQR)	Left median (IQR)	Right median (IQR)	Left median (IQR)	Right median (IQR)
Number	554	554	38	38	516	516
Average diameter (mm)	3.69 (0.88)	3.61 (0.79)	3.30 (0.74)	3.78 (0.73)	3.69 (0.88)	3.60 (0.79)
Average length (mm)	42.91 (11.89)	38.22 (11.09)	85.22 (23.82)	44.80 (15.15)	41.97 (11.49)	37.76 (11.08)

Results are reported as median (IQR) in mm

At the V2 segment on the right side, 3.1% cases of hypoplasia were in females, 4.7% in males ($p=0.488$); on the left side, 2.9% in females, 3.2% in males ($p=0.765$). Hypoplastic arteries were noted bilaterally in five patients (0.9%) at V1 and V2 segment.

Length

The average length at the V1 segment in the typical + variation, variation and typical group is summarized in Table 3. The left VA was significantly larger in all the groups ($p=0.000$).

The average length at the V2 segment is summarized in Table 5. A significant difference was noted between left and right ($p=0.029$). Considering sex differences, the average length in males [right 59.66 (13.19), left 61.25 (12.46)] was significantly larger on the right compared with the females [right 56.96 (12.03), left 59.84 (11.88)]. Right $p=0.021$, Left $p=0.128$. The average length within the racial groups at V2 segment is summarized in Table 4.

Table 4 Average diameter and length of the proximal VAs (V1, V2) and laterality in South African racial groups

	V1		V2	
	Left	Right	Left	Right
Black				
Diameter	3.52 (0.88)[a]	3.43 (0.79) NS	3.43 (0.66)[a]	3.34 (0.79) NS
Length	40.26 (15.26)[c]	35.57 (12.41) NS	59.64 (12.49) NS	59.31 (14.33) NS
Indian				
Diameter	3.82 (0.88)[ab]	3.70 (0.79) NS	3.78 (0.70)[bc]	3.52 (0.71) NS
Length	44.50 (13.18)[c]	39.05 (12.84) NS	62.07 (14.89) NS	59.84 (15.61) NS
White				
Diameter	3.69 (0.79)[a]	3.70 (0.79) NS	3.69 (0.79)[a]	3.52 (0.71) NS
Length	42.53 (10.86) NS	37.97 (10.21) NS	60.37 (10.95) NS	57.86 (11.63) NS

Results are reported as median (IQR) in mm

Significant difference a, b, c $p<0.05$ (Kruskal–Wallis test followed by Wilcoxon Signed Rank test), *NS* No statistical significance

[a]Black vs White

[b]Indian vs White

[c]Indian vs Black

Table 5 Average diameter, length, and laterality at the V2 segment

Parameter	LVA median (IQR)	RVA median (IQR)	Wilcoxon sign rank *p* value
Diameter (mm)	3.60 (0.86)	3.52 (0.71)	0.000*
Length (mm)	60.73 (12.24)	58.25 (12.67)	0.000*

Results are reported as median (IQR) in mm

p value <0.05 was considered statistically significant

LVA left VA, *RVA* right VA

Discussion

Previously, it was suggested that variable origin of the VA did not result in clinical symptoms [21, 27]. However, a recent review of literature has shown that anatomical variations in origin may be symptomatic when they coexist with vascular malformations such as aneurysms, aortic dissection, coarctation, and congenital heart disease [25]. Some researchers have also indicated that knowledge of this variation is crucial for head and neck surgical procedures, angiographies, carotid artery or VA stent placement and during the evaluation of vascular pathologies such as arterial dissection [24, 37]. The most-reported variation in the origin of the VA artery is the emergence of left VA (LVA) directly from the AOA [2, 25]. Our study follows this trend as all variant origins are from the AOA between the left subclavian artery and the left common carotid artery (Fig. 3a, 6a and 7, 2a). The incidence in the current study (6.9%) is similar to previous cadaveric report from South African population (8.5%) (Doctoral dissertation, University of Cape Town). Our result is also comparable to recent reports that used similar imaging modalities (CTA) in an Egyptian population (7%) [1] but slightly higher than reports from Republika Srpska population (4.47%) [40] and Turkish population (3.6%) [2]. In the present study, the comparison of the incidence across the racial groups showed that variation in origin is highest in White (3.6%), followed by Indian (2.5%) and least in Black (0.7%) South African. However, the differences were not significant. All the right VA took their origin from the subclavian artery, although two of the right VA arose from the subclavian artery close to the bifurcation of the innominate artery (brachiocephalic artery) (Fig. 3b). These two VA entered the TF of C4 and C5. The contralateral VA on the left, which originated from the AOA, ascends via the same TF. This type of bilateral variation compares favorably to the study reported by Amgain [3].

Table 6 Incidence of hypoplasia and pattern of dominance at the V1 and V2 segments

VA segment	VAH			VAD		
	Right	Left	Bilateral	Right	Left	Codominance
V1 *n* (%)	39 (7)	33 (6)	5 (0.9)	216 (39.7)	284 (52.2)	44 (8.1)
V2 *n* (%)	43 (7.8)	34 (6.1)	5 (0.9)	206 (37.3)	318 (57.6)	28 (5.1)

VAD VA dominance, *VAH* VA hypoplasia

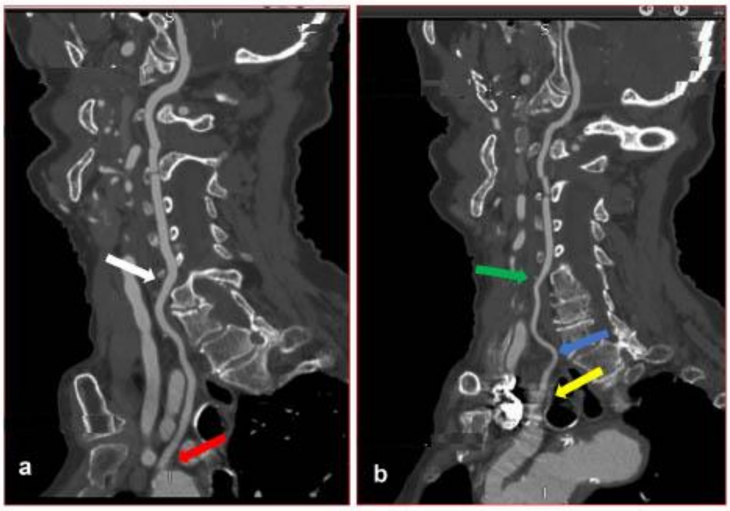

Fig. 6 Sagittal view of the left (**a**) and right (**b**) VA of a female patient. **a** The left VA (red arrow) originates directly from the AOA and enters through the transverse foramen of C5 (white arrow). **b** The right VA took origin from the right subclavian artery (yellow arrow) and ascends through the transverse foramen of C4 vertebra (green arrow). The blue arrow shows single medial loop at the V1 segment (color figure online)

Variation in the origin is often associated with other morphological variations, such as the level of entry into the TF. Complete knowledge of typical anatomy and awareness of possible variation are crucial to prevent iatrogenic injuries to the artery. Preoperative information of anatomical variation with regards to the point of entry of the VA is important to reduce the risk of injury during an anterior and lateral approach to the cervical spine [4]. Interestingly, in the present study, all the left VAs that originated from the AOA entered the TF of cervical vertebrae other than that of C6 vertebra except 1 (2.6%) (Table 1). Previous reports have shown that the highest prevalence of anomalous entry is at C5, followed by C4, C7, and the least reported is at C3 [1, 40]. The typical and variation group on both left

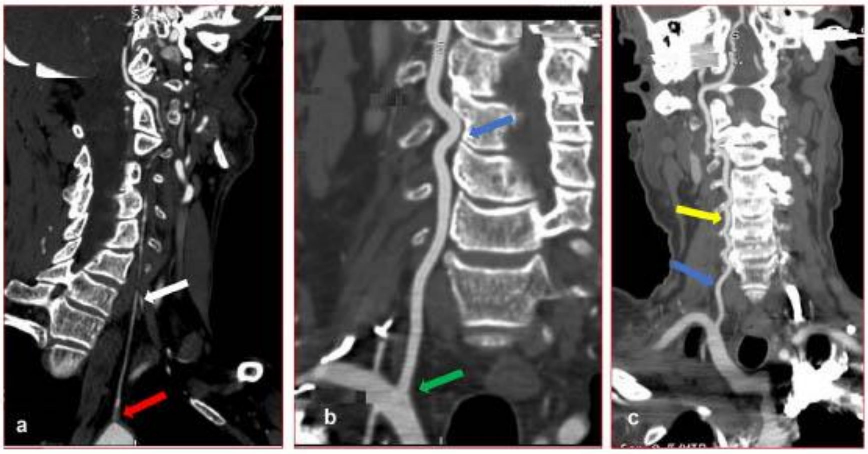

Fig. 7 Coronal view of CTA images of a male (**a**, **b**) and female (**c**) patients showing variation in origin, hypoplasia, medial loop at V2 and mild tortuosity at V1 and V2. **a** Red arrow shows origin of the left hypoplastic vertebral artery (white arrow) from the aortic arch. **b** The dominant right VA emanates from the subclavian artery (green arrow) with a single medial loop into the vertebral body of C4 (blue arrow). **c** Shows mild tortuosity at V1(blue arrow) and V2 segments (yellow arrow) of the right VA (color figure online)

and right sides in our report follows a similar trend. Even though all the right VAs took origin from the subclavian artery, 9.4% (52) exhibited variation in the level of entering the TF (Fig. 7, Table 1). Our results indicate that variation in the point of entry into the TF is not predictable. It can occur even when the artery has a typical origin. However, it should be suspected on the contralateral right VA when there is variation in origin on the left. In the present study, variation in the point of entering the TF appears common on the right when the left VA originates from the AOA, as shown in Fig. 3a, b.

Fundamental knowledge about the complex embryogenesis of the VA can give some clues to understanding the basis of variation in its morphology. As previously known, the VA is formed around the 32nd day of the embryonic stage (during 7–12 mm embryo stage) by the persistence of multiple longitudinal anastomotic chains between the six (or seven) adjacent cervical intersegmental arteries (CIA) formed from the longitudinal arteries of the aortic trunk [14]. According to George and Bruneau, each of these intersegmental arteries is a potential site of arterial agenesis that could result in morphologic variation (George and Bruneau 2011). During the stage of fusion and anastomosis, complications could result in various vascular anomalies like the variation in origin and point of entering the foramina transversarium, tortuosity, hypoplasia, and asymmetry right and left VA as observed in the present study. We hypothesized that complications might set in due to some genetic and environmental factors.

The site of origin of the VA depends on the CIA that persists at the adult stage to become the prevertebral segment, which is usually the sixth CIA [35]. A possible explanation for variation in origin from the AOA, as observed in the present study (Fig. 2a, 3a, 6a and 7a), is the persistence of a single primitive CIA other than the sixth [13]. The persistence of two primitive CIAs simultaneously may duplicate the origin of the VA [13]. However, we did not observe any case of duplicate origin in the present study. Some researchers have suggested that the persistent vessel can be identified by its level of entrance into the TF rather than by its origin [5, 13]. For instance, a VA formed by persistent 5th CIA always enters the C5 TF although may originate from the subclavian artery, AOA, or other previously reported variant origins. According to this theory, anomalous entry of the VA into the TF reported at C3, C4, and C5 in the present study is due to persistent 3rd, 4th, and 5th CIAs. We also report on the point of entry into the TF of the C7 vertebra, but it is unclear which CIA persisted at this level for its occurrence.

Normally, the course of the VA at V1 and V2 segments is straight. However, due to anatomical variation, VA sometimes demonstrates slight loops in all directions. These can result in a significant and potentially dangerous medial or a lateral artery displacement known as tortuosity. VA tortuosity is an uncommon congenital or acquired anomaly mostly reported at the proximal VAs (V1, V2) and rarely reported at the distal part of the artery. The embryogenesis of tortuous VA is not clear [18]. It is also difficult to assess the suggested congenital origin, according to some authors, since vascular tortuosity increases with age [2]. Morris et al. reported that vertebrobasilar artery tortuosity develops in association with connective tissue disorders [32]. Other authors postulate reduced elasticity, degeneration of blood vessels, and vascular wall shear stress as a possible cause [18, 26]. Another study suggested that vascular risk factors (such as hypertension, diabetes, and lipid metabolism disorders) may promote atherosclerosis, aging, and blood vessels' degeneration, thereby aggravating the vertebrobasilar artery tortuosity [20]. However, there is no conclusion on the mechanism of formation. In the present study, tortuosity occurs most frequently at V1 in elderly patients (Fig. 5). We hypothesized that the weakness of the connective tissue that makes up the vascular wall due to aging might contribute to the formation of a tortuous vessel. Also, its frequency at the V1 segment may be because this part of the artery is unconfined while the TF supports the V2 segment in its entire course. Some researchers have suggested that progressive medial deviation of loops of the tortuous VA at the V2 segment (as shown in Fig. 2b 7b) may erode the vertebral body and further cause TF enlargement and nerve root entrapment [2, 4]. A wide range of neurovascular problems has been diagnosed in association with loop formation, as reported in the literature [10, 19]. In contrast, another study suggested that VA loops and tortuosity are asymptomatic and incidentally diagnosed during the evaluation of neck problems and trauma [7]. This information suggests that VA tortuosity may be a co-factor for the clinical symptoms mentioned above and not the primary cause. The prevalence of VA tortuosity has been previously reported in the literature. A Turkish population sample of 35 patients reported 78.3% and 21.6% tortuosity at V1 and V2, respectively [42]. A Japanese study found only one medial loop at V2 out of 1054 patients [41], while a similar study reported 13.6% cases of tortuosity in 110 patients at the V2 segment [2]. Other authors reported no incidence of tortuosity in their population [28]. Most of these reports are from the Asian continent. Incidence of tortuosity seems to exist at a dissimilar rate in different regions, and data from the African population are scarce. In the present work, we report 76.6% and 32.1% tortuosity at the V1 and V2, respectively. This finding is consistent with the previously mentioned report from the Turkish population. Based on our findings, the incidence across the racial groups was similar on the left but significantly high in White on the right at V1 and V2 (Fig. 2c 7c). A possible explanation for the disparity in the rate of occurrence of tortuosity in various populations, as mentioned above, and across the South African racial groups, may be differences in the genetic make-up coupled with other environmental factors. Previous study has shown that tortuosity increases with age [2], and this is probably why it is sometimes described as an acquired anomaly. In agreement with this observation, our result shows that the incidence of tortuosity is common in elderly patients (age range 60–99 years). Tortuosity predisposes the VA to iatrogenic risk during instrumentation procedure especially in corpectomy [2, 8]. In the present study, series of mild, medial, and lateral single; and multiple loops (Figs. 3a, 6b, 7b, c, 2b, c) were seen most at the V1 and less frequently at the V2 segment. Our results indicate that incidence of tortuosity is high in the studied group and should be cautiously look out for during preoperative planning.

Noticeably in the variation group, the VA's width at the V1 segment is significantly larger on the right compared to the left (Table 3). We hypothesized that the left VA of AOA origin frequently has a reduced diameter or sometimes hypoplastic while the right VA is likely to be the dominant artery. A recent anatomic study on Chinese cadavers observed similar significantly larger right VA compared with the left VA in a group with variant LVA origin [28]. This morphologic variation should be considered during the endovascular intervention and preoperative planning around the V1 segment when the origin of the LVA is from the AOA. According to a pathology textbook, 80% of people have a left dominant VA [15]. This theory has also been corroborated by most authors reporting larger left VA in the literature. Our study supports this trend as the average diameter at the V1 segment is similar to that of the Egyptian population ($3.67 \pm 1.07, 3.36 \pm 0.93$) [1], with the left significantly larger than the right side. A consistent significantly larger left was also observed at the V2 segment in the present study. This information is essential during preoperative planning: iatrogenic injury to the dominant VA can result in death [17]. Cervical spine surgery or screw fixation is best carried out on the right side of the cervical vertebrae in this situation so that the left VA can sustain the blood flow in the vertebrobasilar system in case of iatrogenic injury to the right VA.

A condition where the lumen diameter of the VA is exceptionally small in its entire length and terminates at its fusion with the contralateral artery to form the basilar trunk is described as VA hypoplasia (VAH) (Fig. 6a, 7a) [15]. VAH is a frequent morphological variation with a history of underestimated clinical significance. Probably because it is a common finding in asymptomatic population [22]. However, accumulating evidence has shown that VAH is commonly observed in patients with posterior circulation stroke and VA occlusion [22, 31]. This suggests that VAH can predispose to posterior circulation stroke. This may be the possible explanation for the high prevalence of VAH reported by studies using suspected stroke and acute ischemia patients 15.6% [38], and 31.5% [31]. There is no consensus as regards the diameter value for VAH. Authors have used criteria ranging from ≤ 2 mm to ≤ 3 mm [11, 12, 28].

In the present study, a diameter < 2.7 mm is regarded as hypoplastic, as previously described by [12]. Ergun et al. defined VAH using a ≤ 2 mm criterion found an incidence of 7.1% on the right and 9.4% on the left in patients examined by digital subtraction angiographies [11]. In a CT study by Abd El Gawad et al. In a CT study by Abd El Gawad et al. VAH was defined by a diameter ratio of 1:2 between the two VAs and found an incidence rate of 8% on the left, and 3% on the right between the two VAs found an incidence rate of 8% on the left, and 3% on the right [1]. Our findings showed the number of patients with hypoplastic VA on the right at V1 was 7% (39 individuals) and 6% (33 individuals) on the left. At the V2 segment on the right, there was a slight increase in the number of patients, 7.8% (43 individuals), while the number is similar on the left, 6.1% (33 individuals). The prevalence in our study is consistent with the above report by Abd El Gawad et al. using similar imaging protocols and patient characteristics.

Several factors contribute to the challenges of selecting a universal cut-off value of VAH for the general population. The average VA diameter recorded in the literature varies because most of the studies report on different segments of the artery. The differences in the modality of the studies can also contribute to the reported disparity in the average diameter. A recent report has shown a strong correlation between the diameter of the VA and anthropometric parameters like height [12]. All these factors and suspected genetic and environmental factors may be the basis for the differences reported in the literature. The incidence of bilateral hypoplasia in the present study is observed only in 5 patients (0.9%) at V1 and V2. Our findings indicate that the dominant artery can be preserved in most cases during instrumentation procedures since VAH is rare bilaterally.

Vertebral artery dominance (VAD) is a congenital structural variation of the VA characterized by a significant diameter difference between bilateral VAs of the same individual. The prominent VA is now described as the dominant. The embryogenesis of this morphologic variation is not clear, just like that of the VAH. Some researchers hypothesized differences in the origin of bilateral VAs as the possible cause of left dominant VA [29, 44]. The left VA being a second branch of the aorta, while the right VA is the third branch. However, this theory fails to explain the mechanism of the formation of right dominancy. VAD was previously described as mere structural variation without clinical relevance until recently. Researchers now identify VAD as a risk factor for posterior circulation infarction, brainstem infarction, and transient ischemic attack [29, 44].

Scholars have adopted numerous criterion for the definition of VAD in the literature, and till present, there was no agreement on the standard criteria. A recent study using magnetic resonance angiography used a side difference of ≥ 0.3 mm and found left VA to be dominant in 63.6% [43] patients. Other researchers used a size difference of ≥ 1.2 mm and showed similar results in 56.4% of patients with similar image modalities [44]. Ozdemir et al. adopted a standard of VAD using any size difference criteria between the bilateral VAs and observed 64% left dominancy and 31% right dominance with color Doppler ultrasound [34]. As mentioned above, the studies' results were consistently similar even with different dominance criteria. Based on the criteria of any size difference, the VA width in the present study was evaluated as left dominant in 52.2% (V1), 57.6% (V2), right dominant in 39.7% (V1), 37.3% (V2), and codominance in 8.1% (V1), 5.1% (V2) (Table 6). Our result is consistent with the previous report as we report left VAD in most patients. Therefore, it is possible for physicians performing procedures around the VA to preserve the dominant VA, which is expected on the left side in most cases. However, a case-by-case review of preoperative investigations may be required for interventions in the vicinity of the VA as well as for diagnosis of pathologies in the posterior circulatory territory. This is due to the unpredictable nature of variation as noticed in our report.

In the present study, the average length of the variation group at the V1 segment was almost twice the length of the right. This is obviously because all the left VAs in this group emanated directly from the AOA. However, the average length of the left VA in the typical group was also significantly larger than the right. A possible explanation for the side-to-side differences observed in the typical group is the asymmetric origins of the right and left subclavian arteries [39]. However, this theory is yet to be proven and requires further investigation. Few anatomical studies have documented the average length of the first segment of the VA in the literature. Veeramani and Shankar reported a significant difference between left (4.1 ± 1.7 cm equivalent to 41 mm) and right (3.4 ± 1.2 cm equivalent to 34 mm) in 33 Indian cadavers [39]. Our findings are similar to the above study report, as we observe average length 42.91 (11.89) mm and 38.22 (11.09) mm on the left and right VA, respectively. Similar to the V1 segment, the average length of the left VA at the V2 segment is significantly larger than the right (Table 5). We assumed that the above-suggested reason for the V1 segment might have positioned the entire length of the left VA higher than the right.

Generally, because of the unpredictable nature of anatomical variation, the physician performing surgery around the proximal VA needs to be aware of safe technique and standard anatomy and possible anatomical variations [16]. Opinion differs about the necessities of routine preoperative angiographies for evaluating cerebral vasculature due to its downsides such as ionizing radiation and iodinated contrast [33]. While some authors propose CTAs before cervical spine interventions [2], others have suggested that it is unnecessary, especially when the prevalence of anatomical variations of the VAs is low in a population group [33]. The importance of in-depth knowledge of VA anatomy in patients undergoing cervical spine surgery cannot be overemphasized. This is required for a detailed analysis of the preoperative radiograph [8]. Due to morphological variations and frequencies of tortuosity reported in the population in the present study, we hypothesized that CTA might be required for safe surgical interventions around the VA and endovascular treatment of vascular pathologies.

Study limitation

Firstly, this is a single-center retrospective study with the possibility of selection bias. Secondly, specific information about the interracial difference was not provided in the patient's report. Therefore, the authors relied on the available information in the hospital database to deduce patients' race since the study is retrospective.

Conclusion

Anatomical variations of the VA are common in the South African population studied in this work. All variant origin was observed on the left without any significant racial or gender difference. Variation in the point of entry into the TF is similar on both sides. Tortuosity is common in the V1 segment and frequently observed in elderly patients. The average diameter was significantly larger on the left in all the racial groups, but there were no significant gender differences. Hypoplasia occurs at a similar rate on both left and right, and we registered a left dominance pattern. The presence of these morphological variations can influence treatment options for procedures in the head and neck, and regions of the supra-aortic arch. Awareness of the extent of possible anatomical variation will help in interpreting radiographs which will enhance identification of vascular pathologies and will also reduce the risk of iatrogenic injury.

Author contributions All persons listed as authors have contributed substantially to the protocol development, project design, data collection and data analysis of this manuscript. LL, BRO, KSS, RH: conceptualized project. BRO, RH, IGM: collected data. BRO, LL: analyzed data. LL, RH, IGM, BRO: manuscript writing and editing.

Funding Funding was provided by College of Health Sciences, University of Kwazulu-Natal, Durban, South Africa.

Compliance with ethical standards

Conflict of interest The authors declare that they have no conflicts of interest.

Ethics approval The design was approved by the Institutional Review Board/Ethics Committee (Biomedical Research Ethics Committee of the University of KwaZulu-Natal with ethical No: BE 148/19).

Availability of data Available on request.

References

1. Abd El Gawad FA, Shaaban MH, Shuaib DM, Shallan HM (2019) Anatomical variations of the vertebral artery and its relation to the atlas vertebra-radiological and dry bone study. Eur J Anat 23:49–58
2. Alicioglu B, Gulekon N, Akpinar S (2015) Age-related morphologic changes of the vertebral artery in the transverse process. Analysis by multidetector computed tomography angiography. Spine J 15:1981–1987. https://doi.org/10.1016/j.spinee.2015.04.031
3. Amgain K (2019) Role of anatomical variation of vertebral artery in clinical practice. EC Clin Exp Anat ECO 1:27–29
4. Bruneau M, Cornelius JF, Marneffe V, Triffaux M, George B (2006) Anatomical variations of the V2 segment of the vertebral artery. Oper Neurosurg 59:ONS-20-ONS24
5. Caldemeyer KS, Carrico JB, Mathews VP (1998) The radiology and embryology of anomalous arteries of the head and neck. AJR Am J Roentgenol 170:197–203
6. Campero A, Rubino PA, Rhoton AL (2011) Anatomy of the vertebral artery. Pathology and surgery around the vertebral artery. Springer Paris, Paris, pp 29–40. https://doi.org/10.1007/978-2-287-89787-0_4
7. Chibbaro S, Mirone G, Yasuda M, Marsella M, Di Emidio P, George B (2012) Vertebral artery loop—a cause of cervical radiculopathy. World Neurosurg 78(375):e311-375. https://doi.org/10.1016/j.wneu.2011.12.002 (e313)
8. DeCarvalho SA, Abd-El-Barr MM, Groff MW (2019) Vascular complications in cervical spine surgery (anterior and posterior approach). Complications in neurosurgery. Elsevier, Amsterdam, pp 314–319
9. Deng D, Cheng FB, Zhang Y, Zhou HW, Feng Y, Feng JC (2012) Morphological analysis of the vertebral and basilar arteries in the Chinese population provides greater diagnostic accuracy of vertebrobasilar dolichoectasia and reveals gender differences. Surg Radiol Anat 34:645–650. https://doi.org/10.1007/s00276-012-0960-9
10. Doweidar A, Al-Sayed S, Al-Kandery S (2014) Symptomatic vertebral artery loop: a case report and review of literature. Radiol Case Rep 8:35. https://doi.org/10.3941/jrcr.v8i5.1407
11. Ergun O, Tatar IG, Birgi E, Hekimoglu B (2016) Evaluation of vertebral artery dominance, hypoplasia and variations in the origin: angiographic study in 254 patients. Folia Morphol 75:33–37. https://doi.org/10.5603/FM.a2015.0061
12. Gaigalaite V, Vilimas A, Ozeraitiene V, Dementaviciene J, Janilionis R, Kalibatiene D, Rocka S (2016) Association between vertebral artery hypoplasia and posterior circulation stroke. BMC Neurol 16:118. https://doi.org/10.1186/s12883-016-0644-x
13. Gailloud P (2019) Vertebral artery triplication. Surg Radiol Anat 41:841–843. https://doi.org/10.1007/s00276-019-02192-0
14. George B, Bruneau M (2011) Embryology of the vertebral artery. Pathology and surgery around the vertebral artery. Springer, Heidelberg, pp 5–24
15. George B, Laurian C (2012) The vertebral artery: pathology and surgery. Springer Science & Business Media, Heidelberg
16. Gitkind AI, Olson TR, Downie SA (2014) Vertebral artery anatomical variations as they relate to cervical transforaminal epidural steroid injections. Pain Manag 15:1109–1114. https://doi.org/10.1111/pme.12266
17. Guan Q, Chen L, Long Y, Xiang Z (2017) Iatrogenic vertebral artery injury during anterior cervical spine surgery: a systematic review. World Neurosurg 106:715–722. https://doi.org/10.1016/j.wneu.2017.07.027
18. Han H-C (2012) Twisted blood vessels: symptoms, etiology and biomechanical mechanisms. J Vasc Res 49:185–197. https://doi.org/10.1159/000335123
19. Hong-tao Z, Shu-ling Z, Dao-pei Z (2014) Two case reports of bilateral vertebral artery tortuosity and spiral twisting in vascular vertigo. BMC Neurol 14:14. https://doi.org/10.1186/1471-2377-14-14
20. Ikeda K, Nakamura Y, Hirayama T, Sekine T, Nagata R, Kano O, Kawabe K, Kiyozuka T, Tamura M, Iwasaki Y (2010) Cardiovascular risk and neuroradiological profiles in asymptomatic vertebrobasilar dolichoectasia. J Stroke Cerebrovasc Dis 30:23–28. https://doi.org/10.1159/000313440
21. Ka-Tak W, Lam WW, Yu SC (2007) MDCT of an aberrant right subclavian artery and of bilateral vertebral arteries with anomalous origins. AJR Am J Roentgenol 188:W274–W275. https://doi.org/10.2214/AJR.05.0694
22. Katsanos AH, Kosmidou M, Giannopoulos S (2013) Vertebral artery hypoplasia in posterior circulation cerebral ischemia. Clin Neurol Neurosurg 115:1194–1195. https://doi.org/10.1016/j.permed.2012.02.063
23. Khalfani AK, Zuberi T (2001) Racial classification and the modern census in South Africa, 1911–1996. Race and society 4:161–176. https://doi.org/10.1016/S1090-9524(03)00007-X
24. Komiyama M, Morikawa T, Nakajima H, Nishikawa M, Yasui T (2001) High incidence of arterial dissection associated with left vertebral artery of aortic origin. Neurol Med Chir (Tokyo) 41:8–12. https://doi.org/10.2176/nmc.41.8
25. Lazaridis N, Piagkou M, Loukas M, Piperaki E-T, Totlis T, Noussios G, Natsis K (2018) A systematic classification of the vertebral artery variable origin: clinical and surgical implications. Surg Radiol Anat. https://doi.org/10.1007/s00276-018-1987-3
26. Lee SH, Hur N, Jeong S-K (2012) Geometric analysis and blood flow simulation of basilar artery. Atheroscler Thromb 19:397–401. https://doi.org/10.5551/jat.10694
27. Lemke A-J, Benndorf G, Liebig T, Felix R (1999) Anomalous origin of the right vertebral artery: review of the literature and case report of right vertebral artery origin distal to the left subclavian artery. Am J Neuroradiol 20:1318–1321

28. Li X, Guan L, Zilundu PLM, Chen J, Chen Z, Ma M, Zhuang H, Zhuang Z, Qiu Y, Ye F (2019) The applied anatomy and clinical significance of the proximal, V1 segment of vertebral artery. Folia Morphol 78:710–719. https://doi.org/10.5603/FM.a2019.0039
29. Meng X, Ding W, Wu X, Di P (2018) Clinical investigation and characterization of vertebrobasilar dolichoectasia and vertebral artery dominance. Discov Med 25:151–158
30. Mitchell J (2004) Differences between left and right suboccipital and intracranial vertebral artery dimensions: an influence on blood flow to the hindbrain? Physiother Res Int 9:85–95. https://doi.org/10.1002/pri.305
31. Mitsumura H, Miyagawa S, Komatsu T, Hirai T, Kono Y, Iguchi Y (2016) Relationship between vertebral artery hypoplasia and posterior circulation ischemia. J Stroke Cerebrovasc Dis 25:266–269. https://doi.org/10.1016/j.jstrokecerebrovasdis.2015.09.027
32. Morris SA, Orbach DB, Geva T, Singh MN, Gauvreau K, Lacro RVJC (2011) Increased vertebral artery tortuosity index is associated with adverse outcomes in children and young adults with connective tissue disorders. Circ J 124:388–396. https://doi.org/10.1161/CIRCULATIONAHA.110.990549
33. O'Donnell CM, Child ZA, Nguyen Q, Anderson PA, Lee MJ (2014) Vertebral artery anomalies at the craniovertebral junction in the US population. Spine J (Phila Pa 1976) 39:E1053–E1057. https://doi.org/10.1097/brs.0000000000000447
34. Ozdemir S, Yildiz C, Cankur N (2002) Evaluation of vertebral artery system in a healthy population by using colour duplex Doppler ultrasonography. Med School J Uludag 28:95–99
35. Padget DH (1948) The development of the cranial arteries in the human embryo. J Contrib Embryol 32:205–261
36. Piccinin MA, Munakomi S (2019) Neuroanatomy, Vertebrobasilar System. In: StatPearls [Internet]. Treasure Island (FL): StatPearls Publishing; 2020 Jan-. Available from: https://www.ncbi.nlm.nih.gov/books/NBK540995/
37. Poonam SR, Sharma T (2010) Incidence of anomalous origins of vertebral artery–anatomical study and clinical significance. JCDR 4:2626–2631
38. Thierfelder KM, Baumann AB, Sommer WH, Armbruster M, Opherk C, Janssen H, Reiser MF, Straube A, von Baumgarten L (2014) Vertebral artery hypoplasia: frequency and effect on cerebellar blood flow characteristics. Stroke 45:1363–1368. https://doi.org/10.1161/STROKEAHA.113.004188
39. Veeramani R, Shankar N (2014) Anatomical variations of the pre-transverse segment of the vertebral artery in Indian cadavers. Eur J Anat 18:159–163
40. Vujmilović S, Spasojević G, Vujnović S, Malobabić S, Vujković Z (2018) Variability of the vertebral artery origin and transverse foramen entrance level—CT angiographic study. Folia Morphol (Praha) 77:687–692. https://doi.org/10.5603/FM.a2018.0036
41. Wakao N, Takeuchi M, Nishimura M, Riew KD, Kamiya M, Hirasawa A, Imagama S, Kawanami K, Murotani K, Takayasu M (2016) Risks for vascular injury during anterior cervical spine surgery: prevalence of a medial loop of vertebral artery and internal carotid artery. Spine J (Phila Pa 1976) 41:293–298. https://doi.org/10.1097/BRS.0000000000001241
42. Yenigun A, Ustun M, Tugrul S, Dogan R, Ozturan OJTJoL (2016) Classification of vertebral artery loop formation and association with cervicogenic dizziness. J Laryngol Otol 130:1115–1119. https://doi.org/10.1017/S0022215116009117
43. Zhang D-p, Zhang S-l, Zhang J-w, Zhang H-t, Fu S-q, Yu M, Ren Y-f, Ji P (2014) Basilar artery bending length, vascular risk factors, and pontine infarction. J Neurol Sci 338:142–147. https://doi.org/10.1016/j.jns.2013.12.037
44. Zhu W, Wang Y-f, Dong X-f, Feng H-x, Zhao H-q, Liu C-f (2016) Study on the correlation of vertebral artery dominance, basilar artery curvature and posterior circulation infarction. Acta Neurol Belg 116:287–293. https://doi.org/10.1007/s13760-015-0570-5

BRIDGING TEXT

FROM CHAPTER TWO TO THREE

The published article in chapter two investigated the typical anatomy and prevalence of variations at the first (V1) and second (V2) segments of the VAs. Findings from the previous chapter showed that anatomical variations are common at the proximal part of the VA in the South Africa population studied. We also realized that some of the variant anatomies coexist, and when one is present, another can be suspected. The next chapter investigates the anatomy of the suboccipital segment (V3) of the VA, including details of the morphometry and prevalence of variant anatomy in a South Africa population. Details of the findings are compared to reports from other population groups, and the clinical importance of preoperative knowledge of registered variations were highlighted.

CHAPTER THREE

MANUSCRIPT TWO

RADIOLOGICAL ANATOMY OF THE SUBOCCIPITAL SEGMENT OF THE VERTEBRAL ARTERY IN A SELECT SOUTH AFRICAN POPULATION

Bukola R. Omotoso[1], Rohen Harrichandparsad[2], Kapil S. Satyapal[1], Lelika Lazarus[1]

[1]Discipline of Clinical Anatomy, School of Laboratory Medicine and Medical Sciences, College of Health Sciences, University of KwaZulu-Natal, Westville Campus, Private Bag X54001, Durban, South Africa.

[2]Department of Neurosurgery, School of Clinical Medicine, College of Health Sciences, Nelson R Mandela School of Medicine, University of KwaZulu-Natal, Durban, South Africa.

Corresponding Author: Professor L Lazarus

Address: Discipline of Clinical Anatomy, School of Laboratory Medicine and Medical Sciences, College of Health Sciences, University of KwaZulu-Natal, Westville Campus, Private Bag X54001, Durban, South Africa.

Email address: ramsaroopl@ukzn.ac.za

+27 31 260 7899

Submitted to the European Journal of Anatomy on the 25th of January 2021. (Currently under review)

Manuscript number: 210052ll

TITLE PAGE

TITLE:

RADIOLOGICAL ANATOMY OF THE SUBOCCIPITAL SEGMENT OF THE VERTEBRAL ARTERY IN A SELECT SOUTH AFRICAN POPULATION

ABBBREVIATED TITLE

RADIOLOGICAL ANATOMY OF THE SUBOCCIPITAL SEGMENT OF THE VERTEBRAL ARTERY

AUTHORS:

Bukola R. Omotoso[1], Rohen Harrichandparsad[2], Kapil S. Satyapal[1], Lelika Lazarus[1]

PROFESSIONAL / INSTITUSIONAL AFFILIATION

1. Discipline of Clinical Anatomy, School of Laboratory Medicine and Medical Sciences, College of Health Sciences, University of KwaZulu-Natal, Westville Campus, Private Bag X54001 Durban, South Africa.
2. Department of Neurosurgery, School of Clinical Medicine, College of Health Sciences, Nelson R Mandela School of Medicine, University of KwaZulu-Natal, Durban, South Africa.

CORRESPONDING AUTHOR
Name: Lelika Lazarus
Institution: University of KwaZulu-Natal Dept.: Discipline of Clinical Anatomy
Address: Discipline of Clinical Anatomy,
School of Laboratory Medicine and Medical Sciences,
College of Health Sciences, University of KwaZulu-Natal,
Westville Campus.
Zip code: 4000 ; City: Durban; Country: South Africa
E-mail: ramsaroopl@ukzn.ac.za

INSTITUTION RESPONSIBLE FOR RESEARCH SUPPORT
College of Health Sciences (CHS funding), University of KwaZulu-Natal, Durban, South Africa.

DISSEMINATION HISTORY (NOT APPLICABLE)

SECTION OF THE JOURNAL
Original Articles

RADIOLOGICAL ANATOMY OF THE SUBOCCIPITAL SEGMENT OF THE VERTEBRAL ARTERY IN A SELECT SOUTH AFRICAN POPULATION

Bukola R. Omotoso, Rohen Harrichandparsad, Lelika Lazarus

Summary

Vertebral artery (VA) injuries remain one of the most encountered complications during surgical intervention at the craniovertebral junction (CVJ). Anatomically, the suboccipital is the most complicated segment of the VA. The artery undergoes a series of bends to form proximal and distal loops. In addition to this standard anatomical description, previously reported variant anatomies such as fenestration, persistent first intersegmental artery (FIA), hypoplasia, and extradural origin of the posterior inferior cerebellar artery (PICA) also contribute to the complexity of this segment. We evaluated the anatomical features of the V3 component of the VA in a South African population to provide useful data on the prevalence of variation and morphometry of the VA. The study is an observational, retrospective chart review of 554 consecutive South African patients (Black, Indian, and White) who had undergone computed tomography angiography (CTA) at Lenmed Ethekwini Hospital and Heart Centre, Durban, South Africa, from January 2009 to September 2019. Various morphological variations were registered in the course of the VA: (1) Hypoplasia; (2) Extradural (V3) origin of PICA; (3) persistent FIA; and (4) VA fenestration. Hypoplasia was observed in 5.14% of patients. The overall prevalence of the last three variations was 2.1%. Codominance was observed in 42.6% of patients, left dominance in 34.3%, and right dominance in 23.1% of patients. Since failure to identify these morphological variations can result in inadvertent injury to the VA with serious neurological consequences, it is therefore imperative to recognize these variations preoperatively. Knowledge of these variations will also assist in the interpretation of radiographs.

Key words: Suboccipital segment of the vertebral artery – Vertebral artery hypoplasia – Fenestration – Vertebral artery dominance – Posterior inferior cerebellar artery – Persistent first intersegmental artery.

TEXT

INTRODUCTION

Vertebral artery (VA) injuries remain the most common type of injury during cervical spine surgery (DeCarvalho et al., 2019). The risk of injury as a complication of surgery is a major problem, especially at the craniovertebral junction (CVJ) due to the variable course of the artery (Yamazaki et al., 2012). The VA is classically divided into four segments: The first segment (V1) extends from the origin at the subclavian artery to the C6 transverse process. The second segment (V2) extends from C6 to axis vertebra (C2) transverse processes. The third segment (V3) extends from the transverse foramen of the C2 to the point of penetration of the dura mater at the foramen magnum. The intracranial segment (V4) extends from the foramen magnum dura to the vertebrobasilar junction. The V3 part is the segment of the artery at the CVJ, also known as the suboccipital segment (Campero et al., 2011). The V3 is the most anatomically complicated segment of the VA. The artery undergoes a series of bends to form a proximal and a distal loop while passing through the transverse foramen of the axis and atlas vertebrae. Although arterial tortuosity is a morphological variation in the course of the VA frequently reported in the V1 and V2 segments, natural loop formation distinguishes the V3 from other segments of the artery.

The V3 segment of the VA is subdivided into three portions – the vertical part (V3v) ascends through the transverse foramen of C2 and atlas (C1); the horizontal part (V3h) extends from the transverse foramen of C1 and courses in the VA groove on the upper surface of the posterior arch of the atlas; and an oblique part (V3o) extends from the groove to the point of penetration of the posterior atlantooccipital membrane (George and Cornelius, 2001, Ulm et al., 2010). Apart from this standard anatomical description, anatomical variants such as fenestration, persistent first intersegmental artery (FIA), posterior inferior cerebellar artery

(PICA) arising from the V3 segment, and hypoplasia has been reported at this segment (Uchino et al., 2012, Fortuniak et al., 2016). Failure to identify these morphological variations preoperatively may compromise collateral circulation resulting in brainstem infarction (Fortuniak et al., 2016). In FIA, the VA courses below the C1 arch to enter the spinal canal after leaving the transverse foramen of C2 without passing through the transverse foramen of C1. Fenestration was registered when the VA split into two vessels along the V3 segment, which rejoined distally before entering the dura mater. The origin of the PICA from the V3 segment was recognized as the extradural origin of PICA.

The prevalence of fenestration, persistent FIA, and PICA arising from the V3 segment has been observed in the normal population without CVJ anomalies. Most of the reports are from the Asian continent (Uchino et al., 2012, Wakao et al., 2014, Kim, 2016, Arslan et al., 2019), with few reports from Europe and the United States (O'donnell et al., 2014, Fortuniak et al., 2016). Reports from the African continent are scarce. There is no report on the prevalence of morphological variation at the V3 segment in the South African population to the best of our knowledge. Genetic and environmental factors, including local hemodynamic influences, have been suggested to play a specific role in the endmost structure of the VA (Sikka and Jain, 2012). Therefore, racial differences in the Asian and Western populations could account for the disparity in the published reports (Arslan et al., 2019). As a result of this, it was considered crucial to describe the prevalence of these morphologic variations in a South African population. According to a textbook of complications in neurosurgery by DeCarvalho and co-authors, the incidence of anatomical variation increases the likelihood of injury, especially if it is not identified preoperatively (DeCarvalho et al., 2019). Therefore, the overall knowledge of the course of the V3 segment of the VA and prevalence of possible variation is essential to reduce the risk of catastrophic complications associated with vascular injury during a surgical intervention at the base of the skull (Hsu et al., 2017).

We evaluated the anatomical features of the V3 segment of the VA in a South African population using 3D computed tomography angiography (CTA) to provide valuable data on the prevalence of variation and morphometry of the VA. The reports from this study will also contribute to the knowledge of evidence-based anatomy in teaching anatomy and clinical practice.

MATERIALS AND METHODS

Patient Population

We reviewed the records of 554 South African patients who underwent multidetector CTA at Lenmed Ethekwini Hospital and Heart Centre, Durban, South Africa, from January 2009 to September 2019. The patient population represents the KwaZulu-Natal region. The design was approved by the Institutional Review Board/Ethics Committee (Biomedical Research Ethics Committee of the University of KwaZulu-Natal with ethical No: BE 148/19). The angiographies were from 307 males (55.4%) and 247 females (44.6%). The average age of the patients is reported as median (interquartile range): 62 (23) (range: 10-99) years; 62 (25) for female patients and 61 (23) for male patients. A total of 91 (16.4%) were Black, 176 (31.8%) were Indian, and 287 (51.8%) were White South Africans. Images were analyzed using a Picture Archiving Communication system (PACS) tools. The MDCTA images were examined for vascular variations by a neurosurgeon, a neuroradiologist, and an anatomist using the coronal and sagittal view. Patients with congenital abnormalities at the CVJ such as atlantoaxial dislocation, Down syndrome, Klippel-Feil syndrome, or osseous anomalies were excluded from the study to obtain data from the normal population.

Imaging Technique

The imaging examination was performed on a 64-detector row computed tomography (CT) scanner (Lightspeed CT, GE Healthcare Medical Systems, Milwaukee, WI, USA) with the following scanning protocol: 120 kVp, 697 mAs, beam collimation 64 × 0.625 mm, gantry rotation time 0.4 s, section thickness 0.625 mm, pitch 0.969:1 and reconstruction interval of 0.625 mm. During the procedure, 80 mL of non-ionic iodinated contrast followed by 40 mL saline was infused via a double power injector (Medex flowSens, Geubert USA) into the patient's antecubital vein (4 mL/s).

Dimensions of the V3 Segment

The course of the V3 segment and tortuosity (proximal and distal loop) were analyzed. The diameters, lengths, and angles of arteries were measured with the Picture Archiving Communication system (PACS) Tools. The measurement of each part of the V3 was taken on the coronal view of the CTA images (Fig.1). The diameter of the vertical portion was measured before the VA entered the transverse foramen of the atlas vertebra, while the horizontal diameter was measured above the transverse foramen of the atlas. A diameter of ≤ 2.5 mm was described as hypoplasia according to the method provided by Chen and co-authors (Chen et al., 2010). We classified the VA as dominant if the diameter was larger than that of the contralateral side by a difference of ≥ 0.3 mm according to the method described by Zhang et al. (2014). When the bilateral VAs had a similar diameter or the difference between the VAs was less than 0.3 mm, we referred to them as being "equal" or "codominant." We measured the angles between the proximal and distal loops to evaluate the degree of tortuosity. The proximal loop of the V3 is formed as the VA bends to enter the transverse foramen of the C2 vertebra. The distal loop is present at the transition from the vertical to the horizontal portion at the transverse foramen of the C1 vertebra (Fig. 1).

Statistical Analysis

Categorical and continuous variables were analyzed using SPSS version 27 (SPSS Inc., Chicago, IL, USA). Categorical variables were analyzed using the chi-square test. Because the continuous variables are not normally distributed, the Kruskal-Wallis test followed by the Wilcoxon Signed-Rank test was used to detect significant differences in the obtained values for continuous variables. All tests were performed at 95% confidence with a p-value of < 0.05.

RESULTS

Continuous variables are presented as median, interquartile range (IQR), and Range. Categorical variables are presented by a number (N) and percentage. The interclass coefficient correlation for intra-observer reliability testing was 99 % for the V3v length; 97 % for V3v diameter; 99 % for V3h length and diameter; 99 % for V3o length, proximal and distal loop. For inter-observer reliability testing, the intraclass correlation ranges between 72% to 96% for all the parameters.

Vascular Variation

We registered four types of variation at the V3 segment: (1) Hypoplasia; (2) Extradural (V3) origin of PICA; (3) persistent FIA; and (4) VA fenestration. The most frequently observed variation was hypoplasia, found in 5.6% of cases (62/1108). Incidence of bilateral hypoplasia was registered in 1.8% (10/554) of patients. The prevalence of the last three, excluding hypoplasia, was diagnosed in 4.2% (23) of the total patients (23 cases/554). There was no significant ethnic or gender difference in the incidence of variation. The results are summarized in Table 1.

Morphometric Analysis of the Vertebral Artery

Diameter

We observed that the average diameter of the VA increases from the vertical (median (IQR)) (Left- 3.43 (0.61) mm; Right- 3.25 (0.70) mm) to the horizontal part (Left- 3.69 (0.89) mm; Right- 3.60 (0.71) mm) and oblique part (Left- 3.55 (0.79) mm; Right- 3.48 (0.83) mm). The average diameter is significantly larger on the left (vertical portion p=0.000, horizontal portion p=0.001, and oblique portion p=0.006) than on the right side. Most of the VAs had similar diameters (42.6%) with differences of ≤ 0.3 mm between the two sides. We observed a left pattern of dominance in 190 patients (34.3%) and right dominance in 128 patients (23.1%). Concerning the ethnic groups, the diameter of the left V3v was significantly different across the ethnic groups (p=0.002; specifically, between Black and Indian p=0.001; between White and Indian p=0.014). On the right V3v, there was no significant difference across the ethnic groups (p=0.368). The diameter of the left V3h showed a significant difference across the ethnic groups (p=0.002; specifically, between Black and White p=0.03; Black and Indian p=0.001). On the right V3h, there was no significant difference across the ethnic groups (p=0.286). The diameter of the left V3o also showed a significant difference across the ethnic groups (p=0.014; specifically, between White and Black p=0.005; Indian and Black p=0.01). On the right V3o, there was no significant difference across the ethnic groups (p=0.315). The average diameter is summarized in Table 2. For gender, the average diameter of the V3o is significantly larger in females on the left (p=0.000). There were no significant gender differences on the right (p=0.063). The average diameter is summarized in Table 3.

Length

The length of the V3 was significantly greater on the left than the right side in all parts of the artery (median (IQR)). V3v (23.19 (11.72) mm, 21.80 (10.34) mm) p=0.000; V3h (6.75 (3.17) mm, 6.67 (3.01) mm) p=0.000; V3o (4.03 (1.96) mm, 3.82 (1.93)) mm p=0.000. Within the ethnic groups, the length of the left and the right V3v showed a significant difference across the ethnic groups (Left p=0.011, but there was no specific difference between the ethnic groups; Right p=0.005; specifically, between White and Black p=0.035; White and Indian p=0.003). The average length of the horizontal portion (V3h) showed a significant difference across the ethnic groups (Left p=0.000; specifically, between White and Black p=0.008; White and Indian p=0.000; Right p=0.000; specifically, between White and

Black p=0.011; White and Indian p=0.000). The average length of the oblique portion also showed a significant difference across the ethnic groups (Left p=0.000; between White and Black p=0.015; White and Indian p=0.000; Black and Indian p=0.025; Right p=0.000; specifically, between White and Black p=0.001; White and Indian p=0.000). The average length across the ethnic groups and laterality are summarized in Table 2. There were no significant gender differences in the VA length on both sides. The results are summarized in Table 3.

Proximal and Distal Loop Angle

The average angle of the proximal loop was significantly larger on the left (median (IQR)) (67° (24°)) compared to the right (65.66° (25.33°)) side (p=0.001). There was no significant difference in the angle of the distal loop on the right and left sides (Right- 67° (14°), Left- 66° (15°)). We did not observe any significant differences across gender and ethnic groups. The results are summarized in Table 4.

DISCUSSION

Iatrogenic injury to the VA during procedures around C1/2 constitutes a potentially catastrophic complication that may result in permanent neurological deficits or even death (Vergara et al., 2012; Akinduro et al., 2016). Studies have reported rates ranging from 1.7% - 9.0% (Vergara et al., 2012; Elliott et al., 2014; Liang et al., 2004). Adequate information about anatomical variation can influence the choice of surgical procedure at the CVJ. Apart from the risk of injury, morphological variation at the V3 segment of the VA may result in complications such as brainstem infarction if not recognized during preoperative planning (Fortuniak et al., 2016).

Hypoplasia of the VA has been previously described by different criteria in the literature. Using a measure of diameter ≤ 2.5mm according to the method provided by Chen and co-authors (Chen et al., 2010), we observed a 5.6% (62 cases/1108 VAs) incidence of hypoplastic VA (Fig 1B). Our results agreed with the findings of O'Donnell and co-authors (6.26%) in the US population, although hypoplasia was defined by different criteria (O’Donnell et al., 2014). By contrast, a similar study in the Asian population reported an incidence of 10% (Arslan et al., 2019), while another study in the European population reported an incidence of 20% (Fortuniak et al., 2016). In the studies mentioned above, a VA was considered hypoplastic if it was half or less than half of the diameter of its counterpart. We suggested that the disparity in the above studies and the present study may have resulted from the differences in the average diameter of the population studied. Going by the criteria described by Fortunaik et al. (2016) and O’Donnell et al. (2014), it may be practically impossible to report the occurrence of bilateral hypoplasia. Five (out of a total of 57) patients had bilateral hypoplasia in the present study. Because of the compromised blood flow in the VA with a reduced diameter (Chen et al., 2010), surgeons need to be aware of its possibility, which may require special attention during surgical intervention.

PICA is the principal branch of the VA, and it typically originates from the intracranial part of the vertebral artery (4^{th} segment). However, due to numerous embryonic vessels forming the VA and its branches, PICA sometimes emerges from the V3 part. An abnormal course of the VA or its PICA branch below the C1 arch may predispose the arteries to iatrogenic injuries during drilling, tapping, and insertion of lateral mass screws (Arslan et al., 2019). Previous studies have reported the incidence of extracranial origin of PICA between 0.4% to 2.9% (Table 5). The prevalence in the present study is similar to previous reports (Table 5). It is important to note that no perforating arteries emerge from the PICA of extradural origin. Instead, the perforators originate from the intracranial VAs (Mercier et al., 2008). The incidence of PICA arising from the V3 was observed at the oblique part in all the cases. This site of origin is also described as the C1 origin of the PICA. This information is clinically significant to prevent iatrogenic injury to PICA during surgical intervention at the upper cervical spine and posterior approaches to the lower brainstem (Miao et al., 2020).

The prevalence of FIA ranges between 0.01% to 3.2% (Table 5), similar to the prevalence in our series (0.45%; 5 cases/1108 VAs). We observed bilateral persistent FIAs in one of the patients (Fig 2B). The simultaneous persistence of the FIA and the typical branch of the VA results in fenestration at the V3 segment (Uchino et al., 2012), as shown in Fig 3. Both unilateral and bilateral persistent FIA can be easily overlooked (Uchino et al., 2012). An awareness of this variant anatomy and careful review of images will assist in proper identification to prevent VA injury.

Fenestration extended between the vertical and horizontal portion of the V3 segment in the two cases observed in the present study (Fig 3). The two limbs of the fenestrated segment had a similar diameter. The prevalence of fenestration registered in the present study (0.18%; 2 cases/1108 VA arteries) is in agreement with the reports from Western countries (Fortuniak et al., 2016), (O'Donnell et al., 2014) and lesser than the report from a large series study of the Asian population (Uchino et al., 2012) (Table 5). There is a possibility of compromised blood flow at the proximal and distal end of the fenestrated segment of the VA, which may result in transient ischemic attacks (Omotoso et al., 2021). In addition, the passage of the catheter through the normal contralateral VA in patients with this unilateral vascular variation can expose the hindbrain to the risk of ischemia during neuroendovascular procedures (Fortuniak et al., 2016).

In the present study, most patients had equal VA diameters (codominance) (42.6%), the left side was dominant in 34.3%, and right-sided dominance was registered in 23.1%. Our study's pattern of dominance concurs with a previous report in the Asian population (49% equal dominance, 30% left dominance) (Arslan et al., 2019). It is imperative to identify and protect the dominant VA during a surgical intervention at the CVJ. Furthermore, the dominant VA must not be ligated when repairing VA injury, as it can result in permanent neurologic deficit (DeCarvalho et al., 2019).

The ethnic, gender, and side differences in the diameter and length of the V3 segment have been previously reported in the American, South African, and Asian populations (Alfaouri-Kornieieva and Al-Hadidi 2014; Lang and Kessler 1991; Mitchell 2004). According to Mitchell's reports, there were no significant gender or laterality differences based on detailed histological analysis of South African adult cadavers (Witwatersrand region). The average diameter of the horizontal portion in our results is less than but close to the average value of the above histological reports (3.75±0.72 mm) (Mitchell 2004) and MRA reports on the Asian population (3.8±0.51 mm) (Alfaouri-Kornieieva and Al-Hadidi 2014). Noticeably, the average diameter of the vertical portion was smaller than that of the horizontal and oblique portion in our results. On the contrary, Alfaouri-Kornieieva and co-author (2014) reported a gradual decrease from the vertical part to the oblique part in their MRA study. The entire length of the V2 and part of the V3 segment (excluding the horizontal and oblique part) of the VA is restricted within the transverse foramen of the cervical vertebrae, as shown in our CTA series (Fig. 1). We hypothesize that the artery could expand after its exits from the transverse foramen of the atlas (C1) vertebra, which may be a possible explanation for the differences. In agreement with the previous reports by Alfaouri-Kornieieva and co-author (2014) and Arslan et al. (2019), we registered a significantly larger left VA in all parts of the V3 segment (Alfaouri-Kornieieva and Al-Hadidi 2014; Arslan et al., 2019). The total length of the vertical, the horizontal, and the oblique part in the present study agreed with a previous American study, which reported an average length of 38.91±5.53 (Lang and Kessler 1991). In our study, the average length of the vertical part was similar, but the average length of the horizontal and the oblique part was shorter than in the Asian population (23.22±2.7 mm, 17.2±2.85 mm, and 12.31±1.8 mm, respectively). Generally, the disparity noted in the morphometry between the present study and the reports mentioned above may be due to differences in the modality of the studies. In the present study, we observed that the average length showed a significant difference across the ethnic groups. This dissimilarity may be due to some genetic factors. However, more studies may be required from other regions of South Africa to corroborate this theory.

CONCLUSION

We observed the three major atypical vascular variations in the V3 segment of the VA, including persistent FIA, fenestration, and extradural origin of PICA. Additionally, we registered the incidence of unilateral and bilateral hypoplasia. The prevalence of these morphological variations in the South African population studied is similar to the previous report from other population groups. It is imperative to recognize these variations preoperatively. Failure to identify or disregarding the variations can result in inadvertent injury to the VA with neurological consequences. Knowledge of these variations will also assist in the interpretation of radiographs. Complications in the blood flow patterns in the posterior circulation territory can affect important central nervous system structures, including the spinal cord, the brain stem, cerebellum, occipital and temporal lobe of the cerebrum, and inner ear.

REFERENCES

AKINDURO OO, BAUM GR, HOWARD BM, PRADILLA G, GROSSBERG JA, RODTS Jr GE, AHMAD FU (2016) Neurological outcomes following iatrogenic vascular injury during posterior atlanto-axial instrumentation. Clin Neurol Neurosurg, 150: 110-116.

ALFAOURI-KORNIEIEVA M, AL-HADIDI AM (2014) Morphology of the vertebral artery in Asian population. Asian J Med Sci, 5(4): 84-88.

ARSLAN D, OZER MA, GOVSA F, KITIS O (2019) Surgicoanatomical aspect in vascular variations of the V3 segment of vertebral artery as a risk factor for C1 instrumentation. J Clin Neurosci, 68: 243-249.

CAMPERO A, RUBINO PA, RHOTON AL (2011) Anatomy of the vertebral artery. In: Pathology and surgery around the vertebral artery) Springer Paris, Paris, 29-40.

CHEN Y-Y, CHAO A-C, HSU H-Y, CHUNG C-P, HU H-H (2010) Vertebral artery hypoplasia is associated with a decrease in net vertebral flow volume. Ultrasound Med Biol 36(1): 38-43.

DECARVALHO SA, ABD-EL-BARR MM, GROFF MW (2019) Vascular Complications in Cervical Spine Surgery (Anterior and Posterior Approach). In: Complications in Neurosurgery) Elsevier, 314-319.

ELLIOTT RE, TANWEER O, BOAH A, MORSI A, MA T, FREMPONG-BOADU A, SMITH ML (2014) Comparison of screw malposition and vertebral artery injury of C2 pedicle and transarticular screws: meta-analysis and review of the literature. Clin Spine Surg, 27(6): 305-315.

FORTUNIAK J, BOBEFF E, POLGUJ M, KOŚLA K, STEFAŃCZYK L, JASKÓLSKI DJ (2016) Anatomical anomalies of the V3 segment of the vertebral artery in the Polish population. Eur Spine J, 25(12): 4164-4170.

GEORGE B, CORNELIUS J (2001) Vertebral artery: surgical anatomy. Operative techniques in Neurosurgery, 4(4): 168-181.

HSU WK, KANNAN A, MAI HT, FEHLINGS MG, SMITH ZA, TRAYNELIS VC, GOKASLAN ZL, HILIBRAND AS, NASSR A, ARNOLD PM (2017) Epidemiology and outcomes of vertebral artery injury in 16 582 cervical spine surgery patients: an AOSpine North America Multicenter Study. Global Spine J, 7 supl 1: 21S-27S.

KIM MS (2016) Developmental anomalies of the distal vertebral artery and posterior inferior cerebellar artery: diagnosis by CT angiography and literature review. Surg. Radiol. Anat. 38(9): 997-1006.

LANG J, KESSLER B (1991) About the suboccipital part of the vertebral artery and the neighboring bone-joint and nerve relationships. Skull Base Surg, 1(1): 64.

LIANG M-L, HUANG M-C, CHENG H, HUANG W-C, YEN Y-S, SHAO K-N, HUANG C-I, SHIH Y-H, LEE L-S (2004) Posterior transarticular screw fixation for chronic atlanto-axial instability. J Clin Neurosci, 11(4): 368-372.

MERCIER P, BRASSIER G, FOURNIER H, PICQUET J, PAPON X, LASJAUNIAS P (2008). Vascular microanatomy of the pontomedullary junction, posterior inferior cerebellar arteries, and the lateral spinal arteries. Interv. Neuroradiol., 14**,** 49-58.

MIAO H-L, ZHANG D-Y, WANG T, JIAO X-T, JIAO L-Q (2020) Clinical Importance of the Posterior Inferior Cerebellar Artery: A Review of the Literature. Int J Med Sci, 17(18): 3005-3019.

MITCHELL J (2004) Differences between left and right suboccipital and intracranial vertebral artery dimensions: an influence on blood flow to the hindbrain? Physiother Res Int, 9(2): 85-95.

O'DONNELL CM, CHILD ZA, NGUYEN Q, ANDERSON PA, LEE MJ (2014) Vertebral Artery Anomalies at the Craniovertebral Junction in the US Population. Spine, (Phila Pa 1976) 39(18): E1053-E1057.

OMOTOSO BR, HARRICHANDPARSAD R, MOODLEY IG, SATYAPAL KS, LAZARUS L (2021) Fenestration of the Vertebrobasilar Junction Detected with Multidetector Computed Tomography Angiography. Folia Morphol.

SIKKA A, JAIN AJARI (2012) Bilateral variation in the origin and course of the vertebral artery. Anat Res Int, 2012.

UCHINO A, SAITO N, WATADANI T, OKADA Y, KOZAWA E, NISHI N, MIZUKOSHI W, INOUE K, NAKAJIMA R, TAKAHASHI M (2012) Vertebral artery variations at the C1–2 level diagnosed by magnetic resonance angiography. Neuroradiology, 54(1): 19-23.

ULM AJ, QUIROGA M, RUSSO A, RUSSO VM, GRAZIANO F, VELASQUEZ A, ALBANESE E (2010) Normal anatomical variations of the V3 segment of the vertebral artery: surgical implications. J Neurosurg Spine, 13(4): 451-460.

VERGARA P, BAL JS, HICKMAN CASEY AT, CROCKARD HA, CHOI D (2012) C1-C2 posterior fixation: are 4 screws better than 2? Oper Neurosurg, 71 supl 1: ons86-ons95.

WAKAO N, TAKEUCHI M, NISHIMURA M, RIEW KD, KAMIYA M, HIRASAWA A, KAWANAMI K, IMAGAMA S, SATO K, TAKAYASU M (2014) Vertebral artery variations and osseous anomaly at the C1-2 level diagnosed by 3D CT angiography in normal subjects. Neuroradiology, 56(10): 843-849.

ZHANG D-P, ZHANG S-L, ZHANG J-W, ZHANG H-T, FU S-Q, YU M, REN Y-F, JI P (2014) Basilar artery bending length, vascular risk factors, and pontine infarction. J Neurol Sci, 338(1-2): 142-147.

Table 1: Incidence of Anatomical Variations at the suboccipital segment of the VA diagnosed by CTA.

Type of Variation	Total number of patients (incidence %)	Male/Female	Bilateral/ Left/Right	Simultaneous Variation
Persistent FIA	5 (0.45)	1/4	1/0/4	-
FEN	2 (0.18)	0/2	0/1/1	2 with FIA
Extradural PICA Origin	16 (1.44)	11/5	0/8/8	-
Hypoplasia	57 (5.14)	36/21	5/20/32	-

Table 2: Diameter and length of the vertebral artery V3 segment grouped according to ethnicity and laterality in South African patients

Ethnic Group	Parameters	V3v		V3h		V3o	
		Left	**Right**	**Left**	**Right**	**Left**	**Right**
Black	**Diameter**	3.25(0.77) (4.2)	3.16(0.66) (3.3)	3.52(0.64) (4.1)	3.52(0.71) (3.6)	-	-
	Length	24.89(10.3) (78.4)	23.26(8.46) (37.7)	7.17(3.22) (11.4)	7.03(2.72) (10.3)	4.32(1.9) (16.8)	4.01(1.78) (4.5)
Indian	**Diameter**	3.52(0.75) (4.9)	3.44(0.79) (5.1)	3.87(0.88) (5.8)	3.60(0.71) (5.2)	-	-
	Length	24.72(12.63) (36.9)	23.10(9.44) (27.9)	7.55(3.03) (11)	7.26(2.8) (8.8)	4.75(1.98) (5.7)	4.42(1.94) (5.5)
White	**Diameter**	3.43(0.53) (6.1)	3.25(0.64) (3.8)	3.69(0.82) (5.6)	3.60(0.80) (3.6)	-	-
	Length	21.94(11.82) (37.8)	20.60(11.74) (35)	6.19(2.88) (13.8)	6.08(3.15) (11.2)	3.50(1.85) (8.6)	3.36(1.83) (6.2)

Results are reported as median (IQR) (Range) in mm

Table 3: Diameter and length of the vertebral artery V3 segment grouped according to gender and laterality differences in South African patients

		V3v		V3h		V3o	
		Left	Right	Left	Right	Left	Right
Male	Diameter	3.43(0.53) (4.9)	3.25(0.64) (5.1)	3.69(0.97) (4.3)	3.52(0.71) (4.7)	-	-
	Length	24.40(11.76) (40)	22.30(9.95) (33)	6.95(2.98) (13.6)	6.93(3.0) (10.9)	4.08(1.89) (6.3)	3.89(1.91) (6.1)
Female	Diameter	3.43(0.70) (6.2)	3.25(0.70) (3.8)	3.69(0.88) (6.2)	3.69(0.71) (4.2)	-	-
	Length	22.10(11.16) (75.9)	21.57(10.9) (37.7)	6.45(3.22) (12.5)	6.44(3.0) (10.9)	3.96(0.88) (17.6)	3.76(1.98) (5.6)

Results are reported as median (IQR) (Range) in mm

Table 4: Characteristics of proximal and distal loops of the vertebral artery V3 segment grouped according to gender and ethnic group in South African patients

	Proximal Loop		Distal Loop	
	Left	Right	Left	Right
Male	67.33(22.83) (76)	65.66(25.17) (77.7)	66.66(14.67) (72)	67(16) (73.3)
Female	68.16(25.17) (83.6)	65.33(26.17) (75.3)	66(16) (73.6)	66.66(14.16) (53.6)
Black	66(23) (82.3)	68(32) (67.6)	65.50(18.92) (65.9)	69.66(17.17) (62.3)
Indian	68.16(29.17) (77.3)	63.33(24.67) (72)	66(19) (75.6)	65.33(16.67) (71)
White	67.50(22.83) (74.3)	66(22.16) (80.3)	67.16(13.25) (77.3)	67.33(13.83) (66)

Results are reported as median (IQR) (Range) in degrees

Table 5: Prevalence of Anatomical Variations at the V3 segment of the VA in patients CVJ anomalies

Author(year)	Population	Type of study	Sample Size	Anatomical Variations (Patients %)			
				Hypoplasia	Extradural PICA Origin	FEN	Persistent FIA
Uchino et al.,2012	Japan	CTA	2739	0	30(1.1)	25(0.9)	87(3.2)
O'Donnell et al., 2014	US	CTA	975	61(6.26)	4(0.4)	1(0.01)	1(0.01)
Wakao et al., 2014	Japan	CTA	480	0	5(1.3)	5(1.3)	7(1.8)
Fortunaik et al.,2016	Poland	CTA	1800	360(20)	11(0.61)	3(0.16)	0
Kim et al.,2016	South Korea	CTA	546 314	0 0	11 9	2 2	7 8
Arslan et al., 2019	Turkey	CTA	200	10	1.0	0	0.5

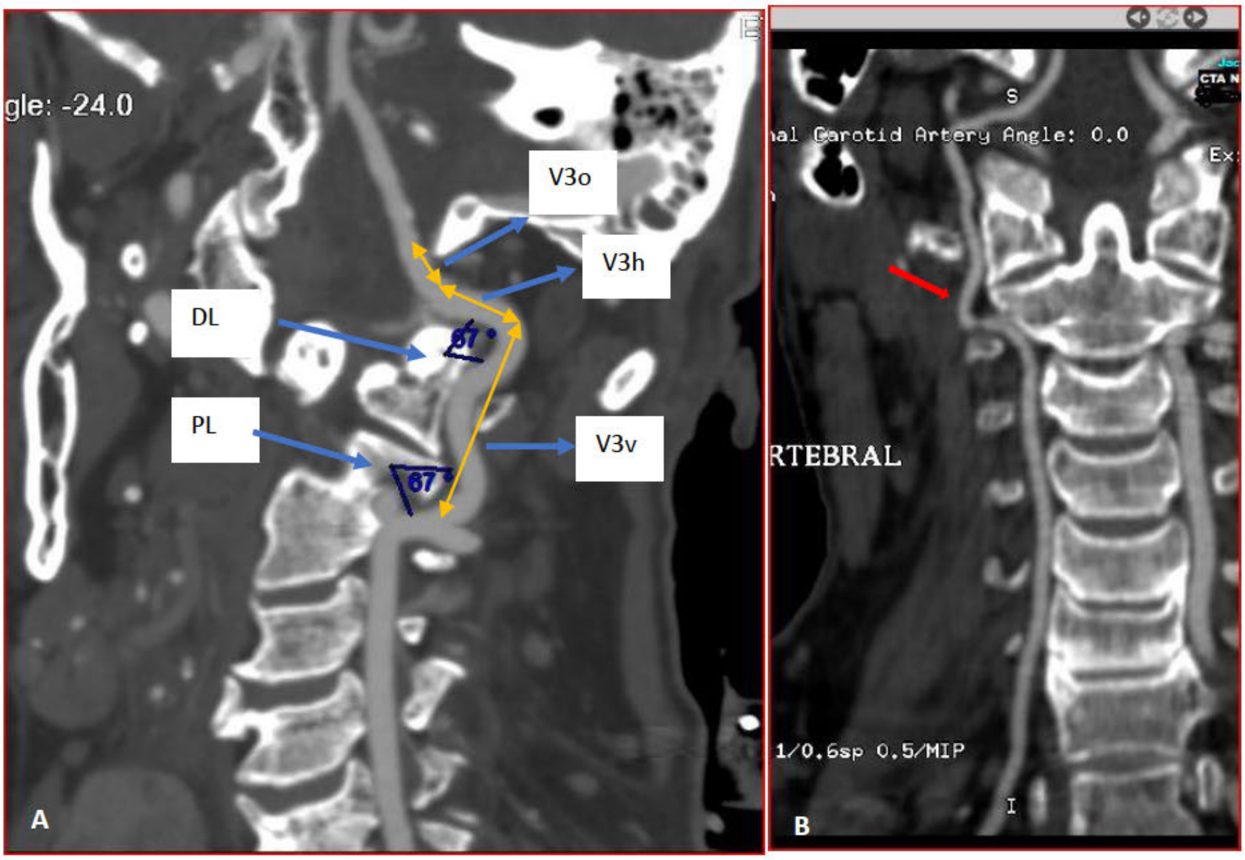
gle: -24.0
V3o
V3h
DL
PL
V3v
67°
67°
A
S
Carotid Artery Angle: 0.0
RTEBRAL
1/0.6sp 0.5/MIP
I
B

Fig. 1

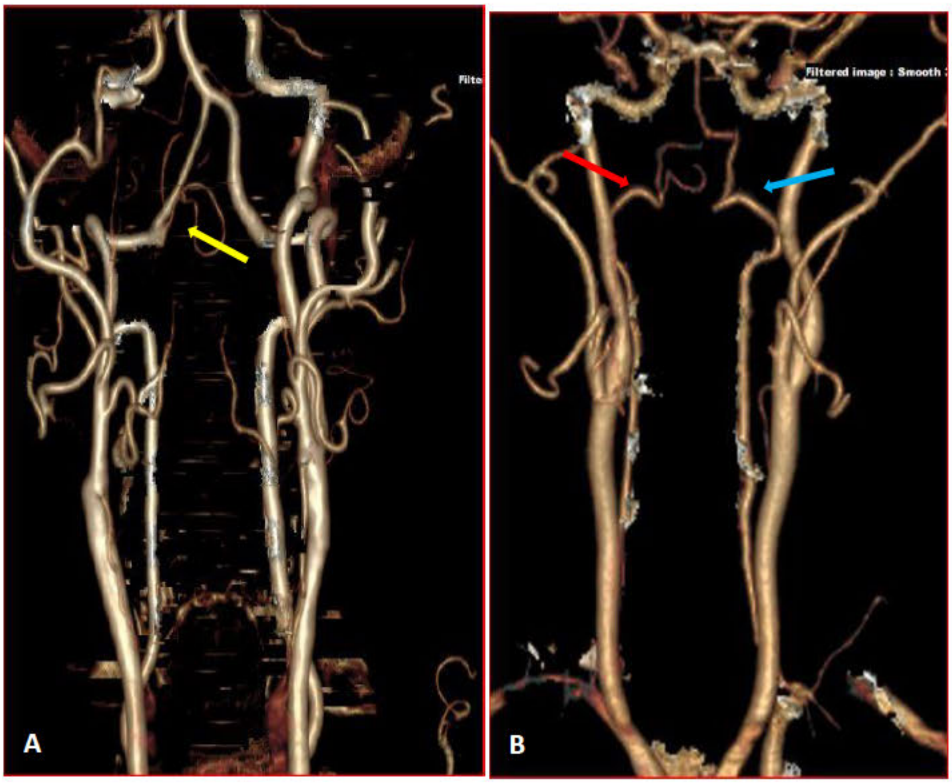
A
Filtered image : Smooth :
B

Fig. 2

Fig. 3

Fig. 1

Oblique (A) and Coronal (B) view of CTA image. **A)** V3 segment of the left VA. V3v – vertical segment of the VA; V3h – horizontal segment of the VA; V3o oblique segment of the VA; PL – proximal loop of V3; DL – distal loop of V3. **B)** The red arrow illustrated right VA hypoplasia.

Fig. 2

Anterior view of 3D-CTA reconstructed images of the vertebral arteries. **A)** PICA (yellow arrow) originates from the oblique part of V3 of the left VA. **B)** The red and blue arrow illustrated bilateral persistent FIA.

Fig. 3

3D-CTA reconstructed images of the vertebral arteries. Anteroposterior view, fenestration and persistent FIA at the V3 segment of the left VA (yellow arrow).

BRIDGING TEXT

FROM CHAPTER THREE TO FOUR

Chapter three investigated the typical anatomy and prevalence of variations at the suboccipital segment of the VA in a South Africa population. We found that the prevalence of variation in this segment is similar to some of the previous reports from international studies. Chapter four evaluates the typical anatomy and prevalence of variation at the most distal part of the VA (intracranial segment) in a South Africa population.

CHAPTER FOUR

MANUSCRIPT THREE

Radiological Anatomy of the Intracranial Vertebral Artery in a Select South African Cohort of Patients

Omotoso, B.R[1], Dr Harrichandparsad, R[2], Dr Moodley, I.G[3], Prof. Satyapal, K.S.[1], Prof. Lazarus, L[1]

[1]Discipline of Clinical Anatomy, School of Laboratory Medicine and Medical Sciences, College of Health Sciences, University of KwaZulu-Natal, Westville Campus, Private Bag X54001, Durban, South Africa.
[2]Department of Neurosurgery, School of Clinical Medicine, College of Health Sciences, Nelson R Mandela School of Medicine, University of KwaZulu-Natal, Durban, South Africa.
[3]Department of Radiology, Jackpersad and Partners Inc., Specialist Diagnostic Radiologists, Lenmed Ethekwini Hospital and Heart Centre, Durban, South Africa.

Corresponding Author: Professor L Lazarus

Address: Discipline of Clinical Anatomy, School of Laboratory Medicine and Medical Sciences, College of Health Sciences, University of KwaZulu-Natal, Westville Campus, Private Bag X54001, Durban, South Africa.

Email address: ramsaroopl@ukzn.ac.za

+27 31 260 7899

Accepted for publication in Scientific Reports on the 20th of May 2021

TITLE PAGE

Title : Radiological Anatomy of the Intracranial Vertebral Artery in a Select South African Cohort of Patients

Authors : Omotoso, B.R[1], Harrichandparsad, R[2], Satyapal, K.S[1]
Moodley, I.G[3], *Lazarus, L[1]

Name of institution : [1]Discipline of Clinical Anatomy
School of Laboratory Medicine and Medical Sciences
College of Health Sciences
University of KwaZulu-Natal
Westville Campus
Private Bag X54001
Durban
4000

[2]Department of Neurosurgery,
School of Clinical Medicine,
College of Health Sciences,
Nelson R Mandela School of Medicine
University of KwaZulu-Natal,
Durban,
South Africa.

[3]Department of Radiology,
Jackpersad and Partners Inc.,
Specialist Diagnostic Radiologists,
Lenmed Ethekwini Hospital and Heart Centre,
South Africa

Total number of figures : 3

Total number of tables : 3

Running headline : Anatomical variations and dimension of the intracranial Vertebral Artery

Corresponding author : Professor L Lazarus
Department of Clinical Anatomy
School of Laboratory Medicine and Medical Sciences
College of Health Sciences
University of KwaZulu-Natal
Private Bag X54001
Durban
4000
South Africa

Telephone number : +27 31 260 7899

Email address : ramsaroopl@ukzn.ac.za

Abstract

The intracranial segment of the vertebral artery (VA) is the unique part of the artery where the two VAs join to form a single vascular channel, viz. the basilar artery. In addition to this typical description, anatomical variations have been described; the presence of anatomical variation has been associated with some pathological processes, neurological complications, and the risk of vascular diseases in the posterior circulatory territory. We evaluated the typical anatomical features and variations of the VA4 component of the VA in a South African population to provide useful data on the prevalence of variation and morphometry of the distal VA. The study is an observational, retrospective chart review of 554 consecutive South African patients (Black, Indian, and Caucasian) who had been examined with multidetector computed tomography angiography (MDCTA) from January 2009 to September 2019. We observed various anatomical variations in the VA4 segment of the VA. We report the incidence of VA hypoplasia, hypoplastic terminal VA, and atresia. Fenestration and duplicate posterior inferior cerebellar artery (PICA) origin were also observed. The left intracranial VA was significantly larger than the right. Our study shows that anatomical variation of the intracranial VA is common in the population studied, with a total prevalence of 36.5%. Understanding the patterns of anatomical variations of the VAs will contribute significantly to the interpretation of ischemic areas and diagnosis of various diseases in the posterior circulatory territory.

Keywords: Vertebral artery hypoplasia, Atresia, Fenestration, Vertebrobasilar junction.

Text

INTRODUCTION

The vertebral artery (VA) emanates from the supero-posterior part of the subclavian artery and proceeds through the foramen transversarium of the sixth to first cervical vertebrae. The left and right VA penetrates the dura mater to enter the intracranial space through the foramen magnum, where they converge to form the basilar trunk at the pontomedullary junction [1]. Anatomically, the VA is divided into four segments. The first three segments (VA1, VA2, VA3) are the extracranial segments, extending from the origin to where they penetrate the dura mater. The fourth segment of the VA (VA4) is intracranial, extending from the foramen magnum to the point where the left and right VA anastomose to form the basilar trunk [1]. The geometry of the basilar trunk depends on the pattern of the bilateral VAs. When there is an asymmetry of bilateral VAs or other anatomical variations, the basilar trunk sometimes bends away from the midline [2]. Previously reported anatomical variations of the intracranial VAs include VA terminating as posterior inferior cerebellar artery (PICA), known as atresia, fenestration, asymmetry, and hypoplasia. Anatomical variations play a significant role in the clinical sequelae of an iatrogenic VA injury, which can vary widely [3]. For instance, damage to the dominant VA when the contralateral VA terminates as PICA can result in devastating complications since the dominant VA solely forms the basilar artery.

The presence of variation has been associated with some pathological processes, neurological complications, and the risk of vascular diseases in the posterior circulatory territory. For instance, atresia and hypoplasia have been associated with hypoperfusion of brain tissues and hemodynamic insufficiency, which may predispose to transient ischaemic attacks or acute brainstem ischaemic stroke [4,5].

Reports on the prevalence of anatomical variations of the intracranial VA are scarce, with few previous reports in the Western population (Caucasians) [1], the Asian population [4], and the Turkish population [6]. Previous studies from the African continent used postmortem and cadaveric histological samples to report on average diameter and incidence of VA hypoplasia [7-9]. Advances in modern imaging technology that led to the establishment of multidetector computed tomography angiography (MDCTA) have made endovascular procedures popular. These procedures require a detailed understanding of typical anatomy and the extent of anatomical variations of the VAs. Consequently, a report on the prevalence of possible variant anatomy will help in the interpretation of radiographs, prevention of iatrogenic injuries, and contribute to the advancement of non-invasive surgical intervention.

In the present study, we assessed the typical anatomical features and variations of the V4 segment of the VA using MDCTA. We aimed to determine the dimensional characteristics and prevalence of anatomical variations of the intracranial VA in a South African population. Due to the multiracial composition of the South African population, in addition to the overall incidence of variation, we also report variations based on three racial groups: Black, Indian, and Caucasian South African. It is necessary to have correct and detailed information about the typical anatomy and prevalence of anatomical variations. Such information is essential before neurosurgery, endovascular and non-invasive procedures. The detailed information from this study will be useful in neurosurgery, anatomy, endovascular, and non-invasive procedures.

MATERIALS AND METHODS

Study population

This study is a retrospective observational review of 554 MDCTA images of South African patients. The patients underwent MDCTA for various reasons between January 2009 and September 2019. Images were obtained from the database of Lenmed Ethekwini Hospital and Heart Center, Durban, South Africa. The Biomedical Research Ethics Committee of the University of KwaZulu-Natal approved the study (Ethical No: BE 148/19) and waived the need for informed consent as this study utilized retrospective chart reviews. There was no patient contact, and no patient details were released from images. All methods were carried out in accordance with relevant guidelines and regulations. Exclusion criteria included MDCTA scans that showed no clarity of the VA's course, scans with motion artifacts or poor-quality imaging, and scans performed on foreign patients or obtained outside a hospital. The angiographies were from 307 males (55.4%) and 247 females (44.6%). The average age of the patients is reported as median (interquartile range〔IQR〕): 62 (23) (range: 10-99) years; 61 (23) for male patients and 62 (25) for female patients. Race was defined according to the guidelines outlined in the modern systems of racial classification in the Republic of South Africa [10]. The criteria used in the scheme of racial classification include skin colour and ancestry. The South African population is divided into four main racial groups: Caucasian, Black, Indian, and Coloured. Three population groups were included in the present study: Black 91 (16.4%), Indian 176 (31.8%), and Caucasian 287 (51.8%). According to the modern system of classification, a Caucasian was defined as a person of European descent. A Black individual was defined as a person having origins in any of indigenous Africa or Native group. An Indian individual was defined as a person of Asian descent [10].

MDCTA Protocol

The imaging examination was performed on a 64-detector row 160-slice helical multidetector computed tomography scanner (Lightspeed CT, GE Healthcare Medical Systems, Milwaukee, WI, USA). In our standard MDCTA protocol for brain examinations, a scan coverage area from the aortic arch to the top of the brain in a supine position (headfirst) was adopted as a field of view (FOV). The scanning protocol was as follows: 120 kVp, 500 mAs, beam collimation 64 × 0.625 mm, speed 20.62mm/rotation, gantry rotation time 0.35s/rotation, the helical thickness of 0.625 mm, pitch 0.516:1, and reconstruction interval of 0.625 mm. Following the acquisition of the nonenhanced CT data, contrast-enhanced MDCTA was performed. During the procedure, a 20 Gauge needle (Pink Nexiva) was used to cannulate patients for IV access in the antecubital region to administer 60 mL of Ioversol (Optiray 350; Guerbet South Africa). This was followed by a 40 mL saline flush via a double power injector (Medex flowSens, Guerbet USA) into the patient's antecubital vein (4 mL/s), and the scan delay was individually adapted using a bolus-tracking technique. First, a single nonenhanced low-dose scan at the upper neck level was obtained for the bolus tracking. With the start of contrast material administration, repeated low dose monitoring scans were obtained every second. Following the appearance of the first contrast in the aortic arch, the MDCTA was triggered automatically without delay. The region of interest was positioned at the aortic arch, and the threshold for the MDCTA was set as 150 Hounsfield Units. When the threshold was surpassed, helical scanning was automatically initiated.

Imaging Reconstruction

Postprocessing of three-dimensional images was performed using multiplanar reformation (MPR), maximum intensity projection (MIP), multiplanar reconstruction (MPR), and volume rendering (VR) algorithms. The volumetric MDCTA data sets were processed on Advanced Workstation 4.2 (GE Healthcare, Milwaukee, WI, USA). A series of 17 projection images at every 20º around the cephalocaudal axis were generated and transfer to the picture archiving communication system (PACS). The MDCTAs were performed for diagnostic purposes in the context of various cerebrovascular accidents or diseases. In some cases, the suspected diseases were not found on the MDCTA; thus, some materials in this study were derived from a healthy population.

Analysis of Anatomical Variations and Dimensions of the V4 Segment

The MDCTA images were analyzed using PACS tools. The images were examined for vascular variations by a neurosurgeon, a neuroradiologist, and an anatomist using the coronal and sagittal view and the 3D reconstructed images. Each MDCTA image was examined for the presence of anatomical variations. In atresia, the VA did not fuse with the contralateral VA but terminates as PICA. The hypoplastic terminal V4 segment was registered when the terminal portion divides into a PICA and a tiny branch that joins the contralateral dominant VA. Fenestration was registered when the VA split into two vessels, which later rejoined distally. The following parameters were measured on a coronal view of the MDCTA (Fig 1): 1) the diameters were measured along the course of the VA at a distance of 11 mm cranial to the entrance of the VA into the foramen magnum, 2) the length of the VAs was measured from the foramen magnum to the point of union with the contralateral VA, and 3) the angle between the bilateral VA at the vertebrobasilar junction. We were unable to appropriately quantify the frequency of the PICA and the spinal arteries because visualization of branches (such as the PICA and spinal arteries) is usually beyond the limits of the MDCTA. A diameter of ≤ 2 mm was described as hypoplasia; we classified the VA as dominant if the diameter was larger than that of the contralateral side by any size difference according to the method provided by Ergun and co-authors [11]. When the bilateral VAs had a similar diameter, we referred to them as "equal" or "codominant." Results were analyzed separately for the left and right sides.

Statistical Analysis

All data were analyzed using SPSS version 27 (SPSS Inc., Chicago, IL, USA). Categorical variables were analyzed using the chi-square test. A Kolmogorov-Smirnov test was used to assess the normal distribution of continuous data. Because the distribution of the data was not normal, nonparametric tests were used. The Kruskal-Wallis test followed by the Wilcoxon Signed-Rank test was used to detect significant differences in the obtained values. The interclass correlation coefficient was used to examine the reliability of measurements. All tests were performed at 95% confidence with a p-value of < 0.05.

RESULTS

Continuous and categorical data are presented as the median and IQR and percentage (N). The interclass correlation coefficient for intra-observer reliability testing was 92% for V4 length, 93% for diameter, and 96% for the angle at the VBJ. For inter-observer reliability testing, the intraclass correlation was 85% for V4 length and diameter; 87% for the angle at the VBJ.

Variation in Morphology

We observed the following variations of the intracranial segment: (1) The hypoplastic terminal VA (Fig 2a) and hypoplasia of VA (Fig 3a). (2) VA terminating as PICA (Atresia) (Fig 2(b) and 3(b)). (3) Fenestration (One was observed at the right intracranial VA (Fig 4a), while the other was observed at the vertebrobasilar junction). (4) Duplicate origin of the PICA (Fig 4b). The incidence of these variations is summarized in Table 1. The incidence of VA hypoplasia is significantly high in Caucasian, followed by Indian on the right (p=0.01). There was no significant difference across the races on the left (p=0.61). Also, there was no significant racial difference in the incidence of hypoplastic terminal VA (p=0.26) and atresia (p=0.54). The incidence of variation across the races is summarized in Table 2. Because visualization of branches of the intracranial VA (PICA and spinal arteries) is usually beyond the limits of MDCTA, the frequency of PICA on the left, right, and bilateral PICA in the present study is low (15.7%, 13.9%, and 14.8%, respectively). We also observed bilateral and unilateral double PICA in 5 patients. Therefore, we cannot appropriately quantify the frequency of the PICA in all the VAs.

Morphometric Analysis of the intracranial Vertebral Arteries

Diameter

The average diameter of the left VA (3.17 (0.62) mm) was similar to that of the right VA (3.17 (0.7) mm). However, the Wilcoxon Signed-Rank test showed a significant difference ($p < 0.001$). This is because the Wilcoxon Signed-Rank test is a rank-sum test and not a median test. The sum of positive Ranks of the left VA was significantly greater than that of the right VA. We observed a left pattern of dominance in 45.3% (251/554) patients; the right side was dominant in 32.7% (181/554) patients. The left and right VAs was equal in diameter in 15.3% (85/554) patients. Concerning the racial groups, no significant differences were observed (Right VA, p=0.567; Left VA, p=0.180). The group diameters are summarized in Table 3. For gender, the diameters are summarized in Table 4. There were no significant gender differences in VA diameter (Right VA, p=0.528; Left VA, p=0.274).

Length

The length of the left (32.36 (7.18) mm) intracranial VA was significantly greater than the right (31.50 (7.22) mm). Within the racial groups, there were no significant differences (Right VA, p=0.386; Left VA, p=0.708). The average length and laterality of the VA across the racial groups are summarized in Table 2. There were no significant gender differences in the length of the VA (Right VA, p=0.665; Left VA, p=0.615). The results are summarized in Table 3.

The angle at the Vertebrobasilar Junction.

The angle at the vertebrobasilar junction was 46° (18°). Within the racial groups, the average angle in Black patients (51° (22°)) was significantly larger than in Caucasian (47° (18°) p=0.037) and Indian (42° (16°) p=0.000) patients. A significant difference was also observed between the Caucasian and Indian (p=0.010) patients. There were no significant gender differences (p=0.103).

DISCUSSION

Our study shows that MDCTA made it possible to evaluate anatomical variations of the intracranial VA. We found that variation is common in the population studied, with a total prevalence of 36.5%. The most frequently observed is VA hypoplasia. The incidence of hypoplasia in the present study (8.3% on the right and 6.5% on the left) is similar to the report of Ergun et al. [11]. These authors defined VA hypoplasia using diameter criteria of ≤ 2 mm and reported an incidence of 7.1% on the right and 9.4% on the left among 254 patients in their angiographic series [11]. By contrast, Songur and co-authors in their autopsy study reported a relatively high incidence of 20.2% on the right, 14.4% on the left, and 4.3% bilaterally using a similar definition of VA hypoplasia [6]. Sometimes it is challenging to compare data from different populations and research groups due to the differences in study modalities, distribution of data, and average diameter. According to a recent report, an individual's VA diameter may depend on anthropometric parameters such as height [12]. All these factors may contribute to the wide range of differences reported in the literature. VA hypoplasia is a congenital anatomical variation that has been previously described with a cut-off diameter between 2.0 mm and 3.0 mm [13]. During embryogenesis, the VA is formed from multiple longitudinal anastomoses between adjacent cervical intersegmental arteries [14,15]. The mechanism of the formation of VA hypoplasia is not precise. However, some authors hypothesized delayed development of the vertebrobasilar artery as the major cause of VA hypoplasia [16].

The reduced diameter of hypoplastic VA has been associated with an increased probability of spontaneous dissection [17] and ipsilateral PICA and lateral medullary infarctions due to suspected atherosclerosis as a result of abnormal hemodynamics [18]. Recently, VA hypoplasia has been associated with an aneurysm of the contralateral dominant VA, most especially at the site of PICA origin [19]. Knowledge of pathologies associated with VA hypoplasia can provide clues and help diagnose pathological processes in the posterior circulatory territory.

In addition to hypoplasia, we also noticed that the hypoplastic terminal portion of the unilateral intracranial VA is a common anatomical variant of the studied population. The VA seems to divide at a spot along its courses to a PICA branch and a tiny branch that joins the contralateral VA. Pekcevik and co-author proposed another terminology for this type of variation; VA continued as PICA [20]. In our own opinion, this suggested anatomical term can be confused with VA terminating as PICA or VA ending as PICA (atresia). We suggest that this variant anatomy can be simply described as hypoplastic terminal VA.

In our series, the percentage of patients having VA atresia is 6.7%. Prevalence of VA atresia has previously been reported as up to 9% [4,21]. Our results were in accordance with the range of the reported prevalence but most similar to that reported by Liu et al. (6.3%) [4]. Clinically, VA atresia has been previously linked to rotational vertebral artery syndrome (RVAS) [22] and bow hunter’s syndrome [23,24], which may result from compression of this variant vessel. Similar to VA hypoplasia, the embryological basis of VA atresia is unclear. The first of the seven cervical intersegmental arteries that formed the VA was designated as the proatlantal intersegmental artery, while the seventh intersegmental artery forms the proximal part of the subclavian artery and point of origin of the VA [15].

Each of these intersegmental arteries is a potential site of arterial agenesis that could result in anatomical variation [25]. Since the point of origin of the VA is at the seventh intersegmental artery, the intracranial VA may have developed from the proatlantal intersegmental artery. Complications during the process of fusion and anastomosis of the proatlantal and other cervical intersegmental arteries could result in anatomical variations of the distal VAs which may include atresia.

We also observed fenestration at the right intracranial VA in one patient and the proximal part of the basilar artery in another patient. Our observation is similar to the report of Dzierzanowski et al., which reported two fenestrations in the Caucasians [1]. Fenestration of the vertebrobasilar artery is a congenital anomaly that involves lumina division of an artery with a single origin into two separate channels that later reunite distally. Embryologically, the VA and the basilar artery develop from different primitive vessels. The VA is formed from the cervical intersegmental arteries, while the basilar artery develops from the longitudinal neural arteries. As a result of these, fenestration at the V4 segment of the VA is due to the absence of obliterations of two intersegmental vessels that fused [25]. Fenestration of the proximal basilar occurs due to partial failure or incomplete fusion of the longitudinal neural arteries and regression of the bridging arteries connecting the longitudinal arteries [26]. Fenestration may predispose to aneurysm around the fenestrated portion of the artery [6,20], and it has also been previously associated with unexplained subarachnoid hemorrhage [27]. In addition to the associated pathologies, knowledge of this variation is essential in clinical diagnosis as fenestration may be misinterpreted as an aneurysm or a dissection on magnetic resonance imaging [20].

In the present study, duplicate PICA origin was registered in one of the patients. It is important to note that duplicate PICA origin is different from the duplication of the PICA. In the duplicate origin, the PICA has two separate origins that later converge distally in the course of the artery. Whereas in duplication of the PICA, there is no distal arterial convergence [28]: each artery courses separately. Duplicate PICA origin is a rare congenital anatomical variation of the PICA with a prevalence of roughly 1.45% previously reported in the Western population (Caucasian and Asian) [28]. Clinically, duplicate PICA origin has been previously reported to highly predispose to intracranial aneurysm formation with an associated incidence between 50% and 71% [28,29]. Embryologically, Lesley and co-authors hypothesized that duplicate PICA origin might be a manifestation of underlying deficient vascular developmental disorganization, which may upraise the tendency toward formation of an intracranial aneurysm [28]. Other authors suggested that this anatomical variation may have resulted from variation in the persistence of standard anastomosis between the lateral spinal artery and the PICA [30]. Considering the unique embryogenesis, adequate perfusion of the regions supplied by the PICA may rely on flow from both origins [29]. Since duplicate PICA origin is an uncommon variation with few previous reports, it should not be overlooked when evaluating the diagnosis and surgical intervention images.

The average diameter and length of the VA in our result is consistent with the previous report on a South American population (Diameter Left- 3.12 ± 0.85 mm, Right- 2.94 ± 0.77 mm; Length Left- 33.86 ± 5.59 mm, Right- 32.47 ± 4.8 mm) [31] based on autopsy samples and another angiographic study of the Caucasians (Diameter Left- 3.16 ± 0.63 mm, Right- 2.78 ± 0.44 mm; Length Left- 31.51 ± 6.51 mm Right- 24.25 ± 6.76 mm) [1]. We observed a significantly larger diameter on the left than the right VA, comparable to the previous reports mentioned above. Interestingly, there was no significant difference across the racial groups and gender in our series. By contrast, a previous histological study of a South African population (Witwatersrand region) reported an average diameter (Left- 2.68 ± 0.86 mm, Right- 2.53 ± 0.75 mm) [7] that was lower than the present study. The differences in the study modalities (MDCTA vs. cadaveric) may be responsible for the contrariety noticed in the results. Tissue shrinkage associated with histological tissue processing may be the reason for the reduced diameter.

We described the pattern of dominance using the criterion of any size difference between the left and right VA; 45.3% showed left dominance, 32.7% showed right dominance, and 15.3% showed codominance. Using a similar criterion, Ozdemir et al. reported similar results of left dominance in 64% of patients and right dominance in 31% of patients [32]. In contrast, Ergun and co-authors reported right VA dominance in 49.5% and left dominance in 47.2% of patients using a similar criterion as described above [11]. Our result shows that most of the patients have left dominant VAs. Noticeably, we observed more VA hypoplasia and atresia on the right. Knowledge of the dominant VA is required for some endovascular procedures. It is also important to preserve the dominant VA since they are likely to predominates the basilar artery. This information is vital to reduce the risk of neurological symptoms that may results from iatrogenic injury.

The angle at the vertebrobasilar junction in the present study is comparable with the report of Songur et al. (52.2 ± 18.2°) [6]. On the contrary, other authors reported a larger mean angle (85.45 ± 10.76°) [1]. The disparity may have resulted from the confluence of the bilateral VA, which can either be a sharp or blunt edge depending on the pattern and frequency of asymmetry. In atresia, the VA did not fuse with the contralateral VA but terminated as PICA. The contralateral VA solely proceeds to form the basilar artery. In the case of hypoplastic terminal VA, the contralateral VA predominates the basilar artery with little contribution from the tapering end of the hypoplastic terminal VA. In addition to asymmetry, these two conditions can also cause the basilar artery to bend from the midline (also known as bending basilar) [33]. Deviation and prominence of a vessel, such as bending basilar due to dominance of one of the VAs, may cause compression of cranial nerves [20]. Furthermore, it is essential to consider the geometry of the vertebrobasilar junction while planning for surgical interventions in this region. This region is of particular interest to neurosurgeons and radiologists due to various interventional neuroradiological procedures conduct in the area to treat vascular diseases such as arterial dissections, aneurysms, arteriovenous malformations, dural fistula, or repair of an occlusive disease [34].

CONCLUSION

Our study shows that anatomical variation of the intracranial VA is common in the population studied, with a total prevalence of 36.5%. Hypoplasia and hypoplastic terminal VA being the most frequent. Understanding the patterns of anatomical variations of the VAs will contribute significantly to the interpretation of ischemic areas and diagnosis of various diseases in the posterior circulatory territory.

Table 1: Incidence of anatomical variations at the intracranial segment (V4) of the VA diagnosed by MDCTA.

Type of Variation	Total number of patients (incidence%)	Left/Right/ Bilateral	Male/Female
Hypoplasia	89 (16.1)	36/46/7	56/33
Hypoplastic terminal VA	73 (13.2)	37/36/0	46/27
VA terminating as PICA (Atresia)	37 (6.7)	15/22/0	24/13
Fenestration	2 (0.4)	0/1/0	1/1
Duplicate PICA origin	1 (0.2)	0/1/0	0/1

Table 2: Incidence of anatomical variations at the intracranial segment (V4) of the VA grouped according to race in South African patients

Type of Variation	Total number of patients (incidence%)	Race		
		Black Left/Right/Bilateral	Indian Left/Right/Bilateral	White Left/Right/Bilateral
Hypoplasia	89 (16.1)	5/5/1	10/19/3	21/22/3
Hypoplastic terminal VA	73 (13.2)	9/3/0	8/15/0	20/18/0
VA terminating as PICA (Atresia)	37 (6.7)	1/2/0	4/9/0	10/11/0
Fenestration	2 (0.4)	0	0	2
Duplicate PICA origin	1 (0.2)	0	0	0/1/0

Table 3: Diameter and length of the vertebral artery V4 segment grouped according to race and laterality in South African patients

	Black		Indian		White	
	Left	Right	Left	Right	Left	Right
V4 Diameter	3.17 (0.7)	3.17 (0.7)	3.17 (0.69)	3.17 (0.7)	3.17 (0.62)	3.17 (0.68)
V4 Length	32.74 (9.13)	30.71 (9.15)	32.20 (7.74)	30.86 (8.6)	32.38 (6.87)	31.61 (6.34)

Results are reported as median (interquartile range〔IQR〕) mm

Table 4: Diameter and length of the vertebral artery V4 segment grouped according to gender and laterality in South African patients

	Male		Female	
	Left	Right	Left	Right
V4 Diameter	3.17 (0.62)	3.17 (0.7)	3.17 (0.62)	3.17 (0.62)
V4 Length	32.29 (7.34)	31.59 (6.92)	32.38 (6.68)	31.48 (7.69)

Results are reported as median (interquartile range〔IQR〕) mm

REFERENCES

1 Dzierzanowski, J. *et al.* Intracranial region of the vertebral artery: morphometric study in the context of clinical usefulness. *Folia Morphol. (Warsz.)* **76**, 379-387, doi:10.5603/FM.a2017.0021 (2017).
2 Hong J, M. *et al.* Vertebral artery dominance contributes to basilar artery curvature and peri-vertebrobasilar junctional infarcts. *J Neurol Neurosurg Psychiatry* **80**, 1087–1092. Available from: https://doi:1010.1136/jnnp.2008.169805 (2009).
3 Schroeder, G. D. & Hsu, W. K. Vertebral artery injuries in cervical spine surgery. *Surg. Neurol. Int.* **4**, S362 (2013).
4 Liu, I.-W. *et al.* Vertebral artery terminating in posterior inferior cerebellar artery: A normal variation with clinical significance. *PLoS One* **12**, e0175264 (2017).
5 Chen, Y.-Y., Chao, A.-C., Hsu, H.-Y., Chung, C.-P. & Hu, H.-H. Vertebral artery hypoplasia is associated with a decrease in net vertebral flow volume. *Ultrasound Med Biol* **36**, 38-43 (2010).
6 Songur, A. *et al.* Variations in the intracranial vertebrobasilar system. *Surg. Radiol. Anat.* **30**, 257-264 (2008).
7 Mitchell, J. Differences between left and right suboccipital and intracranial vertebral artery dimensions: an influence on blood flow to the hindbrain? *Physiother. Res. Int.* **9**, 85-95 (2004).
8 Mitchell, J. & McKay, A. Comparison of left and right vertebral artery intracranial diameters. *The Anatomical Record* **242**, 350-354, doi:10.1002/ar.1092420308 (1995).
9 Ogeng'o, J., Olabu, B., Sinkeet, R., Ogeng'o, N. M. & Elbusaid, H. Vertebral artery hypoplasia in a Black Kenyan population. *J International scholarly research notices* **2014** (2014).
10 Khalfani, A. K. & Zuberi, T. Racial classification and the modern census in South Africa, 1911–1996. *Race and society* **4**, 161-176 (2001).
11 Ergun, O., Tatar, I. G., Birgi, E. & Hekimoglu, B. Evaluation of vertebral artery dominance, hypoplasia and variations in the origin: angiographic study in 254 patients. *Folia Morphologica* **75**, 33-37 (2016).
12 Gaigalaite, V. *et al.* Association between vertebral artery hypoplasia and posterior circulation stroke. *J BMC neurology* **16**, 118 (2016).
13 Katsanos, A. H., Kosmidou, M., Kyritsis, A. P. & Giannopoulos, S. Is vertebral artery hypoplasia a predisposing factor for posterior circulation cerebral ischemic events? A comprehensive review. *Eur. Neurol.* **70**, 78-83 (2013).
14 Luh, G., Dean, B., Tomsick, T. & Wallace, R. The persistent fetal carotid-vertebrobasilar anastomoses. *AJR Am. J. Roentgenol* **172**, 1427-1432 (1999).
15 Padget, D. H. The development of the cranial arteries in the human embryo. *J Contrib Embryol* **32**, 205-261 (1948).
16 Kim, C., Sohn, J.-H. & Choi, H.-C. Are the anomalous vertebral arteries more hypoplastic?: retrospective linear mixed model approach. *BMC neurology* **17**, 168 (2017).
17 Zhou, M. *et al.* Vertebral artery hypoplasia and vertebral artery dissection a hospital-based cohort study. *Neurology*, doi:10.1212/WNL. 0000000000001284 (2015).
18 Chuang, Y.-M., Huang, Y.-C., Hu, H.-H. & Yang, C.-Y. Toward a further elucidation: role of vertebral artery hypoplasia in acute ischemic stroke. *J European neurology* **55**, 193-197 (2006).
19 Harati, A. *et al.* Association between vertebral artery hypoplasia and vertebral artery aneurysms: A case-control study. *J. Clin. Neurosci.* **61**, 73-77 (2019).
20 Pekcevik, Y. & Pekcevik, R. Variations of the cerebellar arteries at CT angiography. *Surg. Radiol. Anat.* **36**, 455-461 (2014).
21 Ohkura, K. *et al.* Vertebral artery variations in thoracic aortic patients. *Eur. J. Cardiothorac. Surg.* **46**, 27-31 (2014).
22 Noh, Y., Kwon, O.-K., Kim, H.-J. & Kim, J. S. Rotational vertebral artery syndrome due to compression of nondominant vertebral artery terminating in posterior inferior cerebellar artery. *J. Neurol.* **258**, 1775-1780 (2011).
23 Yeh, J.-F. *et al.* A case of bow hunter's stroke caused by non-dominant vertebral artery. *Acta Neurol. Taiwan.* **14**, 69-73 (2005).
24 Miao, H.-L., Zhang, D.-Y., Wang, T., Jiao, X.-T. & Jiao, L.-Q. Clinical Importance of the Posterior Inferior Cerebellar Artery: A Review of the Literature. *Int. J. Med. Sci.* **17**, 3005-3019 (2020).
25 George, B., Bruneau, M. & Spetzler, R. F. *Pathology and surgery around the vertebral artery*. (Springer Science & Business Media, 2013).
26 Zhu, D.-Y. *et al.* Treatment of fenestrated vertebrobasilar junction-related aneurysms with endovascular techniques. *J. Clin. Neurosci.* **28**, 112-116 (2016).

27 Hudák, I., Lenzsér, G., Lunenkova, V. & Dóczi, T. Cerebral arterial fenestrations: a common phenomenon in unexplained subarachnoid haemorrhage. *Acta Neurochir. (Wien.)* **155**, 217-222 (2013).
28 Lesley, W. S., Rajab, M. H. & Case, R. S. Double origin of the posterior inferior cerebellar artery: association with intracranial aneurysm on catheter angiography. *American Journal of Roentgenology* **189**, 893-897 (2007).
29 Silva, M. A., See, A. P., Aziz-Sultan, M. A. & Patel, N. J. Surgical treatment of a double origin posterior inferior cerebellar artery aneurysm and insights from embryology: case report and literature review. *Operative Neurosurgery* **13**, E8-E12 (2017).
30 Lasjaunias, P., Vallee, B., Person, H., Ter Brugge, K. & Chiu, M. The lateral spinal artery of the upper cervical spinal cord: anatomy, normal variations, and angiographic aspects. *J. Neurosurg.* **63**, 235-241 (1985).
31 Ballesteros, L., Forero, P. & Quintero, I. Morphological expression of the anterior spinal artery and the intracranial segment of the vertebral artery: a direct anatomic study. *Rom. J. Morphol. Embryol.* **54**, 513-518 (2013).
32 Ozdemir, S., Yildiz, C. & Cankur, N. Evaluation of vertebral artery system in a healthy population by using colour duplex Doppler ultrasonography. *Med School J Uludag* **28**, 95-99 (2002).
33 Meng, X., Ding, W., Wu, X. & Di, P. Clinical investigation and characterization of vertebrobasilar dolichoectasia and vertebral artery dominance. *Discov. Med.* **25**, 151-158 (2018).
34 Mercier, P. *et al.* Vascular microanatomy of the pontomedullary junction, posterior inferior cerebellar arteries, and the lateral spinal arteries. *Interv. Neuroradiol.* **14**, 49-58 (2008).

Declarations

Funding: Funding was provided by the College of Health Sciences, University of Kwazulu-Natal, Durban, South Africa.

Conflict of interest: The authors declare that they have no conflicts of interest.

Ethics approval: The design was approved by the Institutional Review Board/Ethics Committee (Biomedical Research Ethics Committee of the University of KwaZulu-Natal with ethical No: BE 148/19).

Consent to participate: Not applicable

Consent for publication: Not applicable

Availability of data: Available on request

Code availability: Not applicable

Author contributions: All persons listed as authors have contributed substantially to the protocol development, project design, data collection, and data analysis of this manuscript. LL, BRO, KSS, RH: conceptualized project. BRO, RH, IGM: collected data. BRO, LL: analyzed data. LL, RH, IGM, BRO: manuscript writing and editing.

Figure Legends

Fig. 1

Oblique view of CTA image, showing the V3 and V4 segments of the VA. V4L – length of the V4 segment; V4D –Diameter of the V4 segment; VBA – the angle at the vertebrobasilar junction

Fig. 2

3D-CTA reconstructed images showing the vertebral, the subclavian, and the carotid arteries. **a)** The blue arrow indicates PICA. The yellow arrow indicates hypoplastic terminal VA while the white arrow indicates the bending basilar artery. **b)** The blue arrow illustrates the origin of the left VA from the arch of the aorta, and the red arrow shows the termination of ipsilateral VA as PICA

Fig. 3

3D-CTA reconstructed images showing the vertebral, the basilar arteries, and the Circle of Willis. **a)** The yellow arrow illustrates the left dominant VA. The green arrow indicates hypoplastic right VA. **b)** The red arrow illustrates termination of left VA as PICA. The blue arrow indicates dominant right VA

Fig. 4

3D-CTA reconstructed images showing the vertebral, the basilar arteries, and the Circle of Willis. **a)** The green arrow indicates fenestration of right intracranial VA while the white arrow indicates the left VA. **b)** The red arrow illustrates duplicate PICA origin, while the green arrow indicates the left VA

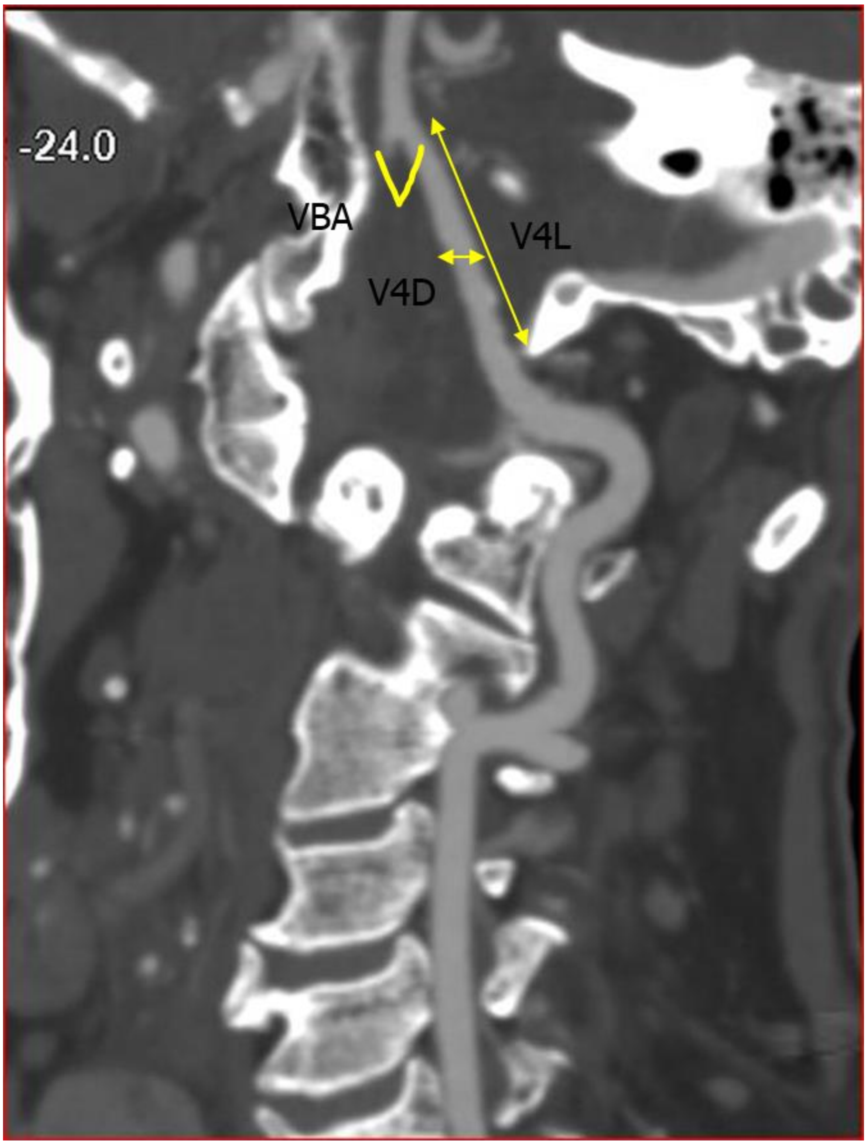

Fig 1.

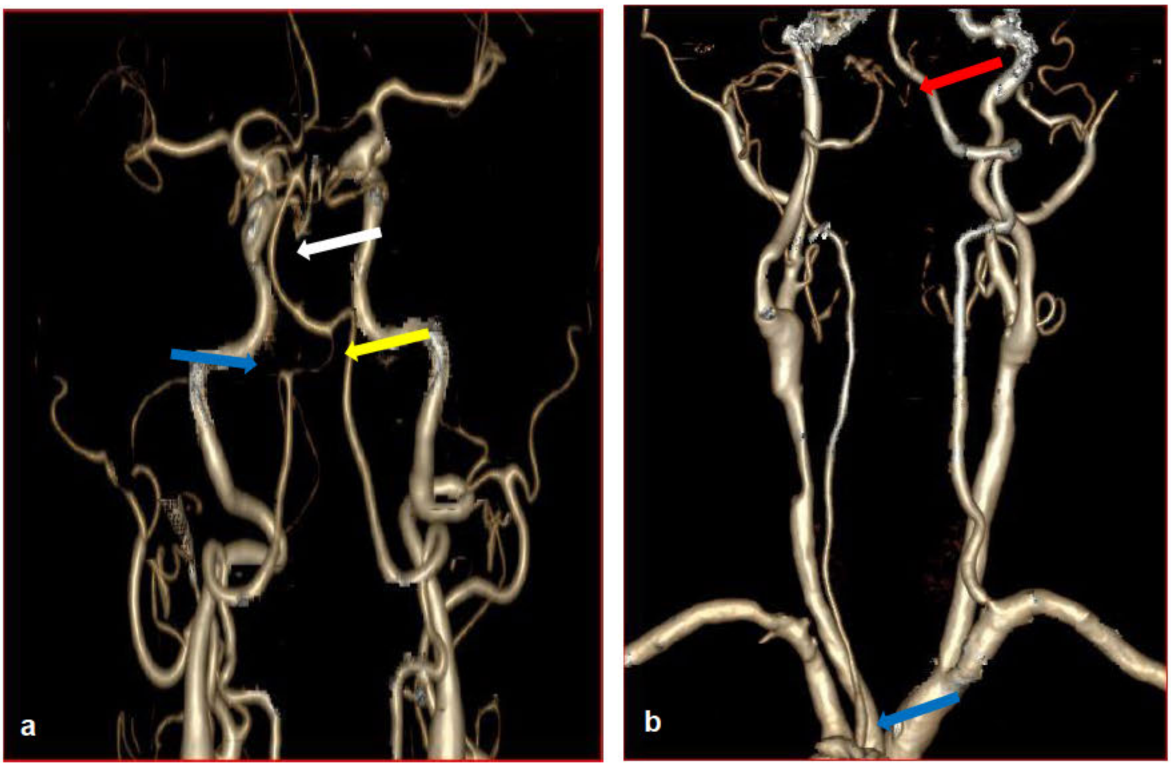
a
b

Fig 2.

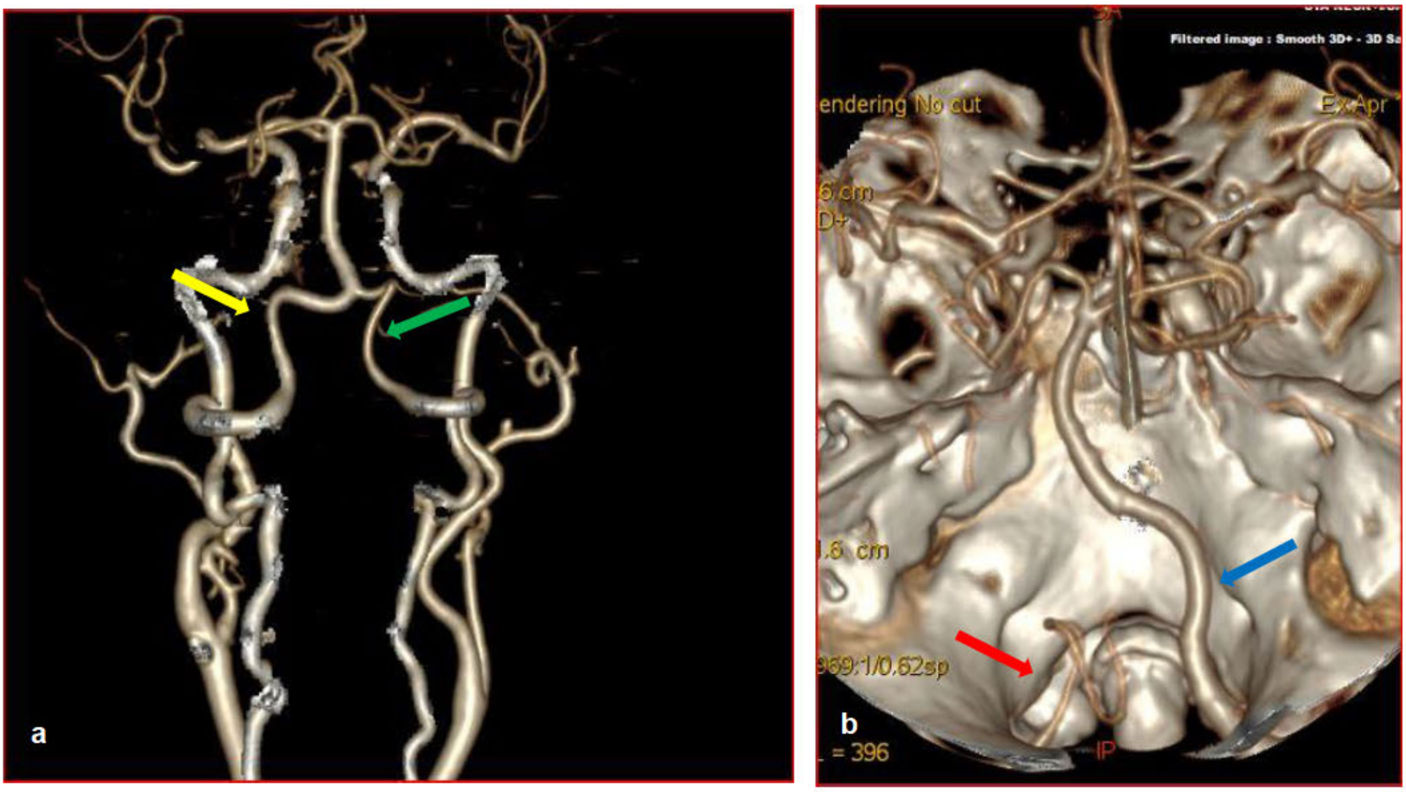
a
b
Filtered image : Smooth 3D+ - 3D Sa
endering No cut
Ex:Apr
6 cm
D+
.6 cm
969:1/0.62sp
= 396
SA
IP

Fig 3

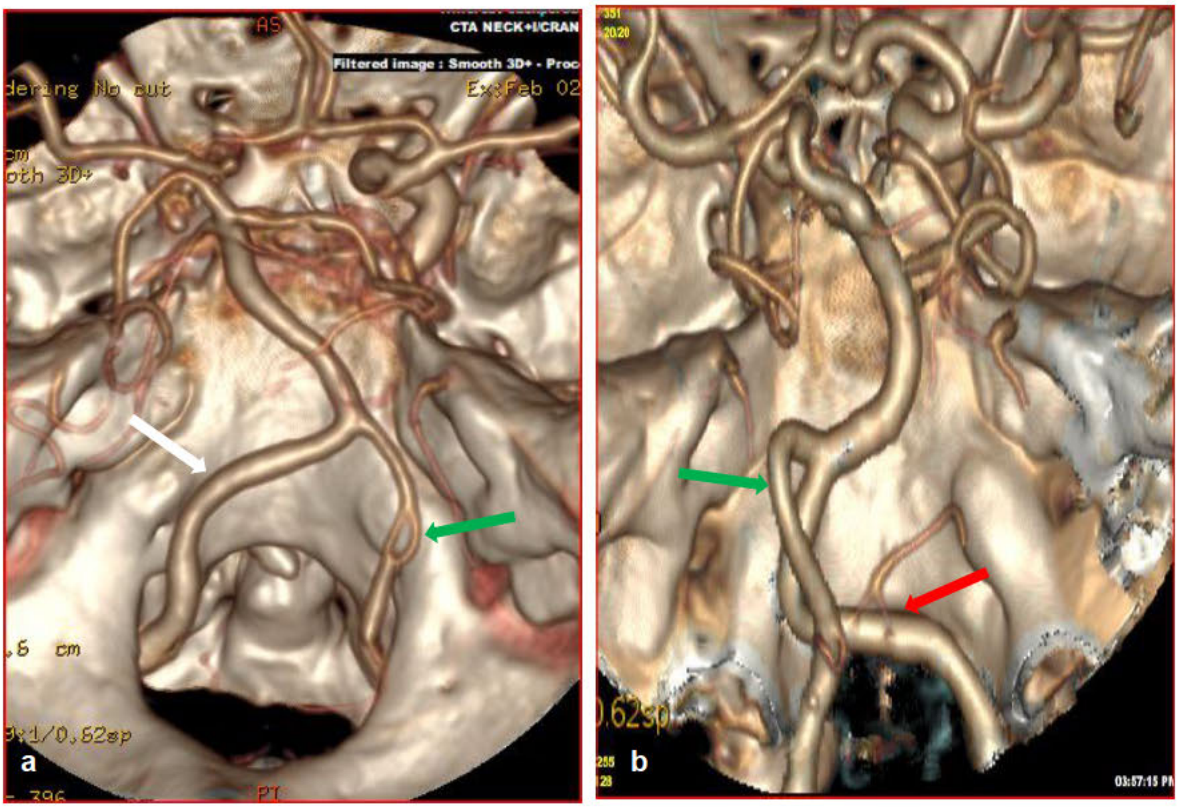
AS
CTA NECK+I/CRAN
Filtered image : Smooth 3D+ - Proc
dering No cut
Ex:Feb 02
oth 3D+
.6 cm
1/0.62sp
a
PI
0.62sp
b
03:57:15 PM

Fig 4.

BRIDGING TEXT

FROM CHAPTER FOUR TO FIVE

Chapter four described the anatomy of the intracranial VA in a South Africa population. Information from this chapter shows that anatomical variations are common in the distal part of the VA in the studied South Africa population. We also found that some variations in the proximal segment coexist with others in the distal part of the artery. Chapter five and six is a combination of various case reports of anatomical variations (in a South Africa population), including details of suspected hemodynamic effects on the posterior circulation territory. The case reports are organized into two separate manuscripts in each of the chapter.

CHAPTER FIVE

MANUSCRIPT FOUR

Fenestration of the Vertebrobasilar Junction Detected with Multidetector Computed Tomography Angiography

Omotoso, B.R[1], Dr Harrichandparsad, R[2], Dr Moodley, I.G[3], Prof. Satyapal, K.S.[1], Prof. Lazarus, L[1]

[1]Discipline of Clinical Anatomy, School of Laboratory Medicine and Medical Sciences, College of Health Sciences, University of KwaZulu-Natal, Westville Campus, Private Bag X54001, Durban, South Africa.
[2]Department of Neurosurgery, School of Clinical Medicine, College of Health Sciences, Nelson R Mandela School of Medicine, University of KwaZulu-Natal, Durban, South Africa.
[3]Department of Radiology, Jackpersad and Partners Inc., Specialist Diagnostic Radiologists, Lenmed Ethekwini Hospital and Heart Centre, Durban, South Africa.

Corresponding Author: Professor L Lazarus

Address: Discipline of Clinical Anatomy, School of Laboratory Medicine and Medical Sciences, College of Health Sciences, University of KwaZulu-Natal, Westville Campus, Private Bag X54001, Durban, South Africa.

Email address: ramsaroopl@ukzn.ac.za

+27 31 260 7899

Published in Folia Morphologica (2021)

DOI: 10.5603/FM.a2021.0028

Published online on 2nd March 2021

ONLINE FIRST

This is a provisional PDF only. Copyedited and fully formatted version will be made available soon.

FOLIA MORPHOLOGICA

ISSN: 0015-5659

e-ISSN: 1644-3284

Fenestration of the vertebrobasilar junction detected with multidetector computed tomography angiography

Authors: B. R. Omotoso, R. Harrichandparsad, I. G. Moodley, K. S. Satyapal, L. Lazarus

DOI: 10.5603/FM.a2021.0028

Article type: Case report

Submitted: 2020-06-05

Accepted: 2020-07-20

Published online: 2021-03-02

Fenestration of the vertebrobasilar junction detected with multidetector computed tomography angiography

B.R. Omotoso et al., Fenestration of the vertebrobasilar junction

B.R. Omotoso[1], R. Harrichandparsad[2], I.G. Moodley[3], K.S. Satyapal[1], L. Lazarus[1]
[1]Discipline of Clinical Anatomy, School of Laboratory Medicine and Medical Sciences, College of Health Sciences, University of KwaZulu-Natal, Westville Campus, Durban, South Africa
[2]Department of Neurosurgery, School of Clinical Medicine, College of Health Sciences, Nelson R Mandela School of Medicine, University of KwaZulu-Natal, Durban, South Africa
[3]Department of Radiology, Jackpersad and Partners Inc., Specialist Diagnostic Radiologists, Lenmed Ethekwini Hospital and Heart Centre, South Africa

Address for correspondence: Prof. L. Lazarus, Department of Clinical Anatomy, School of Laboratory Medicine and Medical Sciences, College of Health Sciences, University of KwaZulu-Natal, Private Bag X54001, Durban, 4000, South Africa, tel: +27 31 260 7899, e-mail: ramsaroopl@ukzn.ac.za

Abstract

The complex embryonic origin of the vertebrobasilar system may result in a wide range of anatomical variations. It has been hypothesized that the formation of fenestrations are likely to occur due to the failure of regression of the bridging arteries that connect the longitudinal neural arteries during embryogenesis. Fenestration of the vertebrobasilar system is a rare anatomical variation that involves a luminal division of the artery, that has a single origin into two separate and parallel channels which are rejoined distally. Fenestrations are important anatomical variants in patients undergoing endovascular and invasive intracranial interventions. Vascular fenestration has been associated with aneurysms, arteriovenous malformations, neuralgia, and vertebrobasilar ischemia. We report on three cases of fenestration at the vertebrobasilar junction in one female and two male patients, respectively, using multidetector computed tomography angiography.

The length of the fenestrated segment of the artery measured 4.41 mm, 3.90 mm, and 5.90 mm, respectively in the patients. Our report is clinically important as the presence of this anatomical variation may influence the management of cervical and intracranial pathologies. Increased awareness of the prevalence of anatomic variations contributes to the advancement of noninvasive imaging capabilities.

Key words: morphological variation, vertebral artery, basilar artery

INTRODUCTION

The vertebrobasilar system is the combination of the two vertebral arteries together with the basilar artery. The vertebrobasilar junction (VBJ) is the point of union of the bilateral vertebral arteries (VA), mostly at the lower border of the pons [19] to form the basilar artery. The vertebrobasilar system provides the blood supply to vital structures like the cervical spinal cord, brainstem, thalamus, cerebellum, and occipital lobes [18]. Therefore, a morphological variation of either of the vertebral artery or basilar trunk can influence vascular supply to the afore mentioned structures. Anatomically, vertebral arteries are divided into 4 segments: prevertebral (V1), vertebral (V2), atlantoaxial (V3) and intracranial (V4) segments [1]. Previous studies regarding the morphology of the vertebral artery have shown the existence of variation in its course [5, 6, 11].

Fenestration is an uncommon anatomical variation that involves a luminal division of an artery that has a common origin into two separate and parallel channels anywhere along its course to rejoin distally. Fenestration is sometimes mistaken for duplication, but should, however, be differentiated. Duplication normally involves double vascular origin which later fuse during the course of the artery [8].

Fenestration of the vertebrobasilar junction has been reported to be a predisposing factor to other vascular malformations like aneurysms [24], arteriovenous malformations [12], and neuralgia [10]. Furthermore, fenestration has been associated with epidermoid cysts and vertebrobasilar ischemia [13, 23]. A thorough understanding of the anatomy and knowledge of anatomical variations of the vertebrobasilar artery is essential for assessing neurologic syndromes and preoperative neurosurgical planning.

In this report, we describe three cases of vertebrobasilar junction fenestration using multidetector computed tomography angiography (MDCTA).

Fenestration of the vertebrobasilar junction is a morphological variation that has been previously reported in the international population, for example in China, United States, Canada and Brazil (Table 1). In this report, we present three cases of fenestration of the VBJ in two White and one Indian South Africans.

CASE PRESENTATION

Our study is retrospective in nature, therefore, written informed consent was not obtained. However, the design of this study was approved by our Institutional Review Board/Ethics Committee (Biomedical Research Ethics Committee of the University of KwaZulu-Natal with ethical No: BE 148/19). No identifying patient information is present in this paper.

Case 1

Computed Tomography Angiography (CTA) scan of intracranial vessels of a 34-year-old Indian South African female at Lenmed Ethekwini Hospital and Heart Centre illustrated fenestration at the vertebrobasilar junction (Fig. 1A). The length of the fenestrated segment at the VBJ is 4.41 mm long with the two limbs having a similar diameter. Clinical examination shows extensive aneurysmal subarachnoid hemorrhage in the right Sylvian fissure with intracerebral extension into the adjacent peri lenticular parenchyma. Ruptured right middle cerebral artery saccular aneurysm, and further multilobulated anterior cerebral artery aneurysm was noted with the incorporation of large left A3 segment.

Case 2

A 79-year-old male White South African presented to Lenmed Ethekwini Hospital and Heart Centre for the history of vertebrobasilar transient ischemic attack

(TIA) and acute unsteadiness. CTA scan revealed fenestration at the vertebrobasilar junction (Fig. 1B). The length of the fenestrated segment at the VBJ is 3.90 mm long with the two limbs having a similar diameter. The posterior communicating artery is hypoplastic on the right when compared to the left and no intracranial aneurysm is demonstrated.

Case 3

An 83-year-old male White South African presented to Lenmed Ethekwini Hospital and Heart Centre for a clinical history of collapse, recurrent transient ischemic attack, ataxia, and diplopia. CTA showed fenestration at the vertebrobasilar junction (Fig. 1C). The length of the fenestrated segment at the VBJ was 5.90 mm long with the two limbs having a similar diameter. The basilar artery is minimally ecstatic involving the medial and lateral margin at its bifurcation.

DISCUSSION

Anatomical variation in the origin of the vertebral artery (VA) is the most reported morphological variation. This has also been reported in the South African population [4, 15]. However, reports on fenestration at the VBJ are scarce and are mostly reported internationally (Table 1). Previous studies regarding the morphology of the vertebral artery have shown the existence of variation with demographic and ethnic/racial differences [5, 6, 11]. Complex embryogenesis of the vertebrobasilar system results in vascular fenestration and it is frequently reported at the extracranial portion of the vertebral artery [12]. In contrast, the three cases we report showed fenestration at the VBJ.

Embryologically, the vertebral artery is formed during the 32nd to 40th days by the development of longitudinal anastomosis between the seven adjacent cervical intersegmental arteries that are formed from the primitive dorsal aorta [17]. Later, however, the first six cervical intersegmental arteries regress, while the seventh persists to form the proximal part of the subclavian artery and the point of origin of the adult vertebral artery. The basilar trunk is formed from the fusion of primitive embryonic longitudinal neural arteries by approximately the fifth foetal week [14]. Generally, fenestration at any of the segments of the VA (V1-V4) is due to the absence of obliterations of two intersegmental vessels which fuse, or by segmental arteries which become short or disappear while a portion of the dorsal aorta remains against the vertebral artery [1]. Basilar artery fenestration occurs as a result of partial failure or incomplete fusion of the longitudinal neural arteries and regression of the bridging arteries connecting the longitudinal arteries [25]. Although fenestration at the vertebrobasilar junction is formed between the confluence of the bilateral distal VA and proximal part of the basilar artery, researchers agree that the best explanation for this morphological variation is the persistence or incomplete fusion of one of the temporary bridging arteries between the embryologic bilateral longitudinal neural arteries that form the basilar artery [7, 25]. This could occur as a result of some genetic or environmental factors [25]. In the cases we observed, fenestration was found at the vertebrobasilar junction in three patients (Figs. 1A, 1B and 1C).

The macroscopic examination of the fenestrated segment revealed a unique fusiform thickened vessel [1]. Furthermore, microscopic and histopathological examination of the limbs has shown irregularities in the lateral and medial wall structure [1, 13]. These irregularities may alter the hemodynamics of blood flow at the proximal and distal end of the fenestrated segment causing transient ischemic attacks (TIA) as reported in two of our patients (cases 2 and 3).

Vertebral artery dominance and bending of the basilar artery have also been reported as risk factors for brainstem infarction and TIA [16]. Morphologically, the VBJ is subjected to the greatest stresses of flow and turbulence from the bilateral vertebral artery below. This complex geometry of the VBJ, in addition to fenestration and basilar bends (Fig 1A, B, C), may also contribute to the clinical history of TIA in cases 2 and 3.

Some authors suggest that fenestration of the VA is an incidental finding and has no pathological and clinical importance [20], while others hypothesized that its occurrence increases the prevalence of aneurysms (most especially at the VBJ) [2, 24]. Fenestration has also been associated with the brain, spinal cord, and spinal column abnormalities in addition to other vascular disorders [21]. In case 1, there is a middle cerebral artery and anterior cerebral artery aneurysm, which is not associated with the fenestration. According to the report by Campos et al., [2] and review of literature (Table 1), fenestration at the VBJ is more common in female subjects while VA fenestration is considered to be more frequent in male subject [12]. This may not be comparable due to different embryological processes in the formation of the basilar artery as opposed to the vertebral arteries. Also, our report is a small series with only three subjects comprising two males and one female.

CONCLUSIONS

The authors presented three cases of fenestration at the VBJ in two White males and one female Indian South African patients. The presence of this morphological variation can increase the incidence of an aneurysm. Since most intracranial vascular disorders such as aneurysm are treated using endovascular procedures, a knowledge of the presence of fenestrations may influence the endovascular strategy. Therefore, knowledge of this anatomical variation will help in the preoperative workup and contribute to the correct interpretation of preoperative images. This report will also contribute to the demography of the South African population.

REFERENCES

[1] Bruneau M, De Witte O, Regli L, et al. Anatomical variations, in Pathology and surgery around the vertebral artery. Paris: Springer Paris. 2011; 53-74.

[2] Campos J, Fox AJ, Vinuela F, et al. Saccular aneurysms in basilar artery fenestration. AJNR Am. J. Neuroradiol. 1987; 8(2): 233-236.

[3] Consoli A, Renieri L, Nappini S, et al. Endovascular treatment with 'kissing'flow diverter stents of two unruptured aneurysms at a fenestrated vertebrobasilar junction. J Neurointerv Surg. 2013; 5(2): e9-e9, doi:10.1136/neurintsurg-2011-010188, PMID:22315285.

[4] Da Silva R, Anatomical study of the variation in the branching patterns and histology of the aorta in a South African population, University of Cape Town, 2013.

[5] Deng D, Cheng FB, Zhang YD, et al. Morphological analysis of the vertebral and basilar arteries in the Chinese population provides greater diagnostic accuracy of vertebrobasilar dolichoectasia and reveals gender differences. Surg Radiol Anat. 2012; 34(7): 645-650, doi: 10.1007/s00276-012-09609, PMID: 22427028.

[6] Gaigalaite V, Vilimas A, Ozeraitiene V, et al. Association between vertebral artery hypoplasia and posterior circulation stroke. BMC Neurol. 2016; 16(1): 118, doi: 10.1186/s12883-016-0644-x , PMID: 27461465.

[7] Gupta V, Ahuja CK, Khandelwal N, et al. Treatment of Ruptured Saccular Aneurysms of the Fenestrated Vertebrobasilar Junction with Balloon Remodeling Technique: A Short Case Series and Review of the Literature. Interv Neuroradiol. 2013; 19(3): 289-298, doi: 10.1177/159101991301900305, PMID: 24070077

[8] Ionete C, Omojola MF, MR angiographic demonstration of bilateral duplication of the extracranial vertebral artery unusual course and review of the literature. AJNR Am. J. Neuroradiol. 2006; 27(6): 1304-1306.

[9] Kan P, Abla AA, Dumont TM, et al. Double- Barrel Stent- Assisted Coiling of a Basilar Artery Fenestration Aneurysm. J Neuroimaging. 2013; 23(3): 496-499, doi:10.1111/j.1552-6569.2012.00720.x , PMID:22607550.

[10] Kim K, Mizunari T, Kobayashi S, et al. Occipital neuralgia caused by the compression of the fenestrated vertebral artery: a case report. J Neurosurg.1999; 27(7): 645-650.

[11] Kornieieva A, Morphology of the vertebral artery in Asian population. Asian J. Med. Sci. 2014; 5(4): 84-88, https://doi.org/10.3126/ajms.v5i4.6150 (E-ISSN 2091-0576; P-ISSN 2467-9100).

[12] Kowada M, Yamaguchi K, Takahashi H, Fenestration of the vertebral artery with a review of 23 cases in Japan. Radiology. 1972; 103(2): 343-346, doi: 10.1148/103.2.343, PMID: 5024559.

[13] Kubo M, Hacein-Bey L, Varelas, PN et al. Ruptured saccular aneurysm of distal vertebral artery fenestration managed with Guglielmi detachable coils and intraventricular tissue plasminogen activator. Surg. Neurol. 2005; 63(3): 244-248, doi:10.1016/j.surneu.2004.02.038, PMID: 15734513.

[14] Luh G, Dean B, Tomsick T, et al. The persistent fetal carotid-vertebrobasilar anastomoses. AJR Am. J. Roentgenol. 1999; 172(5): 1427-1432, doi: 10.2214/ajr.172.5.10227532, PMID: 10227532.

[15] Makhanya N, Mamogale T, Khan N, Variants of the left aortic arch branches. SA Journal of radiology. 2004; 8(4).

[16] Meng XW, Ding X, Wu X, et al. Clinical investigation, and characterization of vertebrobasilar dolichoectasia and vertebral artery dominance. Discov. Med. 2018; 25(138): 151-158.

[17] Padget DH, The development of the cranial arteries in the human embryo. J Contrib Embryol. 1948; 32: 205-261.

[18] Piccinin MA, Munakomi S, Neuroanatomy, Vertebrobasilar System, in StatPearls [Internet]: 2019; StatPearls Publishing.

[19] Standring S. Gray's anatomy e-book: the anatomical basis of clinical practice. Elsevier Health Sciences, 2015.

[20] Tetiker H, Cimen M, Kosar M, Fenestration of the vertebral artery: case presentation. Folia Morphol. (Warsz). 2014; 73(1): 84-86.

[21] Tran- Dinh H, Soo Y, Jayasinghe L, Duplication of the Vertebro- Basilar System, Australas. Radiol, 1991; 35(3): 220-224, doi: 10.1111/j.1440-1673.1991.tb03012.x, PMID:1763984.

[22] Trivelato F, Abud D, Nakiri G, et al. Basilar artery fenestration aneurysms: endovascular treatment strategies based on 3D morphology. Clin. Neuroradiol. 2016; 26(1): 73-79, doi:10.1007/s00062-014-0336-0, PMID: 25164692.

[23] Weis J, Reul J, Mayfrank L, et al. Duplication of a vertebral artery associated with epidermoid cyst of the posterior fossa. Eur. Radiol. 1997; 7(3): 412-414, doi:10.1007/s003300050177, PMID:9087368.

[24] Yoon SM, Chun YI, Kwon Y, et al. Vertebrobasilar junction aneurysms associated with fenestration: experience of five cases treated with Guglielmi detachable coils. Surg. Neurol. 2004; 61(3): 248-254, doi: 10.1016/S0090-3019(03)00485-3, PMID:14984996.

[25] Zhu DY, Fang YB, Wu YN, et al. Treatment of fenestrated vertebrobasilar junction-related aneurysms with endovascular techniques. J Clin Neurosci. 2016; 28: 112-116, doi: 10.1016/j.jocn.2015.09.018, PMID: 26778513

Table 1. Incidence of vertebrobasilar junction fenestration in different population groups

Author (Year)	Country	Type of study	Number of cases	Sex: Male/Female	Segment of VA
Campos et al. (1987) [2]	Canada	DSA	21	7/14	Vertebrobasilar junction
Yoon et al. (2004) [24]	South Korea	CTA	4	2/2	Vertebrobasilar junction
Consoli et al. (2013) [3]	Italy	DSA	2	F	Vertebrobasilar junction
Kan et al. (2013) [9]	USA	DSA	1	F	Vertebrobasilar junction
Gupta et al. (2013) [7]	India	CTA, DSA	4	3/1	Vertebrobasilar junction
Trivelato et al. (2016) [22]	Brazil	DSA	5	1/4	Vertebrobasilar junction
Zhu et al. (2016) [25]	China	DSA	10	6/4	Vertebrobasilar junction
Present study	South Africa	CTA	3	1/2	Vertebrobasilar junction

Figure 1. CTA images of case 1(A), case 2(B) and case 3(C). A) 3D reconstructed image shows vessels of anterior and posterior circulation. Blue arrow shows intracranial segment of right VA while the red arrow shows intracranial segment of the left VA. The white arrow shows fenestration at the vertebrobasilar junction between the confluence of bilateral VAs and proximal part of the basilar artery. **B)** 3D reconstructed image shows the intracranial VA, bending basilar artery and the circle of Willis. The white arrow shows fenestration at the vertebrobasilar junction while the yellow arrow shows the basilar artery. **C)** 3D reconstructed image shows the intracranial VA, bending basilar artery and the circle of Willis. The white arrow shows fenestration at the vertebrobasilar junction while the blue arrow shows the basilar artery.

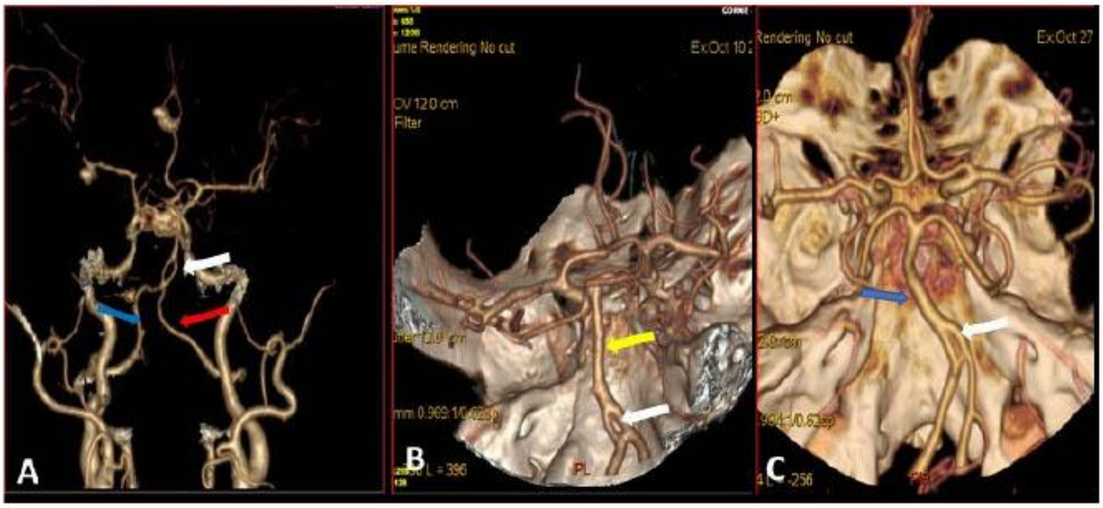
A
B
C
Rendering No cut
Ex:Oct 27
Ex:Oct 10

CHAPTER SIX

MANUSCRIPT FIVE

Anatomical Variations of the Vertebral Arteries in a Select South African Population; Evaluation with Multidetector Computed Tomography Angiography

Bukola R. Omotoso[1], Indresan G. Moodley[2], Rohen Harrichandparsad[3], Kapil S. Satyapal[1], Lelika Lazarus[1]

[1]Discipline of Clinical Anatomy, School of Laboratory Medicine and Medical Sciences, College of Health Sciences, University of KwaZulu-Natal, Westville Campus, Private Bag X54001, Durban, South Africa.
[2]Department of Neurosurgery, School of Clinical Medicine, College of Health Sciences, Nelson R Mandela School of Medicine, University of KwaZulu-Natal, Durban, South Africa.
[3]Department of Radiology, Jackpersad and Partners Inc., Specialist Diagnostic Radiologists, Lenmed Ethekwini Hospital and Heart Centre, Durban, South Africa.

Corresponding Author: Professor L Lazarus

Address: Discipline of Clinical Anatomy, School of Laboratory Medicine and Medical Sciences, College of Health Sciences, University of KwaZulu-Natal, Westville Campus, Private Bag X54001, Durban, South Africa.

Email address: ramsaroopl@ukzn.ac.za

+27 31 260 7899

Accepted for publication in the Italian Journal of Anatomy and Embryology on the 25th of November 2019.

TITLE PAGE

Title: Anatomical Variations of the Vertebral Arteries in a Select South African Population; Evaluation with Multidetector Computed Tomography Angiography

Author: Bukola R. Omotoso[1], Indresan G. Moodley[2], Rohen Harrichandparsad[3], Kapil S. Satyapal[1], Lelika Lazarus[1]

Name of institution: [1]Department of Clinical Anatomy School of Laboratory Medicine and Medical Science College of Health Sciences University of KwaZulu-Natal Westville Campus Private Bag X54001 Durban 4000

[2]Department of Radiology Jackpersad and Partners Inc. Specialist Diagnostic Radiologists Lenmed Ethekwini Hospital and Heart Centre South Africa

[3]Department of Neurosurgery School of Clinical Medicine College of Health Sciences Nelson R Mandela School of Medicine
University of KwaZulu-Natal
PO Box 17039
Congella
4013

Type of article: Original communication

Running headline: Anatomical variations of the vertebral artery

Author to whom prints and offprint requests are to be sent:
Prof Lelika Lazarus
Department of Clinical Anatomy
School of Laboratory Medicine and Medical Science
College of Health Sciences
University of KwaZulu-Natal
Private Bag X54001
Durban
4000
South Africa

Telephone number: +27 31 260 7899

Fax number: +27 31 260 7890

Email Address: ramsaroopl@ukzn.ac.za

Financial Aid: None

Title: Anatomical Variations of The Vertebral Arteries in a Select South African Population; Evaluation with Multidetector Computed Tomography Angiography

Summary

Morphological variation of the vertebral artery has been associated with different clinical symptoms and cerebrovascular disorders in the literature. These include; cerebrovascular lesions, neurological sequalae, ataxia, arterial dissection, potential atherosclerosis vertebrobasilar insufficiency and transient ischemic attacks. Variant anatomy such tortuosity, variation in origin and the level of entering the transverse foramen can also predispose the artery to iatrogenic injury during surgical intervention. We report on four cases of morphological variations of the vertebral artery in 2 Indian, 1white and 1 black South African male and female subject. In three of the cases, there is bilateral tortuosity and a left vertebral artery entering the transverse foramen at C7. In the fourth case, a left vertebral artery took it origin directly from the arch of aorta and was hypoplastic. Tortuosity occurred at V1 and V2 segments leading to a significant and potentially dangerous medial and lateral artery displacement. The hypoplastic vertebral artery has a diameter of 1.58mm compared with 2.38mm of the right. Variations in the origin and anomalous proximal course of the vertebral artery are dangerous during surgery of the lower neck region and cervical spine surgery. In the presence of tortuous vertebral artery, the standard surgical landmarks may not prevent iatrogenic injury thus, it is important to recognize the presence of this morphological variation during preoperative planning to prevent laceration of the artery during anterior and lateral approach to the cervical spine. Increase awareness of prevalence of anatomic variation will contribute to the advancement of noninvasive imaging capabilities.

Keywords: Morphological variation, Vertebral artery, Hypoplasia, Basilar artery, Cervical vertebrae, Tortuosity, Iatrogenic injury.

TEXT

Introduction

Morphological variation of the vertebral artery (VA) has been associated with different clinical symptoms and cerebrovascular disorders (Albayram et al., 2002). It can also predispose the artery to iatrogenic injury during surgical intervention. In-depth knowledge of these variations is essential for surgical operation at the root of the neck as well as during lateral and anterior approaches to the cervical spine, and for diagnosis of some diseases in the posterior circulatory territory. Such morphological variations include variant origin, duplicate origin, variation in the level of entering the transverse foramen, tortuosity, asymmetry, hypoplasia, fenestration of the artery and persistent of the intersegmental artery (PFIA) (Chen et al., 2010, Dodevski and Tosovska-Lazarova, 2012, George and Laurian, 2012).

Anatomically, vertebral arteries are large major arteries of the neck which have their origin from the supero-posterior aspect of the first part of the subclavian artery (George and Laurian, 2012). It runs superior and posterior in the scaleno-vertebral triangle which is formed by scalenus anterior and longus colli muscles (Dodevski and Tosovska-Lazarova, 2012). The vertebral artery enters the transverse foramen at the level of sixth cervical vertebra although this may vary from seventh to third cervical vertebrae (C7-C3) (Wakao et al., 2014). It then proceeds superiorly in the foramina of the cervical transverse process from C6-C1 (Singla et al., 2010) and finally pierces the atlantooccipital membrane and the dura mater to enter the foramen magnum with its intracranial course (Matula et al., 1997). It is segmented into 4 sections: prevertebral (V1), vertebral (V2), atlantoaxial (V3) and intracranial (V4) segment (Jecko et al., 2015). Knowing the exact detail of the origin and course at each of the segment of the VA is very important in preventing catastrophic laceration of the vertebral artery and clinical diagnosis in the posterior circulation. In this article, we describe four cases of morphological variations including tortuosity, variant origin, hypoplasia and variant level of entering the transverse foramen in one of the VA with detailed imaging findings.

Case presentation

Case 1

Computed Tomography Angiography (CTA) scan of the neck and intracranial vessels of a 67-year-old Indian South African female shows marked tortuosity of the distal vertebral arteries with twisting of the 4th segment of the vertebral arteries at the vertebrobasilar junction and variant level of entering the transverse foramen at C7 on the left VA (Figure 1A, E). The patients presented to Lenmed Ethekwini Hospital and Heart Centre for cerebrovascular accident. Clinical examination showed middle cerebral artery infarct, increased peak systolic velocity at the left internal carotid artery. Also, extensive calcification is noted at the aortic arch, origin of the great vessels and carotid arteries bilaterally.

Case 2

CTA scan of the neck and intracranial vessels of a 59-year-old black South African female shows tortuosity of the distal vertebral arteries in the V1 and V2 segment (Figure 1B). The patients presented to Lenmed Ethekwini Hospital and Heart Centre in South Africa for right sided infarct.

Case 3

CTA scan of the neck and intracranial vessels of a 78-year-old Indian South African male shows marked tortuosity of the distal vertebral arteries at the V1 and V2 segment. The patients presented to Lenmed Ethekwini Hospital and Heart Centre for recurring presyncope. Besides tortuosity at the V1, V2, there is slight narrowing of the proximal basilar artery due to noncalcified plaque (Figure 1C).

Case 4

A 39-year-old white South African male presented to the Lenmed Ethekwini Hospital and Heart Centre for episodes of left sided limb weakness and decreased sensation in the left arm. The patient underwent a CTA scan of head and neck and aortic arch and its branches which revealed that the left VA arose directly from the arch of aorta and was hypoplastic with a diameter of 1.58mm compared with diameter of 2.38mm on the right vertebral artery (Figure 1D)**.** Our study is retrospective in nature, therefore, written informed consent was not obtained. However, the design of this study was approved by our Institutional Review Board/Ethics Committee (Biomedical Research Ethics Committee of the University of KwaZulu-Natal with ethical No: BE 148/19) since it forms part of a larger study exploring the anatomy of the vertebral arteries in a select South African population.

Discussion

Apart from variant anatomy like variation in origin, level of entering the transverse foramen and hypoplasia in this study, bilateral tortuosity of the VA is also reported. Tortuosity has been reported mostly by international studies. It occurrence seems to exists at a dissimilar rate in different regions and ethnic groups, data from African population is scarce (Matula et al., 1997, Alicioglu et al., 2015, Yenigun et al., 2016). Complex embryological evolution of the vertebral artery has resulted in a wide range of anatomical variations. During embryological development, the VA develops from fusion of the six transversely oriented cervical intersegmental arteries (CIA) and proatlantal intersegmental artery (PIA) which later regresses except for the sixth cervical intersegmental artery which persist to form the proximal subclavian artery and the point of origin of the adult vertebral artery (Anderson and

Sondheimer, 1976, Luh et al., 1999). Developmental abnormalities at the caudal portion of the intersegmental arteries leads to variant origin of the VA from the aortic arch which may also increase the risk of developing vertebral artery hypoplasia (VAH) compared with VA with normal origin similar to the report in one of the subjects (Figure 1D) (Panicker et al., 2002, Kośla et al., 2014). VAH is defined as the small lumen diameter of the VA. Authors have suggested that persistence of the carotid-vertebrobasilar anastomosis is a compensation for delayed development of vertebrobasilar artery (Luh et al., 1999). Consequently, VAH is formed as a result of the delayed development of vertebrobasilar artery (Kim et al., 2017).

Another important variant anatomy is the level of entering the transverse foramen. Researchers have suggested that the level at which the VA enters the foramen transversarium is related to which specific cervical intersegmental vessel persisted to form the proximal VA (Caldemeyer et al., 1998) but it is not clear the persistence of which of the CIA is responsible for entering the transverse foramen of 7^{th} cervical vertebrae as reported in a left VA of one the subjects (Figure 1A).

It is a general believe that variation in origin and level of entering the transverse foramen of the VA is as result of abnormal arrangement in the fusion process of CIA and PIA. Since the V1 and V2 segment develops from these two primitive arteries while part of PIA becomes the horizontal portion of V3 (Luh et al., 1999), the possibility of these abnormal fusion contributing to tortuosity at V1 and V2 segment cannot be ruled out. The precise mechanism of formation of VA tortuosity is not clear (Han, 2012), and it is difficult to assess the suggested congenital origin (Elgueta et al., 2018). Some authors have suggested that it develops in association with connective tissue disorders (Morris et al., 2011) or as a result of vertebral artery elongation caused by narrowing of the disc space (Sakaida et al., 2001). Others hypothesized reduced elasticity, degeneration of blood vessels, and vascular wall shear stress as possible cause (Han, 2012, Lee et al., 2012). Another study suggested vascular risk factors such as hypertension, diabetes, and lipid metabolism disorders. These factors can promote atherosclerosis, aging, and degeneration of blood vessels, thereby aggravating vertebrobasilar artery tortuosity (Ikeda et al., 2010). It has been reported that tortuosity increases with age as it is mostly reported in older patients (Alicioglu et al., 2015, Elgueta et al., 2018), suggesting aging as one of the predisposing factors to arterial tortuosity. Our findings also support this hypothesis as the average age of subjects with tortuous VA is 68 years.

Origin of the VA from an artery other than the subclavian artery increases blood pressure significantly and has been associated with cerebrovascular lesions, neurological sequalae, ataxia, arterial dissection, and potential atherosclerosis (Dudich et al., 2005, Gabrielli and Rosati, 2013, Yuan, 2016). Hypoplastic VAs are more prone to occlusion, atherosclerosis susceptibility and ipsilateral lesion. Thus, they constitute a risk factor for vertebrobasilar stroke, especially infarcts and hypoperfusion of posterior inferior cerebellar artery (PICA) territory and lateral medullary infarcts (Chaturvedi et al., 1999, Chuang et al., 2006, Giannopoulos et al., 2007, Park et al., 2007, Thierfelder et al., 2014). Tortuosity or loop formation most especially multiple medial loops as reported in this study may predispose the VA to iatrogenic injury during anterior surgical approach to the cervical spine (Wakao et al., 2016). In addition to risk of damage during surgery, vertebral artery tortuosity has been diagnosed in association with various neurovascular problems such as vascular vertigo (Hong-Tao et al., 2014), cervicobrachial pain (Paksoy et al., 2003), cervical radiculopathy (Doweidar et al., 2014) while a similar report suggested that VA loops and tortuosity are asymptomatic and incidentally diagnosed during evaluation of neck problems and trauma (Chibbaro et al., 2012). These wide range of neurovascular problems diagnosed in association with loop formation suggests that VA tortuosity may be a co-factor for these clinical manifestations and not the major cause. We also hypothesized that tortuosity is mostly symptomatic when it co-exists with other cerebrovascular risk factors, its occurrence as a variant anatomy may be asymptomatic. It has been reported that incidence of transient ischemic attacks (TIAs) in the vertebrobasilar system is high in patients with combined carotid and vertebral artery structural disorder compared to patient with isolated carotid artery disease (Delcker et al., 1993). Stenosis of the internal carotid artery and left common carotid artery in addition to vertebral artery tortuosity as reported in two of our subjects (case 1,3) can also predispose the subjects to TIAs.

Presence of anatomical variation of the VA induce wide range of clinical symptoms and pathogenesis is not always well explained. It is also one of the reasons for accidental injury of the VA (Guan et al., 2017). Consequently, in-depth knowledge of anatomical variation in the course of the VA is essential for diagnosis as well as surgical operation in the vicinity of the artery. Awareness of potential anomalies allows surgeons to avoid iatrogenic injury.

In conclusion, this report describes three elderly patients with bilateral tortuosity at V1, V2 and twisting of the V4 at vertebrobasilar junction in one of the patients. Also, the left VA enters the transverse foramen of seventh cervical vertebra in one of the patients. In the fourth patient the left vertebral artery has a variable origin, and it is hypoplastic. Occurrence of anatomical variation of the vertebral artery is diverse and inherent. Therefore, presence of variations should be systematically assessed on preoperative investigations as they sometimes coexist with one another without obvious clinical symptoms. This is to avoid inadvertent tearing of the artery during anterior and lateral approach to the cervical spine. It is necessary to identify morphologic variations preoperatively and alert the surgeon for appropriate modification of surgical procedure to reduce the likelihood of injury.

Conflict of Interest:

The authors declare that they have no conflict of interest.

References

Albayram, S., Gailloud, P. & Wasserman, B (2002). Bilateral arch origin of the vertebral arteries. AJNR Am J Neuroradiol 23**,** 455-458.

Alicioglu, B., Gulekon, N. & Akpinar, S. (2015). Age-related morphologic changes of the vertebral artery in the transverse process. Analysis by multidetector computed tomography angiography. The Spine Journal, 15**,** 1981-1987.

Anderson, R. & Sondheimer, F. (1976). Rare carotid-vertebrobasilar anastomoses with notes on the differentiation between proatlantal and hypoglossal arteries. J Neuroradiology, 11**,** 113-118.

Caldemeyer, K. S., Carrico, J. B. & Mathews, V. P. (1998). The radiology and embryology of anomalous arteries of the head and neck. AJR, 170**,** 197-203.

Chaturvedi, S., Lukovits, T. G., Chen, W. & Gorelick, P. B. (1999). Ischemia in the territory of a hypoplastic vertebrobasilar system. *Neurology,* 52**,** 980-980.

Chen, Y.-Y., Chao, A.-C., Hsu, H.-Y., Chung, C.-P., Hu, H.-H. (2010). Vertebral artery hypoplasia is associated with a decrease in net vertebral flow volume. Ultrasound Med Biol 36**,** 38-43.

Chibbaro, S., Mirone, G., Yasuda, M., Marsella, M., Di Emidio, P. & George, B. (2012). Vertebral artery loop—a cause of cervical radiculopathy. World neurosurgery, 78**,** 375. e11-375. e13.

Chuang, Y.-M., Huang, Y.-C., Hu, H.-H. & Yang, C.-Y. (2006). Toward a further elucidation: role of vertebral artery hypoplasia in acute ischemic stroke. J European neurology,55**,** 193-197.

Delcker, A., Diener, H., Timmann, D. & Faustmann, P. (1993). The role of vertebral and internal carotid artery disease in the pathogenesis of vertebrobasilar transient ischemic attacks. EUR ARCH PSY CLIN N Journal, 242**,** 179-183.

Dodevski, A. & Tosovska-Lazarova, D. (2012). Anatomical features and clinical importance of the vertebral artery. Open Access Maced J Med Sci., 5**,** 328-335.

Doweidar, A., Al-Sayed, S. & Al-Kandery, S. (2014). Symptomatic Vertebral Artery Loop: A case report and review of literature. J. Radiol. Case Rep., 8**,** 35.

Dudich, K., Bhadelia, R. & Srinivasan, J. (2005). Anomalous vertebral artery origin may be an independent risk factor for arterial dissection. Eur. J. Neurol., 12**,** 571-572.

Elgueta, M. F., Jimenez, J. O., Wang, N. N., Lara, A. P., Chankowsky, J., Charghi, R., Tran, D. Q. & Finlayson, R. J. (2018). Anatomical Variations of the Vertebral Artery in the Upper Cervical Spine: Clinical Relevance for Procedures Targeting the C1/C2 and C2/C3 Joints. Regional anesthesia and pain medicine, 43**,** 367-371.

Gabrielli, R. & Rosati, M. S. (2013). Ataxia and vertigo due to anomalous origin of the left vertebral artery. J Vasc Surg, 58**,** 803.

George, B. & Laurian, C. 2012. The vertebral artery: pathology and surgery, Springer Science & Business Media.

Giannopoulos, S., Markoula, S., Kosmidou, M., Pelidou, S.-H. & Kyritsis, A. P. (2007). Lateral medullary ischaemic events in young adults with hypoplastic vertebral artery. J. Neurol. Neurosurg. Psychiatry, 78**,** 987-989.

Guan, Q., Chen, L., Long, Y. & Xiang, Z. (2017). Iatrogenic vertebral artery injury during anterior cervical spine surgery: a systematic review. J World neurosurgery, 106**,** 715-722.

Han, H.-C. (2012). Twisted blood vessels: symptoms, etiology and biomechanical mechanisms. J Vasc Res, 49**,** 185-197.

Hong-Tao, Z., Shu-Ling, Z. & Dao-Pei, Z. J. B. N. (2014). Two case reports of bilateral vertebral artery tortuosity and spiral twisting in vascular vertigo. BMC neurology 14**,** 14.

Ikeda, K., Nakamura, Y., Hirayama, T., Sekine, T., Nagata, R., Kano, O., Kawabe, K., Kiyozuka, T., Tamura, M. & Iwasaki, Y. (2010). Cardiovascular risk and neuroradiological profiles in asymptomatic vertebrobasilar dolichoectasia. J Stroke Cerebrovasc Dis, 30**,** 23-28.

Jecko, V., Rué, M., Castetbon, V., Berge, J. & Vignes, J.-R. J. N. (2015). Vertebral artery (V2) pseudo-aneurysm after surgery for cervical schwannoma. How to prevent it and a review of the literature. Neurochirurgie, 61**,** 38-42.

Kim, C., Sohn, J.-H. & Choi, H.-C. J. B. N. (2017). Are the anomalous vertebral arteries more hypoplastic?: retrospective linear mixed model approach. BMC neurology, 17**,** 168.

Kośla, K. N., Majos, M., Podgórski, M., Polguj, M., Topol, M., Stefańczyk, L. & Majos, A. (2014). Anomalous course and diameter of left-sided vertebral arteries–significance and predisposing factors in clinical practice. Annals of Anatomy-Anatomischer Anzeiger, 196**,** 360-364.

Lee, S. H., Hur, N., Jeong, S.-K. (2012). Geometric analysis and blood flow simulation of basilar artery. Atheroscler Suppl, 19**,** 397-401.

Luh, G., Dean, B., Tomsick, T. & Wallace, R. (1999). The persistent fetal carotid-vertebrobasilar anastomoses. *AJR Am. J. Roentgenol,* 172**,** 1427-1432.

Matula, C., Trattnig, S., Tschabitscher, M., Day, J. & Koos, W. T. (1997). The course of the prevertebral segment of the vertebral artery: anatomy and clinical significance. Surgical neurology, 48**,** 131.

Morris, S. A., Orbach, D. B., Geva, T., Singh, M. N., Gauvreau, K. & Lacro, R. V. J. C. (2011). Increased vertebral artery tortuosity index is associated with adverse outcomes in children and young adults with connective tissue disorders. *J Circulation,* 124**,** 388-396.

Paksoy, Y., Levendoglu, F. D., Ögün, C. Ö., Üstün, M. E. & Ögün, T. C. J. S. (2003). Vertebral artery loop formation: a frequent cause of cervicobrachial pain. Spine J, 28**,** 1183-1188.

Panicker, H., Tarnekar, A., Dhawane, V. & Ghosh, S. (2002). Anomalous origin of left vertebral artery-embryological basis and applied aspects-a case report. J Anat Soc India, 51**,** 234-5.

Park, J.-H., Kim, J.-M. & Roh, J.-K. (2007). Hypoplastic vertebral artery: frequency and associations with ischaemic stroke territory. J. Neurol. Neurosurg. Psychiatry, 78**,** 954-958.

Sakaida, H., Okada, M. & Yamamoto, A. (2001). Vascular reconstruction of a vertebral artery loop causing cervical radiculopathy and vertebrobasilar insufficiency: case report. J. Neurosurg. Spine, 94**,** 145-149.

Singla, R. K., Sharma, T. & Sachdeva, K. (2010). Variant origin of left vertebral arteryin. International Journal of Anatomical Variations, 3, 1.

Thierfelder, K. M., Baumann, A. B., Sommer, W. H., Armbruster, M., Opherk, C., Janssen, H., Reiser, M. F., Straube, A. & Von Baumgarten, L. J. S. (2014). Vertebral artery hypoplasia: frequency and effect on cerebellar blood flow characteristics. 45**,** 1363-1368.

Wakao, N., Takeuchi, M., Nishimura, M., Riew, K. D., Kamiya, M., Hirasawa, A., Imagama, S., Kawanami, K., Murotani, K. & Takayasu, M. (2016). Risks for vascular injury during anterior cervical spine surgery: prevalence of a medial loop of vertebral artery and internal carotid artery. Spine, 41**,** 293-298.

Wakao, N., Takeuchi, M., Nishimura, M., Riew, K. D., Kamiya, M., Hirasawa, A., Kawanami, K., Imagama, S., Sato, K. & Takayasu, M. J. N. (2014). Vertebral artery variations and

osseous anomaly at the C1-2 level diagnosed by 3D CT angiography in normal subjects. Neuroradiology, 56**,** 843-849.
Yenigun, A., Ustun, M., Tugrul, S., Dogan, R., Ozturan, O. J. T. J. O. L. & Otology (2016). Classification of vertebral artery loop formation and association with cervicogenic dizziness. J Laryngol Otol, 130**,** 1115-1119.
Yuan, S.-M. (2016). Aberrant origin of vertebral artery and its clinical implications. BRAZ J CARDIOV SURG, 31**,** 52-59.

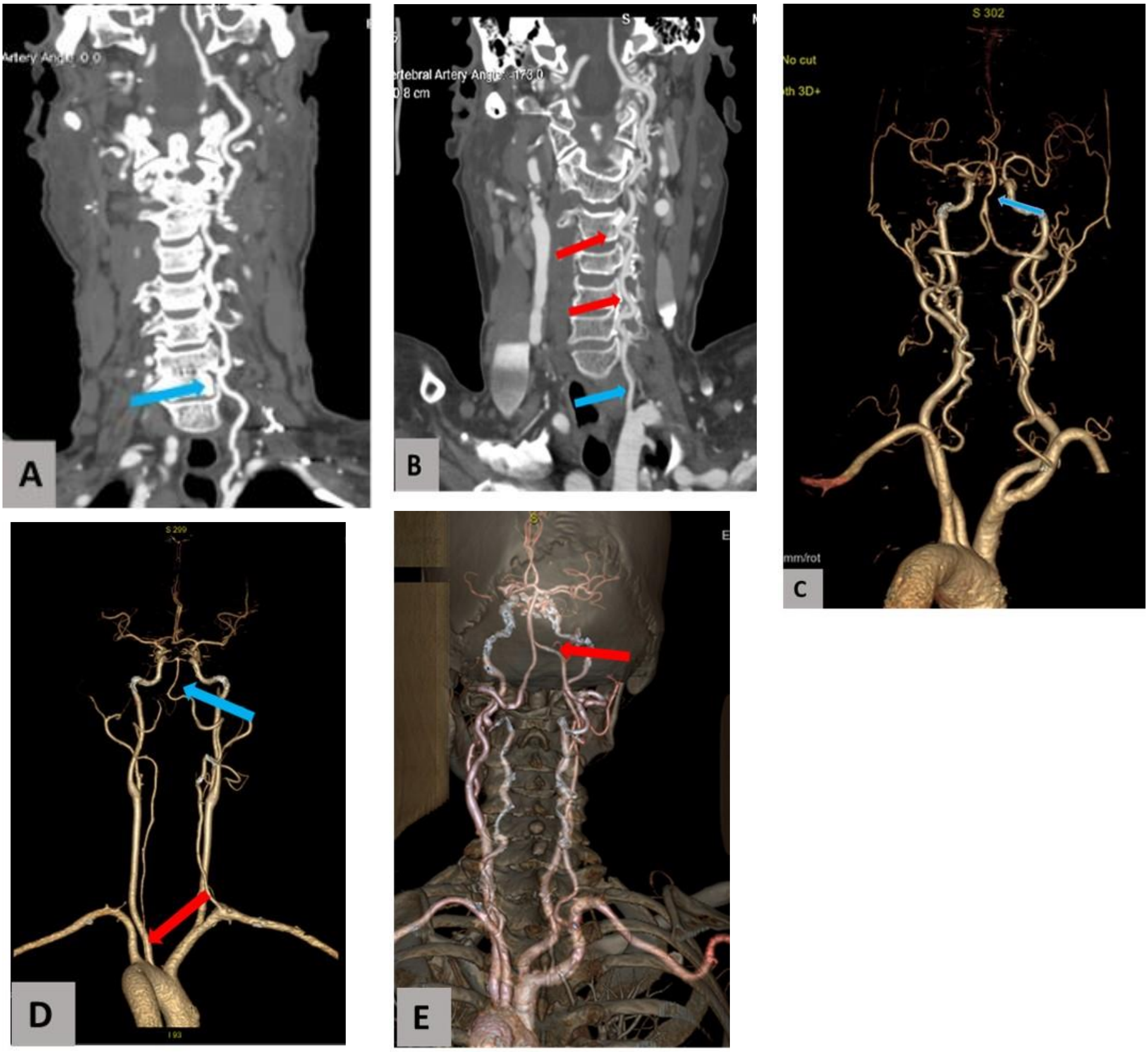
A
B
C
D
E
S 302
No cut
mm/rot

Figure 1

CTA images of case 1(A, E), case 2(B) case 3(C) case 4(D).

A, E) Coronal view and 3D reconstructed image shows tortuosity in the V1-V2 segment. Blue arrow shows entering of the left VA through the transverse foramen of 7th cervical vertebra while the red arrow shows twisting of the 4th segment at the vertebrobasilar junction. **B)** Coronal view shows multiple loops at V2 segment (two red arrows) of the left VA. Blue arrow shows mild tortuosity at V1. **C)** 3D reconstructed image shows tortuosity in the V1-V2 segment of the VA. Blue arrow shows narrowing of the proximal part of the basilar due to uncalcified plaques. **D)** 3D reconstructed image, red arrow shows origin of the left hypoplastic vertebral artery from the aortic arch, blue arrow shows the basilar artery solely formed by the right VA.

CHAPTER SEVEN
SYNTHESIS AND CONCLUSION

7.1 Synthesis

VA injuries are the most common type of injury during cervical spine surgery (Decarvalho et al., 2018). Some authors have quantified the incidence of injury to the VA during the surgical intervention (Madawi et al., 1997, Wright and Lauryssen, 1998). The VA is at risk of damage during anterior, posterior, and lateral approaches to cervical spine surgery and surgical procedures involving the occipito-atlanto-axial region (Wright and Lauryssen, 1998, Neo et al., 2008). Recent updates from researchers have shown that the likelihood of injury is increased by anatomical variation in the course of the VA (Decarvalho et al., 2019). There is limited research on the prevalence of anatomical variations in the course of the VA especially the suboccipital and intracranial segments. Most of the previous studies are international studies that do not necessarily take racial variation into account.

In this observational study, we investigate the anatomical features of the extracranial (V1-V3) and intracranial (V4) components of the VAs in a South African population using MDCTA. After a detailed literature review, it was apparent that this may be the first comprehensive report on the morphology and morphometry of the VA from its origin to the point where they merge to form the basilar artery. This study systematically describes the typical anatomy (including the average length and diameter) and the prevalence of variations in the course of the VA.

The first manuscript (chapter two) focuses on the proximal part of the VA (V1, V2), where we document the prevalence of variation in origin (all on the left), level of entering the transverse foramen, VA tortuosity, VA hypoplasia, and pattern of dominance. The average diameter and length at the V1 and V2 segments are reported and compared to previous literature reports. In the second manuscript (chapter three), we describe the prevalence of morphologic variation and the morphometry of the suboccipital segment (V3) of the VA. Here we registered variations such as the incidence of PICA originating from this segment, persistent first intersegmental artery, fenestration, and VA hypoplasia. For description, the V3 was subdivided into three portions: the vertical, horizontal, and oblique parts. In addition to the prevalence of variation, we also reported the average diameter and length at each part of the V3. The third manuscript (chapter four) describes the typical anatomy and prevalence of variation of the intracranial segment of the VA. Various anatomical variations were recorded at this segment. The most frequent is VA hypoplasia. Others include hypoplastic terminal VA, VA terminating as PICA (atresia), and fenestration. Similar to the previous chapter, we report the average diameter and length and the angle between the bilateral VA at the vertebrobasilar junction.

Another important finding is an anatomical variation involving the proximal and distal VA; the left VA of aortic arch origin terminating as PICA. This variation has been associated with the left VA with no previous report involving the right VA. Only a few studies have reported this type of variant anatomy

(Ohkura et al., 2014, Van Der Weijde et al., 2019). Out of the 554 patients in our series, 38 left VA arose from the arch of the aorta, and 4 of the 38 VAs were atretic. We hypothesize that special attention should be paid to the distal VA of aortic arch origin for the possibility of coexistence with atresia. This can influence the choice of treatment of aortic arch disease and surgical intervention in the supra-aortic arch region. Furthermore, obstruction of this type of VA can increase the risk of posterior circulatory stroke (Ohkura et al., 2014). Knowledge of this variant anatomy is essential when planning for thoracic aortic surgery.

While collating the data on the prevalence of variation, we observed some anatomical variations and reported on the incidence. In the fourth manuscript (chapter five), we report the incidence of fenestration at the vertebrobasilar junction. The fifth manuscript (chapter six) describes various morphological variations, including twisting of the intracranial segment, tortuosity of the proximal VAs, variation in origin and level of entering the transverse foramen, and hypoplasia. Because these two manuscripts are based on case studies, we could hypothesize the link between some anatomical variations and the clinical presentation of patients.

Anatomical variation of the VA is common in the South African population studied. It is worth noting that sometimes anatomical variation coexists involving more than one segment of the VA. For instance, variation in origin can influence the level of entering the transverse foramen. We also observed that variation in the level of entering the transverse foramen is expected on the right when there is variation in origin and level of entering the transverse foramen on the left. In addition, we found cases of variation in the origin of the left VA and atresia of the ipsilateral VA. It is important to note that each of these variant anatomies may have a different clinical significance in diagnosing pathology, interpretation of preoperative images, and endovascular procedure (Kovač et al., 2014). For instance, variation in entry-level could be missed on a non-injected CT scan (Dodevski and Tosovska-Lazarova, 2012). Preoperative knowledge of this type of variation is mandatory for surgical intervention in the vicinity of the VA (Bruneau et al., 2006).

Noticeably, the mean diameter of the VA reduces along its length from its proximal part (V1) to the distal part (V4) except for the horizontal part of the V3, which is larger than the vertical portion. Therefore, we used different criteria (< 2.7, ≤ 2.5, and ≤ 2 mm) to define VA hypoplasia at each segment of the artery (V1, V2; V3; V4). Previous studies have documented similar changes in size along the length of the VA (Cavdar et al., 1996, Mitchell, 2004). The data distribution in the present study showed that the diameter difference between the left and right VA is not so vast though we registered a significantly larger left in all the segments. Furthermore, using the criterion of any size difference to define the pattern of dominance between the bilateral VAs at the intracranial segment for instance, we found 45.3% were left dominant, 32.7% were right dominant, and codominance was observed in 11.9% of patients. Knowledge of the dominant VA is required for some endovascular procedures. It is also important to preserve the dominant VA since they are likely to predominates the basilar artery. This information is vital to reduce the risk of neurological symptoms that may results from iatrogenic injury.

7.2 Study Limitation

Firstly, this is a single-center retrospective study. Data generated might not be adequate to make a generalized conclusion for the whole South Africa population. Secondly, specific information about the interracial difference was not provided in the patient's report. Therefore, the authors relied on the available information in the hospital database to deduce patients' ethnicity since the study is retrospective.

7.3 Conclusion

Conclusion from this study has consequences for safe surgical interventions in the vicinity of the VA. Anatomical variations of the VA are common in the South African population studied in this work. Due to the unpredictable nature of anatomical variation, the physician performing endovascular procedures and surgery around the VA needs to be aware of its prevalence. Opinion differs about the necessities of routine preoperative angiographies for evaluating cerebral vasculature due to its downsides. While some authors propose CTAs before cervical spine interventions, others have suggested that it is unnecessary, especially when the prevalence of anatomical variations of the VAs is low in a population group. Due to the frequencies of variation reported in the present study, we hypothesized that CTA might be required for safe surgical interventions around the VA and endovascular treatment of vascular pathologies. Alternatively, a non-contrast CT scan may be considered. However, non-contrast CT scan do not demonstrate vascular anatomy but may suggest the typical and variable course of the VA. When an anatomical variation is suspected in the course of the VA, CTA may be required for clarification. Except for the incidence of hypoplasia (right intracranial VA) that is high in the White and the Indian compared to the Black group, there was no significant racial or gender difference in the prevalence of other variations at the proximal, suboccipital, and distal segments of the VA. Awareness of the extent of possible anatomical variation will help/assist interpretation of radiographs, which will enhance the identification of vascular pathologies and reduce the risk of iatrogenic injury. Imaging of the entire course of the VA from the origin to the point of convergence to form the basilar artery may be necessary to select a treatment strategy for interventions in the vicinity of the VA. Furthermore, understanding the patterns of anatomical variations of the VAs will contribute significantly to the interpretation of ischemic areas and diagnosis of various diseases in the posterior circulatory territory.

7.3 Recommendation

The present study is retrospective; therefore, we recommend that more prospective and multicenter studies be carried out to corroborate the reported pathophysiological relationship between variant anatomy and associated vascular diseases. Furthermore, reports on the incidence of injury to the VA are scarce in the Africa population. Therefore, we recommend that studies quantifying the risk of injury to the VA are necessary since the recent report has shown that some of the incidences of injury are due to anatomical variations, which are avoidable when there is adequate preoperative knowledge. Lastly, we recommend that information about racial classification should be included in the patient's clinical report. This information is crucial to studies of demography, such as those reporting the prevalence of anatomical variation.

References

Bruneau, M., Cornelius, J. F., Marneffe, V., Triffaux, M. & George, B. (2006). Anatomical variations of the V2 segment of the vertebral artery. *J Operative Neurosurgery,* 59**,** ONS-20-ONS-24.

Cavdar, S., Dalcik, H., Ercan, F., Arbak, S. & Arifoglu, Y. (1996). A morphological study on the V2 segment of the vertebral artery. *Okajimas Folia Anat. Jpn.,* 73**,** 133-137.

Decarvalho, S. A., Abd-El-Barr, M. M. & Groff, M. W. (2018). Vascular Complications in Cervical Spine Surgery (Anterior and Posterior Approach). *Complications in Neurosurgery E-Book***,** 314.

Decarvalho, S. A., Abd-El-Barr, M. M. & Groff, M. W. (2019). Vascular Complications in Cervical Spine Surgery (Anterior and Posterior Approach). *Complications in Neurosurgery*. Elsevier.

Dodevski, A. & Tosovska-Lazarova, D. (2012). Anatomical features and clinical importance of the vertebral artery. *Open Access Maced J Med Sci.,* 5**,** 328-335.

Kovač, J. D., Stanković, A., Stanković, D., Kovač, B. & Šaranović, D. (2014). Intracranial arterial variations: a comprehensive evaluation using CT angiography. *Medical science monitor: international medical journal of experimental and clinical research,* 20**,** 420.

Madawi, A. A., Casey, A. T., Solanki, G. A., Tuite, G., Veres, R. & Crockard, H. A. (1997). Radiological and anatomical evaluation of the atlantoaxial transarticular screw fixation technique. *Journal of neurosurgery,* 86**,** 961-968.

Mitchell, J. (2004). Differences between left and right suboccipital and intracranial vertebral artery dimensions: an influence on blood flow to the hindbrain? *Physiother. Res. Int.,* 9**,** 85-95.

Neo, M., Fujibayashi, S., Miyata, M., Takemoto, M. & Nakamura, T. (2008). Vertebral artery injury during cervical spine surgery: a survey of more than 5600 operations. *Spine (Phila Pa 1976),* 33**,** 779-785.

Ohkura, K., Shiiya, N., Washiyama, N., Yamashita, K., Takahashi, D., Tsuda, K. & Kando, Y. (2014). Vertebral artery variations in thoracic aortic patients. *Eur. J. Cardiothorac. Surg.,* 46**,** 27-31.

Van Der Weijde, E., Bakker, O. J., Sonker, U. & Heijmen, R. H. (2019). Isolated left vertebral artery and its consequences for aortic arch repair. *Journal of vascular surgery cases and innovative techniques,* 5**,** 369-371.

Wright, N. M. & Lauryssen, C. (1998). Vertebral artery injury in C1–2 transarticular screw fixation: results of a survey of the AANS/CNS section on disorders of the spine and peripheral nerves. *J. Neurosurg.,* 88**,** 634-640.

Appendix

UNIVERSITY OF
KWAZULU-NATAL
INYUVESI
YAKWAZULU-NATALI

25 June 2019

Ms B Omotoso (217080986)
School of Laboratory Medicine and Medical Sciences
College of Health Sciences
217080986@stu.ukzn.ac.za

Protocol: An anatomical exploration of the vertebral arteries in a select KwaZulu-Natal population
Degree: PhD
BREC Ref No: BE148/19

EXPEDITED APPLICATION: APPROVAL LETTER

A sub-committee of the Biomedical Research Ethics Committee has considered and noted your application received 07 March 2019.

The study was provisionally approved pending appropriate responses to queries raised. Your response received on 24 June 2019 to BREC letter dated 25 April 2019 has been noted by a sub-committee of the Biomedical Research Ethics Committee. The conditions have been met and the study is given full ethics approval and may begin as from 25 June 2019. **Please ensure that site permissions are obtained and forwarded to BREC for approval before commencing research at a site.**

This approval is valid for one year from **25 June 2019**. To ensure uninterrupted approval of this study beyond the approval expiry date, an application for recertification must be submitted to BREC on the appropriate BREC form 2-3 months before the expiry date.

Any amendments to this study, unless urgently required to ensure safety of participants, must be approved by BREC prior to implementation.

Your acceptance of this approval denotes your compliance with South African National Research Ethics Guidelines (2015), South African National Good Clinical Practice Guidelines (2006) (if applicable) and with UKZN BREC ethics requirements as contained in the UKZN BREC Terms of Reference and Standard Operating Procedures, all available at http://research.ukzn.ac.za/Research-Ethics/Biomedical-Research-Ethics.aspx.

BREC is registered with the South African National Health Research Ethics Council (REC-290408-009). BREC has US Office for Human Research Protections (OHRP) Federal-wide Assurance (FWA 678).

The sub-committee's decision will be noted by a full Committee at its next meeting taking place on **09 July 2019.**

Yours sincerely

Prof D Wassenaar
Acting Chair: Biomedical Research Ethics Committee

cc: Postgrad administrator: [illegible] Supervisor: [illegible] [illegible]

Biomedical Research Ethics Committee
Professor V Rambiritch (Chair)
Westville Campus, Govan Mbeki Building
Postal Address: Private Bag X54001, Durban 4000
Telephone: +27 (0) 31 260 2486 **Facsimile:** +27 (0) 31 260 4609 **Email:** brec@ukzn.ac.za
Website: http://research.ukzn.ac.za/Research-Ethics/Biomedical-Research-Ethics.aspx

1910 - 2010
100 YEARS OF ACADEMIC EXCELLENCE

Founding Campuses: Edgewood ■ Howard College ■ Medical School ■ Pietermaritzburg ■ Westville

28 May 2020

Ms B Omotoso (217080986)
School of Laboratory Medicine and Medical Sciences
College of Health Sciences
217080986@stu.ukzn.ac.za

Dear Ms Omotoso

Protocol: An anatomical exploration of the vertebral arteries in a select KwaZulu-Natal population
Degree: PhD
BREC Ref No: BE148/19

RECERTIFICATION APPLICATION APPROVAL NOTICE

Approved:	25 June 2020
Expiration of Ethical Approval:	24 June 2021

I wish to advise you that your application for Recertification received on 25 May 2020 for the above protocol has been noted and approved by a sub-committee of the Biomedical Research Ethics Committee (BREC) for another approval period. The start and end dates of this period are indicated above.

If any modifications or adverse events occur in the project before your next scheduled review, you must submit them to BREC for review. Except in emergency situations, no change to the protocol may be implemented until you have received written BREC approval for the change.

The committee will be notified of the above approval at its next meeting to be held on 14 July 2020.

Yours sincerely

....
Ms A Marimuthu
(for) Prof D Wassenaar
Chair: Biomedical Research Ethics Committee

cc: Postgrad administrator: dudhraihp@ukzn.ac.za Supervisor: ramsaroopl@ukzn.ac.za harrichandparsad@ukzn.ac.za

Data set

SN	KZCODE	SEX	AGE	RACE	VOR	PTV1R	V1LRmm	V1DR	ELR	V2LR	PTV2R	V2DL	V3VR	V3VDR	V3HR	V3HDR	V3OR	V3ODR	V3PLR
1		1	68	2	1	0	31.2576	3.608	2	51.832	0	3.256	15.98256	2.992	10.34616	3.608	5.0996	2.64	66.66667
2		1	60	2	1	3	62.942	4.048	3	54.74392	0	3.52	26.73792	3.784	10.72632	3.52	5.44896	3.696	60.66667
3		0	71	2	1	0	32.6304	3.872	1	57.024	0	3.784	29.09368	3.344	8.58352	4.224	5.38032	3.65464	53
4		1	45	3	1	0	49.48152	5.016	2	77.37224	0	4.488	30.91986	4.488	9.0288	4.928	5.35744	4.488	103
5		0	44	2	1	0	44.05192	6.424	2	73.128	0	5.808	26.37272	5.72	8.54216	6.072	7.0928	4.24336	108.3333
6		0	46	1	1	0	42.3368	3.52	2	61.952	0	3.08	24.98082	2.992	7.43864	3.08	5.59416	3.168	99
7		0	87	3	1	3	29.5064	4.576	2	57.2352	0	4.664	24.97968	4.488	8.0344	4.224	5.7156	3.82096	43
8		0	69	1	1	0	34.81632	2.992	2	56.232	0	3.52	25.6124	3.344	9.19512	3.168	5.15856	2.728	55.66667
9		0	69	2	1	0	39.78656	2.552	2	61.87456	0	2.376	21.55208	2.376	4.89632	2.552	3.322	2.33112	49
10		0	54	1	1	1	40.11304	3.696	2	59.84	4	3.608	24.6488	3.256	7.87424	3.608	5.39088	3.256	98.66667
11		1	43	2	1	1	34.94744	4.136	2	60.54576	0	3.52	26.77224	3.608	5.42344	3.784	4.994	3.872	53.33333
12		0	54	2	1	3	46.99024	4.84	2	72.51904	1	4.664	30.46648	3.784	5.30816	4.488	4.422	3.96176	79.66667
13		1	64	2	1	1	36.07032	2.992	2	71.50264	0	2.904	26.664	2.992	7.93408	2.992	4.488	2.552	46.33333
14		0	89	2	1	1	40.81528	4.664	2	53.856	1	4.664	32.43504	4.664	6.36328	4.488	5.52816	4.43344	64.33333
15		1	52	3	1	1	31.05256	4.4	2	53.06576	1	4.224	26.69304	4.048	6.90448	4.224	4.73968	3.9644	99.66667
16		0	69	2	1	3	37.356	4.576	2	60.19288	1	4.312	23.14488	4.224	5.6584	4.312	4.57424	4.752	50
17		1	38	2	1	3	39.51992	4.048	2	53.53304	0	3.784	21.64888	3.608	5.80272	3.52	4.1404	3.696	43.33333
18		0	69	2	1	3	44.8712	4.664	3	64.97744	4	4.664	36.06328	4.84	5.17968	5.28	4.488	4.664	49.33333
19		1	57	3	1	1	44.58872	4.136	2	59.972	0	3.872	36.432	3.608	3.31848	3.784	5.44632	3.784	76.33333
20		1	75	3	1	3	40.48	5.456	2	65.29688	0	4.664	30.25704	4.488	7.02328	5.544	5.62672	4.4	84.66667
21		0	72	2	1	1	29.6648	4.048	2	72.91152	1	4.048	26.94208	3.872	5.67776	3.96	4.1184	3.96	62.66667
22		0	67	2	1	3	40.216	3.256	2	64.24	0	3.168	35.8644	3.168	5.74464	3.696	4.63672	3.696	84.66667
23		1	71	3	1	0	30.624	3.696	2	67.848	0	3.432	31.15552	3.432	5.90304	3.432	4.6068	2.992	47.33333
24		0	44	3	1	0	37.01104	5.016	2	68.904	0	4.752	33.03696	4.664	9.05432	4.664	5.19376	4.35776	57.33333
25		1	75	2	1	3	37.58304	4.136	2	70.048	0	4.312	15.87256	4.312	11.79024	3.696	6.75488	5.104	56.33333
26		0	65	2	1	1	34.19152	3.872	2	71.192	0	3.872	30.47088	3.256	6.3008	3.872	4.26448	4.488	93
27		1	54	3	1	0	29.8716	2.904	2	72.336	1	2.904	27.24656	2.904	7.31544	3.08	4.10256	3.1548	61
28		1	16	1	1	0	25.08	3.168	2	73.392	0	3.08	16.192	2.816	5.74728	2.992	3.4012	3.696	90.33333
29		0	75	2	1	1	33.31856	3.696	2	74.536	0	2.112	28.47064	2.112	8.21744	2.25456	3.828	4.49856	56.33333
30		1	59	2	1	0	23.10088	2.992	2	75.68	0	3.08	19.30544	3.168	8.29224	2.816	3.7796	3.344	48
31		1	57	2	1	0	50.512	6.512	2	76.824	0	6.072	30.096	5.984	7.656	NA	NA	NA	59.33333
32		1	74	2	1	0	30.624	3.168	2	77.968	0	3.256	33.16632	3.256	8.0652	3.696	5.10664	3.60712	90.66667
33		1	60	3	1	1	25.872	3.872	2	48.576	0	3.872	21.38576	3.432	7.25824	3.432	4.77576	3.46192	43
34		0	75	2	1	4	37.114	3.432	2	76.16136	3	3.432	29.3832	3.256	7.53368	3.696	5.68392	3.40208	62.66667
35		1	70	3	1	4	34.76	3.784	2	55.37664	1	3.872	13.2	3.432	NA	NA	NA	NA	88.33333
36		0	69	3	1	1	44.01848	6.248	2	64.60872	1	6.336	39.13976	5.72	12.47752	5.368	7.21072	6.424	89
37		1	55	1	1	0	39.78128	4.4	2	69.388	0	4.4	23.07008	4.048	6.9696	4.488	4.67896	3.96	52.66667
38		1	72	3	1	1	31.944	3.96	2	63.8572	0	3.52	29.832	3.52352	9.71344	3.59568	5.9576	3.64496	93
39		0	10	3	1	0	26.81624	3.344	2	40.28904	0	3.52	22.35552	3.432	5.65576	3.432	4.10872	3.32904	50
40		1	77	3	1	1	47.27624	4.224	2	75.37992	1	4.136	NA	4.048	NA	NA	NA	NA	NA
41		1	54	2	1	0	42.65536	3.784	2	60.808	0	3.784	34.1748	3.696	7.38672	3.96	4.65696	4.94912	52
42		0	44	3	1	0	31.77944	4.224	2	51.21776	0	3.784	33.54384	3.96	8.6372	3.432	5.28176	3.64408	90.66667
43		0	59	1	1	1	27.72	2.728	2	42.33328	1	2.728	18.75896	2.904	5.7068	2.904	3.85792	2.6268	85.66667
44		1	62	2	1	1	31.65184	3.256	2	66.2464	0	3.168	17.62376	2.904	5.34688	3.168	3.476	3.08	48
45		1	61	2	1	0	81.37624	3.52	4	54.65064	1	3.432	18.12888	3.432	8.184	NA	NA	NA	45.66667
46		0	65	1	1	1	24.65848	3.872	2	77.63448	4	3.168	45.93688	3.168	9.39928	3.696	6.14064	3.872	59.33333
47		1	58	2	1	0	60.19728	3.52	3	43.67	0	3.432	24.55816	3.344	8.55624	2.904	7.41048	3.09496	47.66667
48		1	52	3	1	0	38.96376	3.96	2	60.92504	0	3.872	19.80264	3.08	12.09032	3.52	4.42992	3.344	46.66667
49		0	52	3	1	0	37.34808	4.4	2	57.38568	0	4.312	32.04168	4.224	10.15872	4.928	3.80336	4.36656	52.33333
50		0	71	2	1	0	31.66592	4.664	1	60.52288	0	4.136	31.41864	3.432	9.05696	4.84	4.34456	5.1128	43.33333
51		0	48	1	1	0	23.26632	4.4	2	59.31288	4	4.048	27.57216	4.488	10.44824	4.752	5.36712	4.32256	42
52		1	67	2	1	0	31.60432	2.728	2	53.3324	0	2.64	18.97456	2.64	3.93448	2.64	4.0436	2.992	73.66667
53		1	60	1	1	0	34.39128	2.64	2	70.35424	0	2.728	#DIV/0!	2.376	NA	NA	NA	NA	92
54		1	69	2	1	1	38.28	3.696	2	63.14088	0	3.52	27.64256	3.52	7.74136	3.872	5.61704	3.872	79.66667
55		1	49	2	1	1	30.16464	3.608	2	55.90904	0	3.52	32.74304	3.52	8.35296	3.696	5.08992	3.696	93.33333
56		1	68	2	1	1	30.09776	3.696	2	56.06128	0	3.344	26.3516	2.904	8.33712	3.696	5.33456	3.784	53.66667
57		1	33	1	1	0	40.04	2.992	2	60.15504	0	3.168	28.08784	3.08	9.1476	3.52	5.74288	3.608	46
58		0	28	2	1	0	45.31384	4.048	2	66.44528	0	3.608	25.8764	3.608	6.79712	3.344	5.27472	3.432	51.66667
59		1	69	2	1	0	38.36976	3.608	2	62.84256	0	3.432	26.16856	2.992	8.45504	3.432	5.31696	3.08	55
60		0	62	2	1	0	41.0608	3.784	2	62.0488	0	3.872	28.45656	3.784	6.95816	3.96	5.17528	3.63	53.66667
61		0	63	3	1	3	31.592	3.08	2	50.6	0	3.08	16.896	2.552	4.18704	3.08	3.36952	2.992	49
62		1	81	2	1	0	27.192	2.728	2	37.22576	0	2.464	20.62368	2.376	6.072	2.904	4.488	2.904	82.33333
63		1	64	1	1	1	34.232	3.168	2	38.72	0	3.08	20.07984	2.464	6.12832	2.904	2.50008	2.904	57
64		1	70	3	1	0	30.88976	3.608	2	42.416	0	3.168	11.616	3.168	5.61704	3.52	2.84328	3.52	70.66667
65		1	74	2	1	0	41.32832	4.488	2	52.91792	0	4.136	28.16792	4.048	8.30632	4.224	5.70416	4.136	73.66667
66		0	65	2	1	1	30.51752	3.52	2	49.66456	0	3.608	24.65672	3.52	9.07632	4.224	5.25536	4.048	53.66667
67		1	85	2	1	0	48.82504	3.96	2	60.86872	0	3.696	31.82784	3.784	8.47264	4.048	5.43136	3.96	57
68		0	70	1	1	1	41.75864	4.224	2	73.40872	0	3.872	31.77152	4.224	9.31216	4.488	5.76488	4.576	74.33333
69		1	62	2	1	0	27.368	3.608	2	59.7256	0	3.52	28.35888	3.432	10.60048	3.52	6.76896	3.52	76.66667
70		0	77	2	1	1	45.94216	3.608	3	46.992	0	3.872	21.96216	3.608	9.8824	3.52	5.85112	3.52	65.33333
71		0	62	2	1	1	40.60936	4.048	2	59.84176	0	3.872	23.34552	3.608	5.3856	3.608	5.11104	3.608	74.33333
72		1	65	3	1	0	39.38088	3.96	2	63.20336	0	3.52	28.07904	3.696	6.63344	3.696	5.13216	3.696	88
73		1	78	2	1	0	42.36056	3.344	2	51.39816	0	3.52	23.76176	3.08	7.25824	3.168	5.06704	3.2076	90
74		1	26	3	1	0	52.03704	3.784	2	59.0964	0	3.344	28.1424	3.52	NA	NA	NA	NA	88.66667
75		1	68	2	1	0	38.14888	3.784	2	72.71616	0	3.52	26.51528	3.52	9.17488	3.608	5.67776	3.432	83.66667
76		0	59	2	1	1	30.17696	3.784	2	41.60904	0	3.696	19.6812	3.432	7.24944	3.52	3.76992	3.4584	84
77		0	61	3	1	0	31.152	3.696	2	56.672	0	3.52	35.79928	3.696	7.07256	3.872	5.92416	3.872	73
78		1	68	3	1	1	44.41272	4.048	2	61.3844	0	3.784	30.59936	3.344	10.88736	3.608	5.35304	3.608	75
79		1	35	1	1	0	48.94032	4.048	2	61.84376	0	4.224	30.25176	3.696	7.73432	4.048	5.73232	4.048	47.33333
80		0	48	2	1	0	35.5784	3.608	2	59.32432	0	3.344	31.79264	3.168	10.9252	3.256	6.12744	3.256	61.66667
81		0	74	3	1	1	43.38488	3.344	2	52.55624	3	3.344	26.49504	2.992	7.77568	3.432	3.80336	3.52	64.66667
82		1	47	1	1	0	34.3948	4.136	2	65.6568	0	4.224	27.0028	3.96	8.89504	4.048	4.84088	4.224	66.33333
83		0	77	1	1	1	30.3512	3.256	2	55.38456	1	2.992	29.97368	3.168	10.17016	3.52	6.16616	3.432	106.6667
84		0	60	1	1	0	42.592	4.136	2	52.712	0	4.136	31.4556	3.608	8.26408	4.048	5.62848	3.872	77.33333
85		1	49	2	1	1	27.74728	3.344	2	59.928	0	3.256	26.07176	3.256	10.16048	3.52	5.11104	3.432	89.66667
86		1	35	3	1	0	40.54512	3.96	2	66.088	0	3.872	29.3788	3.256	9.5612	3.168	4.09728	3.14952	81
87		0	48	1	1	0	35.09968	4.136	2	60.91096	0	4.136	31.5128	3.608	9.6096	3.784	5.34512	4.488	72.66667
88		0	73	2	1	0	36.58776	3.432	2	52.316	0	3.168	25.25776	3.432	8.05552	3.696	5.11456	4.03744	63.33333
89		1	68	1	1	0	41.47792	3.432	2	59.96232	0	3.256	24.4156	3.168	NA	NA	NA	NA	77
90		1	60	2	1	0	48.4	2.992	2	68.11992	0	2.816	26.02248	2.904	11.77264	2.904	6.4724	3.08	69.33333
91		1	73	3	1	0	30.37056	4.136	2	54.13232	0	3.96	21.71312	3.872	4.26272	4.312	3.036	4.664	83.33333
92		1	83	3	1	0	24.728	4.312	2	49.43136	0	4.048	17.31312	4.4	5.6452	4.4	3.76992	4.752	90
93		0	43	1	1	0	30.624	3.256	2	55.72248	0	3.256	23.8348	3.168	9.34912	3.344	4.12544	3.696	88.66667
94		0	63	1	1	1	37.752	4.048	2	70.48888	3	4.048	21.80904	4.048	6.37384	4.048	4.86288	4.224	104
95		1	70	2	1	0	39.864	5.544	2	71.09696	0	5.368	28.43808	4.312	11.79112	5.544	NA	5.456	105
96		0	59	2	1	0	45.144	3.168	2	82.63904	0	3.256	27.08464	2.64	5.96376	2.64	4.15712	2.728	72
97		0	49	2	1	0	36.784	2.64	2	65.42624	0	2.64	NA	NA	NA	NA	NA	NA	NA
98		1	60	2	1	1	27.7288	3.872	2	60.38736	0	3.872	28.12304	3.872	9.08952	3.696	5.60824	3.696	97
99		1	68	2	1	0	34.94392	3.872	2	66.41096	0	4.048	18.30488	3.96	7.6912	3.872	6.19872	3.696	78.33333

100		0	65	1	1	0	34.64208	3.784	2	51.33216	0	3.784	26.664	3.696	8.3512	3.168	4.55664	3.96	76.66667	78.66667
101		1	52	1	1	0	32.51864	2.728	2	55.49544	0	2.464	23.26984	2.376	6.20312	2.2	4.796	2.64	84.33333	77.66667
102		0	40	3	1	0	29.5812	3.344	2	46.43584	0	3.168	29.4316	3.344	8.3028	3.344	7.55568	3.696	39.33333	66.33333
103		0	53	1	1	0	31.24	3.256	2	49.39968	0	3.256	16.66984	2.992	5.64168	3.08	3.74792	3.52	90.66667	94.33333
104		0	62	3	1	1	28.776	3.608	2	55.87472	0	3.608	18.50464	3.696	6.14416	4.136	4.05416	4.224	68.33333	69
105		1	51	2	1	0	45.936	4.312	2	72.6	0	4.224	39.6616	3.784	NA	NA	NA	NA	66.33333	78
106		0	63	1	1	0	48.752	4.048	3	50.10896	0	3.96	14.61152	3.696	5.68832	3.96	3.26128	3.96	92.33333	77.66667
107		0	60	2	1	0	38.72	3.344	2	52.18752	0	3.168	33.13904	2.992	10.72456	3.168	6.40728	3.08	65.33333	78
108		0	55	3	1	0	42.064	4.664	2	70.64728	0	4.136	34.166	3.784	9.69408	4.576	6.55072	4.72472	76.33333	80.66667
109		1	69	2	1	0	37.58656	3.08	2	53.86568	0	2.464	33.88616	2.904	7.56976	2.728	4.59888	2.64	95.66667	85.66667
110		1	39	2	1	0	26.38592	2.64	3	56.94656	0	2.64	16.80888	2.112	4.92888	2.64	2.99376	2.64	60.33333	60.66667
111		1	56	2	1	0	42.3368	3.96	2	63.18576	0	3.784	17.4328	3.696	5.90304	3.784	3.83416	3.784	84.33333	76.33333
112		1	54	3	1	3	44.352	4.048	2	62.83376	3	3.696	20.25144	3.344	7.44832	3.696	3.80952	3.696	53	64.66667
113		1	41	3	1	0	37.94296	4.84	2	53.69232	0	4.488	24.99288	3.96	9.09304	4.224	5.90216	4.224	76.66667	78
114		0	90	1	1	0	25.696	2.992	2	47.04656	1	2.904	22.73744	2.64	8.2984	3.344	5.39352	3.256	85.33333	79.66667
115		1	35	2	1	0	46.552	4.048	2	53.06488	0	3.872	27.30464	3.608	10.21328	3.784	6.688	3.35192	98.66667	110.6667
116		1	55	2	1	0	39.16	4.224	2	55.66352	0	3.784	23.8788	3.344	7.744	4.224	4.89456	3.08	98.66667	89.66667
117		1	59	3	1	1	35.72888	3.784	2	53.85952	0	3.96	17.02448	3.696	5.65312	4.312	3.22344	3.72416	68	82.66667
118		1	40	2	1	0	52.14352	3.872	3	48.67016	0	3.344	25.872	3.432	NA	NA	NA	NA	57.33333	NA
119		0	65	3	1	1	34.056	3.432	2	50.69504	0	3.432	18.00216	3.344	7.57504	3.96	2.43408	3.696	68.66667	67.66667
120		1	72	3	1	1	31.944	3.256	2	58.36776	0	3.344	26.22048	2.992	7.57768	3.432	4.10872	3.366	84	69
121		0	48	1	1	0	35.50184	3.696	2	48.20816	0	3.256	19.65304	3.168	5.95584	3.168	3.49184	3.08	49.66667	72.33333
122		1	80	3	1	4	40.304	3.784	3	57.58896	0	3.608	23.35168	3.432	6.36944	3.696	4.35072	4.224	99.33333	86
123		1	36	3	1	0	37.224	3.52	2	42.25936	0	3.344	11.8008	3.344	5.15328	3.168	2.97088	3.432	84.33333	80.66667
124		0	63	2	1	0	33.94776	3.52	2	52.40928	0	3.608	26.51264	2.816	6.94848	3.432	3.54992	3.784	44.33333	74.66667
125		1	75	2	1	0	28.864	3.256	2	41.08016	0	3.256	18.26528	2.904	6.68448	3.256	3.05536	3.44168	106	87
126		0	80	3	1	4	26.224	3.256	2	46.73592	0	3.168	18.62696	2.992	7.6428	3.52	3.30792	3.52	99	71.33333
127		1	40	1	1	0	50.2656	1.848	4	30.56328	0	2.112	NA	2.024	NA	NA	NA	NA	85.33333	80
128		0	35	2	1	0	34.96064	3.608	2	51.75368	0	3.344	26.5936	3.256	6.512	3.08	3.828	3.344	111.6667	75
129		1	49	3	1	0	39.48208	4.312	2	64.72576	0	4.224	30.184	3.784	10.29512	3.168	4.85584	3.08	63.66667	76.33333
130		0	76	1	1	0	26.6068	3.168	2	38.40672	0	2.992	19.47352	2.64	5.70856	2.64	3.49184	2.992	87.66667	72.33333
131		0	77	1	1	1	30.3512	3.256	2	55.38456	1	2.992	29.97368	3.168	10.17016	3.52	6.16616	3.39064	106.6667	69.66667
132		0	47	3	1	0	37.576	3.872	2	53.3852	0	3.696	32.95072	2.2	8.5492	3.696	6.17584	4.048	82.33333	91
133		1	51	1	1	0	28.248	3.608	2	47.82448	1	3.608	25.21992	3.696	9.62896	3.608	3.88608	3.608	109.6667	76.33333
134		1	32	3	1	0	34.18536	3.432	2	51.81176	0	3.344	43.582	3.168	6.19872	3.432	4.00312	3.67488	107.3333	80.66667
135		1	59	3	1	0	39.6	3.344	2	60.02128	0	3.168	18.65864	3.168	4.10872	3.168	2.24136	3.344	68.66667	65.33333
136		0	68	3	1	0	38.25096	2.376	2	56.96064	0	2.288	13.90136	2.112	3.27624	2.64	2.43408	3.344	67	68.66667
137		1	90	3	1	1	39.16	3.08	2	49.698	0	3.344	12.94744	3.344	4.75992	3.608	2.83976	4.048	79.33333	79.33333
138		1	48	3	1	1	27.28	3.696	2	49.368	0	3.52	28.424	3.168	6.78656	3.696	2.80632	3.88608	99.66667	84
139		0	46	3	1	0	30.536	3.52	2	48.86904	0	3.432	27.984	3.18296	5.36448	3.168	2.43408	3.168	86.33333	68.66667
140		1	84	3	1	0	38.456	5.6408	2	73.24416	0	5.28	24.6928	4.224	4.57864	4.84	2.75088	4.752	71	81.66667
141		1	28	3	1	0	36.80688	2.64	2	55.46376	0	2.64	22.2684	2.64	3.87904	2.64	2.00904	2.728	82.66667	59.66667
142		1	62	3	1	0	37.85144	4.312	2	60.104	0	4.4	28.11512	3.696	8.31072	4.928	2.70512	3.696	57	62
143		1	66	3	1	0	44.088	3.08	3	46.74912	0	3.08	26.97552	3.08	5.2052	2.816	3.32552	2.904	99.66667	68.33333
144		0	58	3	1	0	40.04	3.872	2	70.752	0	3.52	32.57496	3.52	8.8176	3.696	3.61592	3.96	106.3333	70.33333
145		0	59	2	1	0	53.504	4.84	2	76.912	0	4.664	27.368	3.96	7.81352	4.576	5.67776	4.224	103.3333	68.33333
146		0	68	3	1	3	46.46664	2.904	2	52.19368	1	3.168	25.87376	2.728	9.1608	3.344	4.65256	3.696	76.66667	73.66667
147		0	59	2	1	0	39.072	3.696	2	49.632	0	3.168	20.06928	3.168	7.656	NA	NA	NA	82.66667	NA
148		1	51	3	1	0	40.21688	4.136	2	61.424	0	3.872	28.688	4.224	8.54656	4.4	2.80632	4.224	61	75.66667
149		0	71	3	1	1	36.39064	3.608	2	64.60344	0	3.608	27.95408	3.52	11.98472	3.696	4.64464	3.96	74.66667	69.66667
150		0	48	1	1	3	50.688	4.928	2	74.448	0	5.016	27.20168	4.576	7.99128	5.632	3.43552	3.52	64.66667	64.66667
151		1	75	3	1	1	57.0372	3.696	3	45.68256	0	3.17152	19.54392	3.696	8.05728	3.872	4.752	3.696	55.33333	52.66667
152		1	77	3	1	3	39.864	4.576	2	73.04264	0	4.136	28.86664	4.4	9.77856	4.488	NA	4.488	NA	NA
153		1	48	3	1	0	42.7636	4.752	2	67.99408	0	4.576	17.84992	4.048	7.25824	5.104	3.46984	5.016	54.66667	54
154		0	32	3	1	0	36.168	3.432	2	52.27376	0	3.432	27.104	3.08	8.77976	3.784	2.43408	3.696	53.66667	67.66667
155		0	83	3	1	0	44.54384	5.192	2	33.93456	0	4.224	32.13144	4.224	6.1952	4.312	3.5508	4.224	70.66667	64.33333
156		1	15	3	1	0	89.5884	4.136	4	30.71904	0	4.224	29.74664	3.784	8.80704	2.904	2.57312	3.696	68.33333	83.66667
157		1	29	1	1	0	46.816	5.192	2	69.90016	0	5.104	32.03376	5.016	7.24152	5.28	2.43408	4.224	77	72.33333
158		0	47	2	1	0	36.81216	4.312	2	52.8748	0	3.96	21.91288	3.784	8.8616	3.784	4.64464	3.96	110	80.33333
159		1	71	3	1	0	30.448	2.112	2	72.424	0	2.112	24.024	NA	NA	NA	NA	NA	68.33333	61
160		0	27	2	1	0	42.55416	3.96	2	62.03032	0	4.048	34.71512	3.96	10.97272	3.872	5.66984	4.224	111.3333	87.66667
161		0	41	1	1	0	38.0644	3.256	2	64.95544	0	3.432	32.82312	3.256	7.03824	3.696	4.92976	4.048	46.33333	73.66667
162		1	74	3	1	1	25.872	2.288	2	43.21064	0	2.2	23.496	2.112	8.184	NA	NA	NA	NA	NA
163		0	35	3	1	0	42.48112	3.52	2	64.84016	0	3.52	26.28032	3.344	6.73552	3.432	2.99728	3.344	93	82.66667
164		1	58	3	1	1	28.424	3.52	2	60.918	0	3.344	22.34056	3.432	5.37592	3.52	5.17352	3.52	48.33333	103.3333
165		1	81	3	1	3	35.288	3.256	2	51.2468	0	3.256	12.95096	3.168	6.23744	3.608	2.30032	3.39064	98.66667	73.33333
166		1	72	3	1	0	38.0116	3.784	2	59.05152	0	3.432	43.40424	3.52	8.04408	3.784	4.11136	3.784	116.6667	89.33333
167		0	70	2	1	0	45.52944	5.192	3	46.83536	0	5.016	33.11352	4.4	8.52456	4.928	4.29704	4.2636	60	74.33333
168		1	29	3	1	0	73.92	4.048	3	54.90056	0	3.784	29.04352	3.52	6.96784	3.08	5.12072	3.09144	71.33333	95.66667
169		1	54	3	1	0	31.97656	4.312	2	57.772	0	4.136	24.02576	3.696	12.21352	4.136	4.60152	3.872	102.3333	82.66667
170		0	48	1	1	0	34.672	1.936	2	56.49688	4	2.112	24.55376	1.936	7.92	1.936	NA	NA	66.33333	NA
171		1	78	3	1	1	29.39376	2.904	2	57.15688	3	3.08	25.344	2.992	5.67952	2.816	2.6224	2.464	72.66667	91.66667
172		1	56	3	1	3	33.97152	3.08	2	59.664	0	2.904	14.80072	2.904	6.76456	2.904	2.43408	2.904	56.33333	65.33333
173		0	80	3	1	0	55.55264	2.992	3	50.072	0	2.816	15.05152	2.816	3.54464	3.168	2.12784	2.992	44.66667	67.33333
174		0	54	3	1	1	26.312	3.52	2	53.152	0	3.344	20.61136	2.992	5.90304	3.08	1.90344	3.08	80.33333	68.66667
175		1	66	3	1	1	29.26176	3.696	2	59.05328	0	3.168	15.39912	3.168	5.18144	3.696	2.06184	3.21552	57.66667	74.66667
176		0	78	3	1	1	37.09816	3.696	2	58.256	1	3.52	14.36776	3.344	4.79072	3.696	2.80632	3.5596	58	63.66667
177		1	49	2	1	0	29.4052	3.608	2	55.69784	0	3.784	29.36384	3.344	6.19872	3.696	3.17856	3.67928	63	49.66667
178		1	68	3	1	0	32.34352	3.696	2	59.66488	0	3.17152	26.22048	2.816	10.06984	3.344	4.31552	3.21816	66.66667	88.33333
179		1	47	2	1	0	33.19184	2.376	2	57.73592	0	2.464	28.51728	2.112	6.38088	2.376	3.51472	2.376	75	68.66667
180		1	65	3	1	0	29.48	4.312	2	60.544	0	4.048	28.98368	3.432	4.6376	3.432	2.58632	3.696	53.66667	54.33333
181		1	77	3	1	0	22.96888	2.552	2	45.93952	0	2.816	14.29296	2.728	3.432	3.168	2.48952	2.904	72.33333	60.66667
182		1	78	3	1	1	32.208	3.608	2	53.85688	0	3.432	24.28976	3.168	6.4944	3.168	3.44872	3.168	71.33333	57
183		1	70	3	1	3	29.304	3.52	2	49.63376	1	3.34752	15.08672	3.256	5.10664	3.608	2.64	3.168	90.33333	77.33333
184		0	68	2	1	1	33.616	3.168	2	58.256	0	3.168	16.39968	3.168	3.56664	3.696	3.17856	3.08	66	71.33333
185		1	47	3	1	0	38.1216	3.872	2	57.32936	0	3.784	14.78488	3.696	NA	NA	NA	NA	68.66667	NA
186		0	32	2	1	0	49.33984	4.048	2	70.40792	0	3.784	20.4688	3.696	8.0696	3.96	3.5904	3.96	74	81.33333
187		0	48	2	1	3	72.16	3.344	3	47.86584	0	2.816	21.73776	2.816	4.25128	3.168	3.98024	2.992	76	58
188		0	72	3	1	1	33.88	3.696	2	53.24	0	3.52	22.704	3.168	4.81976	3.696	2.99376	3.37392	58.66667	69
189		0	57	2	1	0	61.512	3.52	3	52.7824	0	3.256	30.92672	2.64	8.22448	3.52	4.796	3.23576	71.33333	81.33333
190		1	51	3	1	0	34.41768	3.608	2	69.256	0	3.256	22.18128	3.168	4.30144	3.168	2.43408	3.17152	65.66667	56.66667
191		1	47	3	1	0	36.08	3.872	2	66.52976	0	3.784	21.19832	3.256	6.93616	3.96	3.5904	4.27768	50.66667	51.66667
192		1	47	2	1	0	32.28808	2.376	2	57.83976	0	2.376	29.568	2.64	6.21192	3.08	4.88224	2.904	60.33333	66
193		1	69	3	1	3	29.65776	3.344	2	60.10488	0	3.344	21.32944	2.464	9.23824	2.992	2.49392	2.64	60.66667	63.66667
194		1	67	3	1	0	29.392	3.25952	2	56.23552	1	3.08	14.53056	2.728	4.05768	3.256	2.80632	2.904	63.33333	61.66667
195		1	45	3	1	0	37.14392	3.96	2	63.888	4	3.84032	18.83992	3.168	4.77488	3.608	2.82304	3.34576	68.66667	67.66667
196		1	65	3	1	0	41.888	3.784	2	65.032	0	3.784	18.87424	3.344	6.25944	3.52	3.22344	3.74264	62.33333	68.33333
197		0	78	3	1	0	29.568	3.96	2	53.42128	0	3.344	16.10752	3.344	5.69008	4.048	3.04744	4.17384	62.66667	69.66667
198		0	33	2	1	0	39.512	4.312	2	62.4184	0	4.312	14.25776	3.96	5.58272	4.752	3.89664	4.048	77.33333	66.33333
199		0	59	2	1	0	37.312	3.696	2	59.84	0	3.168	14.35368	3.168	4.81976	3.696	3.17856	3.344	65.66667	57.66667

200		1	42	2	1	0	63.008	2.64	4	22.088	0	2.552	21.37168	2.376	3.7884	2.64	2.80632	3.52	61.66667	60.33333
201		1	54	3	1	0	46.024	3.344	3	36.168	0	2.992	12.79344	2.904	4.32168	3.256	2.06184	3.168	46.33333	48.33333
202		0	76	3	1	0	40.9332	3.608	2	43.47376	0	3.608	15.36832	3.344	5.6628	3.96	2.98584	3.96	65.66667	64.33333
203		0	51	2	1	0	28.776	3.432	2	42.768	0	3.08	13.34256	2.904	4.89632	3.168	2.43408	3.36688	82.66667	84.33333
204		0	40	2	1	1	65.47288	3.696	4	38.36976	0	3.696	21.75184	3.608	2.95152	3.696	2.2704	3.696	66.33333	60.66667
205		0	31	1	1	0	39.00248	3.784	2	67.06216	0	3.696	41.06256	3.256	8.27024	3.696	5.16032	3.432	82.66667	77.66667
206		1	46	3	1	0	49.70592	3.96	2	72.88688	0	3.608	26.3296	3.256	6.76104	3.432	4.86816	3.44432	55.66667	37.33333
207		0	50	2	1	3	45.76	2.904	3	44.704	0	2.904	14.41	2.904	4.8576	2.904	2.43408	2.8556	51.66667	60.33333
208		1	82	3	1	0	30.536	3.608	2	40.832	0	3.43552	14.02016	3.432	5.41112	3.432	2.98584	3.51472	51	57.66667
209		0	84	3	1	0	36.696	3.168	2	55.44264	4	3.168	15.32432	3.168	5.74376	3.696	3.03248	3.696	49.66667	60
210		0	63	2	1	1	31.152	3.872	2	57.8336	1	3.784	23.76	3.432	9.11328	3.872	5.34776	3.96	45	60.33333
211		1	72	3	1	0	45.76	3.696	2	75.73984	0	3.696	23.87968	3.168	3.69864	3.696	3.44256	2.904	95.33333	63.33333
212		1	81	3	1	0	34.14576	2.904	2	58.08352	0	2.64	14.25688	2.376	3.78048	2.904	2.98584	2.64	96	58.33333
213		0	34	3	1	0	40.04	3.168	2	61.16	0	3.168	19.44976	2.904	4.67984	3.52	3.38184	3.608	49.66667	62.66667
214		0	25	3	1	0	33	3.344	2	69.16888	0	3.432	17.35448	2.64	5.12776	3.784	3.17856	3.69248	72	66.33333
215		1	45	3	1	1	29.304	3.168	2	48.75288	0	3.168	13.21496	2.904	5.16208	3.168	2.95152	3.30792	60	68.33333
216		0	77	3	1	1	34.14576	2.64	2	60.72	3	2.64	18.65336	2.64	4.88664	2.64	2.6532	2.904	104.3333	74.66667
217		0	49	3	1	0	39.13448	5.368	2	70.30672	0	5.368	17.76368	4.224	5.73848	4.224	4.09728	3.784	72.66667	77
218		1	55	3	1	0	21.736	3.168	2	41.184	0	3.168	11.088	3.168	3.3396	3.168	1.32	3.168	88.33333	83.33333
219		1	33	3	1	0	38.544	3.344	2	60.456	0	3.256	14.97144	2.992	5.51232	3.5332	3.38184	3.168	54.33333	60
220		0	99	3	1	3	75.328	3.168	4	38.45688	0	3.696	13.46928	3.256	4.57688	3.696	3.38184	3.608	81	80.66667
221		0	75	3	1	1	37.664	3.432	2	56.5004	0	3.432	12.81104	3.168	4.114	3.29736	2.72008	3.32728	87	70.66667
222		1	64	3	1	0	31.856	3.696	2	62.30488	0	3.696	22.088	3.168	5.46656	3.696	3.44256	3.19264	59.33333	71
223		0	77	3	1	3	33.616	1.848	2	45.93688	0	1.848	14.09672	2.112	5.22016	2.112	3.432	2.2	60.66667	85.33333
224		1	81	3	1	0	22.07744	3.168	2	60.56424	0	3.168	32.01264	3.168	7.61376	3.168	NA	3.17152	52.33333	58.66667
225		1	79	3	1	1	79.464	3.9864	3	52.27288	0	3.96	33.8184	3.432	10.64184	3.96	5.39704	3.96	78.33333	67.33333
226		1	74	3	1	1	47.52	3.696	2	75.768	0	3.344	12.67288	3.168	4.5408	3.168	3.07824	3.08	77	58.33333
227		1	55	2	1	0	32.7404	3.52	2	56.41064	0	3.168	31.26904	2.904	9.11152	3.08	4.63232	3.5772	60.33333	62.66667
228		1	52	3	1	0	40.69824	3.696	2	55.088	1	3.432	31.48816	3.344	8.382	3.608	4.5364	4.24864	42	69.66667
229		1	79	3	1	1	48.84088	4.048	2	86.06576	0	3.96	21.12088	3.872	5.544	3.872	NA	NA	NA	NA
230		1	54	3	1	0	44.63448	4.4	2	66.6292	0	4.488	42.504	4.488	8.33272	5.28	5.99016	5.192	60.66667	49.33333
231		1	55	1	1	0	26.7696	3.168	2	59.3912	0	3.168	18.55304	3.168	3.8588	3.168	2.7192	2.904	NA	62
232		1	58	2	1	0	58.344	3.18296	3	44.264	0	3.19792	21.648	2.64	7.27056	2.728	5.07936	3.97144	92.66667	83
233		0	66	2	1	3	36.57896	4.048	2	76.5952	0	4.048	27.016	4.136	11.21208	4.136	6.5208	4.15184	57.66667	77.33333
234		1	74	2	1	1	37.52672	3.784	2	63.82904	0	3.784	17.17672	3.696	7.656	NA	NA	NA	45.33333	NA
235		1	59	1	1	0	30.88448	2.112	2	56.05776	0	2.112	NA	NA	NA	NA	NA	NA	NA	NA
236		1	78	3	1	1	47.53408	3.872	2	56.85152	1	3.872	26.40176	3.608	12.05864	4.048	6.4944	3.96176	98.66667	81
237		1	68	3	1	0	41.008	3.872	2	62.13856	0	3.872	17.25152	3.696	6.47592	4.224	3.61592	4.23456	51.66667	48.66667
238		1	81	3	1	3	39.8948	3.784	2	62.68152	3	3.784	35.47544	3.696	8.62488	3.64936	4.86816	3.5508	100	79.66667
239		0	65	3	1	0	35.992	3.61152	2	60.85904	0	3.52	14.25688	3.696	4.64464	3.696	3.03248	3.696	87.33333	71.33333
240		0	82	3	1	0	33.51656	4.488	2	57.2	1	4.224	15.97024	4.224	6.94584	2.552	3.564	2.87144	74	85
241		1	63	2	1	0	41.81408	3.784	2	76.18864	0	3.696	21.46144	3.52	8.34768	3.96	3.64144	3.96	64	71.66667
242		0	39	1	1	0	38.97784	3.608	2	53.68	0	3.696	14.25688	3.52	5.40144	3.696	3.07824	3.608	90.66667	67.66667
243		0	82	3	1	3	32.648	3.2692	2	52.37496	3	3.256	12.19592	3.168	6.44688	3.256	3.30968	3.256	87	54
244		1	83	3	1	1	26.87696	3.168	2	53.25848	0	3.168	16.38648	2.64	5.346	3.168	3.0096	3.168	50.33333	61.33333
245		0	67	1	1	1	49.3328	4.224	2	71.81592	0	3.872	20.768	3.344	5.28	NA	NA	NA	69.66667	0
246		1	82	3	1	1	32.61984	4.224	2	76.64888	0	3.872	25.5112	3.696	5.37856	4.136	4.37712	4.136	55	52.33333
247		0	80	3	1	0	40.392	4.136	2	53.19072	0	3.784	19.54128	3.256	9.63952	3.96	6.2084	3.73384	66.66667	54.33333
248		0	72	3	1	0	59.57776	4.05064	3	43.92608	0	3.696	22.44088	3.37656	6.98632	3.52	3.84648	3.5508	81.33333	64
249		0	74	3	1	3	40.568	3.608	2	56.59104	0	3.52	16.7816	3.256	5.13216	3.696	3.20848	3.696	61.66667	69
250		1	70	2	1	0	53.152	3.872	2	73.04088	0	4.4	38.01688	3.96	7.20808	4.312	4.29352	4.312	56.33333	75.33333
251		0	58	3	1	1	43.12	3.17152	2	59.66576	0	3.256	21.25112	3.17152	4.52848	3.344	2.48952	3.25952	70.33333	67.66667
252		0	78	2	1	1	58.784	3.96	3	41.096	0	4.048	23.49688	3.96	5.17264	4.488	2.50272	3.96	72.66667	77.66667
253		1	57	3	1	1	39.71704	4.224	2	59.686	0	3.96	15.06824	3.696	5.28	NA	NA	NA	96.66667	NA
254		1	31	1	1	0	35.57312	2.64	2	59.57776	0	2.728	0	2.112	4.43168	2.64	3.3396	2.64	NA	NA
255		1	65	3	1	0	36.96088	3.168	2	58.60888	0	3.168	11.88	3.168	4.30584	3.344	2.64	3.08	46.33333	53.66667
256		0	65	3	1	1	44.39072	3.784	2	61.23744	0	3.696	21.66208	3.696	6.35976	3.784	3.51384	3.35104	56	59.33333
257		1	74	3	1	1	33.52624	3.344	2	54.13408	0	3.344	13.49304	3.168	4.51176	3.696	2.25456	3.432	54.33333	67.66667
258		0	42	2	1	0	37.46248	4.224	2	73.59704	0	3.70832	17.952	3.696	6.67744	4.224	2.99376	3.872	100.6667	70.66667
259		0	30	3	1	0	38.00544	4.752	2	59.0128	0	4.664	17.46624	4.224	5.9444	4.488	2.72184	4.4	52.66667	64
260		1	51	2	1	0	35.816	2.376	2	64.77944	0	2.112	14.6608	2.112	5.37768	2.376	3.27624	2.376	51	79.33333
261		1	37	2	1	0	57.32672	3.784	3	40.1016	0	3.696	16.19112	3.256	5.676	3.96	3.20848	3.696	53	65
262		0	52	3	1	0	37.97112	3.168	2	58.10992	3	3.168	21.64888	2.904	4.30848	3.168	3.07824	3.168	55.33333	60.33333
263		1	78	2	1	0	45.07448	3.608	2	55.12672	0	3.52	21.648	3.432	8.0432	3.608	3.432	2.904	76.66667	54.33333
264		1	61	3	1	1	31.416	3.168	2	53.94488	0	3.168	14.54024	3.168	4.8576	3.608	2.43408	2.992	60	70
265		1	62	3	1	1	39.08784	3.608	2	57.31792	0	3.608	14.81656	3.432	6.2128	3.608	3.19352	3.432	62.66667	65.33333
266		1	57	3	1	0	26.202	3.344	2	49.54752	0	3.256	11.09768	2.464	5.544	NA	NA	NA	54	0
267		0	48	2	1	0	27.84144	2.728	2	45.67288	0	2.728	21.50544	2.464	4.62968	NA	3.17856	NA	53	70.33333
268		1	77	2	1	0	26.69656	3.256	2	55.79112	0	3.168	15.14392	2.728	5.37856	3.15304	3.23928	2.992	58.33333	68.66667
269		1	68	3	1	1	30.976	3.168	2	57.82392	0	3.168	26.3384	3.168	10.15344	3.35896	5.40232	3.344	69	81.33333
270		0	62	2	1	1	43.11384	3.256	2	57.91896	1	3.168	16.94792	2.992	5.62936	3.608	2.43408	3.256	88.33333	67.66667
271		0	71	2	1	0	41.62664	4.664	2	63.21744	0	4.312	18.39464	4.224	3.17856	4.224	4.30848	4.224	88	82.33333
272		0	70	3	1	0	31.68	2.64	2	70.04976	0	2.64	11.18128	2.64	3.03248	2.64	2.45256	2.64	NA	72
273		1	37	1	1	0	41.096	3.256	2	65.032	1	3.344	17.02184	3.168	4.752	NA	NA	NA	67	0
274		1	88	3	1	0	34.56288	3.432	2	57.20352	0	3.256	17.336	3.168	4.03304	3.696	2.85648	3.168	56.66667	66.66667
275		0	58	1	1	0	38.69008	2.112	2	55.9812	1	2.112	NA	NA	NA	NA	NA	NA	NA	NA
276		1	77	3	1	1	36.256	3.52	2	54.208	0	3.432	16.02304	3.256	4.95704	3.784	3.23928	3.608	58.66667	73.66667
277		0	54	3	1	0	27.25536	3.432	2	55.35728	0	3.608	16.93208	3.52	5.1964	3.52	2.5608	3.08	66.66667	76.33333
278		1	68	3	1	1	34.584	2.904	2	52.49024	0	2.904	13.22992	2.904	4.6376	2.904	2.43408	2.992	70.66667	63
279		0	64	3	1	0	27.324	3.432	2	57.93656	0	3.432	15.84088	3.168	4.75464	3.344	2.74824	3.344	52.33333	66
280		1	61	2	1	0	38.54224	3.344	2	64.34208	0	3.256	19.93728	3.168	6.97136	3.432	4.12984	3.72416	91.33333	62
281		0	64	3	1	0	37.77664	4.136	2	62.7088	0	4.048	29.14384	4.048	10.1552	4.048	5.6364	4.312	36.33333	59.33333
282		0	48	2	1	0	38.368	3.168	2	53.25496	0	3.168	14.1328	3.168	4.5716	3.344	2.76056	3.696	51.66667	60.66667
283		0	57	3	1	0	36.87288	3.96	2	58.73296	0	4.048	21.12	3.696	7.06024	3.96	4.15184	3.872	64.66667	66.33333
284		0	72	3	1	0	52.976	2.904	3	49.46128	0	2.992	14.5244	2.64	5.6408	3.168	3.27624	2.992	60.33333	70
285		0	67	3	1	0	33.088	3.344	2	47.19264	0	3.168	21.27136	2.904	5.39088	3.432	3.26128	3.26656	51.66667	60.66667
286		0	68	2	1	1	35.56432	3.256	2	48.488	0	3.256	17.90184	2.64	3.432	3.344	3.48832	3.344	55	60.66667
287		0	57	3	1	0	33.27544	2.904	2	47.16888	1	2.904	31.20216	2.64	11.75592	2.904	5.63112	3.79632	68.33333	80.33333
288		0	67	2	1	0	31.94664	4.224	2	50.30784	0	3.72064	15.05504	3.17152	5.6364	4.224	3.20848	4.224	72.66667	69
289		0	41	3	1	0	60.00632	3.168	3	42.41776	0	3.08	18.568	NA	NA	NA	NA	NA	NA	NA
290		1	76	2	1	0	52.976	4.576	3	42.152	0	4.136	21.27224	3.784	6.94144	4.048	3.5508	4.048	102.3333	57.66667
291		1	36	1	1	0	35.57224	3.46192	2	60.34512	0	3.432	28.57888	3.168	8.3776	3.344	3.85792	3.2956	90.66667	61.66667
292		0	28	2	1	0	37.26272	3.168	2	56.584	0	3.256	23.60688	2.992	4.88488	3.168	2.77024	2.992	75.33333	63.33333
293		0	42	2	1	0	30.46208	2.64	2	63.36264	0	2.64	15.15536	2.64	4.88488	2.64	3.7576	2.816	50.66667	62.33333
294		1	55	3	1	0	39.072	3.70832	2	61.05	0	3.52	15.22488	3.432	3.51912	3.432	2.7192	3.432	53.66667	71
295		0	35	3	1	0	40.92	3.872	2	57.86616	0	3.696	15.4484	2.992	4.62264	3.96	2.26072	3.6476	70.66667	76.66667
296		1	40	3	1	0	42.97216	4.136	2	58.08704	0	3.96	27.104	3.872	8.6372	3.872	2.48952	3.63528	64.66667	66
297		1	62	2	1	0	44.97064	3.608	2	28.53048	0	3.696	27.70152	3.52	8.1312	3.696	2.32496	3.784	46.66667	64.66667
298		1	61	3	1	0	47.10992	3.872	2	66.94248	3	3.696	16.18672	3.52	4.10872	3.784	2.64	3.784	0	66

299		0	64	3	1	0	41.84752	3.52	2	59.4132	0	3.608	32.62072	2.904	8.79384	3.696	3.828	3.52	63.33333	66
300		1	67	3	1	1	41.11536	3.696	2	71.07496	0	3.432	21.92168	3.35896	6.0984	3.696	2.64	3.322	64.66667	71
301		1	37	3	1	0	40.51432	4.224	2	76.76504	0	3.96	29.9948	3.96	7.58032	3.872	4.68952	3.7928	104	80.33333
302		0	43	2	1	0	74.09688	4.84	3	81.88224	0	4.664	37.25216	3.96	8.184	NA	NA	NA	58	61.33333
303		1	34	3	1	0	43.8108	3.696	2	69.01224	0	3.18296	19.81232	3.36248	7.56448	3.432	3.30792	3.256	67.33333	84.33333
304		1	75	3	1	0	36.71184	3.168	2	61.39232	0	3.168	25.18824	2.904	5.81592	2.904	4.64992	3.344	70.66667	57.33333
305		0	66	3	1	0	45.232	3.69952	2	51.6648	0	3.52	15.26976	3.256	4.02864	3.71184	2.43408	2.816	44.66667	58.33333
306		1	26	1	1	0	47.68192	3.784	3	34.364	0	3.344	19.72432	3.52	6.99688	3.608	4.07704	3.608	52	75
307		0	26	1	1	0	38.544	4.224	2	54.64888	0	3.25952	25.69776	3.432	7.392	NA	NA	NA	65.66667	NA
308		0	81	3	1	0	38.7684	3.872	2	50.52344	0	3.784	29.54864	3.696	5.32312	4.224	2.55376	3.76112	82.66667	58.33333
309		1	83	3	1	1	39.18816	3.784	2	52.00976	0	3.96	27.72	3.168	7.79416	3.52	4.53112	3.52	71.66667	73
310		1	53	3	1	0	44.968	4.576	2	62.53016	0	4.224	31.32536	3.696	7.17464	4.4	4.884	4.4	72.66667	95
311		0	28	3	1	0	45.056	4.224	2	73.2424	0	4.048	34.08944	3.87464	13.86176	3.88608	6.59472	4.28032	96	83.66667
312		0	73	1	1	0	0	2.64	2	70.39032	0	2.64	17.29464	2.64	5.41376	2.64	3.476	2.464	81.66667	74.33333
313		0	40	3	1	0	43.58376	3.872	2	57.90752	0	3.4452	16.23248	3.168	4.35336	3.432	2.71216	3.344	84	84.66667
314		1	77	3	1	0	41.37672	4.36656	2	81.78192	0	4.6244	33.3388	4.224	10.56264	4.752	5.97256	4.576	66.33333	73
315		0	85	3	1	1	37.01632	3.168	2	63.34856	1	2.904	31.42216	2.904	6.7452	3.168	5.20608	3.08	69.33333	84
316		1	62	2	1	0	36.15128	4.136	2	55.39776	0	3.784	26.02512	3.432	3.80336	3.608	5.65312	4.312	54	69.33333
317		1	24	3	1	0	38.92152	3.696	2	58.34752	0	3.696	20.59728	3.256	NA	NA	NA	NA	NA	NA
318		0	56	2	1	1	29.00568	3.784	2	70.94208	3	3.52	18.656	3.168	5.808	3.168	NA	NA	NA	NA
319		0	75	3	1	0	35.1824	3.344	2	56.28216	0	3.43552	25.696	3.256	6.47328	3.432	2.12784	3.432	48.66667	68.33333
320		1	68	3	1	0	72.29552	3.168	4	30.53688	0	3.168	12.21088	3.08	5.6628	3.08	3.20848	3.08	61	84.66667
321		1	69	3	1	0	39.36152	4.048	2	65.648	0	3.96	27.63376	3.52	5.96552	3.96	3.23928	3.96	76.33333	70
322		0	81	3	1	1	45.64384	4.928	2	74.51752	1	4.66928	45.5708	3.96	11.76736	5.016	5.6628	5.104	107.3333	69.66667
323		0	79	3	1	3	42.4468	3.52	2	56.35872	0	3.608	23.5708	2.992	4.06384	3.25952	2.43408	3.68896	60.33333	67.33333
324		1	53	3	1	0	48.0832	4.048	2	82.5616	0	3.79632	19.09688	3.168	5.17	3.696	3.05536	3.696	79.33333	70.33333
325		1	73	3	1	1	43.27312	4.048	2	56.62712	0	3.696	14.79104	3.344	5.73936	3.696	2.36016	3.696	72.33333	59.33333
326		0	65	2	1	1	48.5144	3.784	2	62.4052	0	3.696	15.57776	3.344	5.42784	3.872	2.98232	3.872	70.33333	73.66667
327		1	58	2	1	1	41.81144	3.608	2	61.04384	1	3.344	15.87784	3.168	5.016	3.52	1.89112	2.816	62.66667	71.66667
328		0	64	2	1	0	37.928	3.696	2	53.68	0	3.256	22.70576	3.168	6.60704	3.608	NA	3.608	NA	NA
329		1	66	3	1	1	41.81672	4.136	2	79.56872	0	3.96	29.68152	3.696	4.75992	4.224	1.94392	4.24864	59.66667	77
330		1	47	1	1	1	32.736	3.872	2	66.50072	0	3.79632	28.84024	3.872	6.732	3.872	3.80952	3.872	48.33333	70.33333
331		1	62	3	1	0	34.46608	4.488	2	59.99576	0	4.048	30.2456	3.21552	8.8176	3.88432	5.09872	4.136	53.66667	76.66667
332		0	75	3	1	1	21.91288	3.696	2	51.55568	1	3.696	13.46488	3.256	4.93064	3.696	2.2132	3.696	75.66667	70.33333
333		1	75	3	1	1	26.97464	3.08	2	49.36976	0	3.256	16.3768	3.168	5.544	NA	NA	NA	52.33333	NA
334		1	63	3	1	1	34.0604	3.96	2	59.928	0	3.784	12.50832	3.608	5.93208	3.96	2.26072	3.96	107.6667	72.66667
335		0	63	1	1	1	34.04808	2.992	2	55.01672	0	2.992	18.4404	2.904	8.79032	3.08	2.74296	3.08	81.33333	70.33333
336		1	41	1	1	0	43.07424	4.4	2	66.74184	0	3.872	16.42256	3.696	7.28904	4.136	2.84768	3.82096	72.66667	71.66667
337		0	42	1	1	1	69.49888	4.312	3	50.49792	0	3.96	14.12576	3.784	5.72176	4.048	2.32056	3.696	60.33333	68.33333
338		1	58	3	1	0	46.97264	3.52	2	70.40352	1	3.696	11.97856	3.52	4.3472	3.608	1.8788	3.168	68.66667	78.66667
339		0	39	3	1	0	50.424	4.576	2	79.904	0	4.664	22.44	3.696	7.80384	4.488	3.7884	4.488	79.66667	62.66667
340		0	72	2	1	1	52.98392	3.608	3	46.38568	0	3.696	13.58016	3.344	3.50592	3.608	2.22288	2.33112	69	64
341		0	28	3	1	0	27.33368	3.256	2	49.72	0	2.904	12.40888	2.904	4.3296	3.256	2.12784	3.08	84.33333	74.66667
342		1	56	2	1	0	28.42664	2.904	2	47.608	0	3.08	12.9404	2.992	5.40144	3.08	2.72184	3.168	77	75.66667
343		0	10	2	1	0	24.77288	3.43552	2	45.37632	0	3.344	15.73616	3.168	6.63872	3.256	3.34664	3.432	88.33333	81.33333
344		1	63	1	1	1	36.94152	2.992	2	49.64608	0	2.64	11.88528	2.64	4.3824	2.64	2.53704	2.64	104.6667	73
345		0	59	1	1	0	24.99552	2.728	2	52.41544	0	2.728	13.2	2.64	3.20848	2.64	1.86648	2.64	42.66667	60
346		1	78	3	1	1	33.32472	3.784	2	60.896	0	3.608	17.5428	3.608	5.95056	3.96	3.50592	3.8236	70.33333	72
347		1	63	3	1	0	46.21496	4.136	2	67.32176	0	3.96	19.09776	3.608	9.0244	3.872	3.51472	4.224	74.66667	67.66667
348		1	71	2	1	0	40.70616	3.52	2	61.87368	0	3.52	22.54384	3.344	6.41608	3.52	3.17856	3.344	73.33333	69.66667
349		0	55	2	1	1	49.30552	3.872	2	57.94184	0	3.872	15.88488	3.696	5.70328	3.96	2.8116	3.872	72.33333	69.66667
350		0	80	3	1	3	39.27088	3.256	2	50.8156	0	3.168	18.23008	2.816	6.43192	3.08	2.75088	3.256	64.66667	66.66667
351		0	62	3	1	0	29.2556	3.608	2	58.97936	0	3.344	20.50576	3.168	6.78656	3.256	3.98288	3.48832	61.66667	66.66667
352		1	59	3	1	0	46.72712	4.928	2	75.88768	0	4.752	18.21952	4.752	6.98632	4.752	2.64	4.928	66.33333	66.66667
353		1	51	3	1	0	39.63872	1.848	3	41.45944	0	1.848	NA	NA	NA	NA	NA	NA	NA	NA
354		0	50	2	1	0	47.71536	4.048	2	76.11824	0	3.872	18.48264	3.696	7.25648	4.048	2.85648	3.872	64.33333	65.33333
355		1	81	3	1	0	48.04976	3.96	2	88.7084	0	3.784	23.364	3.696	6.38968	4.224	3.828	4.224	100.6667	65.66667
356		0	60	2	1	1	49.61088	3.872	2	69.28768	0	3.872	19.53688	3.696	6.40112	3.872	3.32904	3.696	63.33333	64.33333
357		0	45	3	1	0	35.92072	3.608	2	56.51008	0	3.432	13.2	3.344	3.20056	3.52	2.2088	3.52	64	91.66667
358		1	62	3	1	0	43.208	3.872	2	85.56064	0	4.048	26.18968	3.696	8.04408	3.872	3.44256	4.048	75.66667	74
359		0	38	3	1	0	39.82088	3.168	2	61.78128	0	3.168	13.99288	3.08	3.56664	3.168	3.24632	2.992	64.66667	71
360		1	47	2	1	0	39.18024	3.344	2	60.29144	0	3.256	15.07968	3.168	5.41376	3.256	2.98584	3.168	65	70
361		1	49	2	1	0	47.5904	2.904	4	41.27728	0	2.904	21.12088	2.64	6.4504	2.904	3.17856	2.992	65.66667	68.33333
362		1	72	3	1	0	34.1352	3.256	2	55.352	0	3.168	15.84	2.904	4.6992	3.256	2.71216	2.816	113	78
363		1	56	3	1	0	33.4444	3.08	2	30.36	0	2.816	13.20264	2.728	3.58072	2.816	2.36984	3.168	63.33333	81.33333
364		1	75	3	1	0	31.67032	2.64	2	54.56264	0	2.64	12.77232	2.552	2.80632	2.64	1.71688	2.64	63.66667	73
365		1	27	1	1	0	64.08424	3.872	3	47.62384	0	3.784	16.2228	3.696	4.92008	3.784	2.82304	3.784	83.33333	90.33333
366		0	46	1	1	0	29.64544	2.904	2	49.81328	0	2.64	11.88528	2.64	4.05856	2.376	1.95624	2.464	68	86.33333
367		0	78	3	1	0	33.02904	2.992	2	53.59992	0	2.904	21.57144	NA	NA	NA	NA	NA	NA	NA
368		0	56	1	1	0	30.36	3.432	2	46.9876	0	3.432	20.86392	3.08	9.878	3.256	3.828	3.168	97.33333	73.66667
369		1	73	3	1	0	38.29936	3.608	2	55.88792	0	3.344	12.68696	3.168	3.8676	3.696	2.12784	3.96	71	73.66667
370		0	84	3	1	0	42.25496	3.96	2	66.79728	0	4.048	22.3432	3.96	6.44864	3.96	3.26832	3.872	95.66667	82.33333
371		0	67	3	1	0	36.21552	4.048	2	69.26832	0	3.784	27.544	3.344	5.3328	3.872	2.47104	3.872	51.33333	58.66667
372		0	85	3	1	0	38.96816	3.256	2	60.33016	1	3.168	18.76072	3.168	5.70944	3.344	2.81424	3.344	58.33333	65.66667
373		0	47	1	1	1	29.97456	3.168	2	58.78048	1	3.168	13.20176	2.64	3.51736	3.168	2.00904	3.168	60.66667	78.66667
374		1	73	2	1	0	0	3.696	2	60.59592	0	3.344	25.80424	2.816	9.05696	3.344	3.79984	3.344	48.33333	75.33333
375		0	58	2	1	0	48.23192	4.488	2	75.5392	0	4.488	18.3656	4.224	6.77336	4.224	2.99376	4.16592	57.66667	65.66667
376		1	57	3	1	0	37.2944	3.96	2	70.15888	0	3.608	29.04	3.344	8.0652	3.432	4.05504	3.5596	102.3333	84
377		0	41	3	1	0	42.42744	4.048	2	69.982	0	3.96	22.45496	3.96	6.61584	3.96	3.96	3.696	55.33333	65
378		0	20	3	1	0	41.52896	3.608	2	56.76088	0	3.52	24.55992	3.432	9.58936	3.608	5.11808	4.05768	92.66667	81.33333
379		1	56	2	1	0	34.48984	4.4	2	63.51928	0	3.784	24.99728	3.168	7.74488	3.872	5.78512	4.048	89.66667	64.66667
380		1	47	3	1	1	45.41416	3.608	2	71.91536	1	3.52	26.57776	3.168	5.6628	3.608	4.42992	3.85968	61.66667	68.33333
381		0	35	1	1	1	42.42304	3.608	2	60.78688	1	3.608	25.6168	2.992	5.71296	3.52	4.05416	3.256	53.66667	80.66667
382		0	76	3	1	3	32.64624	3.256	2	48.08232	0	3.344	22.96888	3.256	7.24856	3.344	3.36072	3.256	62	78.33333
383		1	46	1	1	0	62.81792	3.256	3	56.56992	0	3.168	16.2492	3.168	4.88664	3.256	3.75144	3.432	91.66667	74.33333
384		1	68	3	1	0	36.7928	2.992	2	50.6528	0	2.904	15.06824	2.552	3.85	3.08	2.56256	2.904	77.33333	83
385		0	76	2	1	1	38.45688	3.784	2	55.37576	1	3.696	14.1944	3.52	4.93064	3.784	3.52528	3.73912	91.66667	84.33333
386		1	61	1	1	0	46.7676	3.872	2	71.44896	1	3.696	26.664	3.08	5.92064	3.52	4.90776	3.64672	75.33333	72.33333
387		1	31	2	1	0	48.50384	4.4	2	72.1644	0	4.488	30.91792	3.96	8.0564	4.488	5.6628	4.84352	84.66667	46.33333
388		1	52	3	1	0	33.32736	2.64	2	56.36752	0	2.64	12.06832	2.64	4.18088	2.64	2.26072	2.7676	66.33333	68
389		0	68	1	1	1	33.66616	3.256	2	50.16088	1	3.344	20.5964	2.9084	7.29344	3.256	4.02864	3.5508	52.33333	59.33333
390		0	64	3	1	0	32.66472	4.136	2	55.94424	0	3.872	23.88408	3.256	7.49144	3.608	4.26272	4.41936	43.66667	54.66667
391		0	82	3	1	1	48.75288	3.872	2	59.84616	0	3.784	15.84	3.696	5.43136	3.872	2.80632	3.344	66.33333	79.66667
392		1	72	3	1	3	39.62992	3.784	2	62.744	0	3.872	14.52352	3.696	6.91416	3.784	4.05416	3.608	60.33333	64.33333
393		1	31	1	1	0	55.37048	4.05064	2	67.67464	0	3.872	30.09776	3.52	9.37376	3.872	5.37152	4.30848	68	64.33333
394		0	62	3	1	0	33.08008	2.904	2	61.69064	0	2.904	0	2.64	NA	NA	NA	NA	71	NA
395		1	41	1	1	0	34.38952	2.64	2	69.718	0	2.64	0	2.112	8.184	NA	NA	NA	68.33333	NA
396		0	63	2	1	1	34.31208	3.52	2	61.952	0	3.432	15.33224	2.904	5.65928	3.52	3.07824	3.23488	66.33333	67.33333
397		1	72	2	1	1	46.62152	4.136	2	74.7032	0	4.048	32.64712	3.344	7.656	3.344	5.324	3.40824	66.33333	75.66667
398		0	69	3	1	1	36.98552	3.168	2	56.6456	0	3.168	10.57848	3.168	5.51232	3.168	2.43408	3.78488	50.33333	58.33333
399		0	71	3	1	3	46.60656	4.312	2	66.26488	0	3.784	29.57152	3.784	8.55448	4.048	5.41728	5.28	66.66667	63.33333
400		0	58	2	1	0	24.13048	2.64	2	43.00472	0	2.64	NA	NA	NA	NA	NA	NA	NA	NA

401		1	64	2	1	3	46.0064	3.96	2	68.0108	0	3.696	29.23712	3.608	10.62248	3.608	7.44656	3.61416	91.66667	70.33333
402		0	80	3	1	1	42.2312	4.312	2	63.2412	0	3.62032	30.8	3.696	10.38488	3.96	5.58448	4.048	70.66667	61.66667
403		0	80	3	1	1	65.824	4.048	3	44.704	0	3.784	11.61688	3.696	4.31904	3.96	2.69544	3.784	54.66667	57
404		1	52	2	1	0	28.03416	3.52	2	53.504	0	3.432	22.70488	3.168	7.71144	3.52	4.092	3.5992	69.33333	61.66667
405		1	65	3	1	0	31.61136	3.256	2	57.2968	0	3.168	12.69136	3.168	3.8676	3.256	2.6136	3.256	55	75.66667
406		1	67	2	1	4	28.63872	3.08	2	53.15728	4	2.728	22.05808	2.64	8.55448	3.168	5.43488	3.608	84.66667	76.33333
407		0	65	3	1	3	42.47936	4.136	2	69.608	0	3.784	19.27288	3.696	5.66368	4.136	0	0	88.33333	79
408		1	81	3	1	1	24.35312	3.168	2	72.17848	1	3.08	16.24216	2.64	5.75344	2.904	4.37976	2.86528	62.66667	62.66667
409		1	37	2	1	0	44.56056	4.224	2	81.2416	0	3.784	27.984	3.696	7.656	NA	NA	NA	NA	NA
410		0	45	3	1	1	52.74192	4.136	2	68.91456	0	4.136	18.23976	3.784	6.38528	3.784	3.5508	3.08	67.66667	62.33333
411		1	36	2	1	0	NA	NA	2	0	0	2.64	21.66296	2.64	8.23504	2.64	4.52584	3.08	63	67.66667
412		0	53	3	1	1	49.66632	3.784	2	57.18768	0	3.608	14.31496	2.64	7.392	NA	NA	NA	62.33333	NA
413		1	72	2	1	0	33.352	4.136	2	54.0056	0	3.96	21.27752	3.608	9.63336	3.52	6.66248	3.52	64.33333	63.33333
414		1	75	3	1	0	53.7724	4.4	2	69.63176	0	4.136	39.78392	4.224	11.73304	4.224	5.68392	4.224	52.66667	70.66667
415		1	45	2	1	0	41.07752	3.696	2	67.50568	0	3.344	24.926	3.168	8.07928	3.696	0	3.696	100.6667	69.33333
416		0	42	1	1	0	42.16168	4.048	2	60.38824	0	4.136	26.42288	3.62032	9.10888	3.872	4.9148	3.872	53	63.33333
417		1	49	3	1	1	25.85704	3.08	2	50.05264	0	2.64	21.65064	2.64	7.44656	3.08	4.08848	3.168	72.33333	74.66667
418		1	45	3	1	0	48.73704	3.96	2	62.39376	0	3.97144	30.89152	3.96	8.79824	3.872	5.76312	3.86144	76.66667	68.66667
419		1	64	2	1	1	32.17632	3.872	2	58.96264	0	3.784	26.41584	3.432	10.9516	3.872	6.18552	4.576	73.33333	77
420		0	43	3	1	0	70.33488	3.784	3	59.18792	0	3.52	25.34576	3.344	9.8824	3.432	5.59416	5.72	50.33333	68
421		1	65	2	1	0	31.34384	2.728	2	48.63672	0	2.904	18.12184	2.64	4.22664	2.64	3.74528	3.168	106.3333	61
422		1	22	2	1	0	53.16168	4.224	3	51.57416	0	4.224	37.75552	4.224	NA	NA	NA	NA	63.33333	NA
423		1	59	3	1	0	32.03552	3.608	2	59.76608	0	3.34752	22.53768	3.256	8.25	3.608	4.58392	4.752	64.66667	70
424		1	36	3	1	0	46.64704	4.136	2	64.06752	0	3.87552	26.58656	3.784	9.4644	3.96	5.1084	3.96	58.66667	66.66667
425		0	85	3	1	0	40.93848	3.784	2	52.10128	1	3.872	27.23072	3.696	7.50288	3.696	4.99224	3.696	68.66667	72.33333
426		0	35	3	1	0	41.888	3.696	2	68.46664	0	4.048	27.632	3.696	11.088	4.224	NA	4.224	NA	NA
427		1	78	3	1	3	36.8104	3.08	2	58.35456	1	3.256	27.86784	2.904	5.67512	3.696	4.906	3.696	45.33333	71.66667
428		0	69	3	1	1	32.00384	3.52	2	45.672	1	3.256	13.992	2.992	5.4384	3.432	3.05888	3.432	NA	75.33333
429		1	73	3	1	0	37.61032	4.312	2	64.856	0	4.22664	14.78488	3.784	5.28	4.224	3.31496	4.224	69.66667	71.66667
430		0	74	3	1	1	36.20232	3.696	2	49.192	0	3.69952	20.06488	3.344	4.35864	3.71184	2.48952	2.816	59.66667	65
431		1	28	3	1	0	40.04792	3.168	2	53.70376	0	2.728	17.95288	2.288	2.6004	2.64	1.89112	2.64	77.66667	64.66667
432		0	77	3	1	1	33.55176	3.168	2	50.64488	0	3.08	17.072	3.08	NA	NA	3.22344	0	55.66667	NA
433		1	73	3	1	0	27.01776	2.728	2	52.228	1	2.904	19.4172	2.552	4.82504	3.08	3.26568	2.816	66.66667	68.66667
434		1	79	3	1	1	32.66736	3.344	2	55.61776	1	3.168	12.408	2.64	5.18144	3.168	2.55376	2.728	55.33333	60.66667
435		0	46	3	1	0	49.24744	4.136	2	53.99768	0	3.872	10.82928	3.52	3.10904	4.136	2.25456	2.78344	46.33333	59.66667
436		0	17	1	1	0	41.33712	3.696	2	57.29328	0	3.696	19.59584	3.696	6.21544	3.696	3.51472	3.168	69.33333	72.66667
437		1	71	3	1	0	42.4952	3.784	2	64.51192	0	3.344	19.53688	3.168	5.63112	3.256	3.22872	3.168	66	68.33333
438		1	57	3	1	0	42.32096	3.784	2	60.81504	0	3.256	17.26208	2.992	4.9192	3.696	2.49392	3.608	83.33333	67.33333
439		0	65	3	1	1	42.07896	2.64	2	47.57016	1	2.64	14.08616	2.552	4.27592	2.552	2.49392	2.464	87.33333	60.33333
440		1	77	3	1	1	30.04496	2.64	2	50.33776	0	2.64	10.56088	2.552	NA	NA	2.5212	2.464	50	NA
441		0	64	3	1	0	29.19312	2.376	2	42.06488	0	2.2	18.33304	2.376	3.8676	2.64	1.95624	2.6136	68.66667	60.66667
442		0	37	1	1	0	28.55072	2.64	2	55.62128	0	2.64	10.56	2.112	3.432	2.904	2.47104	2.2	70.66667	73.66667
443		0	32	2	1	0	32.7712	2.728	2	61.99072	1	2.728	15.68072	2.64	6.19872	2.112	3.20848	2.376	63.33333	61
444		1	35	3	1	0	49.21928	2.904	3	32.7448	0	2.376	15.15888	2.376	4.3164	2.376	3.80688	2.552	58	62.33333
445		1	71	3	1	0	28.43896	2.64	2	53.51104	0	2.376	12.40888	2.376	4.23456	2.64	2.6136	2.2	74.33333	61
446		0	70	1	1	0	33.35464	4.136	2	56.58752	1	3.784	26.21784	3.52	6.996	3.872	3.7884	5.632	58.66667	59.66667
447		1	67	3	1	0	34.14048	2.728	2	57.99376	0	2.728	10.64888	2.376	4.5716	2.728	3.01752	2.288	72.33333	72.66667
448		1	70	3	1	0	42.95456	3.52	2	31.94576	0	3.432	17.688	3.432	5.30112	0	3.17856	3.256	44.66667	0
449		0	31	3	1	0	38.36888	4.576	2	55.15224	0	4.488	22.792	4.136	9.24	4.136	3.17856	3.50768	61.66667	59.66667
450		0	38	2	1	0	36.1152	3.872	2	73.49848	0	3.872	19.01064	3.696	NA	NA	NA	NA	64.33333	NA
451		0	65	3	1	1	37.02776	3.872	2	56.94304	0	3.872	16.63552	3.696	5.016	0	2.78432	4.53112	0	61
452		1	33	1	1	0	25.28504	2.816	2	42.15552	0	2.816	18.74488	2.552	8.62664	2.816	3.3044	3.17152	100	59.33333
453		0	55	3	1	0	38.66544	3.96	2	55.53328	0	3.784	13.29592	3.696	5.17528	3.872	2.57664	3.872	62	77
454		0	58	1	1	0	29.1632	3.168	2	53.87888	0	3.168	11.52096	2.552	4.40088	3.168	2.7676	3.08	109	69.33333
455		1	69	3	1	0	44.52976	3.696	2	52.7252	0	3.696	12.40888	3.168	4.33488	3.608	3.01752	3.608	62.66667	55.66667
456		0	46	2	1	0	42.76536	3.872	2	60.1128	0	4.048	14.25776	3.696	6.864	3.784	3.81304	3.784	55.33333	0
457		1	76	3	1	0	30.7384	3.256	2	52.9012	0	3.168	12.93688	2.992	4.93152	3.344	3.05536	3.608	95.33333	70
458		1	41	2	1	0	31.85424	3.872	2	57.992	0	3.608	17.688	3.608	8.976	3.608	4.30848	3.696	109.6667	72.66667
459		1	44	2	1	0	23.1924	2.904	2	46.60304	0	2.728	NA	NA	NA	NA	3.8676	NA	NA	NA
460		1	38	2	1	0	39.5956	3.608	2	71.8256	0	3.608	24.288	3.168	6.72584	3.52	4.28032	3.432	68.66667	60.33333
461		1	40	1	1	0	30.16816	3.344	2	58.79984	0	3.344	24.552	3.168	8.184	3.168	4.35864	3.168	54.33333	67.66667
462		1	86	2	1	0	22.1892	3.52	2	52.448	3	3.168	21.12704	2.552	8.97688	3.168	5.20256	3.168	65.66667	68.66667
463		1	72	3	1	1	39.15736	3.256	2	72.47944	0	3.256	39.072	3.08	NA	NA	NA	NA	55.33333	55.66667
464		0	66	3	1	0	35.93304	3.872	2	52.1708	0	3.432	13.46488	3.344	5.544	3.608	2.83976	3.52	94.33333	64.66667
465		0	66	3	1	0	22.2992	1.936	2	43.0364	0	1.848	16.10664	1.848	5.59944	1.848	3.79984	2.20792	81	76.66667
466		1	76	3	1	1	32.92784	3.256	2	44.968	1	2.992	21.75184	2.816	9.05696	3.08	4.14568	3.0888	96.33333	60.33333
467		0	84	3	1	1	44.06512	3.784	2	69.69952	0	3.872	20.32976	3.696	10.648	4.224	6.688	4.312	NA	NA
468		1	31	2	1	0	27.918	3.168	2	41.84048	0	3.08	16.5088	2.728	5.28176	2.816	3.23664	2.816	62.66667	52.33333
469		1	51	1	1	0	52.09424	4.224	2	92.92976	1	4.224	21.26696	3.696	8.448	4.224	3.3	4.4	58.66667	57.66667
470		1	78	3	1	1	35.37952	3.52	2	52.0124	0	3.344	27.456	3.432	9.07456	3.52	5.33456	3.696	66	63.33333
471		0	70	3	1	3	40.20544	3.872	2	52.31072	0	3.608	25.87288	3.52352	7.92	3.96	4.60416	4.60416	57.33333	56
472		1	78	3	1	1	49.87312	5.104	2	60.434	1	5.104	17.68976	4.488	5.11104	4.664	2.75088	4.576	63.66667	74.33333
473		1	59	2	1	0	39.85696	3.256	2	59.40264	0	3.08	29.57152	2.552	9.15288	3.08	4.80744	3.168	53.66667	61.33333
474		0	43	1	1	0	54.91288	5.28	2	89.90872	0	5.28	48.3164	5.28	11.7964	5.2976	6.38616	5.28	53.66667	61.66667
475		1	42	1	1	0	43.44912	3.168	2	82.11984	1	3.696	19.69352	3.168	4.61208	3.696	3.75232	3.696	88.66667	80.66667
476		0	45	3	1	1	44.94424	4.136	2	64.92112	0	3.872	19.94872	3.784	NA	3.784	3.696	3.70656	81.33333	56.33333
477		1	15	3	1	0	47.11608	4.4	2	77.25784	0	4.312	19.29576	3.608	5.41728	4.136	3.90896	4.312	51.66667	61.66667
478		0	60	2	1	0	55.00968	3.52	4	53.00944	0	3.256	29.04	3.256	10.12352	3.168	6.68976	3.168	59.66667	62.33333
479		1	59	3	1	0	37.11576	3.18296	2	63.54216	0	3.256	18.7704	3.168	4.3692	3.696	3.19352	3.26304	64.33333	60.33333
480		1	54	1	1	1	43.1068	4.312	2	56.31472	0	3.872	25.61328	3.608	7.57592	4.224	4.00928	3.87904	59.66667	62.66667
481		1	63	3	1	0	48.774	3.432	2	82.74112	0	3.432	29.91648	3.432	12.79344	3.344	7.4492	3.168	57.66667	56.66667
482		1	73	3	1	1	37.09112	4.224	2	59.49064	1	4.136	30.008	3.432	11.1716	4.136	4.54608	4.28032	82	60.66667
483		1	77	3	1	3	38.77808	3.608	2	45.19416	3	3.608	20.504	3.168	5.28	3.432	2.75088	3.256	57.66667	64.66667
484		1	72	3	1	1	41.70848	4.84	2	68.02752	0	4.224	27.28	3.608	6.22336	3.96	3.19352	3.784	54.33333	61.33333
485		1	55	2	1	1	27.9444	3.52	2	60.71648	1	3.08	24.024	2.816	8.64512	3.432	4.12984	3.344	54.33333	54.66667
486		1	49	2	1	0	32.27664	3.872	2	57.35928	0	3.432	27.874	2.992	6.864	3.52	4.53112	3.47688	52	60
487		1	29	2	1	0	40.23536	4.224	2	72.952	0	4.224	27.192	3.7576	NA	NA	NA	NA	NA	NA
488		1	77	2	1	4	45.056	3.96	2	68.816	4	3.608	24.288	3.608	7.1808	3.872	2.64	3.872	56	60
489		1	72	2	1	0	40.48	2.904	2	56.32	0	3.256	14.784	2.816	3.96	3.256	3.96	3.2076	43.33333	49
490		1	60	2	1	0	44.088	0.792	2	72.248	0	0.792	17.952	0.792	5.808	0.792	5.544	0.792	52	61
491		0	33	1	1	0	55.792	3.872	3	44.704	4	3.96	28.512	3.52	3.96	3.696	3.168	3.61328	50.33333	75
492		0	81	3	1	1	37.58744	3.168	2	58.08	1	3.168	14.52	3.168	3.96	3.168	3.168	3.168	50	61
493		1	59	2	1	0	NA	NA	2	48.69392	0	2.728	22.44	2.288	7.656	2.816	3.696	2.816	107	57
494		1	71	3	1	0	39.16	2.904	2	45.584	0	3.256	22.44	2.904	7.04	2.992	4.224	2.94712	51.66667	61
495		0	81	3	1	3	34.69048	3.52	2	47.17416	0	3.432	20.60784	3.168	6.55424	3.168	4.488	3.168	67.33333	57.66667
496		0	59	2	1	1	49.90656	3.784	2	63.82112	0	3.696	20.3324	3.52	5.31168	3.696	4.224	3.696	55	58.66667
497		1	81	2	1	0	39.03856	2.904	2	58.25688	0	2.904	NA	NA	5.544	NA	NA	NA	NA	NA
498		1	57	3	1	3	40.61904	3.872	2	51.21864	0	3.608	19.536	3.608	7.128	3.73648	3.696	3.73648	50.33333	60
499		0	53	3	1	1	42.19424	3.168	2	64.43096	4	3.168	13.81776	3.168	4.35072	3.168	3.696	3.168	44	47.33333

500		1	68	2	1	0	43.38752	4.048	2	61.6088	0	3.872	18.89448	3.696	8.6592	3.96	5.3856	3.872	54.66667	0
501		0	43	1	1	1	74.90824	3.608	5	39.65104	0	3.52	16.70328	3.256	5.9444	3.608	4.30848	3.608	75.33333	54
502		0	81	1	1	1	48.48536	3.872	2	98.8328	4	3.52	21.79848	3.168	5.4032	3.696	3.564	3.696	0	67.33333
503		0	66	1	1	0	44.0132	3.256	2	75.41688	0	3.168	22.61688	3.168	7.76688	3.168	4.224	3.168	57.66667	65.33333
504		0	32	3	1	0	58.27624	4.312	3	56.144	0	4.488	NA	NA	8.184	4.488	NA	4.4396	49	NA
505		1	45	1	1	0	31.26376	3.52	2	58.3484	0	3.344	25.75232	2.992	13.52912	2.904	4.4176	2.904	107.6667	59.33333
506		1	54	1	1	0	NA	NA	2	64.43448	0	3.96	25.62912	3.696	7.25384	3.696	5.07672	3.696	50.66667	56.33333
507		0	37	1	1	0	NA	NA	2	62.77656	0	3.256	30.36	3.256	6.69768	3.432	5.19728	3.432	49.66667	62.66667
508		1	57	2	1	0	27.55544	3.432	2	48.28032	0	2.992	25.18648	2.64	7.05584	3.432	5.20608	3.432	55.33333	55
509		1	67	3	1	0	29.68064	3.53672	2	55.462	0	3.52	25.52264	3.17152	6.336	3.168	4.488	3.168	52.66667	61
510		1	84	2	1	0	41.82112	4.224	2	80.98376	0	4.84	24.552	4.752	8.8528	4.224	5.78952	4.224	50.66667	49.33333
511		1	66	2	1	1	52.30896	4.136	2	64.24264	0	3.96	20.59288	3.784	6.28408	3.96	5.33456	3.96	55.33333	60.33333
512		1	54	1	1	0	33.83336	3.256	2	60.02216	0	3.168	17.512	3.168	8.45328	3.168	6.38616	3.168	55	61
513		1	31	2	1	0	57.46488	3.344	3	51.04176	0	3.168	25.608	2.904	7.392	NA	NA	NA	70	0
514		0	52	3	1	1	35.62592	3.256	2	56.93776	0	3.432	26.664	3.168	8.0476	3.08	5.49384	3.08	49.66667	60
515		0	51	2	1	0	39.76368	4.488	2	82.28792	0	4.4	23.10176	3.96	7.77568	3.96	4.68776	3.96	49.66667	55.33333
516		1	69	2	1	0	39.36768	3.872	2	68.41384	0	4.048	22.44	3.784	7.656	3.784	5.016	3.784	70	61
517		0	33	2	1	0	47.85088	4.4	2	64.32888	0	4.048	27.88104	3.872	8.976	4.224	6.66336	4.224	51.66667	52.66667
518		1	27	1	1	1	32.80552	3.344	2	71.66104	1	3.432	25.74264	3.168	NA	NA	NA	NA	61	52
519		1	50	1	1	0	39.28936	3.696	2	68.37864	0	3.96	21.23968	3.96	7.54424	3.96	3.85792	3.96	58.33333	58.66667
520		1	65	3	1	0	43.648	4.312	2	84.4448	0	4.4	23.936	4.224	7.744	4.488	3.86144	4.488	45	52.66667
521		0	82	3	1	3	37.84	2.992	2	44.34144	1	3.08	21.32328	2.64	5.1084	2.904	3.96	2.904	42.66667	50
522		0	65	1	1	0	28.864	3.432	2	59.75728	0	3.432	29.33744	3.432	9.24	3.432	5.59944	3.432	55.66667	53.33333
523		0	82	3	1	3	35.59776	3.344	2	60.59064	1	3.344	24.55816	3.168	6.99072	3.168	4.752	3.168	66.33333	49.66667
524		0	28	1	1	0	28.92912	2.992	2	46.17976	0	2.904	21.00912	2.376	6.63344	2.376	4.752	2.376	63.66667	59.33333
525		0	59	1	1	3	30.90032	3.52	3	53.12824	0	3.256	23.232	3.256	7.76248	3.432	4.8268	3.432	44.33333	58.66667
526		0	67	2	1	0	40.5504	3.696	2	57.4068	0	3.696	32.31536	3.52	8.02032	3.696	4.75992	3.696	43	57
527		1	50	1	1	0	40.07344	4.488	2	70.05152	0	4.312	23.562	4.048	6.17584	4.312	3.5508	4.312	47.33333	55
528		0	45	1	1	0	30.0476	3.432	2	47.53584	0	3.256	18.75016	3.168	6.70208	3.344	4.31904	3.344	48.66667	60
529		1	65	2	1	0	40.744	3.168	2	49.88368	0	3.168	15.378	3.168	8.30544	3.168	5.31168	3.168	39.66667	54.66667
530		1	32	1	1	0	49.24832	3.696	2	63.2852	3	3.696	17.81208	3.168	5.44368	3.696	3.96	3.696	53	47.66667
531		1	58	2	1	0	0	3.168	2	51.1456	0	2.992	25.5244	2.904	8.5668	2.904	5.28	2.904	50.66667	52
532		1	60	2	1	0	43.472	4.048	2	74.36	0	3.696	17.688	3.696	8.448	3.96	4.752	3.96	NA	NA
533		0	52	1	1	0	33.9812	3.256	2	59.312	0	3.168	27.72	3.168	4.14568	3.168	2.64	3.168	51	50.33333
534		1	78	2	1	0	28.77072	3.256	2	59.06736	0	3.168	18.48176	2.904	8.5888	3.168	4.49592	2.87144	53.33333	67
535		1	58	3	1	0	43.98592	3.52	2	60.37152	0	3.432	19.53688	3.256	NA	NA	NA	NA	48	NA
536		0	67	3	1	1	45.67112	4.224	2	63.03	0	4.224	21.1288	3.696	6.9696	4.136	4.3296	3.97056	54.33333	56.66667
537		1	78	1	1	0	46.5344	3.432	2	65.93488	0	3.608	26.664	3.432	6.46888	3.344	5.28	3.344	66.66667	54.33333
538		1	59	2	1	0	39.02272	3.344	2	72.2436	0	3.256	17.688	3.168	6.336	3.52	4.224	3.52	58.66667	55
539		0	42	2	1	3	45.39304	2.904	2	72.66688	0	3.608	23.05424	3.168	6.6	3.52	5.3856	3.52	50	50.33333
540		0	78	3	1	0	31.69144	3.52	2	68.01168	0	3.432	28.24976	3.432	7.13328	3.432	5.28	3.432	73.33333	55
541		1	56	3	1	0	30.23944	3.168	2	50.952	0	3.08	22.63536	2.64	7.85312	3.168	4.31904	3.168	44	50
542		0	68	2	1	4	43.70432	3.696	2	61.99072	4	3.696	18.21952	3.52	5.43576	3.696	3.17856	3.696	47.33333	59.66667
543		0	65	3	1	1	28.89216	3.344	2	51.4052	1	3.608	25.65024	2.992	8.33712	3.344	4.57688	3.344	49.33333	52
544		0	69	3	1	1	49.8784	4.224	2	83.11512	0	4.048	34.848	3.96	10.90232	4.224	6.35712	4.224	55.33333	56.66667
545		1	70	3	1	1	33.21384	3.168	2	56.584	3	3.168	16.48944	3.168	6.07728	3.168	3.44256	3.168	53.33333	59
546		1	43	3	1	1	42.87096	3.168	2	61.33776	0	3.168	26.9324	3.168	4.5056	3.168	2.80632	3.168	46.33333	57.33333
547		1	62	3	1	0	28.08696	3.344	2	54.82664	0	3.168	22.44088	3.08	8.86248	3.432	4.86288	3.432	50.66667	60.66667
548		0	44	2	1	0	32.912	3.168	2	46.904	0	3.168	13.464	2.904	3.21288	3.168	2.85648	3.168	63.33333	66.33333
549		0	80	2	1	0	47.30352	4.224	2	70.46424	0	4.752	0	4.224	7.9992	4.224	4.488	4.224	41	55
550		1	69	2	1	0	47.71096	3.608	2	77.71544	0	3.432	22.09416	3.432	8.02824	3.696	5.59944	3.696	47.66667	56.66667
551		1	79	3	1	1	49.24656	3.696	2	71.37768	3	3.608	18.744	3.52	7.92	3.608	4.488	3.608	50.66667	49.66667
552		1	40	3	1	0	35.64704	3.52	2	58.70128	0	3.432	27.72352	2.992	10.32768	3.168	6.864	3.168	53	55
553		1	62	3	1	0	37.048	3.96	2	58.168	0	3.784	28.248	3.168	8.976	3.784	4.752	3.784	39	50.33333
554		1	62	2	1	0	36.31232	3.784	2	62.89272	0	3.52	26.80128	3.608	9.03936	3.52	6.732	3.52	54.33333	65.66667

SN	PTV4R	V4LR	V4DR	PICAR	PICAL	PICAOBLI	PICAOBLI	PICAVERT	PICAHORI	VBA	LGA	DV	RT,LT ATR	HYPTERM	PICA VAR	OTH VAR	VOL	PTV1L
1	0	25.52616	3.08	0	0	0	0		0	33	1	9,16	0	9	0	16	1	3
2	0	24.36984	2.904	0	0	0	0		0	37	1	16	0	9	0	16	1	3
3	2	29.44744	2.904	0	19	0	0		0	46.33333	2	19	0	0	0	0	1	3
4	2	23.936	3.784	0	0	0	0		0	45.33333	2	16	0	0	0	16	1	3
5	0	26.664	4.136	0	0	0	0		0	74.33333	2	16	0	0	0	16	1	0
6	1	27.72	2.112	18	0	0	0		0	34.33333	1	0	0	0	0	0	1	3
7	0	27.104	3.608	0	0	0	0		0	44.66667	2	10,16	0	10	0	16	1	3
8	0	24.11552	2.816	0	0	0	0		0	NA	NA	9,16	0	9	0	16	1	1
9	0	33.88	2.376	0	0	0	0		0	38.33333	1	16	0	0	0	16	1	3
10	4	23.232	3.432	0	0	0	0		0	35.33333	2	16	0	0	0	16	1	3
11	0	37.46072	3.168	0	19	0	8		0	35.33333	1	0	0	0	0	0	2	0
12	0	37.56896	3.96	0	0	0	0		0	36.33333	1	16	0	0	0	16	1	2
13	0	28.512	3.08	0	0	0	0		0	32	1	9,16	0	9	0	16	1	2
14	0	31.504	3.52	0	0	0	0		0	34	2	16	0	0	0	16	1	3
15	0	29.31808	3.168	0	0	0	0		0	67	2	16	0	0	0	16	1	3
16	0	33.6732	3.256	0	0	0	0		0	54	2	16	0	0	0	16	1	3
17	0	25.7092	3.256	0	0	0	0		0	35.33333	2	16	0	0	0	16	1	3
18	3	31.4908	3.608	0	0	0	0		0	50	2	16	0	0	0	16	1	3
19	0	32.16224	3.696	0	0	0	0		0	37.66667	1	16	0	0	0	16	1	3
20	0	21.56352	3.52	0	0	0	0		0	35	1	17	0	0	0	17	1	2
21	0	24.024	3.08	18	0	0	0		0	99.66667	2	0	0	0	0	0	1	3
22	0	42.04024	3.432	18	0	0	0		0	35	1	9,15	0	9	15	0	1	3
23	0	27.67336	3.432	0	0	0	0		0	39.66667	2	16	0	0	0	16	1	4
24	3	33.17952	3.784	18	0	0	0		0	88	2	0	0	0	0	0	1	0
25	0	33.93896	3.784	0	0	0	0		0	32	2	16	0	0	0	16	1	4
26	0	30.1224	2.112	0	0	0	0		0	63	2	16	0	0	0	16	2	0
27	0	26.84704	2.464	0	0	0	0		0	65	2	9,16	0	9	0	16	1	0
28	0	13.40416	2.376	0	0	0	0		0	40.66667	1	16	0	0	0	16	1	0
29	0	24.75088	2.904	1	1	0	0		0	41	1	11	0	0	11	0	1	3
30	0	19.3336	2.552	0	0	0	0		0	38.66667	1	16	0	0	0	16	1	3
31	0	26.136	3.52	0	0	0	0		0	38.66667	2	10,16	0	10	0	16	1	0
32	0	26.664	2.816	18	0	0	0		0	47.33333	1	0	0	9	0	0	1	0
33	3	37.96848	2.992	0	0	0	0		0	31.33333	2	16	0	0	0	16	1	3
34	0	35.64176	2.552	0	0	0	0		0	35.66667	1	16	0	0	0	16	1	3
35	0	37.224	3.08	0	0	0	0		0	50	1	16	0	0	0	16	1	3
36	0	30.03088	5.28	0	0	0	0		0	52	1	10,16	0	10	0	16	1	1
37	0	29.48792	3.432	0	0	0	0		0	61.33333	2	16	0	0	0	16	1	0
38	0	26.62	2.64	0	0	0	0		0	50.66667	1	16	0	0	0	16	1	1
39	0	22.07392	2.64	1	1	0	0		0	56.33333	2	11	0	0	11	0	1	0
40	4	34.39128	1.92544	0	0	0	0		0	29	1	16	0	9	0	16	1	3
41	0	26.0744	3.168	0	0	0	0		0	48.33333	1	16	0	0	0	16	1	1
42	0	31.68088	2.64	18	0	0	0		0	92.33333	2	18	0	0	0	0	1	0
43	0	26.664	2.112	0	0	0	0		0	77	2	16	0	0	0	16	1	3
44	0	22.968	2.728	0	19	0	0		0	59.66667	1	0	0	0	0	0	1	1
45	0	25.872	1.848	0	0	0	0		0	50.66667	2	16	0	0	0	16	1	3
46	0	45.71248	3.168	0	0	0	0		0	90.33333	2	16	0	0	0	16	1	1
47	0	31.944	2.64	0	0	0	0		0	32	1	16	0	0	0	16	1	1
48	0	28.16528	2.816	0	0	0	0		0	43.33333	1	16	0	0	0	16	1	0
49	0	30.70144	5.544	0	2	0	0		0	64.66667	1	12	0	0	12	0	1	0
50	0	29.28904	3.872	0	0	0	0		0	43.66667	2	16	0	0	0	16	1	1
51	0	21.88296	3.168	0	19	0	0		0	40	1	0	0	0	0	0	1	1
52	0	28.91944	2.376	18	0	0	0		0	25.66667	1	0	0	0	0	0	1	0
53	0	NA	NA	0	19	0	0		0	#DIV/0!	NA	0	0	0	0	0	1	0
54	0	26.664	2.904	0	0	0	0		0	41.66667	2	16	0	0	0	16	1	1
55	0	26.56016	3.52	0	19	0	0		0	62	1	0	0	0	0	0	1	2
56	0	29.19224	2.64	18	0	0	0		0	28.33333	1	0	0	0	0	0	1	0
57	0	30.90208	2.728	0	0	0	0		0	68.66667	2	16	0	0	0	16	1	0
58	0	37.11928	2.992	0	0	0	0		0	44.66667	1	16	0	0	0	16	1	0
59	0	32.31888	2.024	0	0	0	0		0	42.66667	1	16	0	0	0	16	1	0
60	0	12.57608	3.08	0	19	0	0		0	24	1	0	0	0	0	0	1	0
61	0	31.31216	2.2	0	0	0	0		0	96	1	16	0	0	0	16	1	0
62	0	19.272	2.376	1	1	0	0		0	76.33333	2	11	0	0	11	0	1	3
63	0	23.00848	2.376	0	0	0	0		0	77	1	16	0	0	0	16	1	0
64	0	30.36	3.168	0	0	0	0		0	27.66667	1	16	0	0	0	16	1	1
65	0	26.928	3.256	0	0	0	0		0	31	1	16	0	0	0	16	1	0
66	0	32.01528	2.552	1	1	0	8		0	22.33333	1	11	0	0	11	0	1	3
67	0	38.016	3.696	18	0	0	0		0	#DIV/0!	0	2	2	0	0	0	2	0
68	0	26.83032	3.344	1	1	0	0		0	56.66667	1	11	0	0	11	0	1	1
69	0	24.024	3.256	0	0	0	0		0	53	1	10,16	0	10	0	16	1	0
70	0	32.56	2.728	0	0	0	0		0	0	1	2,16	2	0	0	16	1	0
71	0	26.928	3.256	0	0	0	0		0	37.66667	1	9,16	0	9	0	16	1	0
72	0	26.76608	3.432	0	0	0	0		0	31	1	16	0	0	0	16	1	0
73	0	26.3472	2.552	0	0	0	0		0	37	1	16	0	0	0	16	1	0
74	0	31.5568	2.904	0	0	0	0		0	50.66667	1	16	0	0	0	16	1	0
75	0	27.5924	3.696	0	0	0	0		0	54.66667	1	16	0	0	0	16	1	1
76	0	18.77392	3.168	0	0	0	0		0	42.33333	1	16	0	0	0	16	1	1
77	0	31.01736	3.256	0	0	0	0		0	42	1	16	0	0	0	16	1	1
78	0	28.6308	3.08	0	19	0	0		0	54.33333	1	0	0	0	0	0	1	0
79	0	27.32576	2.64	0	0	0	0		0	56.66667	1	16	0	0	0	16	1	1
80	0	27.456	2.376	0	0	0	0		0	31.33333	1	9,16	0	9	0	16	1	0
81	0	18.43952	3.08	0	0	0	0		0	39.33333	1	16	0	0	0	16	1	1
82	0	36.696	3.696	18	0	0	0		0	35.66667	2	0	0	0	0	0	1	1
83	0	0	3.168	1	1	0	0		0	#DIV/0!	NA	11	0	0	11	0	1	1
84	0	21.12	3.46544	0	19	0	0		0	69.33333	2	0	0	0	0	0	1	1
85	0	28.776	3.08	0	0	0	0		0	52.33333	1	16	0	0	0	16	1	0
86	0	NA	2.64	0	0	0	0		0	0	2	10, 1,16	1	9	0	16	1	0
87	0	32.37608	3.344	0	0	0	0		0	44.33333	1	16	0	0	0	16	1	0
88	0	21.77384	2.904	0	19	0	0		0	64.66667	2	0	0	0	0	0	1	0
89	0	19.272	NA	0	0	0	0		0	57.33333	2	9,16	0	9	0	16	1	0
90	0	NA	2.64	0	0	0	0		0	#DIV/0!	NA	1,16	1	0	0	16	1	0
91	0	29.9376	3.256	0	0	0	0		0	62.33333	1	16	0	0	0	16	1	3
92	0	33.43472	3.344	0	0	0	0		0	#DIV/0!	NA	16	0	0	0	16	1	0
93	0	15.08672	2.728	0	0	0	0		0	50	1	16	0	0	0	16	1	0
94	0	19.42688	3.784	0	0	0	0		0	37.33333	1	16	0	0	0	16	1	0
95	0	33.264	4.928	0	0	0	0		0	102.3333	1	16	0	0	0	16	1	0
96	0	23.64472	2.09528	1	1	0	0		0	33.66667	1	11	0	0	11	0	1	1
97	NA	NA	NA	0	19	0	0		0	0	NA	0	0	0	0	0	1	0
98	0	29.63136	2.992	0	0	0	0		0	49.33333	1	16	0	0	0	16	1	1
99	0	32.68232	3.6212	0	0	0	0		0	56.66667	1	0	0	0	11	0	1	1

101	0	NA	2.376	0	0	0	0		0	#DIV/0!	NA	16	0	10	0	16	1	0
102	0	29.97192	2.728	18	0	0	0		0	54.66667	2	0	0	0	0	0	1	0
103	0	34.936	2.728	0	0	0	0		0	54.33333	1	16	0	0	0	16	1	0
104	0	31.60872	2.992	0	0	0	0		0	37.66667	1	16	0	0	0	16	1	0
105	0	39.6	3.168	0	19	0	0		0	24.33333	1	0	0	0	0	0	2	0
106	0	33.90464	3.168	18	0	0	0		0	54.66667	1	0	0	0	0	0	1	0
107	0	42.63336	3.168	0	0	0	0		0	56	1	16	0	0	0	16	1	0
108	0	26.5804	3.52	0	0	0	0		0	61	2	16	0	10	0	16	1	0
109	0	#DIV/0!	1.848	0	0	0	0		0	#DIV/0!	NA	1,16	1	0	0	16	1	0
110	0	32.08392	2.376	1	1	0	0		0	46	1	11	0	0	11	0	1	0
111	0	39.4284	3.344	18	0	5	0		0	37.33333	1	0	0	0	0	0	1	0
112	0	35.47632	2.904	0	0	0	0		0	#DIV/0!	2	10,16	0	10	0	16	1	0
113	0	41.72168	3.344	2	0	5	0		0	47.33333	2	10,12	0	10	12	0	1	0
114	0	28.71352	2.992	0	19	0	0		0	74.33333	2	10,19	0	10	0	0	1	0
115	0	31.944	3.256	0	0	0	0		0	34.33333	1	0	0	0	0	0	1	0
116	0	31.73808	3.344	0	0	0	0		0	37.66667	1	16	0	0	0	16	1	0
117	0	36.432	3.08	0	0	0	0		0	44.33333	1	10,16	2	0	0	16	1	1
118	0	0	#DIV/0!	0	0	0	0		0	#DIV/0!	NA	16	1	10	0	16	1	0
119	0	31.416	2.992	1	1	0	0		0	37	2	11	0	0	11	0	1	3
120	0	28.89832	2.464	18	0	0	0		0	48	1	0	0	0	0	0	1	1
121	0	34.4828	3.168	0	0	0	0		0	51.66667	1	16	0	0	0	16	1	0
122	0	35.7852	2.904	18	0	0	0		0	57.66667	2	0	0	0	0	0	2	1
123	0	33.83336	2.64	0	0	0	0		0	53.66667	1	16	0	0	0	16	1	0
124	0	24.70776	3.08	0	0	0	0		0	68	2	10,16	0	10	0	16	1	0
125	0	27.78776	2.992	18	0	0	0		0	76.33333	2	0	0	0	0	0	1	0
126	0	34.232	2.816	0	19	0	0		0	57	1	0	0	0	0	0	1	1
127	0	#DIV/0!	#DIV/0!	1	1	0	0		0	#DIV/0!	NA	1,11	1	0	11	0	2	0
128	0	29.45272	2.64	18	0	0	0		0	47	1	0	0	9	0	0	1	0
129	0	31.944	3.168	0	0	0	0		0	#DIV/0!	2	2,16	2	0	0	16	1	0
130	0	16.10488	2.64	18	0	0	0		0	67	2	10	0	10	0	0	1	0
131	0	0	3.168	1	1	0	0		0	#DIV/0!	NA	11	0	0	11	0	1	1
132	0	29.56888	2.992	0	0	0	0		0	46	1	0	0	0	11	0	1	0
133	0	27.24304	3.344	0	0	0	0		0	58.33333	1	16	0	0	0	16	1	0
134	0	34.73008	2.992	1	1	0	0		0	54	2	11	0	0	11	0	1	0
135	0	34.584	2.64	0	0	0	0		0	0	1	16	1	0	0	16	1	1
136	0	26.03832	1.848	0	0	0	0		0	38	1	16	0	0	0	16	1	3
137	0	29.832	3.344	0	0	0	0		0	32.66667	1	16	0	0	0	16	1	4
138	0	29.392	3.168	0	0	0	0		0	46.33333	1	16	0	0	0	16	1	1
139	0	28.424	3.09584	0	0	0	0		0	32.33333	1	16	0	0	0	16	1	0
140	0	35.288	3.608	1	1	5	0		0	39	1	11	0	0	11	0	1	3
141	0	26.83208	2.376	1	1	0	0		0	48.66667	1	11	0	0	11	0	1	0
142	0	31.34736	3.256	1	1	0	8		0	50.33333	1	10,11	0	10	11	0	1	0
143	0	30.712	2.904	1	2	0	0		0	33.33333	1	12,11	0	0	11	0	1	1
144	0	34.76	3.344	0	0	0	0		0	40.66667	1	16	0	0	12	16	1	3
145	0	34.84976	3.256	0	19	0	0		0	32.33333	1	0	0	0	0	0	1	0
146	0	28.37736	3.256	0	19	0	0		0	60	2	0	0	0	0	0	1	3
147	0	31.06928	2.64	0	0	0	0		0	35.66667	1	9,16	0	9	0	16	1	0
148	0	26.79864	3.432	0	0	0	0		0	36.66667	1	16	0	10	0	16	1	0
149	0	0	2.992	0	0	0	0		0	0	1	16	0	0	0	16	1	1
150	0	38.214	4.048	0	0	0	0		0	52	2	10,16	0	10	0	16	1	1
151	0	30.27552	2.992	0	0	0	0		0	25.66667	1	16	2	0	0	16	2	3
152	0	34.06832	3.784	0	19	0	0		0	31	1	0	0	0	0	0	1	0
153	0	32.41832	3.52	0	19	0	0		0	38.66667	1	0	0	0	0	0	1	0
154	0	33.00528	2.904	0	0	0	0		0	36.66667	1	16	0	0	0	16	1	0
155	0	31.32624	3.344	0	0	0	0		0	40.66667	1	16	0	0	0	16	1	3
156	0	18.062	1.056	0	0	0	0		0	83.66667	2	16	0	0	11	16	1	0
157	0	36.63704	4.312	18	0	0	0		0	42	1	0	0	0	0	0	1	0
158	0	36.62824	3.256	0	19	0	0		0	38.33333	1	0	0	0	0	0	1	0
159	0	28.03504	1.584	0	0	0	0		0	37.66667	1	16	0	0	0	16	1	3
160	0	26.16328	3.432	0	0	0	0		0	31.33333	1	16	0	0	0	16	1	0
161	0	34.44496	2.904	18	0	0	0		0	72.33333	2	16	0	0	0	0	1	0
162	0	27.90216	1.848	0	0	0	0		0	26	1	16	0	0	0	16	1	0
163	0	43.1596	3.168	1	1	0	0		0	44.33333	1	11	0	0	11	0	1	0
164	0	34.24432	3.344	0	0	0	0		0	81.33333	2	16	0	0	0	16	1	1
165	0	18.09016	2.64	0	0	0	0		0	31.66667	1	16	0	0	0	16	1	1
166	0	21.7008	3.608	0	0	0	0		0	65.66667	1	16	0	0	0	16	1	0
167	0	34.3904	3.784	0	0	0	0		0	0	1	16	0	0	0	16	1	1
168	0	28.55952	3.2428	0	0	0	0		0	17	1	16	0	0	0	16	1	0
169	0	33.01936	3.168	0	19	0	0		0	42.66667	1	0	0	0	0	0	1	0
170	0	26.224	2.024	0	19	0	0		0	45.66667	1	0	0	10	0	0	1	0
171	0	27.54576	2.288	1	1	0	0		0	50	1	11	0	0	11	0	1	0
172	0	NA	2.64	0	0	0	0		0	55.66667	1	16	0	0	0	16	1	0
173	0	29.9288	2.112	0	0	0	0		0	43	1	16	0	0	0	16	1	3
174	0	22.968	2.64	0	0	0	0		0	39	1	16	0	0	0	16	1	3
175	0	26.43608	2.816	0	0	0	0		0	49.66667	1	16	0	0	0	16	1	0
176	0	29.1896	3.168	0	0	0	0		0	36.66667	1	16	0	0	0	16	1	1
177	0	25.51208	3.20232	0	19	0	0		0	50.66667	1	0	0	0	0	0	1	1
178	0	25.4672	2.552	0	0	0	0		0	80.33333	2	16	0	0	0	16	1	0
179	0	NA	NA	18	0	0	0		0	0	0	1	1	0	0	0	1	3
180	0	30.448	3.08	1	1	0	0		0	52	1	11	0	9	11	0	1	0
181	0	0	0	0	0	0	0		0	72.33333	2	16	0	0	0	16	1	0
182	0	33.97152	3.432	18	0	0	0		0	0	2	10	0	10	0	0	2	0
183	0	27.016	3.96	0	0	0	0		0	43.66667	1	16	0	0	0	16	1	3
184	0	35.992	2.904	1	1	0	0		0	85.66667	2	10,11	0	10	11	0	1	1
185	0	27.69624	3.256	0	0	0	0		0	26.66667	1	16	0	0	0	16	2	0
186	0	43.7448	3.608	0	0	0	0		0	40	1	16	0	0	0	16	2	0
187	0	0	0	0	0	0	0		0	0	0	1,16	1	0	0	16	1	0
188	0	28.776	3.08	18	0	0	0		0	53	1	0	0	0	0	0	1	1
189	0	28.07992	2.74384	1	1	0	0		0	41	1	11	0	0	11	0	1	3
190	0	28.08608	2.904	0	0	0	0		0	32.33333	1	16	0	0	0	16	1	0
191	0	30.71376	3.432	18	0	0	0		0	70	2	0	0	0	0	0	1	0
192	0	26.928	2.64	0	0	0	0		0	0	0	1,16	1	0	0	16	1	0
193	0	26.66576	2.376	18	0	0	0		0	41	1	9	0	9	0	0	1	3
194	0	31.592	2.728	0	0	0	0		0	42.66667	1	16	0	0	0	16	1	0
195	0	29.568	3.1152	0	0	0	0		0	43	1	16	0	0	0	16	1	0
196	0	31.064	2.728	1	1	0	0		0	35.33333	1	9,11	0	9	11	0	1	3
197	0	32.12	3.16448	0	0	0	0		0	0	2	16	0	0	0	16	1	3
198	0	33.16192	3.696	1	1	0	0		0	40.66667	1	11	0	0	11	0	1	0
199	0	31.68	2.816	1	1	0	0		0	40.33333	2	13,11	0	0	11	13	1	0
200	0	23.04368	2.376	18	0	0	0		0	36	1	0	0	0	0	0	1	3
201	0	33.88	3.168	1	1	0	0		0	77.66667	2	11	0	0	11	0	1	0
202	0	29.7264	3.256	18	0	0	0		0	39	1	0	0	0	0	0	2	0
203	0	31.768	2.64	0	19	0	0		0	53.66667	1	0	0	0	0	0	1	0
204	0	32.208	3.168	18	0	0	0		0	69.33333	2	0	0	0	0	0	1	3
205	0	40.216	3.168	18	0	0	0		0	69.66667	2	0	0	0	0	0	1	0
206	0	26.46512	2.816	18	0	0	0		0	35.33333	1	0	0	0	0	0	1	0
207	0	30.06696	2.904	1	1	0	0	20	0	67.66667	1	11	0	0	11	0	2	3
208	0	37.136	2.904	0	19	0	8		0	34	2	8,19	0	0	0	0	1	0
209	0	33.44	2.904	18	0	0	0		0	63	1	0	0	0	0	0	1	3
210	0	35.61536	3.256	0	0	0	0		0	50.33333	2	16	0	0	0	16	1	3
211	0	NA	NA	0	0	0	0		0	0	0	16	1	10	0	16	1	0
212	0	31.33152	2.992	0	0	0	0		0	41.66667	1	16	0	0	0	16	1	0
213	0	29.92	2.64	0	0	0	0		0	50	1	16	0	0	0	16	1	0
214	0	35.904	2.728	0	0	0	0		0	72	2	16	0	0	0	16	1	0

215	0	32.208	2.904	0	0	0	0		0	43.66667	1	16	0	0	0	16	1	1
216	0	26.928	2.112	0	19	0	0		0	78	2	0	0	0	0	0	1	1
217	0	36.344	3.696	1	1	0	0		0	49.33333	1	11	0	0	11	0	1	0
218	0	27.72	2.64	0	0	0	0		0	78	2	16	0	9	12	16	1	3
219	0	30.624	2.376	1	2	0	0		0	30.66667	1	9,11,12	0	9	11	0	1	0
220	0	38.9136	3.52	1	1	0	0		0	77	2	11	0	0	11	0	2	0
221	0	27.896	2.728	2	0	0	8		0	38	1	13, 14	0	0	14	13	1	0
222	0	23.496	3.168	1	1	0	0		0	31.66667	1	13,11	0	0	11	13	1	1
223	0	33.98648	2.64	18	0	0	0		0	91	2	15	0	0	15	0	1	3
224	0	15.576	0	0	0	0	0		0	0	1	16	0	0	0	16	1	0
225	0	33.98472	3.17152	0	0	0	0		0	57.66667	2	16	0	0	0	16	1	0
226	0	37.4	2.112	0	0	0	0		0	32.33333	1	9,16	0	9	0	16	1	1
227	0	26.84	3.168	18	0	0	0		0	63.66667	2	0	0	0	0	0	1	1
228	0	30.45856	2.992	0	0	0	0		0	30.33333	2	16	0	0	0	16	1	1
229	0	41.49992	3.96	0	0	0	0		0	51.66667	1	16	0	0	0	16	1	3
230	0	37.88928	3.52	0	0	0	0		0	52.66667	1	16	0	0	0	16	2	0
231	0	32.93312	2.64	1	1	0	0		0	50.66667	2	11	0	0	11	0	1	0
232	0	28.92824	2.728	0	0	0	0		0	41.66667	2	9,16	0	9	0	16	1	0
233	0	32.7492	4.048	1	1	0	0		0	58.33333	1	11	0	0	11	0	1	3
234	0	NA	NA	0	0	0	0		0	0	0	16	0	0	0	16	1	1
235	0	NA	NA	0	0	0	0		0	0	0	1,16	1	0	0	16	1	1
236	0	NA	3.256	0	0	0	0		0	0	0	16	0	0	0	16	1	1
237	0	35.728	3.344	0	0	0	0		0	55	0	16	0	0	0	16	1	0
238	0	28.96168	3.03072	0	0	0	0		0	0	0	16	0	0	0	16	1	1
239	0	31.24352	2.57136	0	19	0	0		0	52.66667	1	0	0	0	0	0	1	0
240	0	18.89976	3.43552	0	0	0	0		0	60.66667	2	16	0	0	0	16	1	0
241	0	21.13584	3.168	0	19	0	0		0	0	1	0	0	0	0	0	1	1
242	0	29.84256	3.168	18	0	0	0		0	76	2	0	0	0	0	0	1	0
243	0	31.944	2.64	0	19	0	0		0	22	2	0	0	0	0	0	1	1
244	0	30.73664	2.728	18	0	0	0		0	35.66667	2	0	0	0	0	0	1	1
245	0	29.4272	2.64	18	0	0	0		0	67.66667	2	0	0	0	0	0	1	1
246	0	39.38528	3.696	18	0	0	0		0	85	2	0	0	0	0	0	2	4
247	0	22.15576	3.168	0	0	0	0		0	87	2	16	0	0	0	16	1	0
248	0	36.9864	3.0712	18	0	0	0		0	32.66667	2	0	0	0	0	0	1	1
249	5	37.5276	3.168	1	1	0	0		0	55.66667	2	11	0	0	11	0	1	3
250	0	35.992	3.96	0	0	0	0		0	0	2	16	0	0	0	16	2	0
251	0	35.904	2.728	1	1	0	0		0	50.33333	2	11	0	0	11	0	1	1
252	0	35.46664	3.168	0	19	0	0		0	58.33333	1	0	0	0	0	0	2	1
253	0	31.96336	3.432	0	0	0	0		0	40.33333	1	16	0	10	0	16	1	0
254	0	32.3356	2.112	18	0	0	0		0	69.66667	2	0	0	0	0	0	1	0
255	0	28.90624	2.728	0	19	0	0		0	59.66667	2	0	0	0	0	0	1	0
256	0	33.60544	3.85528	0	19	0	0		0	49.66667	2	0	0	0	0	0	1	3
257	0	32.32416	3.168	18	0	0	0		0	62.66667	2	0	0	0	0	0	1	0
258	0	39.248	3.696	0	19	0	0		0	29.66667	1	13	0	0	0	13	1	0
259	0	27.86872	3.696	0	0	0	0		0	39.33333	1	16	0	0	0	16	1	0
260	0	0	0	0	0	0	0		0	0	1	16	0	0	0	16	1	0
261	0	32.97888	2.85032	1	1	0	0		0	52.66667	1	11	0	0	11	0	1	0
262	0	0	0	0	0	0	0		0	0	0	1,16	1	0	0	16	1	0
263	0	21.85744	3.168	0	0	0	0		0	49	1	16	0	0	0	16	1	1
264	0	33.59136	3.168	1	1	0	0		0	93	2	11	0	0	11	0	1	1
265	0	35.37512	3.256	1	1	0	0		0	46.33333	1	11	0	0	11	0	1	0
266	0	25.2868	2.376	0	0	0	0		0	58.33333	1	16	0	0	0	16	1	0
267	0	27.21136	2.376	0	0	0	0		0	63	1	16	0	0	0	16	1	0
268	0	0	0	0	0	0	0		0	54	1	16	0	0	0	16	1	0
269	0	26.53904	2.64	0	0	0	0		0	73.66667	2	16	0	0	0	16	1	1
270	0	24.7984	2.64	0	0	0	0		0	35	1	16	0	0	0	16	1	1
271	0	33.10648	3.696	1	1	0	0		0	41.33333	1	11	0	0	11	0	1	0
272	0	31.416	2.64	0	19	0	0		0	0	0	0	0	0	0	0	1	3
273	0	36.25336	3.168	0	19	0	0		0	80.33333	2	0	0	0	0	0	1	0
274	0	31.22592	2.904	0	0	0	0		0	49.33333	1	16	0	0	0	16	1	0
275	0	NA	NA	0	0	0	0		0	0	0	16	0	0	0	16	1	0
276	0	32.00912	3.696	0	19	0	0		0	39	1	0	0	0	0	0	1	3
277	0	26.45544	3.168	1	1	0	0		0	53	1	11	0	0	11	0	1	0
278	0	28.46184	2.64	18	0	0	0		0	20.33333	1	0	0	0	0	0	1	1
279	0	31.57616	2.64	1	1	0	0		0	0	0	2,11	2	0	11	0	1	1
280	0	28.73288	3.168	0	19	0	0		0	38.66667	1	0	0	0	0	0	1	0
281	0	26.664	3.696	0	0	0	0		0	66.33333	2	16	0	0	0	16	1	0
282	0	28.78128	2.904	0	0	0	0		0	44.66667	1	16	0	0	0	16	1	0
283	0	32.22648	3.18296	0	19	0	0		0	40.33333	1	0	2	0	0	0	1	0
284	0	33.704	2.64	1	1	0	0		0	38.66667	1	11	0	0	11	0	1	0
285	0	24.00464	2.904	0	19	0	0		0	44	1	0	0	0	0	0	1	0
286	0	36.52	2.64	0	19	0	0		0	87	2	0	0	0	0	0	1	1
287	0	20.80848	2.64	0	0	0	0		0	38.66667	2	16	0	0	0	16	1	0
288	0	36.68456	3.696	0	0	0	0		0	45.66667	1	16	0	0	0	16	1	0
289	0	26.03216	0	0	19	0	0		0	0	1	11	0	10	0	0	2	0
290	0	28.6	3.168	18	0	0	0		0	46	1	0	0	0	0	0	1	0
291	0	32.208	3.168	0	0	0	0		0	37.66667	2	16	0	0	0	16	1	0
292	0	27.2272	2.64	18	0	0	0		0	0	1	0	0	0	0	0	2	0
293	0	20.2312	2.64	0	0	0	0		0	48.33333	1	16	0	0	0	16	1	0
294	0	32.208	2.904	0	19	0	0		0	47.66667	1	0	0	0	0	0	1	1
295	0	28.248	2.9876	0	19	0	0		0	0	0	2	2	0	0	0	1	0
296	3	38.91888	3.432	0	0	0	0		0	0	2	16	0	0	0	16	2	1
297	0	29.04	3.344	0	19	0	0		0	42.66667	2	0	0	0	0	0	1	1
298	0	34.51888	3.52	0	0	0	0		0	72	2	10,16	0	10	0	16	2	0
299	0	36.168	2.64	1	1	0	0		0	53	2	11	0	0	11	0	1	1
300	0	32.60224	3.08	0	0	0	0		0	54	2	16	0	0	0	16	1	1
301	0	36.84032	3.37656	0	0	0	0		0	0	1	16	0	0	0	16	1	0
302	0	0	0	0	0	0	0		0	0	0	16	0	0	0	16	1	0
303	0	38.8168	2.9084	0	0	0	0		0	49.33333	1	16	0	0	0	16	1	0
304	0	0	0	0	0	0	0		0	0	0	16	1	0	0	16	1	0
305	0	33.7304	3.03512	18	0	0	0		0	57.33333	2	0	0	0	0	0	1	0
306	0	22.56672	3.256	0	0	0	0		0	31	2	16	0	0	0	16	1	0
307	0	31.87712	2.816	18	0	0	0		0	39.33333	1	0	0	0	0	0	1	0
308	0	31.35176	3.168	0	1	5	0		0	77	2	11	0	0	11	0	1	0
309	0	28.63168	2.8204	0	19	0	0		0	46	1	0	0	0	0	0	1	3
310	0	32.46936	3.696	0	0	0	0		0	0	2	10,16	0	10	0	16	2	0
311	0	38.368	3.432	0	0	0	0		0	42.66667	1	16	0	0	0	16	1	0
312	0	33.53328	2.64	1	1	0	0		0	40.33333	1	11	0	0	11	0	1	1
313	0	34.02432	3.16976	0	0	0	0		0	44	1	9,16	0	9	0	16	1	0
314	0	34.38336	4.224	1	1	0	0		0	46.66667	1	11	0	0	11	0	1	1

315	1	37.34104	2.376	0	0	0	0		0	0	0	16	1	0	0	16	1	0
316	0	29.09984	2.99552	0	0	0	0		0	37.33333	1	10,16	0	10	0	16	1	0
317	0	35.62768	3.08	18	0	5	0		0	44.66667	1	0	0	0	0	0	1	0
318	0	0	0	0	0	0	0		0	0	1	16	0	0	0	16	1	1
319	0	29.3876	3.08	1	1	0	0		0	42.33333	1	11	0	0	11	0	1	3
320	0	28.66424	2.64	18	0	0	0		0	59.33333	2	9	0	9	0	0	2	0
321	0	34.42736	3.52	0	19	0	8		0	53	1	17	0	0	0	17	1	1
322	0	37.3472	3.94416	18	0	0	0		0	36.66667	1	0	0	0	0	0	1	1
323	0	32.08128	2.64	0	0	0	0		0	74.66667	2	10,16	0	10	0	16	1	3
324	0	29.04	3.168	0	0	0	0		0	0	0	1,16	1	0	0	16	1	1
325	0	34.46344	3.168	18	0	0	0		0	38.66667	1	0	0	10	0	0	2	1
326	5	37.25832	3.256	18	0	0	0		0	0	0	0	0	0	0	0	2	0
327	0	31.6404	2.464	0	0	0	0		0	43	1	16	0	0	0	16	1	1
328	0	33.08976	2.904	0	0	0	0		0	0	1	16	0	0	0	16	2	1
329	0	36.26568	3.696	0	0	0	0		0	45	1	9,16	0	9	0	16	1	1
330	0	30.92408	3.256	18	0	5	0		0	41.33333	2	0	0	0	0	0	1	1
331	0	34.17128	3.784	0	0	0	0		0	69.33333	2	16	0	0	0	16	1	3
332	0	27.48416	3.168	0	0	0	0		0	65.33333	2	17,16	0	0	0	16	1	1
333	0	24.024	3.168	1	1	0	0		0	65.66667	2	11	0	0	11	17	1	1
334	0	34.10352	3.608	0	0	0	0		0	0	2	16	0	0	0	16	1	1
335	0	31.51368	2.64	1	1	0	0		0	49.33333	1	11	0	0	11	0	1	1
336	0	37.74056	3.168	0	0	0	0		0	42.33333	2	16	0	0	16	16	1	0
337	5	26.95176	3.168	0	19	0	0		0	0	0	0	0	0	0	0	1	1
338	0	29.23008	2.464	0	0	0	0		0	44	1	16	0	9	0	16	1	1
339	0	38.85288	3.696	0	0	0	0		0	0	0	16	0	0	0	16	1	0
340	0	31.40896	3.256	0	0	0	0		0	48.33333	0	16	0	0	0	16	1	1
341	0	33.21824	2.64	0	0	0	0		0	50.66667	1	16	0	0	0	16	1	0
342	0	37.22664	2.64	0	0	0	0		0	84.33333	2	16	0	0	0	16	1	1
343	0	20.4116	2.464	18	0	0	0		0	55.33333	2	0	0	0	0	0	1	0
344	0	28.88776	2.64	0	0	0	0		0	46.66667	1	16	0	0	0	16	1	1
345	0	25.61064	2.376	0	0	0	0		0	32.66667	1	17,16	0	0	0	16	1	1
346	0	38.76488	3.256	0	19	0	0		0	44	1	0	0	0	0	17	1	1
347	0	24.8644	3.608	0	0	0	0		0	55	1	16	0	0	0	16	1	0
348	0	33.98912	3.168	0	19	0	0		0	43.66667	1	0	0	0	0	0	1	3
349	0	33.44616	3.256	0	19	0	0		0	42.66667	1	0	2	0	0	0	2	0
350	0	26.664	2.904	0	19	0	0		0	0	0	1	1	0	0	0	1	3
351	0	28.17496	2.816	18	0	0	0		0	59.66667	2	0	0	0	0	0	1	0
352	0	40.04704	3.696	0	0	0	0		0	43.33333	1	16	0	0	0	16	1	0
353	0	37.048	0	0	0	0	0		0	62	2	9,16	0	9	0	16	1	0
354	0	40.84872	3.784	18	0	0	0		0	39.33333	1	0	0	0	0	0	1	1
355	0	43.3136	3.6212	0	0	0	0		0	0	0	16	0	0	0	16	1	0
356	0	43.5028	3.608	0	19	0	0		0	58.66667	2	0	0	0	0	0	1	1
357	0	32.95952	2.728	0	19	0	0		0	48	1	0	0	0	0	0	1	0
358	0	41.01152	3.696	0	0	0	0		0	41.33333	1	16	0	0	0	16	1	0
359	0	33.66088	2.904	0	0	0	0		0	37.33333	1	16	0	0	0	16	1	0
360	0	34.07448	3.168	0	0	0	0		0	60.66667	2	16	0	0	0	16	1	0
361	0	0	2.64	0	19	0	0		7	0	2	0	0	0	0	17	2	0
362	0	35.87408	2.64	0	0	0	0		0	48.66667	2	17,16	0	0	0	16	1	0
363	0	26.78104	2.64	0	0	0	0		0	57.66667	1	16	0	0	0	16	2	0
364	0	0	0	0	0	0	0		0	0	0	16	0	0	0	16	1	3
365	0	36.08352	3.344	0	0	0	0		0	0	0	2,16	2	0	0	16	2	0
366	0	26.4264	2.376	0	0	0	0		0	36.66667	1	17,16	0	0	0	16	1	0
367	0	27.456	0	0	0	0	0		0	54.66667	1	16	0	0	0	16	1	1
368	0	24.94008	3.08	18	0	0	0		0	73.33333	2	0	0	0	0	17	1	0
369	0	31.77064	3.344	0	0	0	0		0	95	2	16	0	0	0	16	1	0
370	0	34.06392	3.96	0	19	0	0		0	47.33333	1	0	0	0	0	0	1	0
371	0	36.49976	3.344	0	19	0	0		0	40.33333	1	0	0	0	0	0	1	0
372	0	31.5524	3.168	1	1	0	0		0	51.66667	2	9,11	0	9	11	0	1	3
373	0	33.154	2.64	1	1	0	0		0	50.33333	2	11	0	0	11	0	1	1
374	0	34.16424	2.464	0	19	0	0		0	51.66667	2	0	0	0	0	0	1	0
375	0	37.2196	3.168	0	0	0	0		0	33	1	16	0	0	0	16	1	0
376	0	35.90312	2.992	1	1	0	0		0	40	1	11	0	0	11	0	1	0
377	0	34.34024	3.696	0	0	0	0		0	44.33333	1	16	0	0	0	16	1	0
378	0	27.104	2.904	1	1	0	0		0	29	1	11	0	0	11	0	1	0
379	0	33.792	3.256	0	0	0	0		0	42	1	16	0	0	0	16	1	0
380	0	33.14784	3.52	0	19	0	0		0	34.33333	1	0	0	0	0	0	1	0
381	0	0	2.904	0	0	0	0		0	0	0	16	0	0	0	16	1	1
382	0	20.91496	3.168	0	0	0	0		0	0	2	16	0	0	0	16	2	0
383	0	0	0	0	0	0	0		0	0	0	16	0	10	0	16	2	3
384	0	40.09984	2.904	1	1	0	0		0	38.66667	1	11	0	0	11	0	1	0
385	0	34.66144	3.256	18	0	5	0		0	31.66667	1	0	0	0	0	0	1	1
386	0	35.552	2.904	1	1	0	0		0	60.33333	2	11	0	0	11	0	1	0
387	0	34.41592	3.17416	18	0	0	0		0	43	1	0	0	0	0	0	1	0
388	0	27.434	1.848	18	0	0	0		0	57	2	9	0	9	0	0	1	1
389	0	23.43264	2.816	18	0	0	0		0	50.66667	2	0	0	0	0	0	1	1
390	0	29.7748	3.608	0	0	0	0		0	48.66667	1	16	0	0	0	16	1	1
391	0	37.25744	3.432	18	0	0	0		0	28	1	0	0	0	0	0	1	0
392	0	41.9892	3.432	0	19	0	0		0	67	2	0	0	0	0	0	1	3
393	0	31.8824	3.168	18	0	0	0		0	50.66667	2	0	0	0	0	0	1	1
394	0	0	0	0	19	0	0		0	0	0	1	1	0	0	0	1	0
395	0	0	0	0	0	0	0		0	0	0	9,16	0	9	0	16	1	1
396	0	28.248	2.904	0	0	0	0		0	48	1	17,16	0	0	0	16	2	3
397	0	29.32072	2.64	18	0	0	0		0	41.33333	1	0	0	0	0	17	1	3
398	0	31.67824	2.64	0	0	0	0		0	62.66667	2	16	0	0	0	16	1	1
399	0	23.10616	3.61152	0	19	0	0		0	70.33333	2	0	0	0	0	17	1	3
400	0	0	0	0	0	0	0		0	0	2	17,16	0	9	0	16	1	1
401	0	30.448	3.696	0	0	0	0		0	36	2	16	0	0	0	16	1	1
402	0	34.20208	3.256	0	0	0	0		0	74.33333	2	10,16	0	10	0	16	1	1
403	0	36.93536	3.344	0	19	0	0		0	45.33333	1	10	0	10	0	0	2	0
404	0	39.35272	3.168	0	19	0	0		0	36.66667	1	0	0	0	0	17	1	0
405	0	31.77064	3.168	0	0	0	0		0	60.33333	1	17,16	0	0	0	16	1	0
406	0	31.58672	2.64	0	0	0	0		0	45	1	9,16	0	9	0	16	1	1
407	0	0	0	0	0	0	0		0	0	0	16	0	0	0	16	1	1
408	0	39.5384	2.64	0	0	0	0		0	75.33333	2	16	0	0	0	16	1	3
409	0	30.86336	3.168	18	0	0	0		0	33.66667	1	0	0	0	0	0	1	0
410	0	35.73592	3.168	0	0	0	0		0	41	1	16	0	0	0	16	1	0
411	0	33.23584	2.64	18	0	0	0		0	45.66667	1	0	0	0	0	0	1	0
412	0	31.61576	2.64	0	19	0	0		0	41.66667	1	0	0	0	0	0	1	1
413	0	42.30072	3.52	1	1	0	0		0	37.66667	1	11	0	0	11	0	1	0
414	0	35.44992	3.52	0	0	0	0		0	38.33333	1	16	0	0	0	16	1	0

415	0	0	0	18	0	0	0		0	76	2	0	0	9	0	0	1	0
416	0	31.84016	3.96	1	1	0	0		0	59.66667	2	11	0	0	11	0	1	1
417	0	25.75936	2.552	1	1	0	0		0	45.33333	1	11	0	0	11	0	1	0
418	0	33.39864	3.432	0	0	0	0		0	86	2	16	0	0	0	16	1	0
419	0	35.57576	3.344	0	0	0	0		0	88	2	16	0	0	0	16	1	1
420	0	33.42064	3.256	0	0	0	0		0	77.66667	2	16	0	0	0	16	1	0
421	0	28.38	2.112	0	19	0	0		0	52.66667	1	9	0	9	0	0	1	0
422	0	0	0	0	0	0	0		0	0	0	16	0	0	0	16	1	0
423	0	30.34768	3.168	0	0	0	0		0	0	0	1,16	2	0	0	16	1	0
424	0	32.58464	3.168	1	1	0	0		0	44.33333	1	11	0	0	11	0	1	0
425	0	31.00504	3.344	1	1	0	0		0	30	1	11	0	0	11	0	1	0
426	0	37.84528	3.168	0	0	0	0		0	48	1	16	0	0	0	16	1	0
427	3	24.49128	2.728	0	0	0	0		0	41	1	16	0	0	0	16	1	3
428	0	31.76008	2.64	0	0	0	0		0	73.66667	2	16	0	0	0	16	2	1
429	0	31.64744	3.696	0	0	0	0		0	47.33333	1	10,16	0	10	0	16	1	0
430	0	32.82136	2.816	0	0	0	0		0	48	1	16	0	0	0	16	1	1
431	0	28.314	2.112	0	0	0	0		0	50.33333	1	16	0	0	0	16	1	0
432	0	27.88896	2.64	1	1	0	0		0	46	1	11	0	0	11	0	1	1
433	0	28.84464	2.8204	18	0	0	0		0	34.33333	1	0	0	0	0	0	1	0
434	0	32.61896	2.904	18	0	0	0		0	45.33333	1	0	0	0	0	0	1	1
435	0	24.54672	3.52	1	1	0	0		0	43.66667	1	11	0	0	11	0	1	0
436	0	35.50976	3.168	0	0	0	0		0	47.33333	1	16	0	0	0	16	1	0
437	0	33.64328	3.344	1	1	0	0		0	45	1	11	0	0	11	0	1	1
438	0	32.52744	3.08	0	19	0	0		0	61.66667	2	0	0	0	0	0	1	0
439	0	23.69752	2.376	1	1	0	0		0	47.66667	1	11	0	0	11	0	1	0
440	0	22.59576	1.848	0	1	0	0		0	42	1	16	0	0	0	16	1	1
441	0	30.20072	2.376	1	1	0	0		0	39.33333	1	11	0	0	11	0	1	0
442	0	22.24816	2.112	1	1	0	0		0	44.66667	1	11	0	0	11	0	1	0
443	0	24.376	0	0	0	0	0		0	0	2	16	1	0	0	16	1	0
444	0	0	0	0	0	0	0		0	0	0	16	0	0	0	16	1	0
445	0	21.33648	2.112	0	0	0	0		0	0	0	10,16	2	0	0	16	1	0
446	0	0	3.96	0	0	0	0		0	0	0	16	0	0	0	16	1	1
447	0	0	2.64	0	19	0	0		0	71.66667	2	0	0	0	0	0	1	1
448	0	32.12088	3.168	18	0	0	0		0	37.66667	1	0	0	0	0	0	1	0
449	0	28.60088	3.52	0	0	0	0		0	46.33333	1	16	0	0	0	16	1	0
450	0	21.83984	3.256	0	19	0	0		0	38.66667	1	0	0	0	0	0	1	0
451	0	36.92392	3.168	1	1	0	0		0	34.33333	1	11	0	0	11	0	1	1
452	0	22.57728	2.376	0	0	0	0		0	34.66667	1	16	0	0	0	16	1	0
453	0	34.79872	3.608	0	19	0	0		0	0	2	0	2	0	0	0	1	0
454	0	43.648	2.64	1	1	0	0		0	37.33333	1	11	0	0	11	0	1	0
455	0	33.3608	3.168	1	1	0	0		0	49	1	11	0	0	11	0	1	0
456	0	27.12512	3.256	1	1	0	0		0	49.66667	2	11	0	0	11	0	1	0
457	0	33.54208	3.168	1	1	0	0		0	39	1	11	0	0	11	0	1	0
458	0	27.46656	3.52	0	0	0	0		0	41.66667	1	16	0	0	0	16	1	0
459	0	0	0	0	0	0	0		0	30.66667	1	16	0	0	0	16	1	0
460	0	39.9124	2.64	0	19	0	0		0	61.33333	2	0	0	0	0	0	1	0
461	0	29.0444	2.904	0	0	0	0		0	65	2	16	0	0	0	16	1	0
462	0	21.49664	2.376	0	0	0	0		0	37.66667	1	16	0	0	0	16	1	0
463	0	0	0	0	19	0	0		0	38.33333	1	0	0	0	0	0	1	1
464	0	29.4404	3.256	0	0	0	0		0	74.66667	2	16	0	10	0	16	1	0
465	0	20.41864	1.32	0	0	0	0		0	41.33333	1	9,16	0	9	0	16	1	0
466	0	22.25608	2.728	1	1	0	0		0	62	2	11	0	0	11	0	1	1
467	0	38.91184	3.696	0	19	0	0		0	36.66667	1	0	0	0	0	0	1	1
468	0	22.58256	2.288	18	0	0	0		0	35.33333	1	0	0	0	0	0	1	0
469	0	32.50192	3.696	0	0	0	0		0	44.33333	2	16	0	0	0	16	1	0
470	0	43.29336	3.256	1	1	0	0		0	31.33333	1	11	0	0	11	0	1	0
471	0	28.29464	3.344	0	0	0	0		0	42.33333	1	16	0	0	0	16	1	1
472	0	33.7436	4.224	18	0	0	0		0	29.33333	1	0	0	0	0	0	1	3
473	0	30.75776	3.08	18	0	0	0		0	40.66667	1	0	0	0	0	0	1	0
474	0	45.5268	4.4	0	19	0	8		0	54	2	0	0	0	0	0	1	1
475	0	41.97688	2.992	0	0	0	0		0	53.66667	2	16	0	0	0	16	1	0
476	0	26.136	3.256	0	0	0	0		0	50.33333	2	16	0	0	0	16	1	1
477	0	41.18576	3.256	0	0	0	0		0	31.33333	1	16	0	0	0	16	1	0
478	0	36.19176	3.432	0	0	0	0		0	41	1	16	0	0	0	16	1	1
479	0	32.6876	3.168	0	0	0	0		0	0	1	16	0	0	0	16	1	0
480	0	27.49384	3.52	0	0	0	0		0	53.66667	1	10,16	0	10	0	16	1	1
481	0	36.52	2.93568	0	0	0	0		0	0	0	1,16	1	0	0	16	1	1
482	0	26.74584	3.432	0	0	0	0		0	38	1	16	0	0	0	16	1	1
483	0	36.74616	3.344	0	19	0	0		0	29.66667	1	0	0	0	0	0	2	0
484	0	32.6788	3.696	0	0	0	0		0	34.66667	1	16	0	0	0	16	1	1
485	5	26.94296	2.64	0	0	0	0		0	38	1	16	0	0	0	16	1	1
486	0	30.31776	3.08	0	19	0	0		0	34.33333	1	0	0	0	0	0	1	1
487	0	45.936	3.432	18	0	0	0		0	0	0	2	2	0	0	0	1	0
488	0	37.488	3.432	0	0	0	0		0	37	1	16	0	0	0	16	1	0
489	0	36.696	2.64	0	0	0	0		0	0	0	16	0	0	0	16	1	1
490	0	28.6	0.792	0	0	0	0		0	55.66667	0	16	0	0	0	16	1	1
491	0	0	3.608	0	0	0	0		0	0	0	16	0	0	0	16	1	0
492	0	26.488	3.168	0	0	0	0		0	46.66667	1	16	0	0	0	16	1	1
493	0	0	2.376	0	0	0	0		0	37.33333	1	16	0	0	0	16	1	1
494	0	27.192	2.464	0	19	0	0		0	37.66667	1	0	0	0	0	0	1	1
495	0	26.928	3.168	0	0	0	0		0	0	0	16	0	0	0	16	1	0
496	0	23.672	3.168	18	0	0	0		0	30	1	0	0	0	0	0	1	0
497	0	0	0	0	0	0	0		0	0	0	1,16	1	0	0	16	1	1
498	0	36.608	2.992	0	0	0	0		0	0	0	16	2	0	0	16	1	0
499	0	30.624	2.728	0	19	0	0		0	59	2	9	0	9	0	0	1	0
500	0	35.88992	3.52	0	0	0	0		0	37.33333	1	16	0	0	0	16	1	0
501	0	42.8164	3.168	0	19	0	0		0	55.33333	2	0	0	0	0	0	1	0
502	0	36.14864	3.696	0	19	0	0		0	46.66667	1	10	0	10	0	0	1	1
503	0	36.4144	3.432	1	1	0	0		0	48	2	11	0	0	11	0	1	0
504	0	40.568	4.312	0	19	0	0		0	55	2	19	0	0	0	0	1	1
505	0	29.49848	3.168	0	0	0	0		0	42.66667	2	16	0	0	0	16	1	0
506	0	28.18904	3.432	0	0	0	0		0	59.66667	2	10,16	0	10	0	16	1	1
507	0	34.12112	3.256	0	0	0	0		0	47.66667	1	16	0	0	0	16	1	0
508	0	32.06192	2.904	0	0	0	0		0	0	1	16	0	0	0	16	1	0
509	0	33.176	3.168	18	0	5	0		0	56.66667	2	0	0	0	0	0	1	1
510	0	37.488	4.752	0	0	0	0		0	0	0	16	0	0	0	16	1	0
511	0	38.55984	3.696	1	1	0	0		0	59.33333	1	10,11	0	10	11	0	1	0
512	0	24.84416	2.64	0	0	0	0		0	69.66667	2	16	0	0	0	16	1	0
513	0	0	0	0	0	0	0		0	0	0	16	0	0	0	16	1	0
514	0	32.64976	3.168	0	0	0	0		0	50.66667	1	16	0	0	0	16	1	0

515	0	37.27152	3.432	0	0	0	0		0	0	0	1,16	1	0	0	16	1	0
516	0	33.62568	3.344	0	0	0	0		0	37	1	16	0	0	0	16	1	0
517	0	32.98768	3.344	0	0	0	0		0	41.33333	1	16	0	0	0	16	1	0
518	0	0	0	0	0	0	0		0	0	0	16	0	0	0	16	1	1
519	0	31.65624	3.168	0	0	0	0		0	38	1	16	0	0	0	16	1	0
520	0	46.1648	4.224	0	0	0	0		0	38.33333	1	16	0	0	0	16	1	0
521	0	31.4864	2.816	0	19	0	0		0	22.33333	1	0	0	0	0	0	1	3
522	0	29.43336	3.432	1	1	0	0		0	63.33333	2	11	0	0	11	0	1	0
523	0	38.17352	3.52	0	0	0	0		0	56.33333	2	16	0	0	0	16	1	1
524	0	36.83856	2.376	0	0	0	0		0	37.66667	1	16	0	0	0	16	1	1
525	0	26.50208	3.08	0	0	0	0		0	41.66667	1	16	0	0	0	16	1	1
526	0	0	3.696	0	0	0	0		0	0	0	16	0	0	0	16	1	1
527	0	43.77736	3.168	0	0	0	0		0	41.33333	1	16	0	0	0	16	1	0
528	0	23.46696	3.168	0	0	0	0		0	46	1	16	0	0	0	16	1	0
529	0	28.87632	3.168	0	0	0	0		0	36.33333	0	16	0	0	0	16	1	0
530	0	39.20664	3.696	0	19	0	0		0	76	2	0	0	0	0	0	1	0
531	0	27.97784	2.904	0	19	0	0		0	52.66667	2	0	0	0	0	0	1	0
532	0	38.808	3.168	0	0	0	0		0	0	1	16	0	0	0	16	1	0
533	0	27.8476	2.64	0	0	0	0		0	38.66667	2	16	0	0	0	16	1	0
534	0	0	2.376	0	0	0	0		0	0	0	16	0	0	0	16	1	0
535	0	0	0	0	0	0	0		0	0	0	16	0	0	0	16	1	0
536	0	36.86584	3.168	0	19	0	0		0	50	1	0	0	0	0	0	1	0
537	0	38.786	3.168	18	0	0	0		0	63.66667	2	0	0	0	0	0	1	0
538	0	0	0	0	0	0	0		0	39	2	16	0	0	0	16	1	0
539	0	38.61352	2.112	0	0	0	0		0	49.66667	2	9,16	0	9	0	16	1	1
540	0	26.928	3.168	0	0	0	0		0	60.33333	2	16	0	0	0	16	1	0
541	0	0	2.64	18	0	0	0		0	54	1	0	0	0	0	0	1	0
542	0	37.07704	3.168	18	0	0	0		0	51.33333	2	0	0	0	0	0	1	0
543	0	29.30312	3.08	0	0	0	0		0	47.66667	1	16	0	0	0	16	1	0
544	0	39.49	3.608	0	19	0	0		0	44.33333	1	0	0	0	0	0	1	1
545	0	32.6964	3.168	1	1	0	0		0	49	1	11	0	0	11	0	1	1
546	0	36.7752	3.168	1	1	0	0		0	50.33333	1	11	0	0	11	0	1	0
547	0	39.53576	3.256	1	1	0	0		0	36.33333	1	11	0	0	11	0	1	0
548	0	30.64688	2.64	0	0	0	0		0	37.66667	2	16	0	0	0	16	1	0
549	0	36.15392	4.224	0	19	0	0		0	37.66667	1	0	0	0	0	0	1	0
550	0	0	3.256	0	0	0	0		0	0	0	16	0	0	0	16	1	0
551	0	22.92928	3.168	0	19	0	0		0	0	0	1	1	0	0	0	1	4
552	0	34.34992	3.432	0	19	0	0		0	56.33333	2	10	0	10	0	0	2	0
553	0	33.88	3.432	0	0	0	0		0	55.33333	2	16	0	0	0	16	1	1
554	0	27.58008	2.904	0	0	0	0		0	31.33333	1	16	0	10	0	16	1	0

SN	V1LL	V1DL	ELL	V2LL	PTV2L	V2DL	V3VL	V3VDL	V3HL	V3HDL	V3OL	V3ODL	V3PLL	V3DLL	PTV4L	V4LL	V4DL	VAD0.3
1	27.37328	3.608	2	57.816	0	3.432	19.272	3.432	8.184	3.52	5.544	3.168	62.66667	56.33333	0	33.88	3.08	0.35
2	45.13432	4.752	2	70.488	1	4.576	29.128	4.136	7.656	4.752	8.2456	4.48976	89	69.33333	0	30.66624	3.96	1.32
3	39.7276	4.84	1	69.96	3	4.664	32.736	3.96	9.504	4.4	5.6936	4.00312	83.33333	88.66667	0	24.02928	4.136	0.97
4	50.14592	3.96	2	73.14296	0	5.192	36.168	4.664	10.56	5.104	5.016	4.36128	58.66667	51.66667	0	22.57112	3.784	1.06
5	49.4824	5.632	2	75.68264	0	5.016	24.728	4.048	8.28432	4.4	5.85904	4.10432	94	81	0	25.872	3.696	0.79
6	37.29528	2.992	2	64.76888	0	3.168	37.928	2.552	9.48728	3.168	4.62968	3.344	103	88	0	128.6366	2.376	0.53
7	41.08984	4.928	2	62.5944	0	4.84	32.65592	4.136	7.45976	4.4	4.54608	4.11928	43.66667	52.66667	0	25.872	3.872	0.35
8	89.32792	3.52	3	53.592	0	3.432	28.44248	2.992	6.49352	3.43552	3.82096	3.24632	69.66667	67	0	24.024	2.728	0.53
9	37.224	2.464	2	58.10112	0	2.376	21.912	2.112	4.60856	2.376	3.25864	2.728	102	71	0	32.912	1.848	0.09
10	39.072	4.576	2	76.736	0	4.576	34.79256	4.4	4.7344	4.136	4.16152	3.344	118.6667	50.66667	0	32.824	3.432	0.88
11	69.78488	4.488	3	45.34552	0	4.224	25.78664	3.784	8.58176	4.312	4.70008	4.30496	95	86	0	40.52664	3.872	0.35
12	37.77136	4.224	2	58.01752	3	3.96	22.98032	3.608	6.80944	4.224	5.54136	3.94328	83	76	0	25.94416	3.608	0.62
13	28.53928	4.752	2	67.40888	1	4.84	31.5568	4.84	6.96344	5.896	5.65576	4.752	46.33333	50.33333	0	25.872	4.136	1.76
14	44.80608	4.488	2	58.90896	0	4.576	31.2576	4.4	8.80792	5.28	5.6408	4.752	49.33333	79	0	30.20776	3.256	0.17
15	34.91752	4.224	2	58.99608	0	4.4	29.09016	4.224	8.71992	4.4	4.99488	3.80248	55.66667	52.33333	0	30.70496	3.344	0.18
16	47.88432	5.632	2	62.87336	1	5.104	34.52416	4.928	3.43816	5.544	4.61648	6.01568	65	85.66667	0	31.32712	3.432	1.05
17	51.98864	3.872	2	62.11656	0	3.872	24.81688	3.696	8.35208	4.224	5.81504	4.67456	92	68.33333	0	27.51232	3.06944	0.18
18	39.864	3.96	3	69.36776	4	3.872	17.45744	4.136	7.436	4.4	5.77104	4.664	75.66667	45.66667	3	36.68984	3.96	0.7
19	61.18376	4.4	2	68.90576	0	4.136	38.89336	3.784	6.2964	4.136	5.23248	4.12192	63.33333	67.66667	0	27.57744	3.432	0.26
20	45.848	4.752	2	59.75376	0	4.4	32.82928	4.048	6.70032	4.928	4.82592	4.6904	73.66667	73.66667	0	25.37744	3.696	0.71
21	55.8756	7.92	2	82.104	1	7.656	48.67016	7.04	7.46944	7.92	5.6232	6.952	106.6667	105.3333	0	27.72	6.688	3.87
22	43.384	4.84	2	71.19376	0	4.488	40.66304	3.96	5.94	3.27536	5.88456	3.14424	82.66667	115	0	40.744	3.696	1.58
23	32.64184	3.696	2	68.4068	0	3.872	35.31616	3.608	7.47912	4.048	5.1656	3.6784	53	56.33333	0	26.4	3.608	0
24	39.83408	6.072	2	57.41472	0	4.84	39.82352	4.84	9.02528	4.928	5.74464	4.664	88	55.66667	0	34.42648	3.432	1.05
25	43.39192	4.136	2	63.97688	0	4.312	29.7	4.224	8.1136	4.312	5.22016	5.192	116	88.33333	0	34.41064	3.432	0
26	91.97144	4.4	2	76.39016	0	4.576	43.84776	4.576	8.07752	4.664	4.8752	4.928	87.66667	62.33333	0	24.376	4.4	0.53
27	29.09808	3.784	2	60.6012	1	3.784	37.89984	3.696	9.02352	3.872	5.6628	3.696	67.33333	78.33333	3	36.50856	3.52	0.88
28	28.72584	2.992	2	41.45592	0	2.904	17.864	2.64	4.1228	2.992	3.6256	3.168	78.66667	64.66667	0	21.79144	2.64	0.18
29	33.616	4.312	2	57.55552	1	4.224	31.50224	4.312	9.11328	4.4	5.8828	4.30144	44	53.66667	0	28.72672	3.696	0.61
30	53.33152	5.192	2	76.1728	0	5.368	38.22984	5.368	8.61256	5.016	5.27032	6.072	45.33333	59.33333	0	28.03064	3.696	2.2
31	45.936	4.84	2	80.81832	0	4.84	39.20048	4.664	9.42128	5.28	5.54224	4.84616	80.33333	81.66667	0	29.568	3.432	1.67
32	40.27408	4.928	2	67.29008	0	4.84	34.20032	3.96	9.64216	4.664	4.42992	3.97848	43.33333	42.66667	0	31.52336	3.96	1.76
33	40.39288	3.52	2	58.5156	1	3.52	36.36864	3.08	7.45272	3.08	5.22896	3.344	63	63.33333	3	32.38488	2.904	0.35
34	39.55688	4.4	2	71.10576	1	4.224	36.29384	3.872	8.58088	4.488	5.98928	4.09728	60	58.33333	0	39.91592	3.344	0.97
35	44.28248	3.344	2	54.4456	3	3.08	23.62184	3.168	5.96376	3.344	4.8752	3.696	46.33333	67.33333	0	20.064	2.64	0.44
36	44.25872	4.312	2	74.07312	1	4.312	42.50576	3.872	8.62928	3.784	5.74288	5.0424	84.33333	68.66667	0	20.34208	3.256	1.94
37	NA	NA	2	NA	0	NA	NA	NA	NA	NA	NA	NA	NA	NA	NA	NA	NA	
38	45.14488	4.488	2	67.7688	1	3.96	32.0716	3.96	9.39752	4.048	4.97464	4.01984	101.6667	67.66667	0	27.30816	3.168	0.53
39	25.52968	3.608	2	39.18464	0	3.52	25.76464	3.432	5.13216	2.992	4.07704	3.08	45.33333	91.66667	0	23.35784	2.376	0.27
40	42.15376	6.864	2	72.33952	0	6.512	NA	NA	NA	NA	NA	NA	NA	NA	0	36.29824	5.104	2.64
41	48.80832	3.96	2	63.096	0	4.048	32.33208	3.96	8.27024	3.96	4.35864	5.07584	78	79.33333	0	21.58904	3.168	0.18
42	33.93016	4.928	2	54.428	0	4.224	38.39352	3.432	8.20688	4.136	5.14096	4.12456	76.66667	67.66667	0	32.3356	2.552	0.71
43	37.13688	3.168	2	62.59264	1	2.992	23.01464	2.904	5.96552	2.904	3.75144	2.464	91	76.66667	0	37.76696	2.64	0.44
44	48.32784	5.28	2	72.96608	0	4.752	22.30272	4.488	NA	NA	NA	NA	48.33333	50	0	23.056	4.048	2.02
45	42.328	4.312	2	57.0284	0	4.136	31.50752	3.96	13.50712	4.488	5.13744	4.488	86	81.33333	0	#DIV/0!	3.696	0.79
46	34.12904	4.488	2	75.85952	1	4.048	50.51024	4.224	10.23528	4.488	8.22096	4.488	71.66667	81	1	39.76632	4.4	0.62
47	61.77688	4.136	3	41.21216	0	3.52	23.496	3.608	7.79504	3.608	6.754	3.432	71.66667	71.33333	0	33.51744	3.344	0.62
48	47.95648	4.224	2	59.68952	0	4.136	35.70336	3.432	10.10416	3.96	5.73232	3.6608	43.33333	51	0	21.57144	3.432	0.26
49	48.70008	5.896	2	59.55488	0	5.808	33.74272	5.808	11.98472	5.456	5.4912	4.67984	57.33333	47	0	29.77832	5.104	1.5
50	36.94328	4.928	2	64.89472	0	5.28	40.92264	4.576	9.6624	4.84	4.61912	5.04064	64.33333	62.33333	0	28.6088	4.84	0.27
51	23.7908	6.16	2	71.71912	3	5.54576	36.344	6.248	10.92344	6.248	5.39528	5.104	37.33333	41.66667	0	29.12184	4.224	1.76
52	37.24336	3.784	2	65.02672	0	3.608	30.53336	3.52	6.42488	3.872	4.5892	3.784	50	77	0	33.93896	2.816	1.05
53	40.2644	4.576	2	56.55232	0	4.488	20.54536	4.224	6.65896	4.488	4.83208	4.048	64	60.66667	0	35.45168	3.784	1.94
54	46.11288	4.312	2	73.79944	3	4.488	31.328	3.784	10.01968	4.312	5.32576	4.09376	46.66667	49.66667	0	21.12	3.432	0.61
55	36.22432	3.608	2	58.43904	0	3.256	28.22072	3.432	8.66712	3.872	4.68776	3.608	42.66667	63	0	28.77248	3.256	0
56	41.27024	3.344	2	71.81152	0	3.08	31.966	2.816	8.5844	3.696	4.8268	3.784	93.66667	75.33333	0	32.95776	3.08	0.36
57	43.98856	3.872	2	67.62712	0	3.696	33.33968	3.872	8.11448	3.96	5.43224	3.71184	59.66667	52.66667	0	33.00528	3.696	0.88
58	37.95176	4.224	2	62.88128	0	3.96	29.9376	3.96	9.09744	3.96	5.15856	4.04008	47.33333	62.33333	0	31.32976	3.52	0.17
59	50.50408	4.488	2	60.56512	0	4.4	31.58584	3.696	9.504	4.224	4.58568	4.224	68	57.33333	0	36.14952	3.432	0.88
60	60.28	4.664	2	71.04328	0	4.488	33.40304	3.784	7.766	5.016	5.104	4.66928	43.66667	47.33333	0	11.8536	2.64	0.88
61	44.35288	2.288	2	52.976	0	2.288	18.8408	2.112	4.66664	2.112	3.2648	2.464	91.33333	87.33333	0	26.56632	1.76	0.79
62	33.7964	3.168	2	45.67464	0	3.168	11.88	2.64	9.09744	2.64	5.15856	4.66928	99.33333	61.33333	0	16.632	2.376	0.44
63	32.296	2.376	2	41.19808	0	2.376	18.33744	2.464	5.66896	2.904	2.99376	2.6796	66	77.33333	0	24.398	2.376	0.79
64	38.192	4.136	2	56.51536	0	3.784	16.57216	3.432	5.37856	4.224	3.54112	3.872	87	72	0	32.296	3.256	0.53
65	48.78368	3.696	2	71.00632	0	3.872	36.3132	3.344	9.11328	3.344	5.37768	3.344	111.6667	61.33333	0	31.15816	2.64	0.79
66	34.40624	4.048	2	48.752	0	4.048	21.22296	3.608	6.66952	4.048	6.36152	3.99256	46.33333	48	0	33.62304	3.168	0.53
67	111.144	3.344	3	46.29064	0	2.904	25.79016	2.904	8.66448	2.904	5.41904	2.904	103.3333	67	0	#DIV/0!	2.376	0.62
68	45.97472	4.224	2	66.01936	0	4.224	35.65144	4.4	12.07272	4.488	5.9928	4.36128	118.3333	74.33333	0	26.68512	4.224	0
69	33.08976	3.784	2	68.46312	0	3.52	23.06392	3.432	10.20624	3.52	7.27144	3.52	98.33333	111.6667	0	24.288	3.256	0.17
70	78.7248	3.696	4	37.3384	0	3.52	32.87152	3.608	9.58848	3.96	6.69328	3.96	45.66667	75	0	32.736	3.168	0.09
71	42.08072	5.456	2	65.824	0	4.224	37.31728	4.224	6.98192	3.96	6.69064	3.96	46.33333	71.66667	0	29.80912	3.168	1.41
72	39.47944	3.344	2	83.23656	0	3.168	31.43272	2.64	7.42016	2.728	6.39936	2.728	93.33333	94	0	24.552	2.64	0.62
73	57.29152	3.96	2	50.39408	0	3.696	26.4	3.432	9.6624	3.96	5.7244	3.93096	97	80.66667	0	25.46104	3.168	0.62
74	60.4912	3.696	2	57.00816	0	3.696	37.36128	3.696	9.0244	3.696	5.49296	3.64584	91.66667	#DIV/0!	0	29.9948	3.432	0.08
75	47.78488	3.52	2	75.74688	0	3.784	35.69192	3.52	9.16256	3.96	5.6936	3.90192	87.33333	108	0	24.024	1.584	0.26
76	51.21864	3.432	2	64.88416	0	3.432	18.74752	3.43816	7.60584	3.608	4.78632	3.32024	102.6667	89.33333	0	30.096	3.168	0.35
77	28.7936	3.784	2	67.4168	0	3.784	28.63696	3.784	10.47552	3.784	5.6188	3.784	84.33333	84.33333	0	29.89448	3.256	0.08
78	41.05992	4.752	2	66.1452	0	4.576	38.72	4.752	9.3324	4.576	5.09256	4.42288	71.33333	82.66667	0	29.07168	4.136	0.7
79	49.28792	3.696	2	69.04744	0	3.608	31.55856	3.168	9.17488	3.784	5.0952	3.784	93.33333	90.66667	0	26.56368	2.992	0.35
80	44.17776	4.048	2	65.3004	0	4.136	35.66464	3.696	10.714	4.224	5.90832	4.00136	69	76	0	30.4348	2.5212	0.44
81	51.89448	4.224	2	61.19696	3	4.048	30.75512	3.432	10.8416	3.96	5.65928	3.96	91	106.3333	0	17.97928	3.432	0.88
82	47.56488	3.608	2	65.55472	0	3.52	37.51968	3.256	9.39928	3.608	4.55136	4.00312	80	89.66667	0	37.752	3.608	0.53
83	37.31552	3.256	2	61.3932	1	3.168	41.10392	3.168	7.17288	3.608	5.41904	3.50856	95.33333	81.33333	0	#DIV/0!	2.904	0
84	48.26888	4.136	2	59.66664	0	4.048	28.63432	3.96	15.02512	4.224	7.25648	4.048	65.33333	77.66667	0	32.91024	3.256	0
85	36.0184	4.048	2	69.784	0	4.136	35.64792	3.784	5.46832	4.048	4.76168	4.312	87.66667	68.33333	0	32.4808	3.96	0.71
86	47.14512	4.928	2	70.2856	0	4.136	26.55576	4.136	12.47224	4.664	5.74464	4.41936	86	91	0	33.26752	3.696	0.97
87	35.24576	3.784	2	65.7668	0	3.784	36.52088	3.872	11.22616	4.048	5.6672	4.47744	52	70.33333	0	33.27544	3.76728	0.36
88	38.58272	4.224	2	53.96072	0	4.048	31.84016	3.432	10.12352	3.81832	4.84704	4.4352	86.66667	77.66667	0	19.47616	4.224	0.79
89	51.10424	4.488	2	65.47816	0	4.4	NA	3.96	NA	NA	NA	0	NA	NA	0	21.912	4.4	1.06
90	44.44968	5.368	2	61.79184	0	4.576	27.78776	4.136	10.43768	4.664	5.23952	4.664	66.66667	68.66667	0	29.09104	3.784	2.38
91	45.02256	3.52	2	61.5604	0	3.256	19.05728	3.256	2.84328	3.608	3.3572	3.73296	90.66667	87.66667	0	31.3324	3.168	0.62
92	43.82576	2.904	2	32.29072	0	2.904	19.35648	2.904	4.93064	2.904	3.2472	3.432	80.33333	100.3333	0	12.408	2.904	1.41
93	28.8992	3.256	2	59.4088	0	3.256	25.24016	3.168	9.16256	3.256	5.16208	3.40384	78.66667	94.33333	0	12.584	2.64	0
94	31.33328	3.52	2	42.306	0	3.344	22.83952	3.344	6.19872	3.608	3.322	3.52	74.33333	66.66667	0	23.54264	2.728	0.53
95	45.30152	4.312	2	73.128	3	3.696	20.89032	3.696	6.75048	4.224	4.5672	4.224	103.3333	69.33333	0	36.46896	3.168	1.23
96	43.30216	3.168	2	37.23456	0	2.64	16.22104	2.112	6.80944	2.112	4.06296	2.2	106	112	0	21.66912	1.672	0
97	45.144	5.456	2	61.688	0	4.84	19.91704	4.84	7.9948	4.84	3.76992	4.84	98.66667	80.66667	0	38.368	3.696	2.82
98	39.776	3.608	2	59.14128	0	3.608	30.78152	3.608	7.97808	3.784	5.4428	3.608	78	64.33333	0	28.39232	2.904	0.26
99	39.70032	3.608	2	65.83544	0	3.872	35.46488	3.696	9.76272	4.752	6.23304	4.576	107	80.33333	0	28.40464	2.816	0.26
100	104.2958	3.432	4	32.57936	0	3.696	28.61848	3.432	8.02824	3.432	5.4032	3.696	89.33333	90.66667	0	27.03008	2.904	0.35
101	34.90696	2.024	2	40.7528	0	2.024	18.74752	2.024	6.12392	2.112	3.86672	2.41384	91.33333	65.66667	0	#DIV/0!	2.112	0.71
102	23.70104	2.992	2	57.03104	0	2.64	26.53728	1.76	8.00536	2.28096	5.63904	3.46984	91.33333	81.33333	0	28.95024	1.672	0.35
103	40.568	5.192	2	65.11208	0	4.576	24.1956	3.784	8.29048	4.312	4.37448	3.696	70.66667	79.33333	0	35.84152	3.96	1.93
104	39.248	4.136	2	62.65688	0	3.784	24.86792	3.872	6.42312	3.784	4.35864	3.88432	98	70.66667	0	35.464	2.992	0.53
105	119.7689	3.872	3	66.00088	0	3.96	NA	3.432	NA	NA	NA	NA	74.33333	NA	0	39.336	3.08	0.44
106	41.98392	3.872	2	60.7288	0	3.608	19.44272	3.432	5.33456	3.784	3.31496	3.784	80	80.33333	0	34.80928	3.432	0.18
107	46.552	3.344	2	60.38912	0	3.08	35.48688	2.904	9.34824	3.168	4.8268	3.168	77.33333	83.33333	0	31.19336	2.376	0
108	39.38616	2.992	2	62.61992	0	2.992	24.03016	2.816	6.776	2.992	#DIV/0!	2.992	84	66.66667	0	37.01368	2.288	1.67
109	33.12056	3.344	2	48.75376	0	2.904	33.6292	3.08	3.26128	2.904	6.65808	2.904	102.3333	96.66667	0	25.19088	2.376	0.26
110	46.55376	3.08	2	62.23976	0	3.168	22.10912	3.08	5.76576	2.64	3.25072	3.168	86	69	0	34.0736	2.552	0.44
111	33.79376	3.432	2	45.30504	0	3.256	20.8868	3.08	6.91328	3.168	4.22576	3.168	81	71.66667	0	36.9028	2.992	0.53
112	34.848	3.168	1	82.45776	1	3.256	24.2088	3.168	5.302	3.168	3.76992	3.168	113.3333	85.33333	4	#DIV/0!	2.64	0.88
113	44.704	2.904	2	59.05416	0	2.728	11.96096	2.376	7.36648	2.112	4.83208	2.024	111	78.66667	0	32.03464	1.056	1.84
114	23.93864	3.344	2	54.99208	1	3.344	26.50384	3.256	9.29368	3.608	7.2908	3.608	84.33333	107.6667	0	36.59656	2.728	0.35

115	51.83464	4.576	2	65.6568	0	4.048	33.88	4.136	9.05432	4.4	6.1864	3.96	94.33333	96.66667	0	30.096	3.256	0.53
116	38.2712	3.784	2	58.6872	0	3.696	28.07904	3.168	5.11984	3.784	4.31904	3.432	65.66667	67.33333	0	30.59408	3.168	0.09
117	37.75992	3.168	2	59.664	0	2.992	21.17808	2.64	6.18552	3.168	3.52792	2.904	96.33333	108.6667	0	28.91416	3.168	0.61
118	37.81624	3.5332	2	66.86592	0	3.784	30.70056	3.344	5.86256	3.96	5.16912	3.96	111.6667	92.66667	0	36.80776	2.904	0.34
119	44.704	3.872	2	53.328	0	3.52	17.16176	3.52	4.02072	3.168	5.00016	3.872	57	65.33333	0	33.79904	2.816	0.44
120	47.256	3.608	2	49.23336	0	3.608	17.95376	3.52	6.7188	3.52	3.84208	3.4012	75	73.33333	0	33.264	3.168	0.35
121	42.504	3.96	2	48.66576	0	3.96	17.07464	3.872	5.41376	3.608	4.03304	3.608	92.66667	76	0	34.45992	3.696	0.26
122	86.06576	3.608	3	39.8684	0	3.344	29.46064	3.168	6.18552	3.696	4.37184	4.224	109	114.6667	0	36.51384	3.168	0.17
123	34.672	4.4	2	61.78128	0	4.136	13.66288	3.96	6.97048	3.96	3.88872	3.608	105.3333	83	0	38.016	3.696	0.88
124	43.56	3.168	2	63.19984	0	3.168	31.48288	2.992	7.4668	2.992	4.422	3.696	73.66667	115.3333	0	34.78376	2.904	0.35
125	32.42624	2.992	2	42.24968	0	2.904	18.06112	2.376	6.996	2.904	2.794	2.80016	81	75	0	23.11672	2.64	0.27
126	31.07368	3.432	2	61.11424	3	3.52	24.1692	3.608	4.6552	3.784	3.24632	3.696	117.6667	78	0	33.704	3.344	0.17
127	78.46872	2.464	4	22.55616	0	2.376	37.87784	2.376	NA	NA	NA	NA	115.6667	NA	0	15.86904	1.056	0.61
128	31.81904	3.432	2	42.57088	0	3.696	25.19528	3.608	9.39136	3.784	3.8192	3.68016	117.6667	80.66667	0	32.34088	3.256	0.18
129	29.6868	3.168	2	60.91096	0	3.168	31.28664	3.168	7.17288	4.224	5.41904	3.696	95.33333	80.33333	0	31.064	2.904	1.14
130	0	0	2	54.1904	0	3.256	26.45808	3.168	7.58384	3.696	3.80952	3.696	76.33333	70.33333	0	14.28944	2.992	
131	37.31552	3.256	2	61.3932	1	3.168	41.10392	3.168	7.17288	3.608	5.41904	3.56048	95.33333	81.33333	0	36.51384	2.904	0
132	NA	NA	2	62.33656	0	4.224	30.77712	3.696	6.70824	4.224	3.78752	3.696	61.66667	76.66667	0	28.69856	3.344	
133	39.46888	3.696	2	61.93	4	3.608	26.2856	3.256	6.72496	3.52	2.794	3.52	63.66667	80.33333	0	26.48184	3.256	0.09
134	43.5952	2.904	1	60.04328	0	3.08	29.13944	2.64	7.4712	2.64	4.3692	2.8996	116.6667	68.66667	0	27.03008	2.464	0.53
135	44.44	5.016	2	68.64	0	4.84	17.68976	4.136	6.18552	3.96	3.29296	3.784	106.3333	94.33333	0	31.064	3.872	1.68
136	22.68728	3.168	2	50.43104	0	3.256	30.24648	3.432	7.26176	4.136	4.12984	3.5508	64	78	0	27.0864	2.552	0.79
137	42.944	3.696	2	51.4976	0	3.696	16.28088	3.608	5.1348	4.048	2.99376	3.92392	108.3333	72.66667	0	29.48	3.696	0.62
138	40.216	4.224	2	67.90608	0	4.048	37.87784	3.696	6.65808	3.52	3.73296	3.696	112	86.33333	0	30.23416	2.904	0.52
139	48.40968	3.432	2	54.912	0	3.432	27.55456	2.904	6.79184	3.432	2.53176	2.992	82	71.33333	0	28.512	2.904	0.09
140	45.76264	5.28	2	67.92192	0	5.192	21.18952	4.752	5.32312	5.896	3.88608	5.896	70	63	0	36.69864	4.928	0.36
141	43.37784	2.728	2	58.05008	0	2.992	13.34608	2.64	4.55664	2.904	3.036	2.904	57.66667	57	0	29.11832	2.64	0.09
142	47.872	3.696	1	66.44	0	3.168	31.85688	3.168	5.84672	3.168	2.28976	3.168	50.33333	62.33333	0	22.4576	2.112	0.61
143	35.992	4.312	2	60.104	0	3.784	31.416	4.048	7.59352	3.872	2.80632	3.696	78	63.33333	0	35.464	3.52	1.23
144	39.61408	4.048	2	66.01232	0	3.696	30.536	3.52	9.37024	4.224	9.69584	3.696	75	69.33333	0	31.70112	3.696	0.18
145	54.30128	4.664	2	65.3004	0	3.96	31.15376	3.432	8.98128	3.872	3.8104	3.696	72.33333	71.66667	0	31.966	2.904	0.18
146	47.85352	3.256	2	52.87832	0	2.904	13.3408	2.64	5.98576	3.344	3.212	3.168	61	64	0	31.58496	3.08	0.36
147	24.0196	3.168	2	44.37048	0	3.872	21.71928	4.224	8.05728	3.696	3.75144	3.696	56	73.33333	0	30.05904	3.256	0.53
148	51.304	3.696	2	69.696	0	3.256	30.184	2.904	9.03672	3.08	2.43408	2.64	90.66667	78.66667	0	21.55912	1.584	0.44
149	44.6512	4.928	2	62.71848	0	4.84	26.97112	3.96	12.74768	4.84	4.51088	3.93008	99.33333	64.33333	0	0	3.608	1.32
150	62.63576	4.224	3	41.4128	0	3.696	26.47656	3.696	7.51608	4.576	3.21464	3.17152	54.66667	59	0	31.42216	3.344	0.71
151	108.768	4.048	3	34.8568	0	4.136	26.4044	3.696	5.126	4.136	4.80128	4.224	78.66667	68.33333	0	35.464	3.608	0.35
152	42.51632	4.048	2	59.90424	0	4.136	29.73872	3.52	10.98944	4.224	5.11984	4.664	80	93.33333	0	33.98912	3.344	0.53
153	NA	NA	2	0	NA	NA	28.776	3.344	4.9368	3.696	3.38184	3.65992	76	68.66667	0	27.53872	3.168	
154	46.11376	4.576	2	55.968	0	4.664	19.9232	3.696	7.02768	4.048	2.74824	4.048	60	70.33333	0	33.44	3.344	1.15
155	51.21864	4.928	2	73.40432	1	4.752	22.62304	3.432	6.40904	5.016	3.38184	4.752	64.33333	64.33333	0	23.8964	3.784	0.26
156	62.76424	3.696	2	61.16	1	3.70832	26.15448	3.168	8.61784	3.608	2.53088	3.52	57.66667	63	0	33.8008	2.992	0.44
157	52.888	5.192	2	77.79464	0	4.664	30.12592	4.136	8.8836	4.664	3.26128	4.224	76	70.33333	0	36.872	4.664	0
158	37.49504	3.608	2	53.152	0	3.608	32.36904	3.696	8.42512	4.048	4.83208	3.96	83	86.33333	0	28.54368	3.608	0.7
159	42.77768	3.696	2	58.52	0	3.784	15.59184	3.696	4.65256	3.696	3.25424	3.696	81.33333	68.66667	0	33.352	3.168	1.59
160	43.30128	4.136	2	64.1916	0	4.048	42.1344	3.784	9.8824	3.96	4.15976	4.30408	120	63.33333	0	29.6912	3.432	0.18
161	50.44864	3.608	2	67.44056	0	3.608	36.56488	3.52	13.05568	3.784	4.52584	3.9072	64	61.33333	0	30.24384	3.168	0.35
162	46.02488	2.904	2	59.752	0	2.816	23.5004	2.552	NA	NA	NA	NA	111	NA	0	31.768	2.2	0.61
163	49.64344	3.608	2	73.70968	0	3.608	27.91536	3.344	5.40496	2.552	3.19352	3.52	114.3333	77	0	43.7976	3.08	0.09
164	37.18704	3.52	2	58.14072	0	3.344	30.36704	3.08	6.9828	3.432	3.54112	3.344	95.33333	55.33333	0	24.15952	3.432	0
165	39.864	3.608	2	54.12	0	3.432	18.54864	2.904	5.4384	3.432	2.74032	3.82888	112	76	0	36.168	2.904	0.35
166	28.16528	3.784	1	66.08536	0	3.52	39.62816	3.168	8.06344	3.52	4.07176	3.432	88	68.33333	0	27.07496	3.11872	0
167	52.36616	4.488	2	48.25128	0	4.136	27.72	4.048	10.7228	3.872	5.11368	4.312	99	69.66667	0	0	3.696	0.7
168	60.04768	4.664	3	67.68696	0	4.136	35.4728	3.696	9.8912	3.696	4.86816	3.8148	101.3333	88	0	29.4404	3.52	0.61
169	38.47272	4.4	2	58.41176	0	4.312	37.80568	4.136	12.81368	4.488	4.91304	4.224	115.3333	76.33333	0	31.8868	3.784	0.09
170	37.22664	3.168	2	66	3	3.168	26.57952	2.904	6.22424	4.576	4.83384	3.8148	90.33333	75.66667	0	34.32	1.584	1.23
171	46.288	3.696	2	56.936	0	4.048	31.064	3.696	6.19872	4.048	2.82304	3.696	68.66667	68.33333	0	31.6008	3.696	0.8
172	42.152	3.52	2	58.96	0	3.432	15.22576	3.168	6.204	3.344	2.2528	3.432	66.33333	54	0	31.152	2.64	0.44
173	37.928	4.752	2	58.08	0	4.4	18.8628	4.752	5.41112	5.368	3.01664	5.28	87.66667	77.66667	0	31.768	4.224	1.76
174	37.4	3.96	2	58.608	0	3.608	18.65952	3.608	5.17	3.344	2.53968	3.168	49.66667	62.66667	0	29.22128	2.992	0.44
175	35.6268	4.224	2	60.66896	0	4.312	18.59	3.696	6.17936	4.576	3.17856	3.96	67.33333	65.66667	0	31.416	3.696	0.52
176	36.12488	2.112	2	56.78464	1	2.112	15.57688	2.112	4.02864	2.112	1.6896	2.2	47	52.33333	0	30.22448	2.64	1.59
177	37.312	4.488	2	62.77744	0	4.048	38.97696	4.048	9.33504	4.312	5.37856	4.1668	59.66667	61.66667	0	32.07424	3.696	0.88
178	38.55632	4.048	2	64.16168	0	3.872	26.93152	3.344	10.14376	3.872	5.3768	3.76112	67	67.33333	0	25.91248	3.608	0.35
179	26.30056	4.136	2	61.97488	0	3.784	30.03792	3.432	11.41096	3.96	4.83384	3.81568	76.66667	66.33333	0	29.546	3.256	1.76
180	34.3508	4.752	2	61.69328	0	4.224	26.49152	3.872	6.75136	4.224	3.43552	3.784	50.66667	74.33333	0	28.64664	3.696	0.44
181	37.488	3.96	2	62.88744	0	3.96	20.43272	3.696	6.22424	3.96	3.1856	3.872	50.33333	75.66667	0	28.512	3.344	1.41
182	61.07376	3.168	1	67.40888	0	3.168	14.87904	2.64	4.818	3.168	3.23664	3.168	73.33333	60.33333	0	33.93808	2.64	0.44
183	33.70576	3.872	2	52.27376	3	3.96	27.984	3.696	5.46656	3.47512	3.322	3.872	49	67	0	34.41856	4.312	0.35
184	48.136	3.168	2	56.86384	1	3.08	23.5752	2.64	5.12776	3.344	3.64936	3.256	76.66667	68.66667	0	33.26752	2.64	0
185	96.096	3.784	3	49.38032	0	3.608	23.76176	3.256	4.61472	3.96	3.27976	3.168	68.33333	77.33333	0	30.448	3.168	0.09
186	75.10888	3.784	3	57.9964	0	3.784	17.96168	3.696	5.6496	4.136	3.30704	4.136	65.66667	69.66667	0	44.2684	3.256	0.27
187	48.0304	4.752	2	72.50056	0	4.224	26.66576	4.224	6.67656	4.4	4.97464	4.4	64.66667	64.66667	0	26.488	3.784	1.41
188	39.51728	3.53232	2	52.27552	0	3.432	23.76352	3.168	4.63232	3.608	3.0096	3.54112	59.33333	72	0	30.712	3.168	0.17
189	48.752	3.608	2	68.92336	1	3.432	31.42568	3.256	8.28432	3.872	5.37856	3.55432	76	69	0	33.43208	2.64	0.09
190	41.99536	4.224	2	71.896	0	3.696	24.2	3.168	4.202	3.4452	2.64	3.26304	65.33333	63	0	28.6	3.344	0.61
191	44.088	5.632	2	67.6764	0	4.928	18.48	4.224	8.01504	4.4	5.58888	4.08056	59.33333	46	0	0	4.224	1.76
192	26.0128	4.224	2	61.25768	0	4.048	28.13536	3.784	9.63776	4.4	4.06384	4.092	65.66667	52.66667	0	27.65224	3.696	1.84
193	36.52	3.256	2	60.72	0	3.96	15.84	3.872	5.61	4.49064	2.82304	4.312	99.66667	65.33333	0	34.584	3.344	0.08
194	32.472	3.872	2	55.616	3	3.432	18.5636	3.432	5.6364	3.52	3.60008	3.42056	68.33333	59.66667	0	31.064	3.256	0.61
195	35.904	3.696	2	55.528	3	3.696	20.36496	3.18296	5.11544	4.048	3.31408	3.278	74.66667	61.66667	0	36.08	3.08	0.26
196	48.4	3.696	2	68.288	0	3.696	19.67944	3.696	5.7332	4.224	3.61592	3.57544	60	69.33333	0	34.144	3.52	0.08
197	27.984	3.872	2	68.1296	0	3.608	27.72	3.256	4.8488	3.96	3.22344	3.5508	70	58	0	27.104	3.08	0.09
198	46.29856	2.288	2	63.36264	0	3.784	27.25712	3.696	4.40088	4.048	3.22344	3.872	59.66667	70.33333	0	32.912	3.57368	2.02
199	41.37408	3.52	2	61.2656	0	3.52	17.95112	3.168	4.56632	3.696	4.026	3.608	50	67.66667	0	32.032	3.168	0.18
200	49.984	3.4452	2	53.85688	0	3.432	22.79112	3.168	4.8884	3.608	2.6004	3.65024	60.33333	65	0	30.36	2.464	0.81
201	53.944	3.168	4	32.77472	0	3.168	19.55624	2.904	5.20256	3.256	3.38184	3.168	66	62.33333	0	32.384	2.904	0.17
202	102.96	2.904	3	33.96888	0	2.904	16.25008	2.64	4.07704	2.904	2.6004	2.904	72.33333	67.66667	0	32.29776	2.64	0.71
203	26.488	3.696	2	54.384	0	3.52	15.92624	3.344	5.41728	3.52	2.6136	3.17856	88.33333	71.33333	0	31.152	3.08	0.27
204	36.96528	3.52	2	65.47288	0	3.344	26.68336	2.992	5.36976	3.168	2.64	3.344	77.33333	70	0	0	3.08	0.18
205	40.49232	4.312	2	71.5924	0	4.224	39.34568	3.52	10.648	3.696	7.13504	3.56048	77.33333	73.33333	0	40.392	3.168	0.53
206	57.18592	4.312	2	69.58776	0	4.224	38.45864	3.96	8.19984	4.4	4.49592	4.18528	46.66667	55	0	28.776	3.432	0.35
207	71.10576	4.224	3	43.25816	0	4.136	16.21928	3.52	5.2052	4.136	3.18912	4.01192	76.33333	58.33333	0	32.65328	3.432	1.32
208	39.688	3.168	2	41.8	0	3.256	14.78488	2.64	4.56192	3.168	3.44256	2.85472	70.66667	66.66667	0	35.816	2.64	0.44
209	41.976	3.696	2	61.24888	4	3.696	16.91272	3.168	5.32752	3.88432	4.30232	3.93888	62.66667	61	0	32.648	2.992	0.53
210	36.784	3.344	2	63.96544	1	3.6212	27.984	3.256	7.7792	3.696	4.89632	3.696	54.33333	61	0	36.13456	2.376	0.53
211	28.688	3.00784	2	60.72	0	2.904	18.60144	4.136	4.56192	3.88432	3.44256	3.56048	98.33333	73.33333	0	31.504	2.112	0.69
212	34.232	3.72416	2	67.584	0	4.048	22.06248	3.608	5.79128	3.696	3.38184	3.696	72.66667	70.66667	0	35.03544	3.88432	0.82
213	49.72	3.696	2	62.48	0	3.696	20.18456	3.168	6.94144	3.872	3.17856	3.79104	68.66667	69.66667	0	28.952	3.344	0.53
214	36.256	4.224	2	64.328	0	4.224	18.48352	4.136	5.4604	4.136	3.44256	4.048	60.66667	64.33333	0	35.2	3.432	0.88
215	33.352	3.08	2	52.27288	0	3.168	12.93776	2.64	4.60944	2.64	2.7192	3.25776	73.66667	65	0	31.328	2.64	0.09
216	34.144	3.168	2	54.56	1	3.168	16.10488	2.64	6.21016	2.64	3.73296	3.256	63.66667	73.33333	0	30.976	2.2	0.53

217	44.62216	5.104	2	56.45112	0	4.752	18.06376	4.752	6.38792	4.752	3.80688	4.4	98.33333	65.66667	0	33.176	3.96	0.27
218	35.90576	4.4	2	60.19464	0	3.96	18.60144	3.96	5.59416	4.224	2.85648	4.4	84.66667	76.66667	0	36.60976	3.696	1.23
219	35.992	3.872	2	55.4576	0	3.696	18.34536	3.696	5.37856	3.696	3.17856	3.696	76.66667	67.33333	0	32.56968	3.168	0.53
220	90.37952	3.168	3	49.45688	0	3.608	16.82472	3.168	4.92448	3.696	4.86024	3.696	88.33333	76.33333	0	39.41608	3.696	0
221	28.776	3.96	2	54.91288	1	3.96	12.96504	3.168	4.50384	3.52	2.85648	3.52	61	54.66667	0	28.952	3.432	0.53
222	39.952	3.696	2	61.77776	0	3.168	15.97112	3.168	5.09432	3.608	3.30792	3.5332	68.33333	61.33333	0	30.448	3.0052	0
223	35.728	4.664	2	47.78576	0	4.488	21.1288	3.872	5.31872	4.488	2.98584	4.488	63.66667	51.66667	0	38.90832	4.224	2.81
224	21.1728	4.224	2	64.152	0	4.224	40.57416	4.224	9.504	4.224	5.68656	3.88432	53	49.66667	0	0	0	1.05
225	41.7956	5.016	2	70.2284	0	5.016	32.736	4.928	12.28216	4.928	6.446	4.928	93.66667	72.66667	0	40.28904	3.96	1.03
226	60.72088	4.224	2	76.73952	0	4.224	15.11224	3.696	5.13216	4.752	3.44256	4.488	83.33333	73.66667	0	37.312	3.696	0.52
227	41.23504	4.224	2	63.0476	0	4.312	35.8468	4.224	9.636	3.432	3.22344	3.96	100.6667	68	0	29.216	3.52	0.7
228	48.7828	3.784	2	62.65336	1	3.97144	34.22936	3.256	7.722	3.62032	4.32608	4.42464	44.66667	64.33333	0	29.38584	2.904	0.08
229	45.936	3.432	2	68.64	0	3.344	28.25152	3.168	8.31776	3.432	6.5208	3.432	55.33333	61.33333	0	40.83376	3.256	0.62
230	115.9858	3.432	3	52.49552	0	3.432	32.59168	3.18296	8.3072	3.696	4.56632	3.608	81	67.66667	0	34.91224	2.904	0.97
231	26.928	3.52	2	51.65952	0	3.432	16.70856	3.256	4.9104	3.432	3.22344	3.08	75.66667	74.33333	0	28.24096	2.64	0.35
232	68.02488	3.168	3	42.83576	0	3.608	22.088	3.256	9.636	3.08	6.69328	4.84	94.33333	91.66667	0	29.34096	3.168	0.01
233	45.936	3.344	2	66	0	3.432	29.942	2.992	10.65416	3.608	5.61264	3.87376	60.33333	74.33333	0	29.34976	3.344	0.71
234	47.6916	4.576	2	54.76152	0	4.4	22.02904	4.224	5.66104	4.664	3.7576	3.608	63	75.66667	0	0	4.136	0.8
235	32.19392	4.03656	2	56.43704	0	4.224	22.792	3.52	6.402	4.4	2.43408	4.4	94.33333	79.33333	0	27.13832	3.23048	1.93
236	52.93552	3.784	2	59.994	1	3.256	35.8468	3.608	12.81808	3.608	7.2512	3.41968	99.33333	74	0	34.496	3.344	0.09
237	39.16	4.312	2	65.65856	0	3.696	16.94088	3.608	5.66104	4.23456	4.39296	4.048	56.33333	60	0	35.65408	3.52	0.44
238	39.67392	3.52	2	60.96376	0	3.784	29.92	3.168	10.19832	3.168	4.906	3.17152	59	75.66667	0	26.97728	3.0272	0.26
239	30.82288	4.4	2	75.33504	0	4.136	21.6524	4.488	5.6628	4.84	3.17856	4.4	67.66667	59	0	31.68	3.784	0.79
240	37.488	4.664	2	58.52	0	4.136	19.33008	4.136	7.72816	4.664	3.59216	4.136	62.33333	61	0	36.96	3.432	0.17
241	45.85856	3.696	2	73.74752	0	3.696	21.38576	3.35104	7.23888	3.96	3.7576	3.96	68.33333	71.66667	0	24.62504	3.2032	0.08
242	41.866	3.168	2	30.2632	0	3.08	14.256	2.904	4.9764	3.168	4.06384	2.992	65.33333	68	0	31.96248	2.65144	0.44
243	38.01952	3.784	2	66.00352	4	3.20936	19.27816	3.696	5.76312	3.96	3.36776	3.81656	85.66667	79.33333	0	34.76	3.168	0.51
244	38.36976	3.432	2	62.72816	0	3.432	15.04932	3.256	5.61	3.432	3.3	3.33432	58.66667	62	0	39.9168	3.168	0.26
245	45.7688	4.136	2	72.57976	0	4.048	17.48384	2.904	5.6672	3.52	3.54288	2.904	114.234	79	0	28.952	3.168	0.08
246	84.92088	3.696	3	61.95552	0	3.608	17.73024	3.696	4.26624	3.52	2.2704	3.52	65	67.33333	0	35.43936	3.432	0.52
247	41.096	3.168	2	59.49944	0	3.08	22.176	2.904	5.98048	3.168	3.96	2.904	55.33333	67	0	20.99592	2.904	0.97
248	48.56632	4.136	2	59.488	0	4.048	30.01768	3.52	15.25744	3.872	6.70472	4.10432	76.66667	62	0	34.39128	3.432	0.09
249	52.97776	3.784	1	61.42752	0	3.784	19.61608	3.608	6.8816	3.96	2.95152	3.96	65	60.33333	5	37.42816	3.168	0.17
250	78.15016	2.992	3	32.5908	0	2.992	18.48352	2.64	7.47648	2.64	3.54288	2.64	59.66667	62.66667	0	26.664	2.64	0.88
251	33.616	2.9964	2	74.976	0	3.168	17.48384	2.904	4.37712	3.432	2.12784	3.2824	70.66667	62	0	32.912	2.83184	0.17
252	102.9609	3.696	3	52.536	0	3.96	17.5296	3.344	4.84704	3.52	2.76496	2.992	83.33333	79.66667	0	32.384	3.168	0.26
253	68.39184	2.64	4	37.53992	0	2.64	19.95312	3.608	5.6672	4.224	2.95152	2.64	67.33333	80.66667	0	0	0	1.58
254	36.88784	3.08	2	57.11288	0	3.168	15.04932	2.64	4.35336	2.64	2.84328	2.64	95.33333	72	0	33.45232	2.376	0.44
255	39.65808	4.048	2	60.984	0	3.784	14.60888	3.696	4.62968	4.048	3.07824	3.52	67.33333	58.33333	0	32.29336	3.168	0.88
256	47.46192	4.048	2	65.49576	2	3.96	23.2584	3.784	6.24272	4.224	3.59216	3.64496	64.33333	68.33333	0	37.84	3.96	0.27
257	45.91136	3.96	2	61.60528	0	3.96	18.25384	3.696	5.70328	3.96	3.01664	3.872	77.66667	64.66667	0	27.8564	3.168	0.62
258	44.06248	3.696	2	70.66576	0	3.70832	18.50464	3.52	5.808	3.52	3.02456	3.784	74.33333	67	0	33.968	3.256	0.52
259	46.82744	3.168	2	76.0936	0	3.168	19.95312	3.168	5.6672	3.168	3.56	2.992	95.33333	65	0	0	2.904	1.58
260	36.56224	4.224	2	63.01064	0	3.70832	17.37032	3.696	5.6672	4.224	3.5772	4.224	117.6667	76	0	38.896	3.696	1.84
261	43.9604	4.048	2	60.49208	0	3.872	17.69152	3.696	6.68888	3.96	3.18912	3.608	75.33333	76.66667	0	31.98712	3.08	0.27
262	43.70344	3.96	2	59.752	3	3.89928	16.99456	3.696	5.36712	3.872	3.66696	3.96	0	80.66667	0	27.12952	3.696	0.79
263	58.256	4.048	2	50.16968	0	3.96	27.20608	3.608	9.65272	4.048	4.29792	3.90896	118.6667	75.66667	0	28.688	3.256	0.44
264	27.984	3.168	2	60.01776	0	2.112	15.62792	3.08	4.05504	3.432	3.0096	2.816	67.33333	70.33333	0	33.29568	3.08	0
265	40.9332	3.784	2	57.59336	0	3.344	13.99728	3.344	7.942	3.696	3.07824	3.608	58.66667	59.66667	0	34.05072	3.256	0.17
266	41.096	2.992	3	51.13504	0	3.09584	13.77992	2.6444	NA	NA	NA	NA	69.66667	67.333	0	32.032	2.64	0.35
267	30.93552	3.608	2	47.56312	0	3.432	25.78048	3.432	NA	NA	NA	NA	0	59.3345	0	29.7748	2.904	0.88
268	38.95232	4.048	2	61.88072	0	4.224	19.90912	3.608	5.69536	4.224	3.31408	4.048	64.66667	67.66667	0	37.246	3.168	0.79
269	37.63056	3.96	2	64.16432	3	3.872	27.73056	3.09496	8.3116	3.96	4.6596	3.69776	84	91.66667	0	29.04	3.432	0.79
270	48.79424	3.256	2	61.02008	3	3.344	18.75192	3.256	4.03216	3.344	2.74824	3.256	70	60.33333	0	32.57672	3.168	0
271	49.28704	3.872	2	70.05504	0	4.224	21.12528	3.872	5.97784	4.224	4.05416	4.224	90	94.33333	0	38.10312	3.696	0.79
272	40.74576	4.048	2	32.33472	0	3.696	13.46752	3.696	0	0	0	0	90.33333	0	0	38.16208	3.168	1.41
273	45.88496	3.52	2	67.1264	1	3.696	0	3.696	0	0	0	0	90.66667	0	0	32.824	3.432	0.26
274	50.4416	4.576	2	61.53224	0	4.488	20.73016	3.96	5.62936	4.224	2.82304	3.432	86	66.66667	0	30.51664	3.168	1.15
275	38.89248	3.872	2	57.99728	3	3.96	13.2	3.52	0	0	0	0	0	0	0	32.11472	3.168	1.76
276	41.624	2.816	2	47.872	0	3.52	14.05008	3.168	4.09728	3.168	3.8192	3.344	62.66667	74	0	30.448	2.728	0.7
277	38.72	3.784	2	60.73936	0	3.784	17.4416	3.696	5.16296	3.696	2.52648	3.08	80.33333	71.33333	0	31.7416	3.168	0.35
278	44.09416	3.784	2	54.52744	0	3.696	16.78512	3.52	5.1172	3.432	2.64	3.432	65.33333	74.66667	0	28.3228	3.432	0.88
279	41.008	2.552	2	64.43272	1	2.552	19.31688	2.464	5.99456	2.64	3.0096	2.64	105	81.66667	0	0	0	0.88
280	48.78896	3.96	2	46.86088	0	4.224	29.12712	3.696	7.53808	4.224	5.62496	3.278	43.33333	69.66667	0	36.608	3.432	0.62
281	46.112	3.696	2	62.69472	0	4.136	28.37296	3.18296	10.23088	4.224	5.82912	4.06384	58.33333	60.66667	0	0	3.432	0.44
282	33.68904	3.52	2	49.808	0	3.344	15.88488	3.168	5.11104	3.696	3.03248	3.23136	51.33333	62.33333	0	29.46768	2.904	0.35
283	42.24176	3.168	2	71.29408	0	3.256	17.07288	3.256	4.61208	3.608	3.24632	3.344	56.33333	80	0	0	2.904	0.79
284	41.976	3.872	2	55.43296	0	3.696	16.632	3.71184	6.644	4.312	2.83976	3.784	74.66667	78.33333	0	34.408	3.344	0.97
285	41.65216	3.256	2	44.4796	0	3.432	20.59552	3.256	6.22512	3.432	3.24632	3.38448	51.66667	73	0	24.12872	2.64	0.08
286	50.3932	3.18296	2	58.44256	1	3.168	23.1088	2.904	4.59184	3.20056	3.2648	3.168	58.66667	65.33333	0	35.552	2.64	0.08
287	39.86488	3.344	2	51.00304	1	2.992	39.33688	2.64	12.85944	3.168	5.346	4.00048	52.33333	67.33333	0	26.34808	2.64	0.44
288	27.59504	3.256	2	54.31976	0	3.344	15.13248	3.168	4.3692	3.61152	3.02456	3.256	59.33333	71	0	0	0	0.96
289	96.44888	3.168	4	32.03464	0	3.168	27.51848	3.08	4.14304	3.168	2.45256	3.168	57.33333	68	0	32.68848	3.168	0
290	48.84	5.192	2	63.21128	0	4.928	32.406	4.224	9.96952	5.104	4.35072	5.104	72.33333	48.66667	0	30.7648	3.784	0.61
291	29.13592	2.992	2	56.1264	0	2.904	27.86432	2.904	8.4128	2.7368	3.59216	2.83184	60	70.33333	0	24.29504	2.376	0.47
292	96.3336	3.784	4	41.00096	0	3.608	18.60584	3.08	5.28352	0	3.2516	2.64	0	0	0	29.128	3.08	0.61
293	28.87104	2.904	2	34.58576	0	2.992	17.50936	2.904	5.566	3.08	4.13688	3.08	52.66667	67.66667	0	23.53912	2.904	0.26
294	42.328	3.784	2	56.04544	0	3.52	15.20904	3.168	4.30056	3.696	3.19352	3.26304	65.33333	63.66667	0	27.35128	2.904	0.07
295	49.016	3.872	2	59.05856	0	3.784	15.54696	3.256	4.83208	3.432	2.99024	3.61152	105	76.33333	0	34.496	2.904	0
296	92.64376	3.08	3	45.34024	0	3.168	25.25952	2.904	4.98168	3.168	2.5212	2.728	55	88.33333	3	32.26432	2.904	1.06
297	35.44464	3.344	2	53.95808	0	3.432	17.54104	2.816	7.56536	2.904	2.53088	3.256	54	56.33333	0	28.88424	2.552	0.27
298	82.38472	2.112	3	57.38304	0	2.288	24.75	2.288	4.69304	2.2	2.25104	2.2	0	64	0	39.182	3.168	1.76
299	44.44	3.256	2	63.60376	0	3.168	34.44584	2.64	7.57592	3.168	5.43048	3.08352	70.66667	76.33333	0	37.312	2.64	0.26
300	46.904	4.048	2	73.83464	0	3.872	28.90536	3.52	7.2688	3.872	3.23928	3.784	77	68.33333	0	33.088	3.872	0.35
301	42.88592	3.696	2	73.23712	0	3.432	28.24976	3.52	8.59848	3.608	3.75144	3.49624	99.66667	76.66667	0	35.56784	2.904	0.52
302	57.64	4.84	2	90.73152	0	5.016	0	0	0	0	0	0	0	0	0	0	0	0
303	39.91064	3.256	2	61.336	0	3.256	19.61432	3.168	6.27	3.432	3.54112	2.992	61.33333	65.66667	0	37.4572	3.168	0.44
304	42.944	4.136	2	53.38784	0	3.96264	32.8944	3.432	7.97808	4.50824	3.7972	4.752	79	71	0	33.8756	3.71624	0.97
305	47.6608	3.872	2	53.48552	0	3.96	23.24256	3.696	5.32136	3.784	2.57664	3.52352	65.33333	65.66667	0	36.542	3.608	0.17
306	50.91152	4.048	2	64.68352	0	3.696	20.06752	3.696	6.1556	3.696	3.542	3.696	61.66667	69.66667	0	35.904	3.696	0.27
307	42.46088	3.696	2	51.15968	0	3.344	13.76056	3.432	4.98256	3.52	2.49392	3.52	55.66667	58.33333	0	32.74832	3.18384	0.52
308	35.992	3.696	2	70.576	0	4.136	34.39392	3.78752	4.95088	3.96	3.00168	4.22048	56.33333	70.66667	0	34.76	3.256	0.17
309	72.27968	5.28	2	85.67944	0	5.104	46.28536	4.01808	10.80904	5.28	5.2448	5.28	69.66667	62.66667	0	35.9524	4.224	1.5
310	82.3944	3.52	3	41.89152	0	3.432	25.62912	3.256	6.42136	3.696	4.56016	3.696	107.3333	75.66667	0	40.11128	3.168	1.06
311	56.86032	4.664	2	67.61304	0	4.224	38.65224	4.84	9.9	4.576	5.97432	4.84	73.33333	88	0	39.952	3.872	0.44
312	45.61392	4.312	2	57.73152	0	4.00576	19.23416	3.696	5.6804	4.224	3.76112	4.312	66.66667	82.66667	0	35.08824	3.3572	1.67
313	48.38416	3.872	2	58.344	0	3.52	16.49296	3.432	5.96552	3.784	2.73944	3.784	73.33333	89.33333	0	36.26128	3.168	0
314	38.42168	3.608	2	53.63864	0	3.696	26.72824	3.344	6.61408	3.344	3.0096	3.344	58.33333	71	0	35.94976	2.9964	0.76
315	36.26832	4.136	2	55.4048	1	3.96	31.4292	4.048	13.07856	3.784	6.60528	3.784	82.33333	98	1	35.82568	3.52	0.97
316	44.71192	3.61152	2	69.4188	0	3.608	32.85744	3.256	6.2128	3.168	5.32312	3.784	65.33333	73.33333	0	29.75896	2.7324	0.53
317	42.75128	3.4452	2	66.9944	0	3.256	21.57936	3.168	8.184	3.344	2.52912	3.344	78.66667	71.66667	0	25.7708	3.23312	0.25

318	30.70056	4.488	2	71.06176	3	4.136	0	3.872	NA	NA	NA	NA	59	NA		0	37.224	3.168	0.71
319	37.80744	3.18296	2	67.84976	0	3.344	19.44536	3.08352	5.13744	3.18296	1.99672	3.27096	60	82		0	28.10544	2.728	0.16
320	101.6118	2.992	4	28.46272	0	2.552	16.89688	2.552	6.79888	2.376	2.32496	2.376	61.66667	67.33333		0	34.12024	2.376	0.18
321	45.15984	3.256	2	61.62024	0	3.168	26.312	2.728	7.5636	2.904	4.45808	2.904	76	65.66667		0	33.792	2.112	0.79
322	45.39832	4.752	2	63.44536	0	4.488	34.43088	3.61152	10.1376	4.576	5.14184	4.576	50	55.66667		0	35.508	3.96	0.18
323	41.18488	3.608	2	56.53032	0	3.25952	18.51344	3.256	4.884	3.256	3.0096	2.89608	56.66667	70.66667		0	32.63392	2.64	0.09
324	45.144	4.752	2	79.66112	0	4.66664	26.32608	4.4	4.61208	4.752	3.52792	4.752	63.66667	79.33333		0	27.72264	4.048	0.7
325	89.42296	2.552	3	47.4232	0	2.552	12.936	2.376	4.31904	2.552	1.93952	2.552	80.33333	60.66667		0	34.10352	1.848	1.5
326	77.88704	2.64	3	44.25872	0	2.64	13.2968	2.64	6.2832	2.64	2.47104	2.64	83.66667	76.66667		0	38.65136	2.376	1.14
327	44.18832	4.488	2	62.70176	1	4.488	0	4.224	5.808	NA	NA	2.992	NA	NA		0	38.53344	3.608	0.88
328	107.272	4.312	3	72.07464	0	4.136	16.37064	3.96	6.80944	4.224	3.02456	4.224	72.66667	63.33333		0	33.61688	3.608	0.61
329	42.7108	3.432	2	61.5956	0	3.608	34.5004	3.696	6.19256	3.96	2.43408	4.488	65.66667	73.33333		0	36.35104	3.52	0.71
330	49.104	3.696	2	68.79224	0	3.37392	37.6772	3.08	7.54512	3.608	5.15856	3.608	67.33333	72		0	31.6712	3.608	0.17
331	36.83504	4.576	2	63.97512	0	4.488	34.67464	4.136	7.99832	4.4	5.41112	4.54608	65	68.66667		0	35.19824	3.872	0.09
332	19.30632	3.696	2	51.49496	0	3.52	15.94736	3.168	4.81008	3.696	2.12784	3.696	84.66667	68.33333		0	32.7756	3.168	0
333	28.006	4.048	2	65.12	0	3.696	19.34768	3.52	5.65312	3.96	3.26128	3.96	78.66667	59.66667		0	36.168	3.696	0.97
334	37.928	3.344	2	68.46488	0	3.432	11.95568	3.168	4.5716	3.256	1.95624	3.256	59	69.66667		0	32.63128	3.168	0.62
335	40.45184	3.696	2	59.026	0	3.52	18.58032	3.432	8.5712	3.872	3.22168	3.872	92.33333	70.33333		0	34.21528	3.344	0.71
336	49.23776	3.608	2	63.558	0	3.608	17.84112	3.52	7.4976	3.696	0	3.696	74.33333	62		0	36.344	3.168	0.79
337	49.21928	3.168	2	63.1048	0	3.08352	16.81416	3.168	5.17528	3.52	3.0096	3.344	58	70.66667		0	34.2716	2.64	1.14
338	39.81032	3.52	2	71.32664	0	3.52	26.61384	3.168	6.18376	3.168	3.4848	3.168	60.33333	63		0	31.6756	2.99552	0
339	45.8172	4.84	2	79.93744	0	4.136	22.08008	3.96	NA	NA	NA	NA	NA	NA		0	0	0	0.26
340	63.04936	3.52	3	52.68912	0	3.432	16.94176	3.344	3.57368	3.432	2.81072	2.992	63.66667	65.33333		0	35.23432	3.08	0.09
341	38.90392	4.048	2	61.56568	0	4.224	11.88	3.96	5.32576	4.048	2.76056	3.47512	74.33333	82.66667		0	34.26016	3.608	0.79
342	64.71696	3.256	3	54.8372	0	3.256	17.54456	3.08	6.18552	3.256	2.7676	3.168	73	71.33333		0	37.84528	2.992	0.36
343	33.63272	3.344	2	43.66296	0	3.432	19.19192	2.904	5.48944	3.168	3.02808	3.168	0	65.33333		0	19.70232	2.64	0.1
344	45.08416	2.728	2	64.76976	0	2.816	13.20176	2.552	3.5508	2.816	1.89112	2.728	60.66667	64.66667		0	32.06104	2.6444	0.26
345	35.61272	3.168	2	53.94576	1	3.168	14.62824	2.64	5.47448	2.64	2.73152	2.64	70.33333	97.33333		0	27.91712	2.64	0.44
346	48.94824	4.224	2	39.03768	0	4.136	18.58296	3.696	7.54424	4.136	3.8192	4.11664	54.66667	59.33333		0	38.33456	3.432	0.44
347	48.55048	4.224	2	68.88024	0	3.872	21.53712	3.696	7.76424	4.136	3.92568	4.136	50.66667	72		0	36.08176	3.784	0.08
348	45.90432	3.872	2	63.86072	0	3.784	20.45824	3.52	6.27528	3.784	3.7972	3.608	63	64.66667		0	35.88288	3.168	0.35
349	78.32	3.256	3	58.47072	0	3.256	17.754	3.168	6.22424	3.256	2.80632	3.256	68.66667	66.66667		0	32.69552	2.64	0.61
350	34.21616	3.168	2	44.70664	0	2.728	22.10912	2.64	5.88632	2.992	4.03744	3.43112	72	62.33333		0	23.64648	2.64	0.09
351	32.74568	2.376	2	56.62096	0	3.344	26.67104	3.08	6.65632	3.432	3.79808	3.2516	75	65.66667		0	28.80416	2.64	-1.23
352	45.85768	4.576	2	93.01952	0	4.928	19.53688	4.224	6.83144	4.488	3.30792	4.664	69.33333	66.66667		0	40.9112	3.696	-0.35
353	58.69776	4.4	2	77.968	0	4.048	21.91288	3.696	6.4592	2.2	3.52792	2.2	58.66667	77.66667		0	38.82648	3.696	2.55
354	54.08568	3.872	2	69.66608	0	3.872	23.36136	3.696	6.90448	3.784	3.3	3.696	56.66667	66.66667		0	37.60592	3.344	-0.18
355	49.64608	6.6	2	93.09256	0	6.424	30.01064	6.952	6.42664	6.424	3.86672	6.424	92	60.66667		0	39.336	5.544	2.64
356	50.55072	4.048	2	66.47696	0	3.96	22.17864	3.872	6.23216	4.136	3.73296	3.96	63.66667	65.33333		0	43.50632	3.52	0.18
357	45.52768	3.344	2	61.7232	0	3.256	16.44984	3.256	3.83416	3.52	2.6312	3.608	66	63		0	35.58456	2.64	-0.27
358	41.096	4.928	2	87.53888	0	4.928	25.24632	4.576	6.95816	5.104	3.18208	5.28	64	66		0	42.63952	4.4	1.06
359	44.462	3.344	2	61.86576	0	3.344	18.8496	3.168	5.38384	3.344	2.80632	3.168	84.33333	72.66667		0	34.11232	3.08	0.17
360	39.91152	3.784	2	59.04976	0	3.696	15.04888	3.256	5.66016	3.608	2.76496	3.432	70	76.66667		0	39.864	3.344	0.44
361	70.04272	3.256	3	26.05328	0	3.432	23.32264	3.168	6.18024	3.432	3.17856	3.37568	60.66667	76.33333		0	0	3.168	0.36
362	36.53584	3.432	2	56.85064	0	3.344	18.54248	3.168	5.98576	3.432	2.6136	3.52	71.66667	78		0	36.7532	3.168	0.17
363	81.6024	3.696	3	44.95128	0	3.696	14.53144	3.432	4.90952	3.432	3.17856	3.6212	69.66667	75.66667		0	32.25728	3.168	0.62
364	31.57528	3.696	2	58.0272	1	3.256	12.14488	3.168	4.81976	3.52	2.58984	3.52	53.33333	70.33333		0	39.94408	3.256	1.06
365	62.744	2.552	3	47.6476	0	2.552	18.36824	2.552	5.8608	2.64	NA	2.64	NA	NA		0	0	0	-1.32
366	32.208	2.904	2	52.18576	0	3.08	15.20904	0	5.2888	3.08	2.12784	2.992	NA	74.66667		0	26.2328	2.904	0
367	57.288	4.136	3	54.56	0	3.784	14.0712	3.696	NA	NA	NA	NA	NA	NA		0	28.31488	3.168	1.15
368	33.09152	3.256	2	47.61152	0	2.992	25.47424	2.904	5.6716	3.52	3.24632	3.5332	36.33333	62.33333		0	25.96	2.64	-0.17
369	31.69936	3.608	2	55.27984	0	3.96	14.12928	3.168	4.37888	3.52	2.49392	4.048	0	83.66667		0	31.65184	3.168	0
370	46.03192	3.872	2	65.736	0	3.784	14.38712	3.696	NA	NA	NA	3.08	NA	NA		0	32.04872	3.344	-0.09
371	33.96888	3.168	2	70.93856	0	3.27096	15.91304	3.08	5.29056	3.696	2.43408	3.696	66.66667	67.66667		0	34.2716	2.992	-0.88
372	44.682	3.784	2	68.09704	4	3.784	22.19096	3.696	5.68128	0	2.7192	0	81.33333	0		0	31.69848	3.168	0.52
373	42.61224	3.608	2	64.47672	2	3.432	16.74728	2.904	4.884	3.256	2.48952	3.256	48.33333	66.33333		0	34.298	3.08	0.44
374	0	3.344	2	48.68776	0	3.432	23.67024	3.168	8.6548	3.432	4.09464	3.432	59.66667	93.33333		0	32.47552	2.728	-0.36
375	44.10032	3.608	2	66.6028	0	3.344	14.72856	3.344	5.6452	3.608	3.03248	3.608	58.66667	66.66667		0	37.9192	3.09584	-0.88
376	42.5348	4.136	2	64.768	0	4.136	30.36	3.784	10.39016	4.224	6.07728	4.91656	74.33333	70		0	38.368	4.224	0.18
377	46.64	3.96	2	67.43088	0	3.872	0	3.872	7.934	3.04	5.23	4.192	67.332	69		0	28.78568	3.696	-0.09
378	49.80888	4.048	2	64.86304	0	3.872	27.46304	3.256	10.03288	4.048	5.13656	3.94856	66.33333	61		0	29.66304	2.904	0.44
379	45.672	3.872	2	67.2276	0	3.344	34.5928	3.168	8.82376	3.696	5.66808	3.87288	66.33333	68.33333		0	32.73952	2.904	-0.53
380	47.8896	3.696	2	63.11272	3	3.608	28.66072	3.344	8.11096	3.696	3.38184	3.74264	46.33333	77		0	34.91048	3.344	0.09
381	43.296	4.488	2	59.62088	1	4.224	27.0468	3.608	6.2304	3.872	3.22344	3.55696	62.33333	64.66667		0	0	3.168	0.88
382	62.8496	2.552	3	38.72528	0	2.552	20.24	2.464	8.184	2.64	4.576	2.552	60.33333	86		0	18.4272	1.848	-0.71
383	39.77952	3.256	3	50.81912	1	3.256	26.13688	2.728	6.10456	3.08	4.40088	3.08	60.66667	85.66667		0	0	0	0
384	39.70912	3.872	2	49.40672	0	3.432	14.36776	3.168	4.95704	3.52	2.98584	2.85824	82	72.33333		0	37.30144	3.168	0.88
385	46.80456	3.608	2	63.09776	3	3.52	13.30648	3.256	4.31728	3.344	3.26216	3.344	79	75		0	40.2644	3.344	-0.17
386	49.16472	3.608	2	74.83696	3	3.52	27.19904	3.432	7.29784	3.344	4.32608	3.98816	66.66667	74.33333		0	38.31872	2.904	-0.26
387	48.89016	4.664	2	78.2232	0	4.136	33.8932	3.96	8.3556	4.4	4.86464	5.016	86.33333	59.33333		0	37.0392	3.3836	0.26
388	36.35544	2.904	2	52.0388	0	2.904	13.84504	2.904	4.38504	2.904	2.64	3.43112	64.66667	70.33333		0	28.15736	2.2	0.26
389	38.81152	3.17152	2	52.36	0	3.168	23.06216	3.168	5.63552	3.168	4.03744	3.29648	64.66667	77		0	22.60896	2.816	-0.09
390	27.46392	3.52	2	57.64352	0	3.696	25.17064	3.256	8.52984	3.432	4.30144	4.42464	66	65		0	31.50312	3.71184	-0.62
391	47.46016	2.64	2	60.19376	0	2.64	16.38032	2.64	4.6376	2.64	3.036	2.288	96.33333	66.33333		0	30.96632	2.64	-1.23
392	43.64624	3.784	2	64.06928	0	3.52	14.60008	3.432	5.7112	3.872	3.47864	3.52	55.66667	71		0	39.19696	3.432	0
393	55.4444	3.432	1	57.11376	0	3.344	32.208	3.256	8.78944	3.4452	4.60944	4.224	80	77.33333		0	31.18456	3.256	-0.62
394	37.57776	3.256	2	53.68088	0	3.168	23.49776	2.992	7.2732	3.168	4.35864	3.6388	69.66667	94		0	31.4028	2.904	0.36
395	28.60792	4.048	2	56.41064	0	4.576	26.01192	3.872	7.74224	4.224	4.57688	3.32552	59.33333	64.66667		0	31.416	3.256	1.41
396	81.04888	3.168	3	38.80976	0	3.256	15.87168	2.64	5.28	2.992	3.44256	3.0228	59.66667	66		0	35.89432	2.64	-0.35
397	45.85856	3.52	2	58.43024	0	3.52	26.59536	3.344	7.75192	3.608	4.86288	3.872	61.66667	75.33333		0	30.7824	3.168	-0.62
398	38.1348	3.696	2	53.2972	0	3.608	16.03272	3.696	4.50384	3.432	5.13392	3.54376	53.33333	70.66667		0	36.7664	3.432	0.53
399	45.15016	4.4	2	72.82792	0	4.136	34.19944	3.96	8.47616	4.4	5.78952	5.368	73.33333	74.66667		0	23.22848	3.52352	0.09
400	46.99288	4.048	2	61.60528	0	3.96	19.66008	3.784	5.7068	4.048	3.23928	4.048	68.66667	68		0	39.0544	3.696	1.41
401	58.24808	5.016	2	75.86832	0	5.104	43.68056	4.576	11.62568	5.016	6.2524	5.016	69.66667	80		0	35.464	4.048	1.06
402	68.6796	3.872	2	75.87712	0	4.048	46.56608	3.52	12.02256	4.224	5.61264	4.928	69.33333	73		0	39.14944	3.432	-0.44
403	84.41576	2.64	3	48.14128	0	2.64	10.8284	2.64	2.6664	2.64	2.01168	2.64	69.66667	58.66667		0	34.59984	2.376	-1.41
404	31.73544	2.904	2	52.18752	0	2.64	20.68704	2.816	7.53808	2.728	4.12896	2.728	61	72.66667		0	39.47504	2.64	-0.62
405	41.88888	3.608	2	63.00888	0	3.696	15.05152	3.168	5.39968	3.696	2.74208	3.608	81.66667	63.66667		0	36.29824	3.168	0.35
406	46.3452	3.608	2	64.86656	1	3.432	33.08536	3.256	11.97768	3.432	6.69416	3.52	117.3333	68.66667		0	33.22352	2.728	0.53
407	46.816	3.52	2	69.35808	0	3.344	26.4	3.168	5.87312	3.52	3.9	4.032	62.66667	69		0	0	0	-0.62
408	42.68264	3.784	2	63.22712	0	3.28856	22.90024	3.3572	5.69184	3.432	3.87112	3.432	79.33333	71.66667		0	39.54984	3.256	0.61
409	58.96176	5.632	2	90.15512	0	4.752	23.144	5.28	9.1456	3.223	4.1	2.904	104	66		0	34.66144	4.224	1.41
410	48.76696	4.224	2	60.19552	0	4.136	16.764	3.696	5.48944	4.224	3.51736	3.256	67	77.66667		0	34.8128	3.696	0.08
411	31.62016	3.432	2	44.59224	0	3.432	20.87536	3.432	6.08168	3.43552	4.51088	4.048	93.33333	74		0	28.36416	2.904	
412	49.25536	3.872	2	64.89208	0	3.872	28.19	2.74	10.19	3.12	2.58984	3.9	75.3448	69		0	37.47568	3.168	0.09
413	37.928	2.992	2	39.1072	0	2.728	14.14952	2.376	7.03208	2.552	5.65488	2.552	64.33333	74.66667		0	35.64	2.2	-1.15
414	47.61944	3.872	2	56.80312	0	3.872	33.01584	3.432	7.99656	3.96	4.6068	3.96	55.66667	59.66667		0	34.17656	3.168	-0.53
415	44.0704	4.576	2	67.58488	0	4.4	24.81688	3.872	9.63776	4.4	4.88224	4.96848	49	77		0	31.62544	3.872	0.88
416	41.65656	4.048	2	61.04472	0	4.224	26.20816	3.608	9.9088	4.048	4.85232	4.048	44.33333	63.33333		0	32.076	3.608	0

417	27.71384	3.344	2	40.07432	0	3.17152	21.23088	2.904	5.236	3.344	3.44256	2.992	86.66667	71	0	29.13416	2.904	0.26
418	73.92088	4.136	3	56.4872	0	3.96	30.45768	3.872	16.47272	4.136	5.68216	4.136	72.33333	66	0	33.29656	3.696	0.18
419	45.01288	3.608	2	64.84544	0	3.52	35.22112	3.344	14.35896	4.136	5.42256	4.928	50	66.33333	0	36.102	3.256	-0.26
420	38.81152	4.136	2	71.98664	0	4.136	24.89344	3.344	10.87328	3.696	5.34776	5.192	81.66667	72.33333	0	33.70576	3.432	0.36
421	31.57616	3.52	2	41.2984	0	3.344	21.12088	3.168	7.46768	3.168	4.2328	3.96	72	60	0	30.25616	2.64	0.79
422	68.2968	6.6	2	87.70432	0	6.16	0	5.016	NA	NA	NA	NA	NA	NA	0	0	0	2.38
423	44.90728	3.17152	2	72.5296	0	2.64	23.36136	2.64	8.58528	2.816	NA	3.696	46.33333	70	0	0	0	-0.44
424	45.54968	4.488	2	67.14488	0	4.4	27.28176	3.52	9.68352	3.97144	4.9104	3.97144	64.33333	65.33333	0	29.788	3.168	0.35
425	45.0604	3.696	2	48.93768	0	3.608	22.704	3.872	9.50928	3.35896	5.07408	3.35896	72.66667	63.33333	0	35.07328	3.4848	-0.08
426	37.92976	3.168	2	61.07728	0	3.168	22.1012	2.64	5.83088	3.168	3.44256	3.168	51.66667	67	0	37.18176	3.168	-0.53
427	48.60416	3.43552	2	78.6984	1	3.432	33.44	3.52	NA	NA	NA	NA	74	0	0	0	0	0.36
428	85.52368	3.432	3	44.89584	0	3.432	19.1796	3.256	6.138	3.432	3.22344	3.344	74	76	0	36.94064	2.904	-0.09
429	38.7508	3.256	2	66.01056	0	3.256	14.256	2.816	5.60384	3.168	2.77728	3.168	80.66667	56.66667	0	0	0	-1.05
430	48.09376	4.224	2	71.71032	0	4.224	26.85144	3.97144	8.0784	4.4	4.40616	3.608	71.33333	69.33333	0	37.0568	3.784	0.52
431	42.35528	3.168	2	61.50848	0	3.09496	24.40768	3.08	5.41376	2.904	2.794	2.904	66.66667	68.33333	0	32.38488	2.552	0
432	39.41256	3.696	2	53.68176	0	3.432	13.2	3.256	4.84352	3.2692	2.7588	3.2692	46.66667	60.66667	0	31.36144	3.08	0.53
433	35.75792	2.992	2	62.75896	3	2.904	16.10488	2.904	4.05768	2.904	2.5212	2.904	85.33333	70	0	31.3456	2.904	0.26
434	42.94136	3.18296	2	51.43072	1,3	2.992	15.31288	2.64	4.34808	3.168	2.57752	2.64	62.66667	81.66667	0	31.73632	2.816	-0.16
435	NA	NA	2	56.69664	0	2.64	12.37104	2.64	4.41056	2.64	2.2704	1.936	58	69.33333	0	27.37328	2.112	
436	46.02312	4.224	2	67.86824	0	4.224	25.432	4.224	7.832	4.224	0	4.576	0	62	0	35.83976	3.696	0.52
437	49.00632	2.552	2	62.9332	0	2.552	11.09064	2.464	5.11104	2.552	3.01312	2.64	0	64	0	0	0	-1.23
438	52.99448	4.312	2	60.9752	0	3.784	26.664	3.52	4.87256	3.696	3.2692	3.608	67	70.66667	0	37.42992	3.256	0.53
439	40.09192	2.2	2	48.85144	0	2.112	12.848	2.112	NA	NA	NA	NA	61	0	0	0	0	-0.44
440	40.83376	3.784	2	56.69312	0	3.432	18.80032	3.168	6.77512	3.696	2.7676	3.344	69.33333	61.66667	0	39.2568	2.992	1.14
441	26.78104	2.728	2	42.196	0	2.728	19.8	2.64	4.5848	2.904	2.26072	2.904	63.66667	67.66667	0	28.23216	2.64	0.35
442	35.97176	3.344	2	60.89776	0	3.168	16.10664	2.992	8.8	3.256	4.61472	2.88376	66.33333	65.33333	0	27.1436	2.728	0.7
443	33.39424	4.312	2	59.18616	0	4.048	20.9836	3.96	6.26472	4.224	4.05768	3.168	45	64.33333	0	40.93496	3.608	1.58
444	44.35288	3.872	2	56.32	0	3.52	26.18	3.432	5.7024	3.784	3.17856	3.08	62.66667	61.66667	0	34.2848	3.168	0.97
445	42.24968	2.64	2	56.09208	0	2.552	11.94512	2.112	4.84968	2.64	0	1.76	67.33333	55.33333	0	0	0	0
446	49.81328	6.864	2	106.5187	0	6.864	84.70792	5.632	NA	NA	NA	NA	72	59	0	0	0	2.72
447	37.40704	3.344	2	58.12136	0	3.256	17.16088	2.64	3.8676	2.64	2.56608	2.728	83.33333	59.66667	0	19.37936	2.64	0.61
448	33.86856	3.52	2	55.36168	0	3.168	13.82744	3.08	3.8368	3.52	2.50272	2.83272	66.33333	56.33333	0	28.864	3.168	0
449	NA	NA	2	58.08176	0	2.904	26.32344	2.992	7.12976	2.728	4.87872	2.992	109.3333	64	0	27.9092	2.112	
450	52.51752	3.256	2	24.8336	0	3.168	12.936	3.08	0	0	0	#DIV/0!	57	0	0	22.374	2.64	-0.61
451	43.41656	4.664	2	30.36176	0	4.312	14.7884	3.96	5.43136	4.224	3.07824	4.82504	86.33333	66.33333	0	37.312	3.696	0.79
452	28.17232	3.256	2	42.06136	0	2.64	21.73512	2.552	6.42664	2.904	4.06912	3.168	50.66667	69.66667	0	25.04568	2.376	0.44
453	54.30568	2.376	2	61.6308	0	2.376	NA	NA	NA	NA	NA	NA	NA	NA	0	0	0	-1.58
454	27.9048	3.168	2	55.17776	0	3.168	12.5312	2.64	4.3208	3.168	2.58984	3.08	86.66667	82.33333	0	42.064	2.64	0
455	49.21224	3.432	2	52.80528	0	3.432	17.05616	3.168	5.94792	3.256	2.76056	3.608	76.66667	73.66667	0	30.81672	2.816	-0.27
456	49.3416	4.224	2	63.01856	0	4.048	14.2648	3.784	6.72496	4.048	3.00168	4.048	113.6667	63.33333	0	37.88224	3.52	0.35
457	39.74872	3.784	2	61.68184	0	3.696	17.32896	3.608	6.17056	3.784	2.75088	3.784	105.6667	77	0	38.1964	3.256	0.52
458	30.02296	4.312	2	53.5524	0	4.224	20.97568	4.048	7.2864	4.224	4.3472	4.224	95	74	0	26.89368	3.696	0.44
459	24.89432	3.344	2	47.53232	0	3.256	16.98048	2.64	7.48264	3.168	4.81976	3.168	82.66667	75.33333	0	24.74736	3.08	0.44
460	42.11592	4.4	2	69.1724	0	4.312	25.34488	4.048	8.45328	4.224	3.97056	4.224	49.66667	47.66667	0	40.03384	3.696	0.79
461	30.23592	3.52	2	57.73064	0	3.608	23.9096	3.432	9.86656	3.168	4.45368	3.168	64.33333	59	0	2.992	2.992	0.18
462	24.40944	2.816	2	39.66336	0	2.816	20.34736	2.552	7.3392	3.168	3.85176	3.168	70	65	0	24.92336	2.376	-0.7
463	51.13416	4.048	2	80.69864	4	3.784	43.03376	3.784	NA	NA	NA	NA	57.66667	60.66667	0	0	0	0.79
464	40.39288	2.464	2	57.11552	1	2.288	15.47568	2.376	4.224	2.464	2.5652	2.376	72	70.33333	0	32.17808	1.32	-1.41
465	32.0012	3.52	2	52.80264	0	3.168	27.45952	3.168	6.79712	3.696	4.63144	3.696	93.66667	68	0	27.88544	3.08	1.58
466	34.80664	3.52	2	47.2428	1	3.432	25.87288	3.344	7.9904	3.344	5.28	3.344	56.33333	64.66667	0	28.02624	2.64	0.26
467	30.53864	2.64	2	41.49992	0	2.64	21.19392	2.64	7.03912	2.64	1.04544	2.64	83	63	0	27.65136	2.64	-1.14
468	30.26144	3.344	2	47.78664	0	3.168	16.9048	2.728	7.04616	3.168	3.3264	3.168	60	53	0	26.02688	2.64	0.17
469	49.54136	4.224	2	98.16576	1	3.696	23.11144	3.696	8.888	3.696	4.488	3.696	49	48.66667	0	34.21968	3.344	0
470	44.46816	3.344	2	60.632	0	3.608	33.26576	3.168	9.32536	3.872	6.8024	4.136	55.33333	90.66667	0	42.47056	3.168	-0.18
471	48.87608	3.432	2	57.99992	0	3.168	29.304	3.08	11.23584	3.432	5.13216	3.41528	56.33333	80.66667	0	29.19224	2.64	-0.44
472	57.47104	3.96	2	67.55496	1	3.96	21.30656	3.696	5.44368	4.048	3.33432	4.048	59.66667	64.66667	0	30.31424	3.256	-1.14
473	54.098	3.96	2	67.52152	0	3.52	31.23384	3.696	NA	3.52	NA	3.52	81.66667	0	0	35.34256	3.168	0.7
474	38.25096	3.256	2	56.87176	1	3.168	15.05944	2.64	4.3692	3.168	2.50184	3.168	51.66667	61.66667	0	39.3536	2.64	-2.02
475	44.78232	4.224	2	78.23288	0	3.96	26.3208	3.256	6.6704	4.224	3.64144	4.4	79.33333	76.66667	0	42.36848	3.696	1.05
476	70.49064	4.048	3	62.15792	0	3.96	20.32976	3.696	NA	NA	NA	NA	58.66667	66	0	24.64	3.17152	-0.09
477	34.94304	4.4	2	69.43288	0	4.18176	19.184	4.224	4.752	4.136	3.44256	4.576	62.33333	60.33333	0	41.67768	3.696	0
478	39.072	3.784	2	56.92984	0	4.136	38.43928	3.256	10.61456	4.136	6.95992	4.048	88.33333	80.66667	0	35.7764	3.168	0.26
479	35.816	3.61152	2	60.0028	0	3.70832	24.04248	3.608	6.20312	3.608	2.85208	3.256	61.66667	74.66667	0	35.04248	3.696	0.43
480	52.09688	3.256	1	75.59728	1	3.08	33.06336	2.904	8.28784	2.992	5.34688	2.728	63.66667	59.66667	0	37.25656	2.904	-1.05
481	35.992	4.664	2	58.608	0	3.784	25.344	3.872	4.72296	4.576	3.036	4.312	57.66667	59.66667	0	37.10256	3.696	1.23
482	41.27376	3.608	2	61.6	0	3.608	29.744	3.27096	8.6152	3.52352	4.39296	3.17504	64.33333	66.66667	0	26.7036	2.85472	-0.61
483	104.6637	3.696	3	23.76352	1	3.872	12.67288	3.432	5.60384	3.608	3.0096	3.60976	57.33333	64	0	32.94632	3.256	0.09
484	46.47368	3.432	2	60.8124	1	2.904	18.31104	2.91984	4.95792	3.08	2.75088	3.168	62.66667	62	0	31.80936	2.904	-1.41
485	43.67616	4.224	2	69.52264	3	3.872	28.16176	3.52	11.9592	4.136	6.42224	3.93096	70.66667	58.33333	0	29.57856	3.43552	0.7
486	38.42784	4.048	2	62.04264	0	3.82272	34.35256	3.784	8.28256	4.224	5.43488	4.224	54	67	0	34.01376	3.256	0.18
487	42.68	2.816	2	66.528	0	2.816	23.76	2.552	0	NA	NA	NA	NA	NA	0	44.616	2.376	-1.4
488	71.104	3.96	2	81.664	2	3.432	28.248	3.432	5.016	3.96	4.224	3.96	54	67	0	37.84	3.432	0
489	52.888	4.4	2	43.032	0	4.576	17.16	NA	NA	NA	NA	NA	43	49	5	36.696	3.696	1.5
490	53.856	4.224	2	72.08696	0	4.752	17.424	4.224	8.184	4.752	4.752	4.752	54	67	0	29.656	3.696	3.43
491	35.112	3.168	2	56.232	4	3.168	21.296	2.728	5.544	3.08	2.904	3.08	56.66667	50.33333	0	0	2.64	-0.7
492	38.37328	3.696	2	63.8	1	3.696	25.87992	3.696	6.38528	3.52	5.016	3.52	50.66667	60.66667	0	32.912	3.168	0.53
493	0	3.608	2	56.32	0	3.256	29.832	2.904	7.656	3.344	5.808	3.344	87	64	0	0	3.168	
494	49.03448	4.752	2	60.5572	0	4.312	33.5456	3.608	10.6744	4.136	5.05296	4.136	57.33333	60	0	28.04296	2.992	1.85
495	27.192	0.792	2	38.808	0	0.792	19.008	0.792	5.544	0.792	3.96	0.792	63	60	0	23.496	0.792	-2.73
496	32.67264	3.608	2	53.26288	0	3.608	20.328	3.432	5.632	NA	NA	NA	NA	NA	0	27.368	3.432	-0.17
497	37.70096	4.4	2	59.312	0	4.136	19.71288	4.136	5.544	4.136	3.168	4.136	NA	NA	0	43.384	3.872	1.5
498	44.00264	3.344	2	64.108	0	3.432	19.53688	2.64	4.752	NA	NA	NA	48.33333	NA	0	0	2.64	-0.53
499	34.13256	4.048	2	57.904	4	4.136	21.94808	3.872	4.752	3.872	4.752	3.872	54	62	0	33.16632	3.168	0.88
500	52.01768	3.608	2	57.99728	0	3.52	17.18376	3.432	4.488	3.52	3.432	3.52	62	56.66667	0	35.95768	3.432	-0.44
501	58.43728	4.664	3	57.32232	4	4.576	21.77736	4.048	5.544	4.488	4.752	4.488	65.33333	66	0	43.032	3.96	1.05
502	52.47792	3.696	2	87.21064	4	3.696	22.84656	3.696	6.96608	3.696	3.432	3.696	0	72.66667	0	34.18448	3.168	-0.17
503	33.352	3.168	2	64.71608	0	2.904	20.97832	2.376	6.97312	2.816	5.15152	2.816	72.33333	57.33333	0	38.808	3.168	-0.09
504	50.34216	5.104	2	68.08032	0	5.016	20.856	5.016	NA	NA	NA	NA	61.66667	0	0	42.064	4.224	0.79
505	36.87728	3.52	2	55.704	0	3.52	26.74936	3.168	9.92728	3.168	5.54928	3.168	75	51.33333	0	27.68216	3.168	0
506	31.21536	3.168	2	56.83304	0	3.168	29.39024	2.992	7.97016	2.992	4.39296	2.992	59.33333	55.66667	0	34.07624	2.816	
507	NA	NA	2	59.73968	0	3.608	24.55288	3.168	NA	NA	NA	NA	67.33333	57	0	26.73352	3.19352	
508	30.48672	3.168	2	54.38312	0	3.08	27.72352	2.816	7.03648	2.64	4.86816	2.64	56.66667	66.33333	0	30.712	2.376	-0.26
509	48.75728	4.048	2	67.22848	0	3.96	15.93152	3.784	6.9564	4.048	3.90632	4.048	64.66667	61	0	37.0524	3.168	0.51
510	0	4.224	2	77.65912	1	4.224	25.49624	3.696	9.812	4.224	4.90776	4.224	52.66667	65	0	37.488	3.696	0
511	43.4148	2.64	2	57.02664	0	2.64	25.344	2.64	7.656	2.64	4.752	2.64	65	58	0	28.9828	2.64	-1.5
512	31.13176	2.904	2	49.05472	0	2.904	23.04896	2.64	9.67384	2.64	5.96728	2.64	55.66667	62	0	25.88872	2.376	-0.36
513	44.7788	4.664	2	65.83632	0	4.576	25.608	4.224	NA	NA	NA	NA	67.33333	0	0	0	0	1.32
514	43.3356	4.224	2	64.196	0	3.872	30.89152	3.168	8.73312	3.872	5.44368	3.872	43.66667	50.33333	0	33.18656	3.168	0.96
515	44.8536	3.96	2	83.07288	0	3.608	22.57464	3.432	7.01976	3.96	5.12688	3.96	52.66667	55.33333	0	38.27648	3.432	-0.53

516	47.35192	4.048	2	78.10352	0	4.136	NA	NA	NA	NA	NA	NA	67	55	0	30.3512	3.344	0.18
517	44.55968	3.96	2	59.84088	0	3.784	29.95872	3.696	9.96336	3.872	6.0192	3.872	53.66667	52	0	33.56584	3.168	-0.44
518	35.83888	2.64	3	41.02296	1	2.64	29.656	2.64	8.87128	2.464	4.5408	2.464	52.66667	63.33333	0	0	2.288	-0.7
519	48.61032	2.904	2	75.54008	0	3.344	26.25568	3.256	6.77512	3.52	4.554	3.52	102.6667	59.66667	0	32.8284	3.256	-0.8
520	42.21096	4.224	2	70.1844	0	4.224	20.43976	3.696	6.77864	4.224	4.796	4.224	93	82.66667	0	43.9076	3.696	-0.09
521	33.17424	4.312	2	60.13568	4	4.136	24.20088	3.96	6.48032	4.224	4.35072	4.224	45.66667	50.66667	0	31.49608	3.432	1.32
522	26.4088	3.696	2	63.36352	0	3.696	28.88248	3.432	10.12352	3.256	6.4504	3.256	55.33333	52.33333	0	30.31248	3.344	0.27
523	52.72432	3.344	3	40.65864	0	3.432	21.9472	2.904	NA	NA	NA	NA	69.33333	62.66667	0	0	2.728	0
524	30.0124	3.344	2	51.30576	1	3.432	29.392	2.904	9.82256	3.168	6.17848	3.168	54.33333	57	0	37.708	2.904	0.35
525	31.15024	3.432	2	45.67904	1	2.992	20.26288	2.904	8.37672	3.256	18.74224	3.256	43.33333	53.66667	0	26.69304	2.904	-0.09
526	37.928	3.872	2	63.272	0	4.136	24.55376	3.52	8.59848	3.872	5.28	3.872	62.66667	54	0	0	0	0.17
527	0	3.168	2	65.81256	0	3.168	22.71016	3.08	6.10368	3.168	3.17856	3.168	47	59	0	43.57936	3.168	-1.32
528	36.784	3.696	2	57.904	0	3.696	19.272	3.52	7.28816	3.52	4.49592	3.52	55	59.66667	0	25.08616	3.432	0.27
529	40.39112	2.112	2	48.19672	0	2.112	11.75856	2.112	6.64752	2.112	5.12688	2.112	42.66667	49.33333	0	36.9336	0	-1.06
530	52.4612	3.168	2	30.096	4	3.168	18.21776	3.168	4.39296	3.168	2.43408	3.168	47.66667	49	0	39.40376	3.168	-0.53
531	0	3.96	2	58.35544	0	3.608	25.24192	3.432	8.7868	3.432	6.50232	3.432	51.33333	50.33333	0	31.94488	3.256	0.79
532	35.024	3.696	2	76.56	0	3.696	18.744	3.696	8.448	3.696	6.336	3.696	44.33333	44	0	38.984	3.168	-0.35
533	33.12936	3.52	2	62.33216	0	3.52	15.57776	3.432	3.96	3.432	2.64	3.432	52.33333	50	0	33.34496	3.168	0.26
534	33.1364	3.168	2	56.41944	0	3.432	24.55288	3.168	8.5844	2.904	5.96552	2.7632	53.66667	49.33333	0	38.09168	3.168	-0.09
535	28.73376	4.048	2	48.86112	0	4.136	23.9052	3.872	8.01416	3.784	5.41728	3.81128	64.66667	59.33333	0	24.464	3.08	0.53
536	41.10128	3.168	2	42.47936	0	3.168	18.48176	3.168	6.38616	3.168	4.29792	3.168	44.33333	55.66667	0	28.39496	2.904	-1.05
537	46.112	3.608	2	64.52952	0	3.432	28.85432	3.256	8.97864	3.432	4.9104	3.432	53	50.66667	0	36.65816	3.168	0.18
538	41.85808	3.168	2	67.68696	0	3.168	20.064	3.168	8.448	3.168	4.752	3.1196	50.66667	50	0	0	0	-0.17
539	45.39304	3.784	2	75.78648	0	4.136	21.67528	3.872	8.976	3.52	6.4944	3.52	59.66667	54.66667	0	39.37472	2.992	0.88
540	33.17864	3.432	2	56.9624	0	3.432	22.53152	3.168	8.85192	3.168	6.18552	3.168	57.33333	54.33333	0	27.808	3.168	-0.09
541	NA	3.432	2	56.4212	0	3.168	25.9556	3.168	8.13384	3.168	4.85232	3.168	67.66667	67	0	32.06192	2.376	0.26
542	48.55312	3.696	2	70.57952	0	3.344	18.61464	3.168	6.2964	3.696	3.17856	3.696	60.66667	65.33333	0	37.21168	3.168	0
543	NA	3.432	2	54.68408	0	3.608	32.41656	3.256	8.82464	3.432	6.1864	3.432	68.66667	51.33333	0	31.8604	3.08	0.09
544	58.46984	3.432	3	46.30208	0	3.432	30.60552	3.432	8.36	3.52	5.6496	3.52	80.66667	66.66667	0	36.70216	2.904	-0.79
545	39.43456	3.168	2	54.03552	4	3.168	18.5944	3.168	6.62112	3.168	4.10784	3.168	55.66667	66.33333	0	39.11864	2.64	0
546	48.84352	3.696	2	64.29456	0	3.696	16.37504	3.608	5.28	3.696	3.66696	3.696	49.33333	47.33333	0	39.49792	3.608	0.53
547	31.86128	3.344	2	55.17864	0	3.168	24.55728	3.168	9.79968	3.432	4.3692	3.432	66.66667	57.33333	0	39.16792	3.432	0
548	41.30544	3.168	2	24.0504	0	3.168	13.992	2.904	3.78048	3.168	3.0096	3.168	47.33333	60	0	34.056	2.64	0
549	61.67216	4.488	2	60.5088	0	4.576	18.18432	3.96	8.59848	4.488	5.016	4.4396	54.33333	44.66667	0	44.5764	3.432	0.27
550	51.20104	3.344	2	77.46816	0	3.168	25.08176	2.904	10.03464	2.288	6.1644	2.288	59.66667	52	0	0	3.168	-0.27
551	41.71288	3.608	2	81.66488	4	3.696	18.29696	3.696	5.544	3.696	3.432	3.696	47.33333	50.66667	0	42.47232	3.168	-0.09
552	83.24976	2.904	3	44.73832	0	2.904	26.136	2.904	9.52688	2.904	7.01976	2.904	43.33333	47	0	29.56624	2.64	-0.62
553	35.552	3.96	2	62.48	0	4.136	34.32	3.696	8.712	4.224	4.488	4.224	48.66667	51	0	34.584	3.432	0
554	43.61544	3.696	2	66.40744	0	3.256	27.89688	3.52	10.04696	3.344	7.128	3.344	53.66667	43.66667	0	26.52232	3.256	-0.08

Description of CTA data set

Variable description and characteristics in the cross-sectional dataset (data.txt)

Variable	Description	Coding	Notes
KZCODE	Patient ID		
SEX		1=male 0=female	
AGE		continuous	
RACE		1=black 2=Indian 3=white 4=colored	
VOR or L	VA origin on right or left	1=SCA 2=AOA 3=BCT 4= RCCA 5= LCCA	
PTV1R or L	Presence of tortuosity at V1 right or left	0=no 1= mild 2=Coil 3=single loop 4=multiple loop 5=twisting	

Pattern of Dominance		1=left dominance 2=right dominance 3=codominance	
Variation at Distal VA		0=No variation 1=Rt Atresia 2=Lt Atresia 3=PICA at V3vR 4=PICA at V3hR 5=PICA at V3oR 6=PICA at V3vL 7=PICA at V3hL 8=PICA at V3oL 9=Hypoplastic terminal right 10=Hypoplastic terminal left 11=Bilateral PICA 12=Unilateral double PICA 14= Bilateral double PICA 15=fenestration 16= Bilateral absence of PICA 17=AICA ss area of PICA 18=Unilateral PICA RT 19 =Unilateral PICA LT	
V4 VAR		1=Rt Atresia 2=Lt Atresia 9=Hypoplastic terminal right 10=Hypoplastic terminal left	
V1LR or L	Length of V1 right or left	Continuous	
V1DR or L	Diameter of V1 right or left	Continuous	
ELR or L	Level of entry to the transverse foramen	1=C7 2=C6 3=C5 4=C4 5=C3	

V2LR or L	Length of V2 right or left	continuous	
PTV2R or L	Presence of tortuosity at V2 right or left	1=yes 0=no	
V2DR or L	Diameter of V2 right or left	continuous	
V3VR or L	Vertical length of V3 right or left	continuous	
V3VDR or L	Vertical diameter of V3 right or left	continuous	
V3HR or L	Horizontal length of V3 right or left	continuous	
V3HDR or L	Horizontal diameter of V3 right or left	continuous	
V3OR or L	Oblique length of V3 right or left	continuous	
V3ODR or L	Oblique diameter of V3 right or left	continuous	
V3PLR or L	Proximal loop at V3 right or left	continuous	
V3DLR or L	Distal loop at V3 right or left	continuous	
V4LR or L	Length of V4 right or left	continuous	
V4DR or L	Diameter of V4 right or left	continuous	
PICAR or L	Presence of PICA right or left	1=yes 0=no 3=PICA at V3vR 4=PICA at V3hR 5=PICA at V3oR 6=PICA at V3vL 7=PICA at V3hL 8=PICA at V3oL 18=Unilateral PICA RT	

		19 =Unilateral PICA LT	
VBA	Angle at vertebrobasilar junction	continuous	
LGA	Local geometry of the apex	1=sharp edge 2=blunt edge	
NA	Missing data		

Abbreviations: VA = vertebral artery, SCA= subclavian artery, AOA=arch of aorta, BCT=brachiocephalic trunk, RCCA= right common carotid artery, LCCA=left common carotid artery, PICA=posterior inferior cerebral artery

www.nature.com/scientificreports

scientific reports

OPEN

Radiological anatomy of the intracranial vertebral artery in a select South African cohort of patients

B. R. Omotoso[1], R. Harrichandparsad[2], K. S. Satyapal[1], I. G. Moodley[3] & L. Lazarus[1]✉

The intracranial segment of the vertebral artery (VA) is the unique part of the artery where the two VAs join to form a single vascular channel, viz. the basilar artery. In addition to this typical description, anatomical variations have been described; the presence of anatomical variation has been associated with some pathological processes, neurological complications, and the risk of vascular diseases in the posterior circulatory territory. We evaluated the typical anatomical features and variations of the VA4 component of the VA in a South African population to provide useful data on the prevalence of variation and morphometry of the distal VA. The study is an observational, retrospective chart review of 554 consecutive South African patients (Black, Indian, and Caucasian) who had been examined with multidetector computed tomography angiography (MDCTA) from January 2009 to September 2019. We observed various anatomical variations in the VA4 segment of the VA. We report the incidence of VA hypoplasia, hypoplastic terminal VA, and atresia. Fenestration and duplicate posterior inferior cerebellar artery (PICA) origin were also observed. The left intracranial VA was significantly larger than the right. Our study shows that anatomical variation of the intracranial VA is common in the population studied, with a total prevalence of 36.5%. Understanding the patterns of anatomical variations of the VAs will contribute significantly to the interpretation of ischemic areas and diagnosis of various diseases in the posterior circulatory territory.

The vertebral artery (VA) emanates from the supero-posterior part of the subclavian artery and proceeds through the foramen transversarium of the sixth to first cervical vertebrae. The left and right VA penetrates the dura mater to enter the intracranial space through the foramen magnum, where they converge to form the basilar trunk at the pontomedullary junction[1]. Anatomically, the VA is divided into four segments. The first three segments (VA1, VA2, VA3) are the extracranial segments, extending from the origin to where they penetrate the dura mater. The fourth segment of the VA (VA4) is intracranial, extending from the foramen magnum to the point where the left and right VA anastomose to form the basilar trunk[1]. The geometry of the basilar trunk depends on the pattern of the bilateral VAs. When there is an asymmetry of bilateral VAs or other anatomical variations, the basilar trunk sometimes bends away from the midline[2]. Previously reported anatomical variations of the intracranial VAs include VA terminating as posterior inferior cerebellar artery (PICA), known as atresia, fenestration, asymmetry, and hypoplasia. Anatomical variations play a significant role in the clinical sequelae of an iatrogenic VA injury, which can vary widely[3]. For instance, damage to the dominant VA when the contralateral VA terminates as PICA can result in devastating complications since the dominant VA solely forms the basilar artery.

The presence of variation has been associated with some pathological processes, neurological complications, and the risk of vascular diseases in the posterior circulatory territory. For instance, atresia and hypoplasia have been associated with hypoperfusion of brain tissues and hemodynamic insufficiency, which may predispose to transient ischaemic attacks or acute brainstem ischaemic stroke[4,5].

Reports on the prevalence of anatomical variations of the intracranial VA are scarce, with few previous reports in the Western population (Caucasians)[1], the Asian population[4], and the Turkish population[6]. Previous studies

[1]Discipline of Clinical Anatomy, School of Laboratory Medicine and Medical Sciences, College of Health Sciences, University of KwaZulu-Natal, Westville Campus, Private Bag X54001, Durban 4000, South Africa. [2]Department of Neurosurgery, School of Clinical Medicine, College of Health Sciences, Nelson R Mandela School of Medicine, University of KwaZulu-Natal, Durban, South Africa. [3]Department of Radiology, Jackpersad and Partners Inc, Specialist Diagnostic Radiologists, Lenmed Ethekwini Hospital and Heart Centre, Durban, South Africa. ✉email: ramsaroopl@ukzn.ac.za

from the African continent used postmortem and cadaveric histological samples to report on average diameter and incidence of VA hypoplasia[7–9]. Advances in modern imaging technology that led to the establishment of multidetector computed tomography angiography (MDCTA) have made endovascular procedures popular. These procedures require a detailed understanding of typical anatomy and the extent of anatomical variations of the VAs. Consequently, a report on the prevalence of possible variant anatomy will help in the interpretation of radiographs, prevention of iatrogenic injuries, and contribute to the advancement of non-invasive surgical intervention.

In the present study, we assessed the typical anatomical features and variations of the V4 segment of the VA using MDCTA. We aimed to determine the dimensional characteristics and prevalence of anatomical variations of the intracranial VA in a South African population. Due to the multiracial composition of the South African population, in addition to the overall incidence of variation, we also report variations based on three racial groups: Black, Indian, and Caucasian South African. It is necessary to have correct and detailed information about the typical anatomy and prevalence of anatomical variations. Such information is essential before neurosurgery, endovascular and non-invasive procedures. The detailed information from this study will be useful in neurosurgery, anatomy, endovascular, and non-invasive procedures.

Materials and methods

Study population. This study is a retrospective observational review of 554 MDCTA images of South African patients. The patients underwent MDCTA for various reasons between January 2009 and September 2019. Images were obtained from the database of Lenmed Ethekwini Hospital and Heart Center, Durban, South Africa. The Biomedical Research Ethics Committee of the University of KwaZulu-Natal approved the study (Ethical No: BE 148/19) and waived the need for informed consent as this study utilized retrospective chart reviews. There was no patient contact, and no patient details were released from images. All methods were carried out in accordance with relevant guidelines and regulations. Exclusion criteria included MDCTA scans that showed no clarity of the VA's course, scans with motion artifacts or poor-quality imaging, and scans performed on foreign patients or obtained outside a hospital. The angiographies were from 307 males (55.4%) and 247 females (44.6%). The average age of the patients is reported as median (interquartile range 〔IQR〕): 62 (23) (range: 10–99) years; 61 (23) for male patients and 62 (25) for female patients. Race was defined according to the guidelines outlined in the modern systems of racial classification in the Republic of South Africa[10]. The criteria used in the scheme of racial classification include skin colour and ancestry. The South African population is divided into four main racial groups: Caucasian, Black, Indian, and Coloured. Three population groups were included in the present study: Black 91 (16.4%), Indian 176 (31.8%), and Caucasian 287 (51.8%). According to the modern system of classification, a Caucasian was defined as a person of European descent. A Black individual was defined as a person having origins in any of indigenous Africa or Native group. An Indian individual was defined as a person of Asian descent[10].

MDCTA protocol. The imaging examination was performed on a 64-detector row 160-slice helical multidetector computed tomography scanner (Lightspeed CT, GE Healthcare Medical Systems, Milwaukee, WI, USA). In our standard MDCTA protocol for brain examinations, a scan coverage area from the aortic arch to the top of the brain in a supine position (headfirst) was adopted as a field of view (FOV). The scanning protocol was as follows: 120 kVp, 500 mAs, beam collimation 64 × 0.625 mm, speed 20.62 mm/rotation, gantry rotation time 0.35 s/rotation, the helical thickness of 0.625 mm, pitch 0.516:1, and reconstruction interval of 0.625 mm. Following the acquisition of the nonenhanced CT data, contrast-enhanced MDCTA was performed. During the procedure, a 20 Gauge needle (Pink Nexiva) was used to cannulate patients for IV access in the antecubital region to administer 60 mL of Ioversol (Optiray 350; Guerbet South Africa). This was followed by a 40 mL saline flush via a double power injector (Medex flowSens, Guerbet USA) into the patient's antecubital vein (4 mL/s), and the scan delay was individually adapted using a bolus-tracking technique. First, a single nonenhanced low-dose scan at the upper neck level was obtained for the bolus tracking. With the start of contrast material administration, repeated low dose monitoring scans were obtained every second. Following the appearance of the first contrast in the aortic arch, the MDCTA was triggered automatically without delay. The region of interest was positioned at the aortic arch, and the threshold for the MDCTA was set as 150 Hounsfield Units. When the threshold was surpassed, helical scanning was automatically initiated.

Imaging reconstruction. Postprocessing of three-dimensional images was performed using multiplanar reformation (MPR), maximum intensity projection (MIP), multiplanar reconstruction (MPR), and volume rendering (VR) algorithms. The volumetric MDCTA data sets were processed on Advanced Workstation 4.2 (GE Healthcare, Milwaukee, WI, USA). A series of 17 projection images at every 20° around the cephalocaudal axis were generated and transfer to the picture archiving communication system (PACS). The MDCTAs were performed for diagnostic purposes in the context of various cerebrovascular accidents or diseases. In some cases, the suspected diseases were not found on the MDCTA; thus, some materials in this study were derived from a healthy population.

Analysis of anatomical variations and dimensions of the V4 segment. The MDCTA images were analyzed using PACS tools. The images were examined for vascular variations by a neurosurgeon, a neuroradiologist, and an anatomist using the coronal and sagittal view and the 3D reconstructed images. Each MDCTA image was examined for the presence of anatomical variations. In atresia, the VA did not fuse with the contralateral VA but terminates as PICA. The hypoplastic terminal V4 segment was registered when the terminal portion divides into a PICA and a tiny branch that joins the contralateral dominant VA. Fenestration was registered

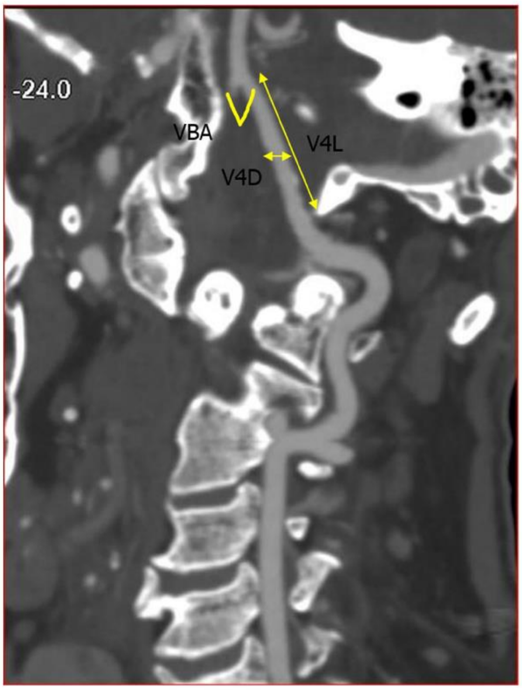

Figure 1. Oblique view of CTA image, showing the V3 and V4 segments of the VA. V4L length of the V4 segment; V4D Diameter of the V4 segment; VBA the angle at the vertebrobasilar junction.

when the VA split into two vessels, which later rejoined distally. The following parameters were measured on a coronal and oblique view of the MDCTA (Fig. 1): 1) the diameters were measured along the course of the VA at a distance of 11 mm cranial to the entrance of the VA into the foramen magnum, 2) the length of the VAs was measured from the foramen magnum to the point of union with the contralateral VA, and 3) the angle between the bilateral VA at the vertebrobasilar junction. We were unable to appropriately quantify the frequency of the PICA and the spinal arteries because visualization of branches (such as the PICA and spinal arteries) is usually beyond the limits of the MDCTA. A diameter of ≤ 2 mm was described as hypoplasia; we classified the VA as dominant if the diameter was larger than that of the contralateral side by any size difference according to the method provided by Ergun and co-authors[11]. When the bilateral VAs had a similar diameter, we referred to them as "equal" or "codominant." Results were analyzed separately for the left and right sides.

Statistical analysis. All data were analyzed using SPSS version 27 (SPSS Inc., Chicago, IL, USA). Categorical variables were analyzed using the chi-square test. A Kolmogorov–Smirnov test was used to assess the normal distribution of continuous data. Because the distribution of the data was not normal, nonparametric tests were used. The Kruskal–Wallis test followed by the Wilcoxon Signed-Rank test was used to detect significant differences in the obtained values. The interclass correlation coefficient was used to examine the reliability of measurements. All tests were performed at 95% confidence with a p-value of <0.05.

Ethics approval. The design was approved by the Institutional Review Board/Ethics Committee (Biomedical Research Ethics Committee of the University of KwaZulu-Natal with ethical No: BE 148/19).

Results

Continuous and categorical data are presented as the median and IQR and percentage (N). The interclass correlation coefficient for intra-observer reliability testing was 92% for V4 length, 93% for diameter, and 96% for the angle at the VBJ. For inter-observer reliability testing, the intraclass correlation was 85% for V4 length and diameter; 87% for the angle at the VBJ.

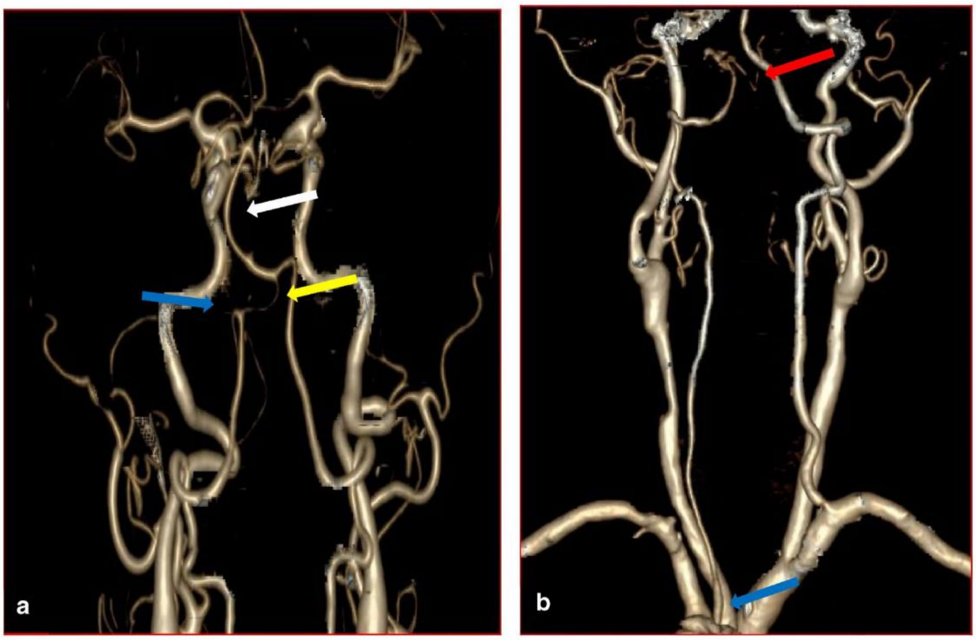

Figure 2. 3D-CTA reconstructed images showing the vertebral, the subclavian, and the carotid arteries. (**a**) The blue arrow indicates PICA. The yellow arrow indicates hypoplastic terminal VA while the white arrow indicates the bending basilar artery. (**b**) The blue arrow illustrates the origin of the left VA from the arch of the aorta, and the red arrow shows the termination of ipsilateral VA as PICA.

Variation in morphology. We observed the following variations of the intracranial segment: (1) The hypoplastic terminal VA (Fig. 2a) and hypoplasia of VA (Fig. 3a). (2) VA terminating as PICA (Atresia) (Figs. 2b and 3b). (3) Fenestration (One was observed at the right intracranial VA (Fig. 4a), while the other was observed at the vertebrobasilar junction). (4) Duplicate origin of the PICA (Fig. 4b). The incidence of these variations is summarized in Table 1. The incidence of VA hypoplasia is significantly high in Caucasian, followed by Indian on the right ($p=0.01$). There was no significant difference across the races on the left ($p=0.61$). Also, there was no significant racial difference in the incidence of hypoplastic terminal VA ($p=0.26$) and atresia ($p=0.54$). The incidence of variation across the races is summarized in Table 2. Because visualization of branches of the intracranial VA (PICA and spinal arteries) is usually beyond the limits of MDCTA, the frequency of PICA on the left, right, and bilateral PICA in the present study is low (15.7%, 13.9%, and 14.8%, respectively). We also observed bilateral and unilateral double PICA in 5 patients. Therefore, we cannot appropriately quantify the frequency of the PICA in all the VAs.

Morphometric analysis of the intracranial vertebral arteries. *Diameter.* The average diameter of the left VA (3.17 (0.62) mm) was similar to that of the right VA (3.17 (0.7) mm). However, the Wilcoxon Signed-Rank test showed a significant difference ($p<0.001$). This is because the Wilcoxon Signed-Rank test is a rank-sum test and not a median test. The sum of positive Ranks of the left VA was significantly greater than that of the right VA. We observed a left pattern of dominance in 45.3% (251/554) patients; the right side was dominant in 32.7% (181/554) patients. The left and right VAs was equal in diameter in 15.3% (85/554) patients. Concerning the racial groups, no significant differences were observed (Right VA, $p=0.567$; Left VA, $p=0.180$). The group diameters are summarized in Table 3. For gender, the diameters are summarized in Table 4. There were no significant gender differences in VA diameter (Right VA, $p=0.528$; Left VA, $p=0.274$).

Length. The length of the left (32.36 (7.18) mm) intracranial VA was significantly greater than the right (31.50 (7.22) mm). Within the racial groups, there were no significant differences (Right VA, $p=0.386$; Left VA, $p=0.708$). The average length and laterality of the VA across the racial groups are summarized in Table 3. There were no significant gender differences in the length of the VA (Right VA, $p=0.665$; Left VA, $p=0.615$). The results are summarized in Table 4.

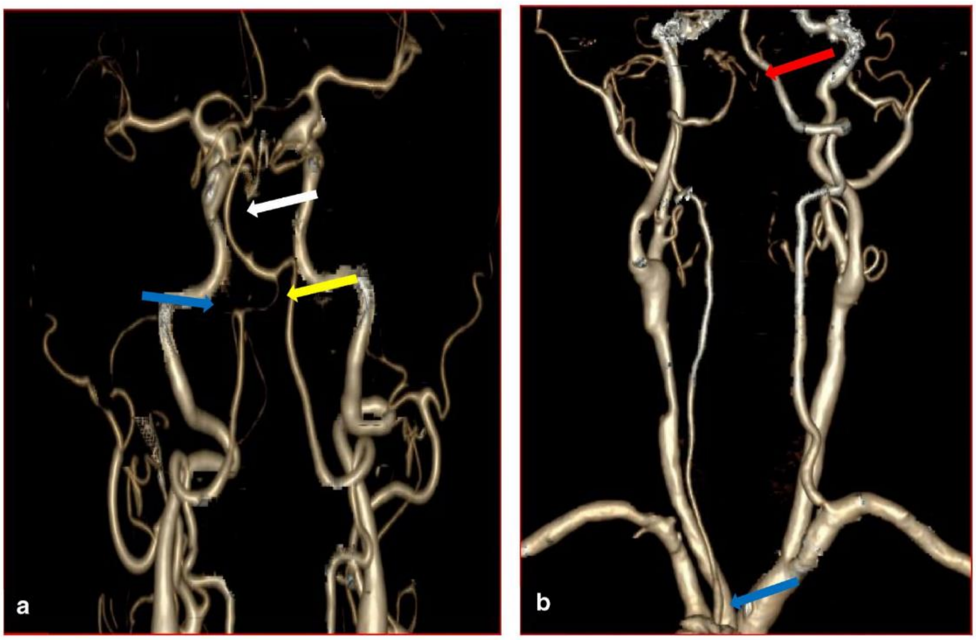

Figure 2. 3D-CTA reconstructed images showing the vertebral, the subclavian, and the carotid arteries. (**a**) The blue arrow indicates PICA. The yellow arrow indicates hypoplastic terminal VA while the white arrow indicates the bending basilar artery. (**b**) The blue arrow illustrates the origin of the left VA from the arch of the aorta, and the red arrow shows the termination of ipsilateral VA as PICA.

Variation in morphology. We observed the following variations of the intracranial segment: (1) The hypoplastic terminal VA (Fig. 2a) and hypoplasia of VA (Fig. 3a). (2) VA terminating as PICA (Atresia) (Figs. 2b and 3b). (3) Fenestration (One was observed at the right intracranial VA (Fig. 4a), while the other was observed at the vertebrobasilar junction). (4) Duplicate origin of the PICA (Fig. 4b). The incidence of these variations is summarized in Table 1. The incidence of VA hypoplasia is significantly high in Caucasian, followed by Indian on the right ($p=0.01$). There was no significant difference across the races on the left ($p=0.61$). Also, there was no significant racial difference in the incidence of hypoplastic terminal VA ($p=0.26$) and atresia ($p=0.54$). The incidence of variation across the races is summarized in Table 2. Because visualization of branches of the intracranial VA (PICA and spinal arteries) is usually beyond the limits of MDCTA, the frequency of PICA on the left, right, and bilateral PICA in the present study is low (15.7%, 13.9%, and 14.8%, respectively). We also observed bilateral and unilateral double PICA in 5 patients. Therefore, we cannot appropriately quantify the frequency of the PICA in all the VAs.

Morphometric analysis of the intracranial vertebral arteries. *Diameter.* The average diameter of the left VA (3.17 (0.62) mm) was similar to that of the right VA (3.17 (0.7) mm). However, the Wilcoxon Signed-Rank test showed a significant difference ($p<0.001$). This is because the Wilcoxon Signed-Rank test is a rank-sum test and not a median test. The sum of positive Ranks of the left VA was significantly greater than that of the right VA. We observed a left pattern of dominance in 45.3% (251/554) patients; the right side was dominant in 32.7% (181/554) patients. The left and right VAs was equal in diameter in 15.3% (85/554) patients. Concerning the racial groups, no significant differences were observed (Right VA, $p=0.567$; Left VA, $p=0.180$). The group diameters are summarized in Table 3. For gender, the diameters are summarized in Table 4. There were no significant gender differences in VA diameter (Right VA, $p=0.528$; Left VA, $p=0.274$).

Length. The length of the left (32.36 (7.18) mm) intracranial VA was significantly greater than the right (31.50 (7.22) mm). Within the racial groups, there were no significant differences (Right VA, $p=0.386$; Left VA, $p=0.708$). The average length and laterality of the VA across the racial groups are summarized in Table 3. There were no significant gender differences in the length of the VA (Right VA, $p=0.665$; Left VA, $p=0.615$). The results are summarized in Table 4.

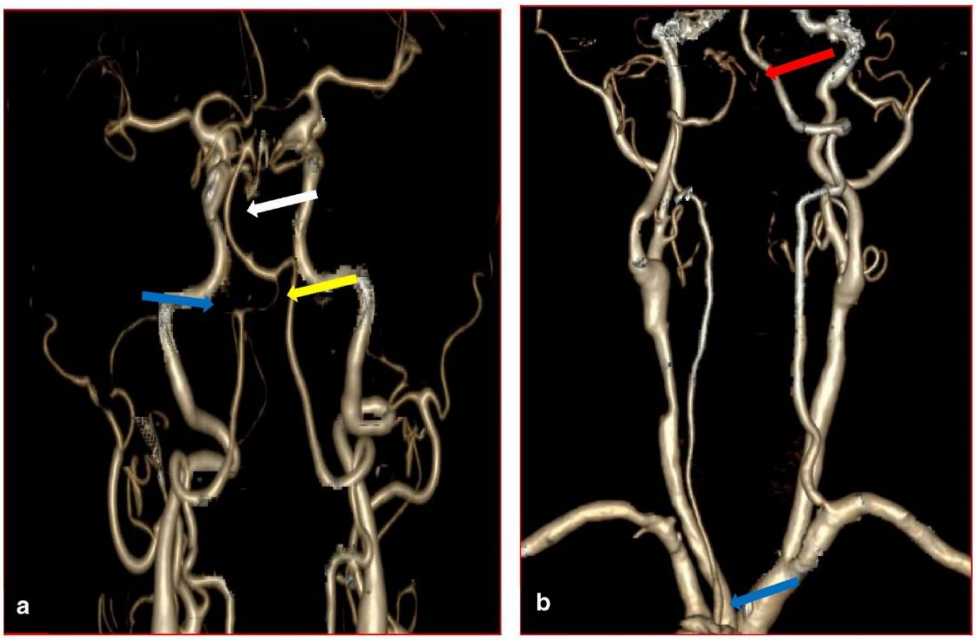

Figure 2. 3D-CTA reconstructed images showing the vertebral, the subclavian, and the carotid arteries. (**a**) The blue arrow indicates PICA. The yellow arrow indicates hypoplastic terminal VA while the white arrow indicates the bending basilar artery. (**b**) The blue arrow illustrates the origin of the left VA from the arch of the aorta, and the red arrow shows the termination of ipsilateral VA as PICA.

Variation in morphology. We observed the following variations of the intracranial segment: (1) The hypoplastic terminal VA (Fig. 2a) and hypoplasia of VA (Fig. 3a). (2) VA terminating as PICA (Atresia) (Figs. 2b and 3b). (3) Fenestration (One was observed at the right intracranial VA (Fig. 4a), while the other was observed at the vertebrobasilar junction). (4) Duplicate origin of the PICA (Fig. 4b). The incidence of these variations is summarized in Table 1. The incidence of VA hypoplasia is significantly high in Caucasian, followed by Indian on the right ($p=0.01$). There was no significant difference across the races on the left ($p=0.61$). Also, there was no significant racial difference in the incidence of hypoplastic terminal VA ($p=0.26$) and atresia ($p=0.54$). The incidence of variation across the races is summarized in Table 2. Because visualization of branches of the intracranial VA (PICA and spinal arteries) is usually beyond the limits of MDCTA, the frequency of PICA on the left, right, and bilateral PICA in the present study is low (15.7%, 13.9%, and 14.8%, respectively). We also observed bilateral and unilateral double PICA in 5 patients. Therefore, we cannot appropriately quantify the frequency of the PICA in all the VAs.

Morphometric analysis of the intracranial vertebral arteries. *Diameter.* The average diameter of the left VA (3.17 (0.62) mm) was similar to that of the right VA (3.17 (0.7) mm). However, the Wilcoxon Signed-Rank test showed a significant difference ($p<0.001$). This is because the Wilcoxon Signed-Rank test is a rank-sum test and not a median test. The sum of positive Ranks of the left VA was significantly greater than that of the right VA. We observed a left pattern of dominance in 45.3% (251/554) patients; the right side was dominant in 32.7% (181/554) patients. The left and right VAs was equal in diameter in 15.3% (85/554) patients. Concerning the racial groups, no significant differences were observed (Right VA, $p=0.567$; Left VA, $p=0.180$). The group diameters are summarized in Table 3. For gender, the diameters are summarized in Table 4. There were no significant gender differences in VA diameter (Right VA, $p=0.528$; Left VA, $p=0.274$).

Length. The length of the left (32.36 (7.18) mm) intracranial VA was significantly greater than the right (31.50 (7.22) mm). Within the racial groups, there were no significant differences (Right VA, $p=0.386$; Left VA, $p=0.708$). The average length and laterality of the VA across the racial groups are summarized in Table 3. There were no significant gender differences in the length of the VA (Right VA, $p=0.665$; Left VA, $p=0.615$). The results are summarized in Table 4.

Type of Variation	Total number of patients (incidence%)	Left/Right/Bilateral	Male/Female
Hypoplasia	89 (16.1)	36/46/7	56/33
Hypoplastic terminal VA	73 (13.2)	37/36/0	46/27
VA terminating as PICA (Atresia)	37 (6.7)	15/22/0	24/13
Fenestration	2 (0.4)	0/1/0	1/1
Duplicate PICA origin	1 (0.2)	0/1/0	0/1

Table 1. Incidence of anatomical variations at the intracranial segment (V4) of the VA diagnosed by MDCTA.

		Race		
		Black	Indian	White
Type of Variation	Total number of patients (incidence%)	Left/Right/Bilateral	Left/Right/Bilateral	Left/Right/Bilateral
Hypoplasia	89 (16.1)	5/5/1	10/19/3	21/22/3
Hypoplastic terminal VA	73 (13.2)	9/3/0	8/15/0	20/18/0
VA terminating as PICA (Atresia)	37 (6.7)	1/2/0	4/9/0	10/11/0
Fenestration	2 (0.4)	0	0	0/1/1
Duplicate PICA origin	1 (0.2)	0	0	0/1/0

Table 2. Incidence of anatomical variations at the intracranial segment (V4) of the VA grouped according to race in South African patients.

	Black		Indian		White	
	Left	Right	Left	Right	Left	Right
V4 Diameter	3.17 (0.7)	3.17 (0.7)	3.17 (0.69)	3.17 (0.7)	3.17 (0.62)	3.17 (0.68)
V4 Length	32.74 (9.13)	30.71 (9.15)	32.20 (7.74)	30.86 (8.6)	32.38 (6.87)	31.61 (6.34)

Table 3. Diameter and length of the vertebral artery V4 segment grouped according to race and laterality in South African patients. Results are reported as median (*IQR* interquartile range) mm.

	Male		Female	
	Left	Right	Left	Right
V4 Diameter	3.17 (0.62)	3.17 (0.7)	3.17 (0.62)	3.17 (0.62)
V4 Length	32.29 (7.34)	31.59 (6.92)	32.38 (6.68)	31.48 (7.69)

Table 4. Diameter and length of the vertebral artery V4 segment grouped according to gender and laterality in South African patients. Results are reported as median (*IQR* interquartile range) mm.

Other authors suggested that this anatomical variation may have resulted from variation in the persistence of standard anastomosis between the lateral spinal artery and the PICA[30]. Considering the unique embryogenesis, adequate perfusion of the regions supplied by the PICA may rely on flow from both origins[29]. Since duplicate PICA origin is an uncommon variation with few previous reports, it should not be overlooked when evaluating the diagnosis and surgical intervention images.

The average diameter and length of the VA in our result is consistent with the previous report on a South American population (Diameter Left- 3.12 ± 0.85 mm, Right- 2.94 ± 0.77 mm; Length Left- 33.86 ± 5.59 mm, Right- 32.47 ± 4.8 mm)[31] based on autopsy samples and another angiographic study of the Caucasians (Diameter Left- 3.16 ± 0.63 mm, Right- 2.78 ± 0.44 mm; Length Left- 31.51 ± 6.51 mm Right- 24.25 ± 6.76 mm)[1]. We observed a significantly larger diameter on the left than the right VA, comparable to the previous reports mentioned above. Interestingly, there was no significant difference across the racial groups and gender in our series. By contrast, a previous histological study of a South African population (Witwatersrand region) reported an average diameter (Left- 2.68 ± 0.86 mm, Right- 2.53 ± 0.75 mm)[7] that was lower than the present study. The differences in the study modalities (MDCTA vs. cadaveric) may be responsible for the contrariety noticed in the results. Tissue shrinkage associated with histological tissue processing may be the reason for the reduced diameter.

We described the pattern of dominance using the criterion of any size difference between the left and right VA; 45.3% showed left dominance, 32.7% showed right dominance, and 15.3% showed codominance. Using a similar criterion, Ozdemir et al. reported similar results of left dominance in 64% of patients and right dominance in 31% of patients[32]. In contrast, Ergun and co-authors reported right VA dominance in 49.5% and left dominance in 47.2% of patients using a similar criterion as described above[11]. Our result shows that most of the patients have left dominant VAs. Noticeably, we observed more VA hypoplasia and atresia on the right. Knowledge of the dominant VA is required for some endovascular procedures. It is also important to preserve the dominant VA since they are likely to predominates the basilar artery. This information is vital to reduce the risk of neurological symptoms that may results from iatrogenic injury.

The angle at the vertebrobasilar junction in the present study is comparable with the report of Songur et al. ($52.2 \pm 18.2°$)[6]. On the contrary, other authors reported a larger mean angle ($85.45 \pm 10.76°$)[1]. The disparity may have resulted from the confluence of the bilateral VA, which can either be a sharp or blunt edge depending on the pattern and frequency of asymmetry. In atresia, the VA did not fuse with the contralateral VA but terminated as PICA. The contralateral VA solely proceeds to form the basilar artery. In the case of hypoplastic terminal VA, the contralateral VA predominates the basilar artery with little contribution from the tapering end of the hypoplastic terminal VA. In addition to asymmetry, these two conditions can also cause the basilar artery to bend from the midline (also known as bending basilar)[33]. Deviation and prominence of a vessel, such as bending basilar due to dominance of one of the VAs, may cause compression of cranial nerves[20]. Furthermore, it is essential to consider the geometry of the vertebrobasilar junction while planning for surgical interventions in this region. This region is of particular interest to neurosurgeons and radiologists due to various interventional neuroradiological procedures conduct in the area to treat vascular diseases such as arterial dissections, aneurysms, arteriovenous malformations, dural fistula, or repair of an occlusive disease[34].

Conclusion

Our study shows that anatomical variation of the intracranial VA is common in the population studied, with a total prevalence of 36.5%. Hypoplasia and hypoplastic terminal VA being the most frequent. Understanding the patterns of anatomical variations of the VAs will contribute significantly to the interpretation of ischemic areas and diagnosis of various diseases in the posterior circulatory territory.

Data availability

Available on request.

Code availability

Not applicable.

Received: 13 March 2021; Accepted: 20 May 2021
Published online: 09 June 2021

References

1. Dzierzanowski, J. *et al.* Intracranial region of the vertebral artery: morphometric study in the context of clinical usefulness. *Folia Morphol. (Warsz.)* **76**, 379–387. https://doi.org/10.5603/FM.a2017.0021 (2017).
2. Hong, J. *et al.* Vertebral artery dominance contributes to basilar artery curvature and peri-vertebrobasilar junctional infarcts. *J. Neurol. Neurosurg. Psychiatr.* **80**(1087–1092), 10. https://doi.org/10.1136/jnnp.2008.169805 (2009).
3. Schroeder, G. D. & Hsu, W. K. Vertebral artery injuries in cervical spine surgery. *Surg. Neurol. Int.* **4**, S362 (2013).
4. Liu, I.-W. *et al.* Vertebral artery terminating in posterior inferior cerebellar artery: A normal variation with clinical significance. *PLoS One* **12**, e0175264 (2017).
5. Chen, Y.-Y., Chao, A.-C., Hsu, H.-Y., Chung, C.-P. & Hu, H.-H. Vertebral artery hypoplasia is associated with a decrease in net vertebral flow volume. *Ultrasound Med. Biol.* **36**, 38–43 (2010).
6. Songur, A. *et al.* Variations in the intracranial vertebrobasilar system. *Surg. Radiol. Anat.* **30**, 257–264 (2008).
7. Mitchell, J. Differences between left and right suboccipital and intracranial vertebral artery dimensions: an influence on blood flow to the hindbrain?. *Physiother. Res. Int.* **9**, 85–95 (2004).
8. Mitchell, J. & McKay, A. Comparison of left and right vertebral artery intracranial diameters. *Anat. Rec.* **242**, 350–354. https://doi.org/10.1002/ar.1092420308 (1995).
9. Ogengo, J., Olabu, B., Sinkeet, R., Ogengo, N. M. & Elbusaid, H. Vertebral artery hypoplasia in a Black Kenyan population. *J. Int. Sch. Res. Not.* **2014**, 15 (2014).
10. Khalfani, A. K. & Zuberi, T. Racial classification and the modern census in South Africa, 1911–1996. *Race Soc.* **4**, 161–176 (2001).
11. Ergun, O., Tatar, I. G., Birgi, E. & Hekimoglu, B. Evaluation of vertebral artery dominance, hypoplasia and variations in the origin: angiographic study in 254 patients. *Folia Morphol.* **75**, 33–37 (2016).
12. Gaigalaite, V. *et al.* Association between vertebral artery hypoplasia and posterior circulation stroke. *J. BMC Neurol.* **16**, 118 (2016).
13. Katsanos, A. H., Kosmidou, M., Kyritsis, A. P. & Giannopoulos, S. Is vertebral artery hypoplasia a predisposing factor for posterior circulation cerebral ischemic events? A comprehensive review. *Eur. Neurol.* **70**, 78–83 (2013).
14. Luh, G., Dean, B., Tomsick, T. & Wallace, R. The persistent fetal carotid-vertebrobasilar anastomoses. *AJR Am. J. Roentgenol* **172**, 1427–1432 (1999).
15. Padget, D. H. The development of the cranial arteries in the human embryo. *J. Contrib. Embryol.* **32**, 205–261 (1948).
16. Kim, C., Sohn, J.-H. & Choi, H.-C. Are the anomalous vertebral arteries more hypoplastic?: retrospective linear mixed model approach. *BMC Neurol.* **17**, 168 (2017).
17. Zhou, M. *et al.* Vertebral artery hypoplasia and vertebral artery dissection a hospital-based cohort study. *Neurology* https://doi.org/10.1212/WNL.0000000000001284 (2015).
18. Chuang, Y.-M., Huang, Y.-C., Hu, H.-H. & Yang, C.-Y. Toward a further elucidation: role of vertebral artery hypoplasia in acute ischemic stroke. *J. Eur. Neurol.* **55**, 193–197 (2006).
19. Harati, A. *et al.* Association between vertebral artery hypoplasia and vertebral artery aneurysms: A case-control study. *J. Clin. Neurosci.* **61**, 73–77 (2019).
20. Pekcevik, Y. & Pekcevik, R. Variations of the cerebellar arteries at CT angiography. *Surg. Radiol. Anat.* **36**, 455–461 (2014).
21. Ohkura, K. *et al.* Vertebral artery variations in thoracic aortic patients. *Eur. J. Cardiothorac. Surg.* **46**, 27–31 (2014).
22. Noh, Y., Kwon, O.-K., Kim, H.-J. & Kim, J. S. Rotational vertebral artery syndrome due to compression of nondominant vertebral artery terminating in posterior inferior cerebellar artery. *J. Neurol.* **258**, 1775–1780 (2011).

23. Yeh, J.-F. *et al.* A case of bow hunter's stroke caused by non-dominant vertebral artery. *Acta Neurol. Taiwan.* **14**, 69–73 (2005).
24. Miao, H.-L., Zhang, D.-Y., Wang, T., Jiao, X.-T. & Jiao, L.-Q. Clinical Importance of the Posterior Inferior Cerebellar Artery: A Review of the Literature. *Int. J. Med. Sci.* **17**, 3005–3019 (2020).
25. George, B., Bruneau, M. & Spetzler, R. F. *Pathology and surgery around the vertebral artery* (Springer, 2013).
26. Zhu, D.-Y. *et al.* Treatment of fenestrated vertebrobasilar junction-related aneurysms with endovascular techniques. *J. Clin. Neurosci.* **28**, 112–116 (2016).
27. Hudák, I., Lenzsér, G., Lunenkova, V. & Dóczi, T. Cerebral arterial fenestrations: a common phenomenon in unexplained subarachnoid haemorrhage. *Acta Neurochir. (Wien.)* **155**, 217–222 (2013).
28. Lesley, W. S., Rajab, M. H. & Case, R. S. Double origin of the posterior inferior cerebellar artery: association with intracranial aneurysm on catheter angiography. *Am. J. Roentgenol.* **189**, 893–897 (2007).
29. Silva, M. A., See, A. P., Aziz-Sultan, M. A. & Patel, N. J. Surgical treatment of a double origin posterior inferior cerebellar artery aneurysm and insights from embryology: case report and literature review. *Oper. Neurosurg.* **13**, E8–E12 (2017).
30. Lasjaunias, P., Vallee, B., Person, H., Ter Brugge, K. & Chiu, M. The lateral spinal artery of the upper cervical spinal cord: anatomy, normal variations, and angiographic aspects. *J. Neurosurg.* **63**, 235–241 (1985).
31. Ballesteros, L., Forero, P. & Quintero, I. Morphological expression of the anterior spinal artery and the intracranial segment of the vertebral artery: a direct anatomic study. *Rom. J. Morphol. Embryol.* **54**, 513–518 (2013).
32. Ozdemir, S., Yildiz, C. & Cankur, N. Evaluation of vertebral artery system in a healthy population by using colour duplex Doppler ultrasonography. *Med School J Uludag* **28**, 95–99 (2002).
33. Meng, X., Ding, W., Wu, X. & Di, P. Clinical investigation and characterization of vertebrobasilar dolichoectasia and vertebral artery dominance. *Discov. Med.* **25**, 151–158 (2018).
34. Mercier, P. *et al.* Vascular microanatomy of the pontomedullary junction, posterior inferior cerebellar arteries, and the lateral spinal arteries. *Interv. Neuroradiol.* **14**, 49–58 (2008).

Author contributions

All persons listed as authors have contributed substantially to the protocol development, project design, data collection, and data analysis of this manuscript. L.L., B.R.O., K.S.S., R.H.: conceptualized project. B.R.O., R.H., I.G.M.: collected data. B.R.O., L.L.: analyzed data. L.L., R.H., I.G.M., B.R.O.: manuscript writing and editing.

Funding

Funding was provided by the College of Health Sciences, University of Kwazulu-Natal, Durban, South Africa.

Competing interests

The authors declare no competing interests.

Additional information

Correspondence and requests for materials should be addressed to L.L.

Reprints and permissions information is available at www.nature.com/reprints.

Publisher's note Springer Nature remains neutral with regard to jurisdictional claims in published maps and institutional affiliations.

Radiological anatomy of the suboccipital segment of the vertebral artery in a select South African population

Bukola R. Omotoso[1], **Rohen Harrichandparsad**[2], **Kapil S. Satyapal**[1], **Lelika Lazarus**[1]

[1] Discipline of Clinical Anatomy, School of Laboratory Medicine and Medical Sciences, College of Health Sciences, University of KwaZulu-Natal, Westville Campus, Durban, South Africa

[2] Department of Neurosurgery, School of Clinical Medicine, College of Health Sciences, Nelson R Mandela School of Medicine, University of KwaZulu-Natal, Durban, South Africa

SUMMARY

Vertebral artery (VA) injuries remain one of the most encountered complications during surgical intervention at the craniovertebral junction (CVJ). Anatomically, the suboccipital segment is the most complicated segment of the VA. The artery undergoes a series of bends to form proximal and distal loops. In addition to this standard anatomical description, previously reported variant anatomies such as fenestration, persistent first intersegmental artery (FIA), hypoplasia, and extradural origin of the posterior inferior cerebellar artery (PICA) also contribute to the complexity of this segment. We evaluated the anatomical features of the V3 component of the VA in a South African population to provide useful data on the prevalence of variation and morphometry of the VA. The study is an observational, retrospective chart review of 554 consecutive South African patients (Black, Indian, and White) who had undergone computed tomography angiography (CTA) at Lenmed Ethekwini Hospital and Heart Centre, Durban, South Africa, from January 2009 to September 2019. Various morphological variations were registered in the course of the VA: (1) Hypoplasia; (2) Extradural (V3) origin of PICA; (3) persistent FIA; and (4) VA fenestration. Hypoplasia was observed in 5.6% of cases. The overall prevalence of the last three variations was 4.2% of the total patients. Codominance was observed in 42.6% of patients, left dominance in 34.3%, and right dominance in 23.1% of patients. Since failure to identify these morphological variations can result in inadvertent injury to the VA with serious neurological consequences, it is therefore imperative to recognize these variations preoperatively. Knowledge of these variations will also assist in the interpretation of radiographs.

Key words: Suboccipital segment of the vertebral artery – Vertebral artery hypoplasia – Fenestration – Vertebral artery dominance – Posterior inferior cerebellar artery – Persistent first intersegmental artery

INTRODUCTION

Vertebral artery (VA) injuries remain the most common type of injury during cervical spine

Corresponding author:
Lelika Lazarus. University of KwaZulu-Natal, Discipline of Clinical Anatomy, School of Laboratory Medicine and Medical Sciences, College of Health Sciences, University of KwaZulu-Natal, Westville Campus, 4000 Durban, South Africa. E-mail: ramsaroopl@ukzn.ac.za

Submitted: January 25, 2021. **Accepted:** May 31, 2021

surgery (DeCarvalho et al., 2019). The risk of injury as a complication of surgery is a major problem, especially at the craniovertebral junction (CVJ) due to the variable course of the artery (Yamazaki et al., 2012). The VA is classically divided into four segments. The first segment (V1) extends from the origin at the subclavian artery to the C6 transverse process. The second segment (V2) extends from C6 to axis vertebra (C2) transverse processes. The third segment (V3) extends from the transverse foramen of the C2 to the point of penetration of the dura mater at the foramen magnum. The intracranial segment (V4) extends from the foramen magnum dura to the vertebrobasilar junction. The V3 part is the segment of the artery at the CVJ, also known as the suboccipital segment (Campero et al., 2011). The V3 is the most anatomically complicated segment of the VA. The artery undergoes a series of bends to form a proximal and a distal loop while passing through the transverse foramen of the axis and atlas vertebrae. Although arterial tortuosity is a morphological variation in the course of the VA frequently reported in the V1 and V2 segments, natural loop formation distinguishes the V3 from other segments of the artery.

The V3 segment of the VA is subdivided into three portions: the vertical part (V3v) ascends through the transverse foramen of C2 and atlas (C1); the horizontal part (V3h) extends from the transverse foramen of C1 and courses in the VA groove on the upper surface of the posterior arch of the atlas; and an oblique part (V3o) extends from the groove to the point of penetration of the posterior atlantooccipital membrane (George and Cornelius, 2001, Ulm et al., 2010). Apart from this standard anatomical description, anatomical variants such as fenestration, persistent first intersegmental artery (FIA), posterior inferior cerebellar artery (PICA) arising from the V3 segment, and hypoplasia have been reported at this segment (Uchino et al., 2012; Fortuniak et al., 2016). Failure to identify these morphological variations preoperatively may compromise collateral circulation resulting in brainstem infarction (Fortuniak et al., 2016). In FIA, the VA courses below the C1 arch to enter the spinal canal after leaving the transverse foramen of C2 without passing through the transverse foramen of C1. Fenestration was registered when the VA split into two vessels along the V3 segment, which rejoined distally before entering the dura mater. The origin of the PICA from the V3 segment was recognized as the extradural origin of PICA.

The prevalence of fenestration, persistent FIA, and PICA arising from the V3 segment have been observed in the normal population without CVJ anomalies. Most of the reports are from the Asian continent (Uchino et al., 2012; Wakao et al., 2014; Kim, 2016, Arslan et al., 2019), with few reports from Europe and the United States (O'Donnell et al., 2014; Fortuniak et al., 2016). Reports from the African continent are scarce. There is no report on the prevalence of morphological variation at the V3 segment in the South African population to the best of our knowledge. Genetic and environmental factors, including local hemodynamic influences, have been suggested to play a specific role in the endmost structure of the VA (Sikka and Jain, 2012). Therefore, racial differences in the Asian and Western populations could account for the disparity in the published reports (Arslan et al., 2019). As a result, it was considered crucial to describe the prevalence of these morphologic variations in a South African population. According to a textbook of complications in neurosurgery by DeCarvalho and co-authors, the incidence of anatomical variation increases the likelihood of injury, especially if it is not identified preoperatively (DeCarvalho et al., 2019). Therefore, the overall knowledge of the course of the V3 segment of the VA and prevalence of possible variation is essential to reduce the risk of catastrophic complications associated with vascular injury during a surgical intervention at the skull base (Hsu et al., 2017).

We evaluated the anatomical features of the V3 segment of the VA in a South African population using 3D computed tomography angiography (CTA) to provide valuable data on the prevalence of variation and morphometry of the VA. The reports from this study will also contribute to the knowledge of evidence-based anatomy in teaching anatomy and clinical practice.

MATERIALS AND METHODS

Patient Population

We reviewed the records of 554 South African patients who underwent multidetector CTA at Lenmed Ethekwini Hospital and Heart Centre, Durban, South Africa, from January 2009 to September 2019. The patient population represents the KwaZulu-Natal region. The design was approved by the Institutional Review Board/ Ethics Committee (Biomedical Research Ethics Committee of the University of KwaZulu-Natal with ethical No: BE 148/19). The angiographies were from 307 males (55.4%) and 247 females (44.6%). The average age of the patients is reported as median (interquartile range): 62 (23) (range: 10-99) years; 62 (25) for female patients and 61 (23) for male patients. Race was defined according to the guidelines outlined in the modern systems of racial classification in the Republic of South Africa (Khalfani and Zuberi, 2001). The South African population is divided into four main racial groups: White, Black, Indian, and Colored. Three population groups were included in the present study: Indian 176 (31.8%), White 287 (51.8%), and Black (16.4%). Images were analyzed using a Picture Archiving Communication System (PACS) Tools. The MDCTA images were examined for vascular variations by a neurosurgeon, a neuroradiologist, and an anatomist using the coronal and sagittal view. Patients with congenital abnormalities at the CVJ such as atlantoaxial dislocation, Down syndrome, Klippel-Feil syndrome, or osseous anomalies were excluded from the study to obtain data from the normal population.

Imaging Technique

The imaging examination was performed on a 64-detector row computed tomography (CT) scanner (Lightspeed CT, GE Healthcare Medical Systems, Milwaukee, WI, USA) with the following scanning protocol: 120 kVp, 697 mAs, beam collimation 64 × 0.625 mm, gantry rotation time 0.4 s, section thickness 0.625 mm, pitch 0.969:1 and reconstruction interval of 0.625 mm. During the procedure, 80 mL of non-ionic iodinated contrast followed by 40 mL saline was infused via a double power injector (Medex flowSens, Guerbet USA) into the patient's antecubital vein (4 mL/s).

Dimensions of the V3 Segment

The course of the V3 segment and tortuosity (proximal and distal loop) were analyzed. The diameters, lengths, and angles of arteries were measured with the Picture Archiving Communication System (PACS) Tools. The measurement of each part of the V3 was taken on the coronal view of the CTA images (Fig.1). The diameter of the vertical portion was measured before the VA entered the transverse foramen of the atlas vertebra, while the horizontal diameter was measured above the transverse foramen of the atlas. A diameter of ≤ 2.5 mm was described as hypoplasia according to the method provided by Chen and co- authors (Chen et al., 2010). We classified the VA as dominant if the diameter was larger than that of the contralateral side by a difference of ≥ 0.3 mm according to the method described by Zhang et al. (2014). When the bilateral VAs had a similar diameter or the difference between the VAs was less than 0.3 mm, we referred to them as being "equal" or "codominant." We measured the angles between the proximal and distal loops to evaluate the degree of tortuosity. The proximal loop of the V3 is formed as the VA bends to enter the transverse foramen of the C2 vertebra. The distal loop is present at the transition from the vertical to the horizontal portion at the transverse foramen of the C1 vertebra (Fig. 1).

Statistical Analysis

Categorical and continuous variables were analyzed using SPSS version 27 (SPSS Inc., Chicago, IL, USA). Categorical variables were analyzed using the chi-square test. Because the continuous variables are not normally distributed, the Kruskal-Wallis test followed by the Wilcoxon Signed-Rank test was used to detect significant differences in the obtained values for continuous variables. All tests were performed at 95% confidence with a p-value of < 0.05.

RESULTS

Continuous variables are presented as median, interquartile range (IQR), and Range. Categorical variables are presented by a number (N) and percentage. The interclass coefficient correlation for intra-observer reliability testing was 99 % for the V3v length; 97 % for V3v diameter; 99 % for V3h length and diameter; 99 % for V3o length, proximal and distal loop.

For inter-observer reliability testing, the intraclass correlation ranges between 72% to 96% for all the parameters.

Vascular Variation

We registered four types of variation at the V3 segment: (1) hypoplasia; (2) extradural (V3) origin of PICA; (3) persistent FIA; and (4) VA fenestration. The most frequently observed variation was hypoplasia, found in 5.6% of cases (62/1108). Incidence of bilateral hypoplasia was registered in 0.9% (5/554) of patients. The prevalence of the last three, excluding hypoplasia, was diagnosed in 4.2% (23) of the total patients (23 cases/554). There was no significant racial or gender difference in the incidence of variation. The results are summarized in Table 1.

Morphometric Analysis of the Vertebral Artery Diameter

We observed that the average diameter of the VA increases from the vertical (median (IQR)) (Left- 3.43 (0.61) mm; Right- 3.25 (0.70) mm) to the horizontal part (Left- 3.69 (0.89) mm; Right- 3.60 (0.71) mm) and oblique part (Left- 3.55 (0.79) mm; Right- 3.48 (0.83) mm). The average diameter is significantly larger on the left (vertical portion p=0.000, horizontal portion p=0.001, and oblique portion p=0.006) than on the right side. Most of the VAs had similar diameters (42.6%) with differences of ≤ 0.3 mm between the two sides. We observed a left pattern of dominance in 190 patients (34.3%) and right dominance in 128 patients (23.1%). Concerning the racial groups, the diameter of the left V3v was significantly different across the racial groups (p=0.002; specifically, between Black and Indian p=0.001; between White and Indian p=0.014). On the right V3v, there was no significant difference across the racial groups (p=0.368). The diameter of the left V3h showed a significant difference across the

Fig. 1.- Oblique (**A**) and Coronal (**B**) view of CTA image. **A)** V3 segment of the left VA. V3v – vertical segment of the VA; V3h – horizontal segment of the VA; V3o oblique segment of the VA; PL – proximal loop of V3; DL – distal loop of V3. **B)** The red arrow illustrated right VA hypoplasia.

racial groups (p=0.002; specifically, between Black and White p=0.03; Black and Indian p=0.001). On the right V3h, there was no significant difference across the racial groups (p=0.286). The diameter of the left V3o also showed a significant difference across the racial groups (p=0.014; specifically, between White and Black p=0.005; Indian and Black p=0.01).

On the right V3o, there was no significant difference across the racial groups (p=0.315). The average diameter is summarized in Table 2. For gender, the average diameter of the V3o is significantly larger in females on the left (p=0.000). There were no significant gender differences on the right (p=0.063). The average diameter is summarized in Table 3.

Table 1. Incidence of Anatomical Variations at the suboccipital segment of the VA diagnosed by CTA FIA- Persistent first intersegmental artery, FEN- fenestration, PICA- posterior inferior cerebellar artery.

Type of Variation	Total number of cases (incidence %)	Male/Female	Left/Right	Simultaneous Variation
Hypoplasia	62 (5.6)	36/21	25/37	-
Extradural PICA Origin	16 (1.44)	11/5	8/8	-
Persistent FIA	5 (0.45)	1/4	1/4	-
FEN	2 (0.18)	0/2	1/1	2 with FIA

Table 2. Diameter and length of the vertebral artery V3 segment grouped according to race and laterality in South African patients. Results are in mm. Median and (IQR). Range in mm.

Racial Group	Parameters	V3v		V3h		V3o	
		Left	Right	Left	Right	Left	Right
Black	**Diameter**	3.25(0.77) (2.02-6.25)	3.16(0.66) (1.93-5.28)	3.52(0.64) (2.11-6.25)	3.52(0.71) (1.94-5.63)	3.69(1.14) (2.46-6.95)	3.45(0.97) (2.33-6.42)
	Length	24.89(10.3) (6.21-84.7)	23.26(8.46) (10.6-48.3)	7.17(3.22) (3.55-15.0)	7.03(2.72) (3.21-13.5)	4.32(1.9) (1.89-18.74)	4.01(1.78) (1.86-6.39)
Indian	**Diameter**	3.52(0.75) (2.11-7.04)	3.44(0.79) (0.79-5.98)	3.87(0.88) (2.11-7.92)	3.60(0.71) (0.79-6.07)	3.61(0.79) (2.02-6.42)	3.52(0.79) (2.33-5.46)
	Length	24.72(12.63) (11.8-48.7)	23.10(9.44) (11.7-39.7)	7.55(3.03) 3.69(0.82)	7.26(2.8) (2.95-11.8)	4.75(1.98) (2.47-8.25)	4.42(1.94) (1.89-7.44)
White	**Diameter**	3.43(0.53) (0.79-6.95)	3.25(0.64) (1.85-5.72)	3.69(0.82) (0.79-6.42)	3.60(0.80) (1.85-5.54)	3.52(0.8) (0.79-5.9)	3.43(0.7) (0.79-5.72)
	Length	21.94(11.82) (10.6-45.6)	20.60(11.74) (8.71-46.6)	6.19(2.88) (2.67-16.5)	6.08(3.15) (2.6-13.9)	3.50(1.85) (1.05-9.7)	3.36(1.83) (1.32-7.56)

Table 3. Diameter and length of the vertebral artery V3 segment grouped according to gender and laterality differences in South African patients. Results are in mm. Median and (IQR). Range in mm.

		V3v		V3h		V3o	
		Left	Right	Left	Right	Left	Right
Male	**Diameter**	3.43(0.53) (2.02-6.95)	3.25(0.64) (0.79-5.98)	3.69(0.97) (2.11-6.42)	3.52(0.71) (0.79-5.54)	3.45(0.79) (0.79-6.42)	3.52(0.7) (0.79-5.72)
	Length	24.40(11.76) (6.22-46.3)	22.30(9.95) (10.6-43.6)	6.95(2.98) (2.84-16.5)	6.93(3.0) (2.60-13.5)	4.08(1.89) (1.32-7.45)	3.89(1.91) (1.89-8.25)
Female	**Diameter**	3.43(0.70) (0.79-7.04)	3.25(0.70) (1.85-5.72)	3.69(0.88) (0.79-7.92)	3.69(0.71) (1.85-6.07)	3.77(0.72) (2.02-6.95)	3.61(0.79) (2.2-6.42)
	Length	22.10(11.16) (8.71-48.7)	21.57(10.9) (10.6-48.3)	6.45(3.22) (2.67-15.3)	6.44(3.0) (2.95-13.9)	3.96(0.88) (1.05-18.7)	3.76(1.98) (1.87-7.56)

Length

The length of the V3 was significantly greater on the left than the right side in all parts of the artery (median (IQR)). V3v (23.19 (11.72) mm, 21.80 (10.34) mm) p=0.000; V3h (6.75 (3.17) mm, 6.67 (3.01) mm) p=0.000; V3o (4.03 (1.96) mm, 3.82 (1.93)) mm p=0.000. Within the racial groups, the length of the left and the right V3v showed a significant difference across the racial groups (Left p=0.011, but there was no specific difference between the racial groups; Right p=0.005; specifically, between White and Black p=0.035; White and Indian p=0.003). The average length of the horizontal portion (V3h) showed a significant difference across the racial groups (Left p=0.000; specifically, between White and Black p=0.008; White and Indian p=0.000; Right p=0.000; specifically, between White and Black p=0.011; White and Indian p=0.000). The average length of the oblique portion also showed a significant difference across the racial groups (Left p=0.000; between White and Black p=0.015; White and Indian p=0.000; Black and Indian p=0.025; Right p=0.000; specifically, between White and Black p=0.001; White and Indian p=0.000). The average length across the racial groups and laterality are summarized in Table 2. There were no significant gender differences in the VA length on both sides. The results are summarized in Table 3.

Proximal and Distal Loop Angle

The average angle of the proximal loop was significantly larger on the left (median (IQR)) (67° (24°)) compared to the right (65.66° (25.33°)) side (p=0.001). There was no significant difference in the angle of the distal loop on the right and left sides (Right- 67° (14°), Left- 66° (15°)). We did not observe any significant differences across gender and racial groups. The results are summarized in Table 4.

DISCUSSION

Iatrogenic injury to the VA during procedures around C1/2 constitutes a potentially catastrophic complication that may result in permanent neurological deficits or even death (Vergara et al., 2012; Akinduro et al., 2016). Studies have reported rates ranging from 1.7% - 9.0% (Vergara et al., 2012; Elliott et al., 2014; Liang et al., 2004). Adequate information about anatomical variation can influence the choice of surgical procedure at the CVJ. Apart from the risk of injury, morphological variation at the V3 segment of the VA may result in complications such as brainstem infarction if not recognized during preoperative planning (Fortuniak et al., 2016).

Hypoplasia of the VA has been previously described by different criteria in the literature. Using a measure of diameter ≤ 2.5mm according to the method provided by Chen et al. (2010), we observed a 5.6% (62 cases/1108 VAs) incidence of hypoplastic VA (Fig. 1B). Our results agreed with the findings of O'Donnell and co-authors (6.26%) in the US population, although hypoplasia was defined by different criteria (O'Donnell et al., 2014). By contrast, a similar study in the Asian population reported an incidence of 10% (Arslan et al., 2019), while another study in the European

Table 4. Characteristics of proximal and distal loops of the vertebral artery V3 segment grouped according to gender and racial group in South African patients. Results are in degrees. Median and (IQR). Range in degrees.

	Proximal Loop		Distal Loop	
	Left	Right	Left	Right
Male	67.33(22.83) (42.7-118.7)	65.66(25.17) (39-116.7)	66.66(14.67) (42.7-114.7)	67(16) (37.3-110.7)
Female	68.16(25.17) (36.3-120)	65.33(26.17) (36.3-111.7)	66(16) (41.7-115.3)	66.66(14.16) (43.4-97.3)
Black	66(23) (36.3-118.6)	68(32) (42-109.6)	65.50(18.92) (41.7-107.6)	69.66(17.17) (43-105.3)
Indian	68.16(29.17) (42.7-120)	63.33(24.67) (39.7-111.7)	66(19) (39.7-115.3)	65.33(16.67) (39.7-110.7)
White	67.50(22.83) (43.3-116.7)	66(22.16) (36.3-116.7)	67.16(13.25) (37.4-114.7)	67.33(13.83) (37.4-114.7)

population reported an incidence of 20% (Fortuniak et al., 2016). In the studies mentioned above, a VA was considered hypoplastic if it was half or less than half of the diameter of its counterpart. We suggest that the disparity in the above studies and the present study may have resulted from the differences in the average diameter of the population studied. Going by the criteria described by Fortunaik et al. (2016) and O'Donnell et al. (2014), it may be practically impossible to report the occurrence of bilateral hypoplasia. Five (out of a total of 57) patients had bilateral hypoplasia in the present study. Because of the compromised blood flow in the VA with a reduced diameter (Chen et al., 2010), surgeons need to be aware of its possibility, which may require special attention during surgical intervention.

PICA is the principal branch of the VA, and it typically originates from the intracranial part of the vertebral artery (4th segment). However, due to numerous embryonic vessels forming the VA and its branches, PICA sometimes emerges from the V3 part. An abnormal course of the VA or its PICA branch below the C1 arch may predispose the arteries to iatrogenic injuries during drilling, tapping and insertion of lateral mass screws (Arslan et al., 2019). Previous studies have reported the incidence of extracranial origin of PICA between 0.4% to 2.9% (Table 5). The prevalence in the present study is similar to previous reports (Table 5). It is important to note that no perforating arteries emerge from the PICA of extradural origin. Instead, the perforators originate from the intracranial VAs (Mercier et al., 2008). The incidence of PICA arising from the V3 was observed at the oblique part in all the cases. This site of origin is also described as the C1 origin of the PICA. This information is clinically significant to prevent iatrogenic injury to PICA during surgical interventions at the upper cervical spine and posterior approaches to the lower brainstem (Miao et al., 2020).

The prevalence of FIA ranges between 0.01% to 3.2% (Table 5), similar to the prevalence in our series (0.45%; 5 cases/1108 VAs). We observed bilateral persistent FIAs in one of the patients (Fig. 2B). The simultaneous persistence of the FIA and the typical branch of the VA results in fenestration at the V3 segment (Uchino et al., 2012), as shown in Fig. 3. Both unilateral and bilateral persistent FIA can be easily overlooked (Uchino et al., 2012). An awareness of this variant anatomy and careful review of images will assist in proper identification to prevent VA injury.

Fenestration extended between the vertical and horizontal portion of the V3 segment in the two cases observed in the present study (Fig. 3). The two limbs of the fenestrated segment had a similar diameter. The prevalence of fenestration registered in the present study (0.18%; 2

Table 5. Prevalence of anatomical variations at the V3 segment of the VA in different population groups.

Author (year)	Population	Type of study	Sample Size	Anatomical Variations (Patients %)			
				Hypoplasia	Extradural PICA Origin	FEN	Persistent FIA
Uchino et al., 2012	Japan	MRA	2739	0	30(1.1)	25(0.9)	87(3.2)
O'Donnell et al., 2014	US	CTA	975	61(6.26)	4(0.4)	1(0.01)	1(0.01)
Wakao et al., 2014	Japan	CTA	480	0	5(1.3)	5(1.3)	7(1.8)
Fortuniak et al., 2016	Poland	CTA	1800	360(20)	11(0.61)	3(0.16)	0
Kim et al., 2016	South Korea	CTA	546 314	0 0	11(2.0) 9(2.9)	2(0.4) 2(0.6)	7(1.3) 8(2.5)
Arslan et al., 2019	Turkey	CTA	200	10	2(1)	0	1(0.5)
Present study	**South Africa**	**CTA**	**554**	**57(10.3)**	**16(2.9)**	**2(0.4)**	**5(1.0)**

cases/1108 VA arteries) agrees with the reports from Western countries (Fortuniak et al., 2016), (O'Donnell et al., 2014), and is lesser than the report from a large series study of the Asian population (Uchino et al., 2012) (Table 5). There is a possibility of compromised blood flow at the proximal and distal end of the fenestrated segment of the VA, which may result in transient ischemic attacks (Omotoso et al., 2021). In addition, the passage of the catheter through the normal contralateral VA in patients with this unilateral vascular variation can expose the hindbrain to the risk of ischemia during neuroendovascular procedures (Fortuniak et al., 2016).

In the present study, most patients had equal VA diameters (codominance) (42.6%), the left side was dominant in 34.3%, and right-sided dominance was registered in 23.1%. Our study's pattern of dominance concurs with a previous report in the Asian population (49% equal dominance, 30% left dominance) (Arslan et al., 2019). It is imperative to identify and protect the dominant VA during a surgical intervention at the CVJ. Furthermore, the dominant VA must not be ligated when repairing VA injury, as it can result in permanent neurologic deficit (DeCarvalho et al., 2019).

The race, gender and side differences in the diameter and length of the V3 segment have been previously reported in the American, South African, and Asian populations (Alfaouri-Kornieieva and Al-Hadidi, 2014; Lang and Kessler, 1991; Mitchell, 2004). According to Mitchell's reports, there were no significant gender or laterality differences based on detailed histological analysis of South African adult cadavers (Witwatersrand region). The average diameter of the horizontal portion in our results is less than, but close to, the average value of the above histological reports (3.75±0.72 mm) (Mitchell, 2004) and MRA reports on the Asian population (3.8±0.51 mm) (Alfaouri-Kornieieva and Al-Hadidi, 2014). Noticeably, the average diameter of the vertical portion was smaller than that of the horizontal and oblique portion in our results. On the contrary, Alfaouri-Kornieieva and co-author (2014) reported a gradual decrease

Fig. 2.- Anterior view of 3D-CTA reconstructed images showing the vertebral, basilar, and carotid arteries. **A)** PICA (yellow arrow) originates from the oblique part of V3 of the left VA. The green arrow illustrated the basilar artery. The white arrow illustrated the right common carotid artery **B)** The red and blue arrow illustrated bilateral persistent FIA. The yellow arrow illustrated the left common carotid artery.

from the vertical part to the oblique part in their MRA study. The entire length of the V2 and part of the V3 segment (excluding the horizontal and oblique part) of the VA is restricted within the transverse foramen of the cervical vertebrae, as shown in our CTA series (Fig. 1). We hypothesize that the artery could expand after its exits from the transverse foramen of the atlas (C1) vertebra, which may be a possible explanation for the differences. In agreement with the previous reports by Alfaouri-Kornieieva and co-author (2014) and Arslan et al. (2019), we registered a significantly larger left VA in all parts of the V3 segment (Alfaouri-Kornieieva and Al-Hadidi, 2014; Arslan et al., 2019). The total length of the vertical, the horizontal, and the oblique part in the present study agreed with a previous American study, which reported an average length of 38.91±5.53 (Lang and Kessler, 1991). In our study, the average length of the vertical part was similar, but the average length of the horizontal and the oblique part was shorter than in the Asian population (23.22±2.7 mm, 17.2±2.85 mm, and 12.31±1.8 mm, respectively) (Alfaouri-Kornieieva and Al-Hadidi, 2014). Generally, the disparity noted in the morphometry between the present study and the reports mentioned above may be due to differences in the modality of the studies. In the present study, we observed that the average length showed a significant difference across the racial groups. This dissimilarity may be due to some genetic factors. However, more studies may be required from other regions of South Africa to corroborate this theory.

ACKNOWLEDGEMENTS

Institution responsible for research support: College of Health Sciences (CHS funding), University of KwaZulu-Natal, Durban, South Africa.

REFERENCES

AKINDURO OO, BAUM GR, HOWARD BM, PRADILLA G, GROSSBERG JA, RODTS Jr GE, AHMAD FU (2016) Neurological outcomes following iatrogenic vascular injury during posterior atlanto-axial instrumentation. *Clin Neurol Neurosurg*, 150: 110-116.

ALFAOURI-KORNIEIEVA M, AL-HADIDI AM (2014) Morphology of the vertebral artery in Asian population. *Asian J Med Sci*, 5(4): 84-88.

Fig. 3.- 3D-CTA reconstructed images showing the vertebral, basilar, and carotid arteries. Anteroposterior view, fenestration, and persistent FIA at the V3 segment of the left VA (yellow arrow). The white arrow illustrated the left internal carotid artery.

ARSLAN D, OZER MA, GOVSA F, KITIS O (2019) Surgicoanatomical aspect in vascular variations of the V3 segment of vertebral artery as a risk factor for C1 instrumentation. *J Clin Neurosci*, 68: 243-249.

CAMPERO A, RUBINO PA, RHOTON AL (2011) Anatomy of the vertebral artery. In: *Pathology and surgery around the vertebral artery*. Springer Paris, pp 29-40.

CHEN Y-Y, CHAO A-C, HSU H-Y, CHUNG C-P, HU H-H (2010) Vertebral artery hypoplasia is associated with a decrease in net vertebral flow volume. *Ultrasound Med Biol*, 36(1): 38-43.

DECARVALHO SA, ABD-EL-BARR MM, GROFF MW (2019) Vascular complications in cervical spine surgery (anterior and posterior approach). In: *Complications in Neurosurgery*. Elsevier, pp 314-319.

ELLIOTT RE, TANWEER O, BOAH A, MORSI A, MA T, FREMPONG-BOADU A, SMITH ML (2014) Comparison of screw malposition and vertebral artery injury of C2 pedicle and transarticular screws: meta-analysis and review of the literature. *Clin Spine Surg*, 27(6): 305-315.

FORTUNIAK J, BOBEFF E, POLGUJ M, KOŚLA K, STEFAŃCZYK L, JASKÓLSKI DJ (2016) Anatomical anomalies of the V3 segment of the vertebral artery in the Polish population. *Eur Spine J*, 25(12): 4164-4170.

GEORGE B, CORNELIUS J (2001) Vertebral artery: surgical anatomy. Operative techniques in *Neurosurgery*, 4(4): 168-181.

HSU WK, KANNAN A, MAI HT, FEHLINGS MG, SMITH ZA, TRAYNELIS VC, GOKASLAN ZL, HILIBRAND AS, NASSR A, ARNOLD PM (2017) Epidemiology and outcomes of vertebral artery injury in 16582 cervical spine surgery patients: an AO Spine North America Multicenter Study. *Global Spine J*, 7 suppl 1: 21S-27S.

KHALFANI AK, ZUBERI T (2001) Racial classification and the modern census in South Africa, 1911-1996. *Race and Society*, 4(2): 161-176.

KIM MS (2016) Developmental anomalies of the distal vertebral artery and posterior inferior cerebellar artery: diagnosis by CT angiography and literature review. *Surg Radiol Anat*, 38(9): 997-1006.

LANG J, KESSLER B (1991) About the suboccipital part of the vertebral artery and the neighboring bone-joint and nerve relationships. *Skull Base Surg*, 1(1): 64.

LIANG M-L, HUANG M-C, CHENG H, HUANG W-C, YEN Y-S, SHAO K-N, HUANG C-I, SHIH Y-H, LEE L-S (2004) Posterior transarticular screw fixation for chronic atlanto-axial instability. *J Clin Neurosci*, 11(4): 368-372.

MERCIER P, BRASSIER G, FOURNIER H, PICQUET J, PAPON X, LASJAUNIAS P (2008) Vascular microanatomy of the pontomedullary junction, posterior inferior cerebellar arteries, and the lateral spinal arteries. *Interv Neuroradiol*, 14: 49-58.

MIAO H-L, ZHANG D-Y, WANG T, JIAO X-T, JIAO L-Q (2020) Clinical importance of the posterior inferior cerebellar artery: a review of the literature. *Int J Med Sci*, 17(18): 3005-3019.

MITCHELL J (2004) Differences between left and right suboccipital and intracranial vertebral artery dimensions: an influence on blood flow to the hindbrain? *Physiother Res Int*, 9(2): 85-95.

O'DONNELL CM, CHILD ZA, NGUYEN Q, ANDERSON PA, LEE MJ (2014) Vertebral artery anomalies at the craniovertebral junction in the US population. *Spine, (Phila Pa 1976)* 39(18): E1053-E1057.

OMOTOSO BR, HARRICHANDPARSAD R, MOODLEY IG, SATYAPAL KS, LAZARUS L (2021) Fenestration of the vertebrobasilar junction detected with multidetector computed tomography angiography. *Folia Morphol*, doi: 10.5603/FM.a2021.0028.

SIKKA A, JAIN AJARI (2012) Bilateral variation in the origin and course of the vertebral artery. *Anat Res Int*, 2012: 580765.

UCHINO A, SAITO N, WATADANI T, OKADA Y, KOZAWA E, NISHI N, MIZUKOSHI W, INOUE K, NAKAJIMA R, TAKAHASHI M (2012) Vertebral artery variations at the C1-C2 level diagnosed by magnetic resonance angiography. *Neuroradiology*, 54(1): 19-23.

ULM AJ, QUIROGA M, RUSSO A, RUSSO VM, GRAZIANO F, VELASQUEZ A, ALBANESE E (2010) Normal anatomical variations of the V3 segment of the vertebral artery: surgical implications. *J Neurosurg Spine*, 13(4): 451-460.

VERGARA P, BAL JS, HICKMAN CASEY AT, CROCKARD HA, CHOI D (2012) C1-C2 posterior fixation: are 4 screws better than 2? *Oper Neurosurg*, 71 supl 1: ons86-ons95.

WAKAO N, TAKEUCHI M, NISHIMURA M, RIEW KD, KAMIYA M, HIRASAWA A, KAWANAMI K, IMAGAMA S, SATO K, TAKAYASU M (2014) Vertebral artery variations and osseous anomaly at the C1-C2 level diagnosed by 3D CT angiography in normal subjects. *Neuroradiology*, 56(10): 843-849.

ZHANG D-P, ZHANG S-L, ZHANG J-W, ZHANG H-T, FU S-Q, YU M, REN Y-F, JI P (2014) Basilar artery bending length, vascular risk factors, and pontine infarction. *J Neurol Sci*, 338(1-2): 142-147.

PhD Thesis

by bukola omotoso

Submission date: 19-May-2021 11:08PM (UTC+0200)
Submission ID: 1584638165
File name: PhD_Thesis_Titin_plain_2.docx (8.36M)
Word count: 9501
Character count: 51612

PhD Thesis

ORIGINALITY REPORT

5%	2%	4%	0%
SIMILARITY INDEX	INTERNET SOURCES	PUBLICATIONS	STUDENT PAPERS

PRIMARY SOURCES

1	B. R. Omotoso, R. Harrichandparsad, I. G. Moodley, K. S. Satyapal, L. Lazarus. "An anatomical investigation of the proximal vertebral arteries (V1, V2) in a select South African population", Surgical and Radiologic Anatomy, 2021 Publication	1%
2	Bukola Omotoso, Rohen Harrichandparsad, Kapil Satyapal, Indheresan Moodley, Lelika Lazarus. "Anatomical Variations and Dimension of the Intracranial Vertebral Artery: Evaluation With Multidetector Computed Tomography Angiography", Research Square, 2021 Publication	1%
3	Pathology and surgery around the vertebral artery, 2011. Publication	<1%
4	B. R. Omotoso, R. Harrichandparsad, I. G. Moodley, K. S. Satyapal, L. Lazarus. "Fenestration of the vertebrobasilar junction	<1%

detected with multidetector computed tomography angiography", Folia Morphologica, 2021
Publication

5	monitoringthefuture.org Internet Source	<1 %
6	Myoung Soo Kim. "Developmental anomalies of the distal vertebral artery and posterior inferior cerebellar artery: diagnosis by CT angiography and literature review", Surgical and Radiologic Anatomy, 2016 Publication	<1 %
7	epdf.pub Internet Source	<1 %
8	www.ijpsr.info Internet Source	<1 %
9	www.hindawi.com Internet Source	<1 %
10	people.beocat.ksu.edu Internet Source	<1 %
11	Vishal Bhadkaria, Harsh Kumar Chawre, Joshi S S, Joshi S D. "HISTOLOGICAL VARIATIONS IN VARIOUS SEGMENTS OF VERTEBRAL ARTERY", Journal of Evolution of Medical and Dental Sciences, 2016 Publication	<1 %

12	pdfs.semanticscholar.org Internet Source	<1 %
13	R. Shane Tubbs. "Surgical anatomy and quantitation of the branches of the V_2 and V_3 segments of the vertebral artery", Journal of Neurosurgery Spine, 07/2009 Publication	<1 %
14	link.springer.com Internet Source	<1 %
15	www.mdpi.com Internet Source	<1 %
16	files.givewell.org Internet Source	<1 %
17	Sergio Paulo Brasil Lima. "Acurácia da angiografia por tomografia computadorizada no diagnóstico de morte encefálica", Universidade de Sao Paulo, Agencia USP de Gestao da Informacao Academica (AGUIA), 2020 Publication	<1 %
18	Yunsuk Choi, Sang Bong Chung, Myoung Soo Kim. "Prevalence and anatomy of anomalous left vertebral artery originated from aorta evaluated by computed tomographic angiography", Surgical and Radiologic Anatomy, 2018 Publication	<1 %

19	Worawut Woraputtaporn, Tansita Ananteerakul, Sitthichai Iamsaard, Malivalaya Namking. "Incidence of vertebral artery of aortic arch origin, its level of entry into transverse foramen, length, diameter and clinical significance", Anatomical Science International, 2019 Publication	<1 %
20	"Arterial Revascularization of the Head and Neck", Springer Science and Business Media LLC, 2016 Publication	<1 %
21	Gowthaman Gunabushanam, Lauren Kummant, Leslie M. Scoutt. "Vertebral Artery Ultrasound", Radiologic Clinics of North America, 2019 Publication	<1 %
22	www.earthjournals.org Internet Source	<1 %
23	Jong Un Moon, Myoung Soo Kim. "C3 segmental vertebral artery diagnosed by computed tomography angiography", Surgical and Radiologic Anatomy, 2019 Publication	<1 %
24	openknowledge.worldbank.org Internet Source	<1 %

31	periodicos.unifor.br Internet Source	<1%
32	www.jemds.com Internet Source	<1%
33	archive.org Internet Source	<1%
34	www.ckinetics.com Internet Source	<1%
35	ddfe.curtin.edu.au Internet Source	<1%
36	A. Mishra, H. Pendharkar, E.R. Jayadaevan, N. Bodhey. "Anomalous Origins of Bilateral Vertebral Arteries in a Child with down Syndrome and Moyamoya Disease", Interventional Neuroradiology, 2012 Publication	<1%
37	Pasaoglu Lale, Ugur Toprak, Tunca Kaya. "Variations in the Branching Pattern of the Aortic Arch Detected with Computerized Tomography Angiography", Advances in Radiology, 2014 Publication	<1%
38	Rashmi N Gitte, Chenna Reddy Ganji, Vishal M Salve. "Fourth branch of arch of aorta and its clinical implication", Journal of Biomedical Sciences, 2016	<1%

Publication

39	Staffan Hallerstam. "Blood flow and flow resistance in the vertebral arteries of patients with and without carotid atherosclerosis", Clinical Physiology and Functional Imaging, 3/2004 Publication	<1 %
40	downloads.hindawi.com Internet Source	<1 %
41	hdl.handle.net Internet Source	<1 %
42	www.adelaide.edu.au Internet Source	<1 %
43	www.nber.com Internet Source	<1 %
44	Shao-wei Zhu, Yang Yang, Yu-guang Liu, Jing-wei Cao, Feng Li. "Anatomical Features and Clinical Significance of Radiculomuscular Artery Variants Involving the Suboccipital Segment of Vertebral Artery", Clinical Neuroradiology, 2016 Publication	<1 %
45	website60s.com Internet Source	<1 %
46	www.krepublishers.com Internet Source	<1 %

47	Constantine C. Phatouros, Randall T. Higashida, Adel M. Malek, Philip M. Meyers et al. "Endovascular Treatment of Noncarotid Extracranial Cerebrovascular Disease", Neurosurgery Clinics of North America, 2000 Publication	<1 %
48	Submitted to Hong Kong Baptist University Student Paper	<1 %
49	Submitted to University of KwaZulu-Natal Student Paper	<1 %
50	dspace.mit.edu Internet Source	<1 %
51	hwbdocuments.env.nm.gov Internet Source	<1 %
52	www.azdeq.gov Internet Source	<1 %
53	www.pubmedcentral.nih.gov Internet Source	<1 %
54	Siniša Vujmilović, Goran Spasojević, Saša Vujnović, Slobodan Malobabić, Zoran Vujković. "Variability of the vertebral artery origin and transverse foramen entrance level — CT angiographic study", Folia Morphologica, 2015 Publication	<1 %
55	academic.oup.com Internet Source	<1 %

56	profiles.uonbi.ac.ke Internet Source	<1%
57	repository-tnmgrmu.ac.in Internet Source	<1%
58	ros.kpi.ua Internet Source	<1%
59	Akira Uchino, Naoko Saito, Takeyuki Watadani, Yoshitaka Okada et al. "Vertebral artery variations at the C1–2 level diagnosed by magnetic resonance angiography", Neuroradiology, 2011 Publication	<1%
60	data.ub.uni-muenchen.de Internet Source	<1%
61	G S Bhatia. "Severe left ventricular hypertrophy in Anderson-Fabry disease", Heart, 2004 Publication	<1%
62	Wilhelm Schäberle. "Extracranial Cerebral Arteries", Ultrasonography in Vascular Diagnosis, 2011 Publication	<1%
63	manualzz.com Internet Source	<1%
64	pssjournal.biomedcentral.com Internet Source	<1%

65	recycle4colorado.ipower.com Internet Source	<1%
66	semspub.epa.gov Internet Source	<1%
67	www.docstoc.com Internet Source	<1%
68	"2 Microsurgical Anatomy of the Internal Carotid and Vertebral Arteries", Neurovascular Surgery, 2015. Publication	<1%
69	Sikka, Aprajita, and Anjali Jain. "Bilateral Variation in the Origin and Course of the Vertebral Artery", Anatomy Research International, 2012. Publication	<1%

Exclude quotes	Off	Exclude matches	Off
Exclude bibliography	Off		